Alaska Power Authority
Susitna Hydroelectric Project

Subtasks 4.09 through 4.15

FINAL REPORT ON SEISMIC STUDIES FOR SUSITNA HYDROELECTRIC PROJECT

February 1982

Prepared by

Woodward-Clyde Consultants

for

Acres American Incorporated

1000 Liberty Bank Building
Main at Court
Buffalo, New York 14202
Telephone: (716) 853-7525

PREFACE

This report presents the results of the seismic studies conducted during 1980 and 1981 for the Feasibility Study of the proposed Susitna Hydroelectric Project site. These studies included geologic evaluation of faults and lineaments, a historical and microearthquake seismicity study, an assessment of the potential for reservoir-induced seismicity, and the estimation of ground-motion parameters.

The report includes ten sections which summarize the results of the studies to date. The three appendices present support data for the interpretations and conclusions presented in Sections 1 through 10. Tables and figures appear at the end of each section and appendix.

In most cases, measurements reported in this volume were made in the metric system and then converted to U.S. Customary Units. For these conversions, the measurements reported in the U.S. system are rounded off to the nearest single unit (e.g., 70 km converts to 43 miles) even when in the context of the sentence the conversion should be rounded off to the nearest ten units (e.g., 70 km converted to 40 miles). This was done to retain the original number used to make the conversion. Conversely, some measurements were made using the U.S. system; in these cases, the conversion to the metric system also have been rounded off to the nearest single unit. Both sets of numbers have been presented for the convenience of the reader.

The results and conclusions presented in this report refine those presented in the Interim Report (Woodward-Clyde Consultants, 1980b).

Figures 3-5(A and B) and 3-6(A) incorrectly depict the distribution of ice disintegration deposits. On Figure 3-5(A), the area northwest of the Black River shown to be ice disintegration deposits of Early Wisconsin age is, in fact, an area of till. On Figure 3-5(B), ice disintegration deposits of Late Wisconsin age should be shown only on the valley floor; other areas indicated as ice disintegration deposits are areas covered by till. On Figure 3-6(A), the area of ice disintegration deposits of Early Wisconsin age east of Butte Lake should have been shown as till.

The above corrections address errors in graphical presentation and do not affect the conclusions of the report.

TABLE OF CONTENTS

TABLE OF CONTENTS (CONTINUED)

TABLE OF CONTENTS (CONTINUED)

TABLE OF CONTENTS (CONTINUED)

LIST OF TABLES

LIST OF FIGURES

LIST OF FIGURES (CONTINUED)

LIST OF FIGURES (CONTINUED)

DEFINITION OF KEY TERMS

Site Region:	The area within a 62-mile (100-km) radius about either site.
Project Area:	This generally includes the Devil Canyon and Watana areas and the region in between.
Devil Canyon Area:	The area within a 6-mile (10-km) radius about the Devil Canyon site.
Devil Canyon Site:	The presently proposed location of the Devil Canyon Dam and related facilities.
Devil Canyon Reservoir:	The area of the Susitna River upstream from the proposed Devil Canyon site which will be inundated by impoundment by the dam.
Watana Area:	The area within a 6-mile (10-km) radius about the Watana site.
Watana Site:	The presently proposed location of the Watana Dam and related facilities.
Watana Reservoir:	The area of the Susitna River upstream from the proposed Watana site which will be inundated by impoundment by the dam.

DEFINITION OF KEY TERMS (CONTINUED)

Microearthquake Study Area:	The area in which microearthquake monitoring was conducted in 1980. The boundaries are 62.3° to 63.3° north latitude and 147.5° to 150.4° west longitude.

ACKNOWLEDGMENTS

The Woodward-Clyde Consultants' personnel who participated in the geological portion of the investigation during the two-year study included: Phillip Birkhahn, George Brogan, Dan Collins, Tom Freeman, Bob Goodwin, Paul Guptill, Jon Lovegreen, Ron Mees, Hector Reyes, Ed Sabins, Ray Sugiura, John Waggoner, Dennis Welsch, and Jerry Williams. Dr. Norm Ten Brink of Grand Valley State College, Michigan, assisted with the Quaternary studies. Dr. Kerry Sieh of the California Institute of Technology assisted with trench logging and Quaternary studies.

The Woodward-Clyde Consultants' personnel who participated in the seismological portion of the seismic geology investigation during the two-year study were: Jim Agnew, Jean Briggs, Jim Cullen, Don Helmberger, John Hobgood, Barbara Leitner, Jose Rial, Bette Shepard, William Savage, and Paul Somerville. Jason McBride and Richard Thompson, both of Woodward-Clyde Consultants, and Milton Mayr, Dianne Marshall, Cole Jonafrauk, and Rodney Viereck, all of the University of Alaska Geophysical Institute, assisted with operation of the micro-earthquake network in 1980. Jose Rial analyzed and interpreted synthetic seismograms and first-motion parameters to estimate focal-mechanism parameters. These results were reviewed by Don Helmberger. Reservoir-induced seismicity studies were conducted by Thalia Anagnos, Ram Kulkarni, Peter Knuepfer, and Duane Packer. The earthquake engineering portion of the investigation was conducted by Ezio Alviti, Barbara Bogaert, John Egan, Maurice Power, and Jim Rafidi.

Discussions were held with members of the Alaska Geological Survey, the University of Alaska Geophysical Institute, the Lamont-Doherty Geological Observatory, the University of Alaska, and the U.S. Geological Survey.

Dr. Ulrich Luscher was principal-in-charge of the investigation in 1980. In 1981, George Brogan assumed Dr. Luscher's position. Jon Lovegreen was the project manager and directed the geology study along

with Phillip Birkhahn. Dr. William Savage directed the seismology study; Dr. Packer directed the reservoir-induced seismicity study; and Maurice Power directed the earthquake engineering study.

Project peer review was provided by: Dr. Robert Forbes, Professor Emeritus of Geology of the University of Alaska (geology); and Dr. I. M. Idriss (earthquake engineering), Dr. George Linkletter (Quaternary geology), Dr. Duane Packer (geology), Dr. William Savage (reservoir-induced seismicity), and Dr. Tom Turcotte (seismology), all of Woodward-Clyde Consultants.

Tha Alaska Power Authority authorized the project and provided funding for this investigation. Among those involved were Eric Yould (Director), Nancy Blunck, Robert Mohn, and Dave Wozniak.

Acres American Inc. (Acres) provided logistical support during the field work and participated in discussions which ultimately led to the technical conclusions presented in this report. Among those directly involved were John Lawrence (Project Manager), Mike Bruen, Lance Duncan, Jim Gill, Robert Henschel, Don MacDonald, Virendra Singh, Stuart Thompson, and Leib Wolofsky.

Radiometric (K-Ar) age dates along with thin sections and analyses were provided by Dr. Ken Foland and his colleagues at Ohio State University. Krueger Enterprises, Inc., of Massachusetts provided radiocarbon (C^{14}) age dates. Air Photo Tech, Inc., of Anchorage, Alaska, provided low-sun-angle color near-infrared aerial photography.

Aircraft support was provided by Akland Helicopter, Inc., Air Logistics, Inc., ERA Helicopters, Inc., and Kenai Air, Inc., and was arranged by Acres American Inc. Lodging and logistics in the field were also arranged by Acres.

This report and the Interim Report were prepared by Woodward-Clyde Consultants under subcontract to Acres. Technical support and typing were provided by Jill Pelayo and Carole Wilson, assisted by Barbara Belton, Esther Martin, and Hazel Boyd. Illustrations were prepared by Arlene Padamada, assisted by Dennis Fischer, Al Herron, Robyn Sherrill, Chairoach Siripatanapaibul, and Mark Winters. Technical editing was done by Karen Lundegaard. Printing and binding of the Interim Report was done by Continental Graphics, of Los Angeles. This report was printed and bound by Woodward-Clyde Consultants and Hendricks Printing Company, Inc., of Irvine, California, under the direction of Marcel Arboleda, assisted by Belinda Spicer.

1 - SUMMARY

1.1 - Project Description

The Susitna Hydroelectic Project as currently proposed involves two dams and reservoirs on the Susitna River in the Talkeetna Mountains of south central Alaska. The Project is approximately 50 miles (80 km) northeast of Talkeetna, Alaska, and 118 miles (190 km) north-northeast of Anchorage, Alaska (Figures 1-1 and 2-1). The downstream dam at Devil Canyon (62.8° north latitude, 149.3° west longitude) is currently being considered as an arch dam to be approximately 645 feet (197 m) high. It would impound a 26-mile- (42-km-) long reservoir with a capacity of approximately 1,092,000 acre-feet (1,348 x $10^6 m^3$). The upstream dam at Watana (62.8° north latitude, 148.6° west longitude) is currently being considered as an earthfill or rockfill dam to be approximately 885 feet (270 m) high. It would impound a 48-mile- (77-km-) long reservoir with a capacity of approximately 9,515,000 acre-feet (11,741 x $10^6 m^3$). These dimensions are approximate and subject to revision during design of the project.

Collectively, the proposed dams and related structures are referred to as the Project. This report is part of a feasibility study for the Project being managed and conducted by Acres American Inc. for the Alaska Power Authority. The purpose of this report is to summarize the results of the seismic geology, seismology, and earthquake ground-motion investigation conducted during 1980 and 1981.

The primary objectives of this two-year investigation were to provide values of earthquake ground-motion parameters that would be used for dam design and assessment of feasibility of the Project and to identify faults that have the potential for surface rupture through the area of the Project.

The 1980 study included: review of available geologic and seismologic literature and data; monitoring of microearthquake activity for three months within approximately 30 miles (48 km) of both proposed dam sites using a 10-station microearthquake network; a preliminary review of the potential for reservoir-induced seismicity; interpretation of existing remotely sensed data; a 10 person-month geologic field reconnaissance of mapped faults and lineaments within 62 miles (100 km) of the Project; analysis and interpretation of these data for selection of 13 features (faults and lineaments) for detailed study in 1981; and an estimate of potential earthquake ground motions for the Project. The results of the 1980 study were reported in an Interim Report (Woodward-Clyde Consultants, 1980b).

The 1981 study included: the acquisition and interpretation of low-sun-angle color near-infrared aerial photography; a 10 person-month field program of geologic field mapping, aerial reconnaissance, and trench excavation and logging of 13 features; a three person-month field program of Quaternary geologic studies; geophysical surveys; potassium-argon and radiocarbon age dating; analysis of seismograms for moderate to large earthquakes that have occurred within or adjacent to the Talkeetna Terrain; review of the Benioff zone seismicity and refinement of the location and size of the maximum credible earthquake for the zone; analysis of focal mechanisms of selected earthquakes to refine understanding of the regional stress regime; and development of a model for reservoir-induced seismicity that incorporates the relationship of natural seismicity with reservoir-induced earthquakes. From this work, seismic sources were identified, and the maximum credible earthquake for each source and its recurrence interval were estimated. These data were used to estimate the potential ground motions for the Project. A manual was also prepared for the operation of a long-term seismic monitoring network.

The results presented in this report were developed for two reasons: 1) for the purpose of evaluating Project feasibility; and 2) to support submittal of a license application for the Project to the Federal Energy Regulatory Commission. The results should be reviewed when final dam design is considered.

This summary abstracts many important details that should be considered in any application of the results to seismic design. Consequently, the concepts, interpretations, and conclusions presented in this summary should be used only within the context of corresponding sections in the text.

1.2 - Fault Study Rationale

According to the present understanding of plate tectonics, the earth's lithosphere contains 12 to 22 miles (20 to 35 km) or so of relatively light, brittle crust that overlies the mantle, which is denser and less brittle than the crust. Major horizontal movements of the crustal plates are considered to be related to, or caused by, thermal convective processes within the mantle.

Within the plate-tectonic framework, faults that have the potential for generating earthquakes have had recent displacement and may be subject to repeated displacements as long as they are in the same tectonic stress regime. In regions of plate collision such as Alaska, the tectonic stress regime is the result of one plate being subducted, or underthrust, beneath the adjacent plate.

Faults with recent displacement both in the downgoing plate and in the upper plate can generate earthquakes, which cause ground motions at the surface that need to be considered for seismic design purposes. However,

faults in the downgoing plate are not considered when evaluating potential for ground-surface rupture, because these faults do not extend into the upper plate.

A guideline for defining "recent displacement" was prepared by Acres American Inc. and is discussed in Section 3 of the Interim Report (Woodward-Clyde Consultants, 1980b). According to that guideline, faults that have caused rupture of the ground surface within approximately the past 100,000 years are classified as being faults with recent displacement and should be considered in seismic design. Conversely, faults that have not caused rupture of the ground surface during the past 100,000 years are classified as faults without recent displacement. These faults are considered to be of no additional importance to Project feasibility and dam design because faults without recent displacement are not known to be sources of large earthquakes or surface rupture.

To be identified as a fault with recent displacement, earthquakes that occurred on the fault during the past 100,000 years need to have been large enough to produce geological evidence of surface rupture that could be detected by our investigation. Consequently, an estimate was made of the magnitude of the largest earthquake that might have occurred without leaving any detectable geologic evidence. This earthquake was designated the "detection level earthquake" and is considered to be a potential seismic source.

1.3 - Approach

The 1980 study led to the identification of features considered to be potentially important to seismic design. The rationale and methods for identifying these features is discussed in Section 8 of the Interim Report (Woodward-Clyde Consultants, 1980b).

The purpose of the 1981 study was to evaluate the feasibility and design significance of three potentially important earthquake sources with known recent displacement; these included the Castle Mountain and Denali faults and the Benioff zone. The 1980 study also identified 13 features (four faults and nine lineaments) in the vicinity of the proposed dam sites that required additional study to evaluate whether they had been subject to surface displacement during the past 100,000 years and, therefore, might need to be considered as seismic sources for purposes of dam design. These 13 features were examined in detail during the 1981 field study. The study involved the following objectives:

a) Assessing the likelihood that each of the 13 features is a fault.

b) Assessing the age of the sediments overlying each of the 13 features.

c) Selecting and excavating trenches across topographic features that resembled topographic expression of faults in the young geologic deposits.

d) Evaluating the likelihood that each of the 13 features is a fault with recent displacement using the guideline established for the project, i.e., rupture of the ground surface during the past 100,000 years.

e) Assessing the detectability of faults that may have ruptured the ground surface during moderate to large earthquakes in the past 100,000 years and estimating a detection level earthquake that could theoretically occur on a fault that might be below the detection level of geologic investigation.

f) Evaluating seismological records of moderate to large historical earthquakes in the project region to estimate focal mechanism parameters and assess the relation of the earthquakes to recognized faults with recent displacement.

g) Applying judgment and experience gained from the study of other faults with recent displacement in Alaska and in similar tectonic environments (e.g., Japan and South America).

h) Estimating the maximum credible earthquake and recurrence interval 1) for each fault that is considered to be a seismic source, 2) for the Benioff zone, and 3) for a detection level earthquake.

i) Estimating the potential for surface rupture on any faults with recent displacement within 6 miles (10 km) of the dam sites.

j) Estimating the values of ground-motion parameters for the seismic sources identified in objective (h) above that are appropriate for seismic design.

1.4 - Tectonic Model

A tectonic model for the area encompassing the Project region was developed in 1980 to provide a framework in which to: assess fault activity; estimate maximum credible earthquakes; evaluate the potential for surface fault rupture; and evaluate the potential for reservoir-induced seismicity.

On the basis of the tectonic model, a relatively stable tectonic unit was identified in which the Project is located. This tectonic unit was named the Talkeetna Terrain (Woodward-Clyde Consultants, 1980b). The Terrain boundaries are the Denali and Totschunda faults to the north and

east, the Castle Mountain fault to the south, and a zone of deformation with volcanoes to the west. The thickness of the Talkeetna Terrain is limited by the Benioff zone or base of the crust at depth (Figure 1-1). With the exception of the western boundary, which is primarily a broad zone of uplift marked by Cenozoic age volcanoes, all of the boundaries are (or contain) recognized faults with recent displacement. The Terrain is part of the North American plate.

Because the Talkeetna Terrain is a relatively stable tectonic unit, major strain release occurs along its boundaries rather than within the Terrain. The basis for this conclusion is: the clear evidence for recent displacement along the Castle Mountain, Denali, and Totschunda faults and the subducting plate defined by the Benioff zone; the general absence of large historical earthquakes within the Terrain; and the absence of faults within the Terrain that display evidence of recent displacement. Some compression-related crustal adjustment within the Terrain is probably occurring as a result of the plate movement and the stresses related to the subduction process. This crustal adjustment is expressed by small earthquakes such as those recorded during the 1980 microearthquake study.

1.5 - Quaternary Geology

Surfaces and sediments of late Quaternary were studied in detail to provide information on the recency of fault displacement. These studies were designed to: a) prepare a map showing the geographic extent and age of surficial glacial sediments and surfaces; and b) evaluate the likelihood that each of the 13 significant features is a fault with recent displacement. In the site region, the Quaternary surfaces and sediments are primarily glacial in origin. This origin reflects the wide-spread glacial activity in south central Alaska during late Quaternary time.

Four distinct Quaternary glacial episodes are evident: pre-Wisconsin, >100,000 years before present (y.b.p.); Early Wisconsin, 75,000 to 40,000 y.b.p.; Late Wisconsin, 25,000 to 9,000 y.b.p.; and Holocene, <9,000 y.b.p. (Figure 3-2). Each glacial episode was less extensive than the preceding one. The limits of each are defined by the elevation and geographic distribution of glacial erosional or depositional features. Glaciers advanced repeatedly from three main source areas: the Alaska Range to the north; the southern and southeastern Talkeetna Mountains; and the Talkeetna Mountains north and northwest of the Susitna River. Glacial flow was dominantly south and southwest, following the regional slope and structural grain. Multi-directional and convergent flow, differing glacial magnitudes, topographic influences, and other parameters make the glacial chronology of the Project region complex.

The four features near the Watana site are located in areas where Late Wisconsin (25,000 to 9,000 y.b.p.) surfaces predominate except in the vicinity of the Talkeetna River where pre-Wisconsin (>100,000 y.b.p.) surfaces are present (Figure 3-4). The nine features near the Devil Canyon site are in areas of Early Wisconsin and older (>40,000 y.b.p.) erosional surfaces, except in the vicinity of the Susitna River and major creeks where Late Wisconsin (25,000 to 9,000 y.b.p.) surfaces predominate (Figure 3-4).

1.6 - Faults with Recent Displacement

Faults for which evidence of recent displacement was found were considered to be potential seismic sources. Each potential seismic source was evaluated during this study to estimate its potential seismic ground motions at the Watana and Devil Canyon sites and its potential for surface rupture within 6 miles (10 km) of the sites.

On the basis of the 1980 study, the Talkeetna Terrain boundary faults were identified as seismic sources that need to be considered as potential sources of seismic ground motion at the sites. These include: the Castle Mountain fault, the Denali fault, the Benioff zone interplate region, and the Benioff zone intraplate region (Figure 1-1). These sources are considered to be or to contain faults with recent displacement that could cause seismic ground motions at the Watana and Devil Canyon sites; however, because of their distance from the sites, these faults do not have the potential for rupture through the sites. The 1980 study also identified 13 features near the sites that required detailed evaluation during the 1981 study to assess their importance for seimsic design.

On the basis of the 1981 study, no evidence for faults with recent displacement other than the Talkeetna Terrain boundary faults has been observed within 62 miles (100 km) of either site and none of the 13 features near the sites are judged to be faults with recent displacement. Therefore, when applying the guideline defining faults with recent displacement to the results of our investigation, the 13 features are considered not to be potential seismic sources that could cause seismic ground motions at the sites or surface rupture through the sites.

Our interpretation that none of the 13 features are faults with recent displacement is based on data collected during our investigation. The data are limited in the sense that a continuous 100,000 year-old stratum or surface was not found along the entire length of each of the features. For this reason, the available data were analyzed and professional judgment was applied to reach conclusions concerning the recency of displacement on each of the 13 features.

As discussed previously, earthquakes up to a given magnitude could occur on faults with recent displacement that might not be detectable by our

geologic investigation. The size of such an earthquake, designated the detection level earthquake, varies according to the degree of natural preservation of fault-related geomorphic features and from one tectonic environment to another. The detection level earthquake has been estimated by: 1) evaluating the dimensions of surface faulting associated with worldwide historical earthquakes in tectonic environments similar to the Talkeetna Terrain; 2) identifying the threshold of surface faulting using a group of thoroughly studied earthquakes in California; and 3) evaluating the degree of preservation of fault-related geomorphic features in the Talkeetna Terrain. For this project, we have judged that the detection level earthquake is magnitude (M_S) 6.

1.7 - Seismicity

Historical earthquake activity within 200 miles (322 km) of the Project is associated with displacement along crustal faults in the upper plate and with the subducting (downgoing) plate. The largest earthquake within 200 miles (322 km) of the Project is the 1964 Prince William Sound earthquake of magnitude (M_S) 8.4. This earthquake occurred outside the Talkeetna Terrain on the interface between the North American plate and the Pacific plate (Figure 1-1); the associated rupture and deformation extended to within approximately 88 miles (142 km) of the Project.

Within the site region (62 miles [100 km] from the Project), the level of historical seismicity on the Benioff zone is at least several times greater than that of the crustal region. The largest reported earthquake in the site region (magnitude [M_S] 6-1/4) occurred on 3 July 1929. The focal depth appears to be below the crust, possibly in the depth range of 25 to 31 miles (40 to 50 km). This depth suggests that this earthquake may have occurred on the Benioff zone.

During three months of mid-1980, a ten-station microearthquake array was operated to study the area within 30 miles (48 km) of the Project. More than 260 earthquakes in the magnitude (M_L) range 0.0 to 3.7 were analyzed.

Earthquake activity recorded by the microearthquake array clearly delineates two seismic zones. The upper zone of crustal activity occurs predominantly in the depth range of 5 to 12 miles (8 to 20 km). The lower zone of activity defines a northwestward dipping zone (the Benioff zone) at a depth of 25 miles (40 km) in the southeast to 50 miles (80 km) in the northwest portion of the microearthquake study area (Woodward-Clyde Consultants, 1980b). The Benioff zone is approximately 6 to 9 miles (10 to 15 km) thick and is characterized by widely distributed seismicity.

During the three-month period of monitoring, 13 earthquakes of magnitude (M_L) 3.0 and larger were located in the Benioff zone. This level of activity is about ten times greater than that recorded for the shallow (crustal) zone. The slope of the magnitude-frequency relationship for the Benioff zone microearthquakes is 0.68, similar to that for many areas worldwide. The magnitude-frequency relationship suggests a relatively low number of larger earthquakes compared to smaller earthquakes. These results are consistent with the historical seismicity record.

The crustal earthquake activity was found to contain relatively few events at depths shallower than 5 miles (8 km) or deeper than 12 miles (20 km). No seismic activity that appeared to be associated with the crust was deeper than 19 miles (30 km). The level of seismicity within the crustal zone within 30 miles (48 km) of the Project is very low, about one-tenth of the Benioff zone activity. The slope of the associated magnitude-frequency relationship is 1.48.

The 1981 seismicity study included: an evaluation of the tectonic association of moderate to large earthquakes within or adjacent to the Talkeetna Terrain; review of small earthquakes within the Talkeetna Terrain to assess the nature of the stress regime; review of Benioff zone seismicity to refine the assessment of the magnitude and location of the largest earthquake that could be expected to occur on the Benioff zone; and development of a manual for a long-term seismic monitoring network. The first three topics are discussed in Section 5 and are summarized below. The network manual has been prepared as a separate document from this report.

The evaluation of moderate to large historical earthquakes shows that all of these events larger than magnitude (M_S) 5.6 in the Talkeetna Terrain occurred in the Benioff zone, adjacent to recognized faults with recent displacement (such as the Castle Mountain fault), or in the crust adjacent to the western boundary of the Talkeetna Terrain. The event near the western boundary of the Terrain is the 1943 earthquake of magnitude (M_S) 7.3, which had a focal depth of 11 miles (17 km) and was located approximately 90 miles (145 km) southwest of the Project. A review of available small-scale satellite imagery and aerial photography showed several lineaments that could have been sources for this earthquake. However, no obvious source was observed during an aerial reconnaissance of the epicentral region.

Evaluation of the regional stress regime, using records obtained from the microearthquake network operated during the 1980 study and records from the University of Alaska Geophysical Institute (UAGI), supports a northwest-direction of compression. This orientation is consistent with regional plate tectonic motion and with the tectonic setting of the Talkeetna Terrain.

Review of worldwide and Alaskan Benioff zone seismicity resulted in a refined configuration of the Benioff zone. The Benioff zone in

south central Alaska is comprised of two regions. In the interplate region, earthquakes occur along the interface between the subducting Pacific plate and the overlying North American plate (Figure 1-1). Relatively large earthquakes, such as the 1964 magnitude (M_S) 8.4 Prince William Sound earthquake, occur along this region. In the intraplate region, earthquakes occur within the subducting Pacific plate where it is decoupled from and dips beneath the North American plate. The maximum earthquakes in this region of the Benioff zone are of moderate to large size and are smaller than the maximum earthquakes in the interplate region.

1.8 - Maximum Credible Earthquakes (MCEs)

Maximum credible earthquakes (MCEs) were estimated for the boundary faults (in the crust and in the Benioff zone) and for the detection level earthquake (discussed in Section 1.6). The MCEs for the crustal faults (the Castle Mountain and Denali faults) were estimated using the magnitude-rupture-length relationships developed by Slemmons (1977b) and relationships based on Slemmons' data base (U.S. Nuclear Regulatory Commission, 1981). The rupture area relationship of Wyss (1979) was also considered. Application of these relationships represents the state-of-the-practice in the estimation of maximum credible earthquakes. (Appendix E in the Interim Report [Woodward-Clyde Consultants, 1980b] describes the details of these relationships.) These relationships provide essentially the same results for the crustal boundary faults.

The estimated magnitude of the MCE for the Denali fault was revised from the estimate that was presented in the Interim Report (Woodward-Clyde Consultants, 1980b). The revision resulted from the evaluation of recent data, such as that of Slemmons (U.S. Nuclear Regulatory Commission, 1981).

The refined configuration of the Benioff zone (discussed in Sections 1.7 and 5.2) distinguishes between the shallow interplate region (where earthquakes accommodate relative plate motion) and a deeper intraplate region (where earthquakes accommodate internal deformation within the Pacific plate) (Figures 1-1 and 5-7). Review of the historical seismicity in analogous interplate and intraplate regions of the world, including Japan and South America, was used to estimate the MCE for both regions of the Benioff zone.

Sources of moderate earthquakes appear to exist within the Talkeetna Terrain, although no faults with recent displacement were detected by our investigation. Therefore, an MCE was estimated for the detection level earthquake that would be associated with a fault along which no surface rupture was observed. In summary, the MCEs for the crustal and Benioff zone seismic sources are estimated as follows:

Source	MCE (M_S)	Closest Approach to Proposed Dam Sites: Devil Canyon miles/(km)		Watana miles/(km)	
Castle Mountain fault	7-1/2	71	(115)	65	(105)
Denali fault	8	40	(64)	43	(70)
Benioff zone (interplate)	8-1/2	57	(91)	40	(64)
Benioff zone (intraplate)	7-1/2	38	(61)	31	(50)
Detection level earthquake	6	<6	(<10)	<6	(<10)

Note:

1. This MCE accommodates the 1964 Prince William Sound earthquake of magnitude (M_S) 8.4. As discussed by Kanamori (1977), the M_S magnitude scale appears to saturate for this size event, and the M_W scale more accurately describes the size of the energy release. The M_W magnitude of the 1964 earthquake is 9.2; this M_W magnitude is represented in the table and in the report by M_S 8-1/2 for comparison to the other MCEs.

1.9 - Effect of Reservoir-Induced Seismicity (RIS)

The reservoir that would be impounded behind the proposed Devil Canyon dam would be 551 feet (168 m) deep, and that behind the Watana dam would be 725 feet (221 m) deep. The volume of the Devil Canyon reservoir would be 1.09×10^6 acre-feet ($1,348 \times 10^6 m^3$). The volume of the Watana reservoir would be 9.56×10^6 acre-feet ($11,741 \times 10^6 m^3$). Using classifications cited by Packer and others (1977), both reservoirs would be very deep; the Devil Canyon reservoir would be large, and the Watana reservoir would be very large. Because of the proximity of the two reservoirs to each other, they would constitute a combined hydrologic unit that would be very deep and very large.

Given that the combined hydrologic unit described above will be very deep and very large, the potential for reservoir-induced seismicity (RIS) was estimated by evaluating reservoir-induced seismicity at other deep, very deep, and very large reservoirs. Our interpretation of the results of this comparison indicates that the expected likelihood of a reservoir-induced earthquake (including microearthquakes) at the proposed reservoir is 0.46 (on a scale of 0 to 1).

Since the likelihood of a reservoir-induced event is high, it is important to understand what the maximum reservoir-induced earthquake is likely to be. Previous studies (Packer and others, 1977; Packer and others, 1979) have presented data that support the concept that reservoirs can trigger earthquakes by means of increases in pore pressure or by incremental increases in stress. Because reservoirs act as triggering mechanisms, they are not expected to cause an earthquake larger than that which could occur in a given region "naturally." Rather, the reservoirs are expected to have a potential effect on the length of time between events and possibly on the location of the event. Thus, if the tectonic and seismologic setting of a region is known, and if the maximum earthquake for the region has been adequately

defined, the maximum size of a reservoir-induced event is limited by the maximum earthquake that would occur in the region independently of RIS.

Review of historical RIS data (Packer and others, 1977; Packer and others, 1979) strongly suggests that reservoir-induced earthquakes of magnitude (M_S) larger than 5 occur where faults with recent displacement lie within the hydrologic regime of the reservoir. Since no faults with recent displacement were found within the hydrologic regime of the proposed reservoirs (discussed in Sections 1.6 and 4.4), the likelihood of an RIS event of magnitude (M_S) greater than 5 is considered to be very low. However, the detection limits for faults with recent displacement in this region suggest the theoretical possibility of the presence of a fault within the hydrologic regime of the reservoirs that could generate a magnitude (M_S) 6 earthquake (Section 1.6). Consequently, there is some likelihood that a reservoir-induced earthquake of up to magnitude (M_S) 6 could occur.

A model was developed to estimate the likelihood that earthquakes of magnitude (M_S) ≥ 4 could occur within the hydrologic regime of the reservoir during the design life of the Project (Section 6). Application of the model shows that a moderate to large RIS earthquake is unlikely and that RIS has little effect on values for ground-motion parameters. The limited effect is due in large part to there being no faults with recent displacement within the hydrologic regime of the reservoir and the remote possibility of the presence of an undetected fault that could be the source of the detection level earthquake. The results of using this model were incorporated into design analysis (Section 8.2).

1.10 - Ground Motions

Both deterministic and probabilistic assessments were made of earthquake ground motions at the sites. The parameters of ground motions addressed in these studies included peak horizontal ground acceleration, response spectra, and duration of strong shaking. Estimated mean peak horizontal ground accelerations and duration of strong ground shaking (significant duration) at the sites due to maximum credible earthquakes are the following:

Earthquake Source	Maximum Magnitude	Mean Peak Acceleration (g's)		Significant Duration (sec)
		Watana Site	Devil Canyon Site	
Benioff zone (interplate)	8-1/2	0.35	0.3	45
Denali fault	8	0.2	0.2	35
Detection level earthquake	6	0.5	0.5	6

Response spectra of site ground motions for these maximum credible earthquakes are presented in Section 8.

Probabilities of exceedance were estimated for various levels of peak ground acceleration at the Watana site. For probability of exceedance levels of 50 percent, 30 percent, 10 percent, 5 percent, and 1 percent in 100 years, the corresponding peak ground accelerations are the following:

Probability of Exceedence in 100 years	Peak Ground Acceleration at Watana Site (g)
50 percent	0.28
30 percent	0.32
10 percent	0.41
5 percent	0.48
1 percent	0.64

The interplate region of the Benioff zone was found to dominate the contributions to the probabilities of exceedance. Other sources of earthquakes, including the Denali fault and the detection level earthquake contributed only slightly to the probabilities of exceedance.

At the Devil Canyon site, peak ground accelerations for given probabilities of exceedance would be slightly lower than those at the Watana site because the Devil Canyon site is somewhat farther from the Benioff zone.

Possible design ground-motion criteria were formulated for a maximum credible earthquake occurring on the interplate region of the Benioff zone. The criteria are consistent with those typically used for critical facilities. These criteria, which are presented in Section 8, included 84th percentile smooth response spectra and an acceleration time history for use in the seismic analysis of Watana Dam. The acceleration time history has an appropriately long duration and a response spectrum that closely fits the 84th percentile response spectra at the anticipated fundamental natural period of Watana Dam.

Design ground-motion criteria for a detection level earthquake can be formulated using the same approach as that used for a maximum Benioff zone earthquake. However, it is also appropriate to consider the relatively low probability of detection level earthquakes in comparison to Benioff zone earthquakes in selecting design criteria for a detection level earthquake.

For non-critical facilities, such as a powerhouse or transmission towers, the results of the probabilistic studies can be used to aid in selecting design criteria. Selection of the design criteria may include consideration of acceptable levels of probabilities of exceedence, economics, and acceptable risks of damage to these facilities.

1.11 - Conclusions

Two sets of conclusions were drawn from the results of the investigation. The feasibility conclusions are those considered important in evaluating the feasibility of the Project. The technical conclusions are those related to the scientific data collected. Both sets are presented in Section 10. The feasibility conclusions, in summary, are the following:

1) The faults with known recent displacement closest to the Project sites are the Castle Mountain and Denali faults. These faults, and the Benioff zone associated with the subducting Pacific plate, are considered to be seismic sources. Maximum credible earthquakes (MCEs) for the Castle Mountain and Denali faults, and the interplate and intraplate regions of the Benioff zone, have been estimated as: a magnitude (M_S) 7-1/2 earthquake on the Castle Mountain fault, 71 miles (115 km) from the Devil Canyon site and 65 miles (105 km) from the Watana site; a magnitude (M_S) 8 earthquake on the Denali fault, 40 miles (64 km) from the Devil Canyon site and 43 miles (70 km) from the Watana site; a magnitude (M_S) 8-1/2 earthquake on the interplate region of the Benioff zone, 57 miles (91 km) from the Devil Canyon site and 40 miles (64 km) from the Watana site; and a magnitude (M_S) 7-1/2 earthquake on the intraplate region of the Benioff zone, 38 miles (61 km) from the Devil Canyon site and 31 miles (50 km) from the Watana site.

2) Of the 13 significant features, nine were found to be lineaments and four were found to be faults. No evidence of faults with recent displacement (displacement in the past 100,000 years) was found on features that pass through or adjacent to the Project sites; therefore, none of the 13 significant features near the sites are judged to be faults with recent displacement for purposes of seismic design.

3) The detection level earthquake (an earthquake that theoretically could occur on an undetected fault with recent displacement) was judged to be a magnitude (M_S) 6 earthquake that could occur within 6 miles (10 km) of either site.

4) Estimates of peak acceleration, response spectra, and duration of strong shaking at the sites were made for the Denali fault, the interplate region of the Benioff zone, and the detection level earthquake. The results of the probabilistic ground-motion (seismic exposure) study indicate that the source most likely to cause ground shaking at the site is the interplate region of the Benioff zone. Possible design criteria have been formulated for the Benioff zone earthquake.

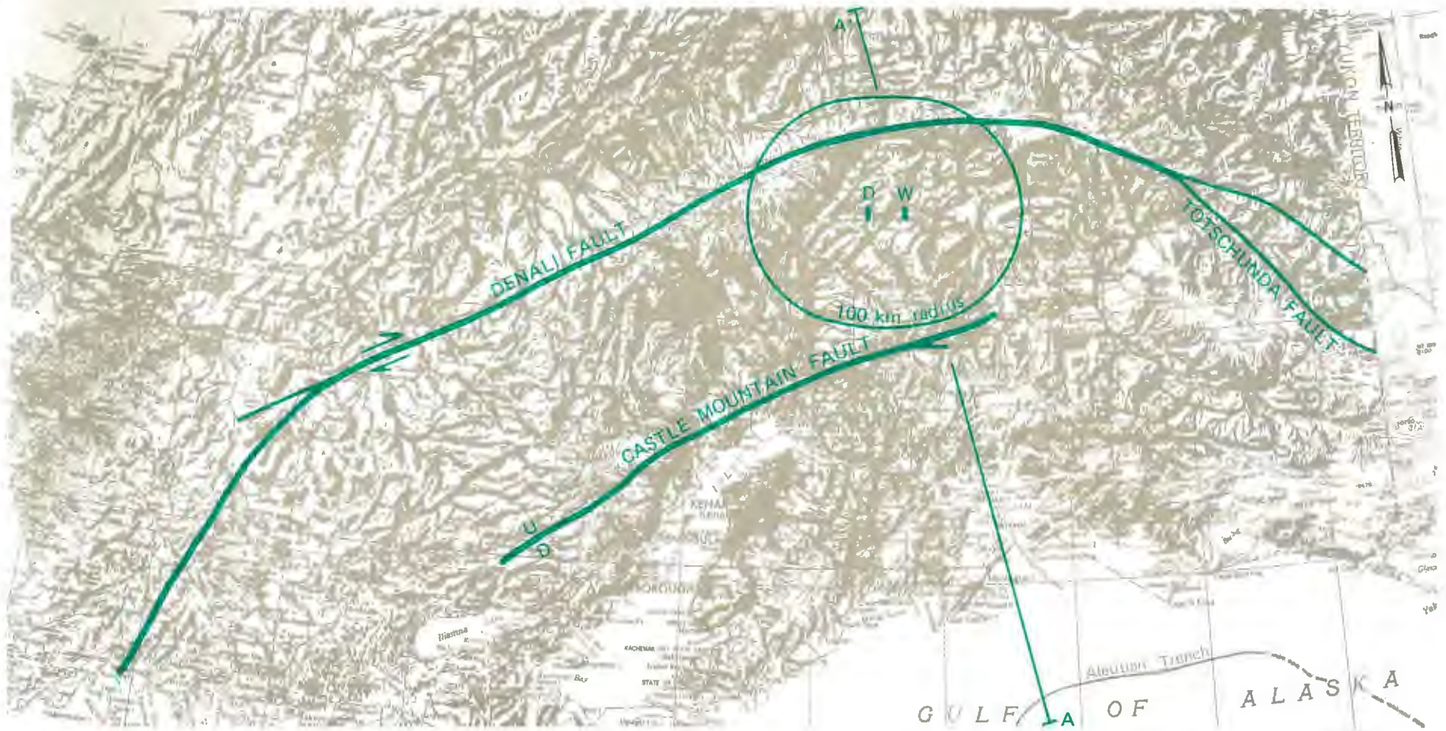

A. MAP VIEW OF SEISMIC SOURCES

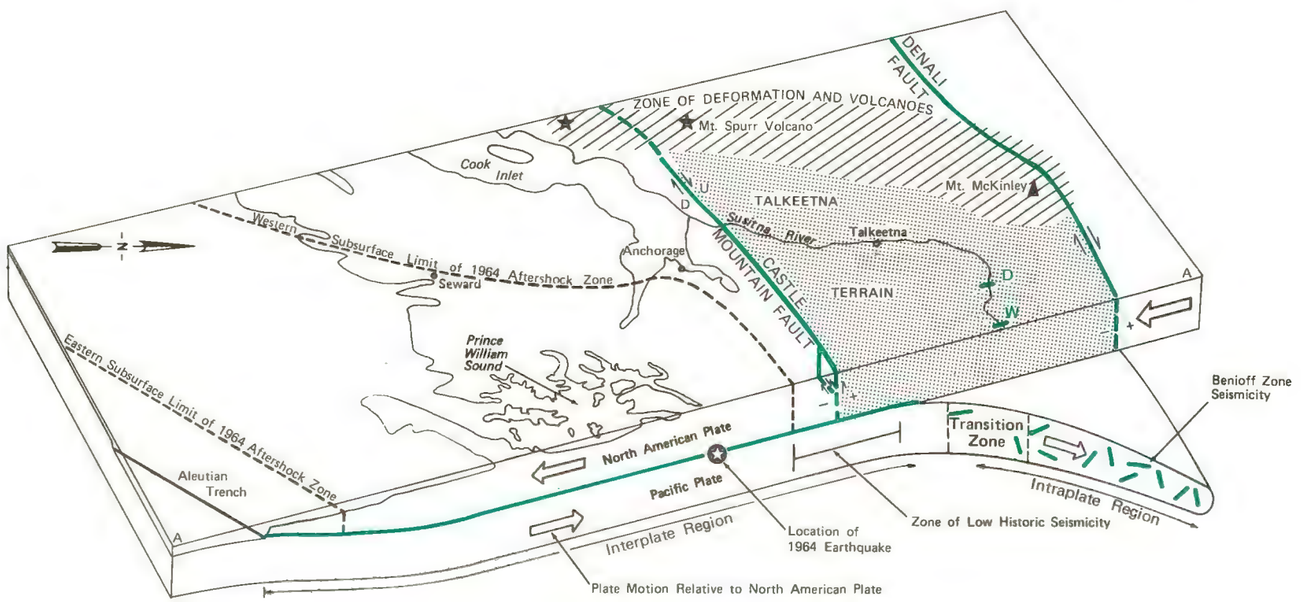

B. THREE DIMENSIONAL VIEW OF SEISMIC SOURCES

LEGEND

Active crustal fault considered as a seismic source. Arrows show sense of horizontal displacement: U is up; D is down.

Active crustal fault segment not considered as a seismic source

W — Watana Site

D — Devil Canyon Site

NOTES

1. Fault locations after Beikman (1974a; 1974b)
2. A—A' is the section orientation shown below in the three dimensional view of seismic sources.

SUMMARY OF SEISMIC SOURCES

2 - INTRODUCTION

2.1 - Project Description and Location

Present conceptual plans for the Susitna Hydroelectric Project (referred to hereafter as the Project) include two dams and reservoirs in the Talkeetna Mountains of south central Alaska (Figure 2-1). This study to evaluate the feasibility of the Project was authorized by the Board of Directors of the Alaska Power Authority (APA) on 2 November 1979. Acres American Inc. (Acres) was selected by the Alaska Power Authority (APA) to conduct the feasibility study. A Plan of Study (POS) was developed by Acres that identified the scope of services to be conducted for the feasibility study (Acres American Inc., 1980).

The overall objectives of the feasibility study were to:

1) Establish the technical, economic, and financial feasibility of the Project to meet the future power needs of the Railbelt Region of the State of Alaska;

2) Evaluate the environmental consequences of designing and constructing the Susitna Project; and

3) File a complete license application with the Federal Energy Regulatory Commission.

Woodward-Clyde Consultants was one of a six-member team of consultants assembled by Acres to meet the objectives of the study. The objectives and scope of participation in the feasibility study by Woodward-Clyde Consultants are described in Sections 2.2 and 2.3.

The Project is located on the Susitna River, 50 miles (80 km) northeast of Talkeetna, Alaska, in the Talkeetna Mountains (Figures 1-1 and 2-1). The Devil Canyon site is located at river mile 133 (62.8° north latitude, 149.3° west longitude); the Watana site is located at river mile 165 (62.8° north latitude, 148.6° west longitude). This report encompasses the region within 62 miles (100 km) of either site. Thus, the Project site region includes the Talkeetna Mountains, the north-central portion of the Alaska Range, and portions of the Susitna and Copper River lowlands.

The Project, as presently planned, would involve two dams on the Susitna River (Figure 2-1). Plans for the downstream location--the Devil Canyon site--call for a concrete arch dam having a structural height of approximately 645 feet (197 meters) and an estimated maximum water depth of 545 feet (166 meters). The impounded reservoir would be approximately 26 miles (42 km) long and have a storage capacity of approximately 1,092,000 acre-feet ($1,348 \times 10^6$ m^3). Plans for the upstream location--the Watana site--include an earthfill or rockfill dam having a structural height of approximately 885 feet (270 meters) and an estimated maximum water depth of 725 feet (449 m). Its impounded reservoir would be approximately 48 miles (77 km) long and have a storage capacity of 9,515,000 acre-feet ($11,741 \times 10^6$ m^3) (Acres American Inc., in press). A transmission line, approximately 365 miles (588 km) long, is planned to connect the power plants at the dam sites with existing transmission lines.

2.2 - Objectives

The responsibility of Woodward-Clyde Consultants for the Project feasibility study was defined in Task 4 of the POS prepared by Acres and issued by the APA in February 1980. The objectives of the POS assigned to Woodward-Clyde Consultants were to:

a) Identify faults that have the potential for surface rupture through the Project or the potential for significant ground motions at the Project;

b) Estimate the dimensions of surface rupture and estimate the ground motions at the Project;

c) Undertake preliminary evaluations of the seismic stability of proposed earth-rockfill and concrete dams;

d) Assess the potential for reservoir-induced seismicity and seismically induced landslides in the reservoir area; and

e) Identify soils that would be susceptible to seismically induced failure along the proposed transmission line and access routes.

Task 4 of the POS is subdivided into subtasks 4.01 through 4.15. These subtasks were identified by Acres to meet the overall objectives of Task 4 of the POS. The subtasks were established to provide the geologic, seismologic, and earthquake engineering data needed to assess the feasibility of the Project. The correspondence of the subtasks identified by Acres to the objectives of Task 4 of the POS are listed in Table 2-1.

The objectives (a through e) described above are addressed by the following subtasks and sections of the report:

- Objective (a) is addressed by Subtask 4.11, and the results are presented in Section 4;

- Objective (b) is addressed by Subtasks 4.11 and 4.13, and the results are presented in Sections 4 and 8;

° Objective (c) is addressed by Subtask 4.14 as a consulting service, as described below;

° Objective (d) is addressed by Subtask 4.10, and the results are presented in Section 6; and

° Objective (e) is addressed by Subtask 4.15, and the results are presented in Section 9.

Subtasks 4.01 through 4.08, reported in the Interim Report (Woodward-Clyde Consultants, 1980b), were conducted in 1980 to provide data for a preliminary assessment of project feasibility. Subtasks 4.09 through 4.15 were conducted in 1981. This Final Report presents the results from all subtasks conducted during the two-year investigation, except Subtasks 4.09 and 4.14. Subtask 4.09 is a manual for a long-term earthquake monitoring system that is presented in a separate document. Subtask 4.14 consisted of consultation without a report requirement.

The results presented in this report were developed for the purpose of evaluating Project feasibility and should be reviewed when final dam design is considered. The results are provided in support of the license application to be submitted to the Federal Energy Regulatory Commission (FERC) by Acres on behalf of the APA.

.3 - Scope

This report is the product of a two-year investigation intended to provide data for seismic design feasibility considerations. In this report, the work conducted during the first year will be referred to by the term "1980 study"; work conducted during the second year will be referred to by the term "1981 study." The term "investigation" will be used for the two-year program.

The multidisciplinary approach used during this investigation involved interaction among a team of structural geologists, Quaternary geologists, seismologists, and earthquake engineers. Their task was the analysis of potential seismic sources, recency of fault displacement, surface rupture potential, and ground-motion parameters. The scope of work for Subtasks 4.01 through 4.08 is discussed in Section 2 of the Interim Report (Woodward-Clyde Consultants, 1980b). For subtasks 4.09 through 4.15, a scope of work was developed which included the following:

a) a detailed compilation and review of information describing the Quaternary geology of the site region; this information included aerial photography at scales of 1:24,000, 1:44,000, and 1:125,000 and LANDSAT imagery at a scale of 1:250,000;

b) acquisition and interpretation of low-sun-angle aerial photography of the area within 6 miles (10 km) of each dam site and along selected segments of the Talkeetna thrust fault and the Susitna feature;

c) geological field studies of the Quaternary geology and of 13 significant features. These studies included aerial reconnaissance, field mapping, interpretation of aerial photographs, geophysical surveys, age dating, trench excavation and logging, and review of pertinent mine data;

d) development of a plan for a long-term seismic monitoring network and preparation of a manual for use in implementing the network;

e) review and analysis of records of selected historical moderate to large earthquakes within or adjacent to the Talkeetna Terrain;

f) review and analysis of records of selected earthquakes in the Talkeetna Terrain to provide additional insights into the stress regime of the Terrain;

g) review and analysis of worldwide Benioff zone earthquakes to refine preliminary estimates of the maximum credible earthquakes (MCEs);

h) review and analysis of worldwide moderate to large earthquakes to assess the magnitude of the detection level earthquake;

i) development of a statistical model to incorporate the effect of reservoir-induced seismicity on seismic design parameters;

j) assessment of the potential for reservoir-induced seismicity;

k) estimation of maximum credible earthquakes (MCEs) for Talkeetna Terrain boundary faults and estimation for each MCE recurrence interval and rupture length;

l) evaluation of attenuation relationships for crustal and Benioff zone seismicity in Alaska and selection of appropriate relationships for establishing seismic design parameters;

m) selection of seismic design parameters using both deterministic and probabilistic approaches;

n) interpretation of aerial photography along the rights-of-way of the proposed access road and transmission line to identify potential areas of seismically induced failure, such as landslides and liquefaction; and

o) preparation of this report to summarize the results of the two-year investigation.

Completion of the scope of the two-year investigation involved approximately a 130-person-month level of effort. This included: approximately 30 person-months for the data compilation, 70 person-months for the field studies, and 30 person-months for data analysis and report preparation.

2.4 - Fault Study Rationale

2.4.1 - Conceptual Approach

The conceptual approach to studies of faults, including faults with recent displacement, was reviewed in detail in the Interim Report (Woodward-Clyde Consultants, 1980b). The following is a summary of the key aspects of the approach used to guide the overall investigation.

a) The earth's crust is comprised of a series of plates that are moving in relation to one another. Plate movement can result in collisions with resultant subduction (underthrusting of one plate beneath another).

b) When two crustal plates collide, the plate with the heavier crust is usually subducted (underthrust) beneath the other. Eventually the subducted plate falls or is thrust downward into the upper mantle and becomes detached from the overriding plate. Since plates from the oceanic crust are heavier than continental plates, the oceanic plates are generally underthrust.

c) Where subduction is occurring, the subduction process generates tectonic stress: within the downgoing plate, within the overriding crustal plate, and along the interface between the two plates where they are in contact with one another.

d) The subduction process leads to a complex pattern of deformation, faulting, and seismic activity. An understanding of the subduction process provides the seismotectonic framework within which to evaluate the significance of faults and earthquakes.

e) Tectonic stress can lead to displacement along fault planes. The resulting instantaneous release of energy (an earthquake) produces seismic waves; these waves are propagated through the earth's crust and mantle and result in ground motion that is commonly referred to as earthquake shaking.

f) Faults that are sources of earthquakes are typically subject to repeated displacements as long as the tectonic stress environment remains unchanged. Therefore, faults that show evidence of recent displacement are assumed to have the potential for future displacement.

g) Rupture of the ground surface occurs during an earthquake if the energy is released at a sufficiently shallow depth along a fault that intersects the ground surface. When the energy release occurs deeper in the crust or beneath the crust, or when the energy release is small relative to the depth of release, the fault does not rupture the ground surface.

h) The direction and rate of movement between plates has changed during geologic time, resulting in a changed tectonic stress environment. After such a change, displacement may occur on some pre-existing faults and cease on other faults. Therefore, faults that were sources of earthquakes in a previous tectonic environment, and are found to be faults without recent displacement in the current tectonic environment, are not likely to be sources of earthquakes in the current tectonic environment.

i) The frequency of earthquakes is related to the cyclic elastic strain buildup and release by fault rupture; therefore, the frequency varies greatly from one part of the earth's crust to another. The interval between earthquakes on the same fault or fault system may be longer than the period for which historical records of earthquakes are available. Therefore, the most reliable approach to evaluating the frequency of earthquakes is one which utilizes an understanding of both the geologic record and the historic seismicity record.

j) Earthquakes and the related surface rupture potential at a given location in the earth's crust or lithosphere can be evaluated by using the history of surface fault rupture (or displacement) that is expressed in the geologic record of the past. As most commonly applied, if displacement has occurred on a fault within a specified past time period, the fault is classified as having recent displacement. Faults with recent displacement (as defined for a particular project) are then inferred to have a potential for surface rupture and earthquakes. This potential is considered in the design of that project. Guidelines defining what is considered "recent displacement" for this project are described in Section 2.4.2.

k) A fault that has been subject to frequently occurring and large recent displacement appreciably affects the surface geology and topography. For these faults, the record of past earthquakes in the surface geology and topography is clearly recognizable. A fault that has been subject to relatively infrequent and small displacement may not greatly affect the landscape. The evidence of these displacements may be difficult to detect and to evaluate; however, it is improbable that all evidence of young faulting would be

completely obliterated by weathering, erosion, and deposition. Experience during the past decade or so indicates that it is very unlikely for faults with recent displacement to have no effect on the landscape. Geologists that are experienced in assessment of recent fault displacement can detect these faults (Sherard and others, 1974).

2.4.2 Guidelines for the Identification of Faults with Recent Displacement

Regulatory definitions of a fault with recent displacement, such as those discussed in the Interim Report (Woodward-Clyde Consultants, 1980b), can lead to a simplistic and possibly misleading concept of the significance of a particular fault. If a fault has been subject to displacement within a specified past period of time, whether it is 11,000 years, 35,000 years, or 100,000 years, it is important to understand how much displacement has occurred, how often it has occurred, and the sense of displacement. For example, consider a fault that has been subject to 0.2 inches (5 mm) of displacement every 75,000 years and a second fault that has been the source of 3.3 feet (1 m) of displacement every 10,000 years. Both faults can be considered to have recent displacement (if displacement within the past 100,000 years is used as the definition of a fault with recent displacement); however, the first fault is a much less important source of earthquakes than the second fault when measured in terms of the size of the displacement and the frequency of occurrence. For purposes of dam design, the effect of displacement on these two faults can be significantly different. In addition, the sense of relative displacement is also important. As discussed by Sherard and others (1974), the effect on dam design of displacements on thrust faults, normal faults, and strike-slip faults is different for each type of fault.

Dams have been designed to accommodate ground motions from relatively large earthquakes that may occur relatively close to the dam. For example, the San Pablo Dam in California is designed to accommodate the ground motions of a magnitude (M_S) 8-1/2 event on the San Andreas fault and a magnitude (M_S) 7-1/2 event on the Hayward fault, approximately 12 miles (20 km) and 10 miles (16 km) from the dam, respectively. Dams have also been designed to accommodate surface rupture. For example, the Coyote Springs Dam, built in California in 1936, was designed as an earth dam to accommodate 20 feet (6 meters) of horizontal displacement and 3.3 feet (1 meter) of vertical displacement in the foundation.

Consequently, any consideration of faults with recent displacement ultimately needs to address not only how recently fault displacement has occurred, but also how much displacement has occurred, how often it has occurred, and what the sense of displacement has been. From these data, an assessment can be made of the likelihood that the fault will have these characteristics in the future. From this assessment, the seismic source potential and potential for surface rupture for a particular fault can be considered in an appropriate manner by the designer of the dam. Explicit geologic evidence for the recency of displacement along a fault may not exist; for these faults, the available data and experience with other faults are used in the final evaluation.

The guidelines for this investigation were conservatively selected by Acres in the absence of criteria established by FERC, the review agency to whom the license application will be submitted. The guidelines were selected after available regulatory and dam-building agency guidelines were reviewed (these agency guidelines are summarized in the Interim Report [Woodward-Clyde Consultants, 1980b]) and after discussions were held with project team members. The guidelines were based on state-of-the-practice

knowledge for identifying faults with recent displacement that should be considered in dam design; further refinements of this knowledge should be incorporated into future studies and into these guidelines. The guidelines are as follows:

1) All lineaments or faults that have been identified by the geology and seismology community as having been subject to recent displacement should be included in assessing the seismic design criteria for the Project.

2) All features identified as faults that have been subject to displacement in approximately the past 100,000 years should be considered to have had recent displacement. All faults having recent displacement should be considered when assigning design criteria for ground motions or for surface displacement at the structure sites.

3) If a lineament or a suspected branch of a lineament is within 6 miles (10 km) of either site, then a detailed investigation should be made to establish whether or not the lineament or branch can be considered to have recent displacement and whether the potential exists for displacement in the dam foundation.

4) Lineaments more distant than 6 miles (10 km) from a dam site that could cause significant ground motion at the site if they were faults with recent displacement should be investigated in detail. An assessment should be made of whether or not a lineament is a fault and if it has been subject to recent displacement.

2.5 - Methodology

The purpose of this investigation was to estimate, for consideration of Project feasibility, the values of seismic design parameters for ground motion and rupture of the ground surface during earthquakes. The interrelationship of each step of our interdisciplinary program is shown in Figure 2-2.

The methodology used to identify seismic source parameters and sources of potential fault rupture through the sites included the following key items:

1) Identification of faults with recent displacement. This included studies of crustal faults and lineaments using the methods discussed in Section 4 and Appendix A.

2) Identification of seismic sources, including crustal faults with recent displacement and Benioff zone sources. This included studies of historical earthquakes using methods discussed in Section 5 and the studies of faults with recent displacement discussed in item (1) above.

3) Evaluation of and selection of a detection level earthquake, which represents an earthquake whose source (a fault with recent displacement) would not be detected at the surface. The detailed methology for this work is discussed in Section 4.2.

4) Estimation of maximum credible earthquakes for each of the seismic sources. The methodology for this work is discussed in Section 7.

5) Development of attenuation relationships for the seismic sources using methodologies described in Section 8.

6) Estimation of ground-motion parameters for the seismic sources. A deterministic approach has been used; that is, the maximum earthquakes is assumed to occur during the lifetime of the Project at the closest approach of the seismic source to the Project.

TABLE 2-1

PROJECT SUBTASKS AND OBJECTIVES

Subtask Number and Description	Objective
4.01 - Review of Available Data	Acquire, compile, and review existing data, and identify the earthquake setting of the Susitna River area.
4.02 - Short-term Seismologic Monitoring Program	Establish initial monitoring system, obtain and analyze basic seismologic data on potential earthquake sources within the Susitna River area and supply information required to implement a more thorough long-term monitoring program (Subtask 4.09).
4.03 - Preliminary Reservoir-Induced Seismicity	Evaluate the potential for the possible future occurrence of reservoir-induced seismicity (RIS) in the Susitna Project area.
4.04 - Remote Sensing Image Analysis	Select and interpret available remote sensing imagery to identify topographic features that may be associated with active faulting.
4.05 - Seismic Geology Reconnaissance	Perform a reconnaissance investigation of known faults in the Susitna River area, and of lineaments that may be faults, identify active faults, and establish priorities for more detailed field investigations.
4.06 - Evaluation and Reporting	Complete a preliminary evaluation of the seismic environment of the project, define the earthquake source parameters required for earthquake engineering input in design, and document the studies in reports suitable for use in design studies.
4.07 - Preliminary Ground-Motion Studies	Undertake a preliminary estimate of the ground motions (ground shaking) to which proposed project facilities may be subjected during earthquakes.
4.08 - Preliminary Analysis of Dam Stability	Provide input for preliminary evaluations of the seismic stability of proposed earthfill, rockfill, and/or concrete dams during maximum credible earthquakes.
4.09 - Long-term Seismologic Monitoring Program	Develop a long-term seismologic monitoring program to provide a continuing source of seismological data for refinement of the seismic design aspects of the project during the detailed design phase.
4.10 - Reservoir-Induced Seismicity	Refine the estimate for the potential for reservoir-induced seismicity made in Subtask 4.03.
4.11 - Seismic Geology Field Studies	Perform seismic geology field studies to identify faults that may be active and in the vicinity of the selected dam sites.
4.12 - Evaluation and Reporting	Refine the evaluation of the seismic environment and the earthquake source parameters derived in Subtask 4.06, complete the reporting of all the fieldwork and studies undertaken in Subtasks 4.01, 4.05, and 4.09 to 4.11, and provide coordination and management to Subtasks 4.09 to 4.11.
4.13 - Ground-Motion Studies	Refine the estimate of ground-motion characteristics made in Subtask 4.07.
4.14 - Dam Stability Consulting Services	To provide consulting assistance to the Acres design group engaged in the feasibility design of the dams.
4.15 - Soil Susceptibility to Seismically-Induced Failure	Provide input on behavior of those areas along the transmission line and major access road routes that appear to be underlain by soils particularly susceptible to seismically-induced ground failure such as liquefaction or landsliding.

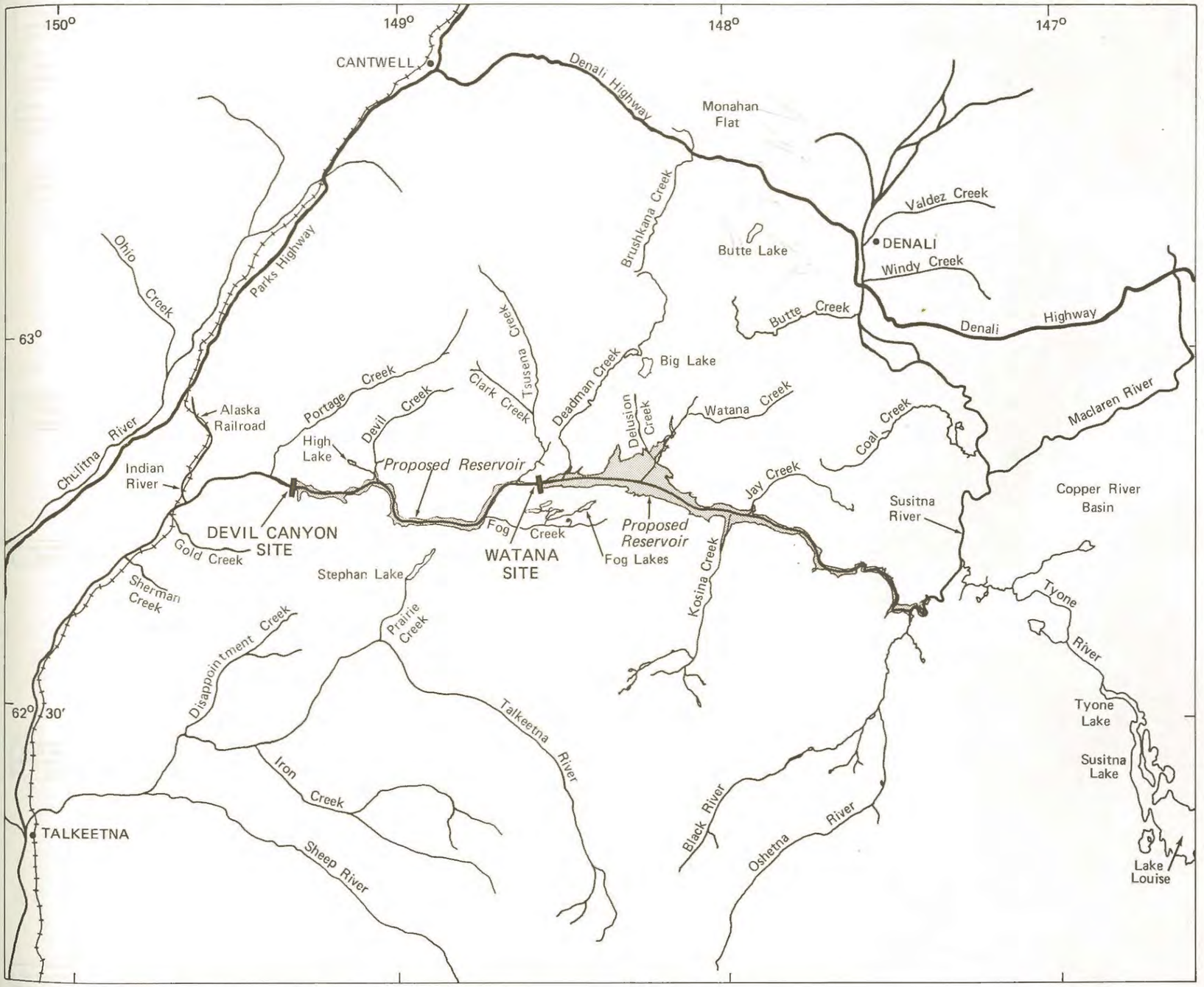

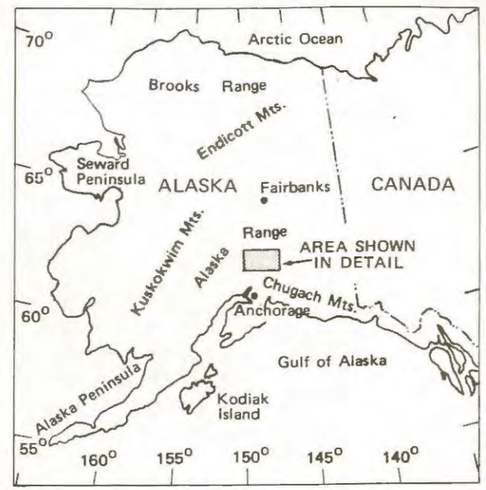

NOTE

1. Proposed reservoir configuration is after Acres American Inc. (In Press).

N

PROJECT LOCATION MAP

0 5 10 15 20 Miles

0 10 20 30 Kilometers

WOODWARD-CLYDE CONSULTANTS 41410A February 1982

FIGURE 2-1

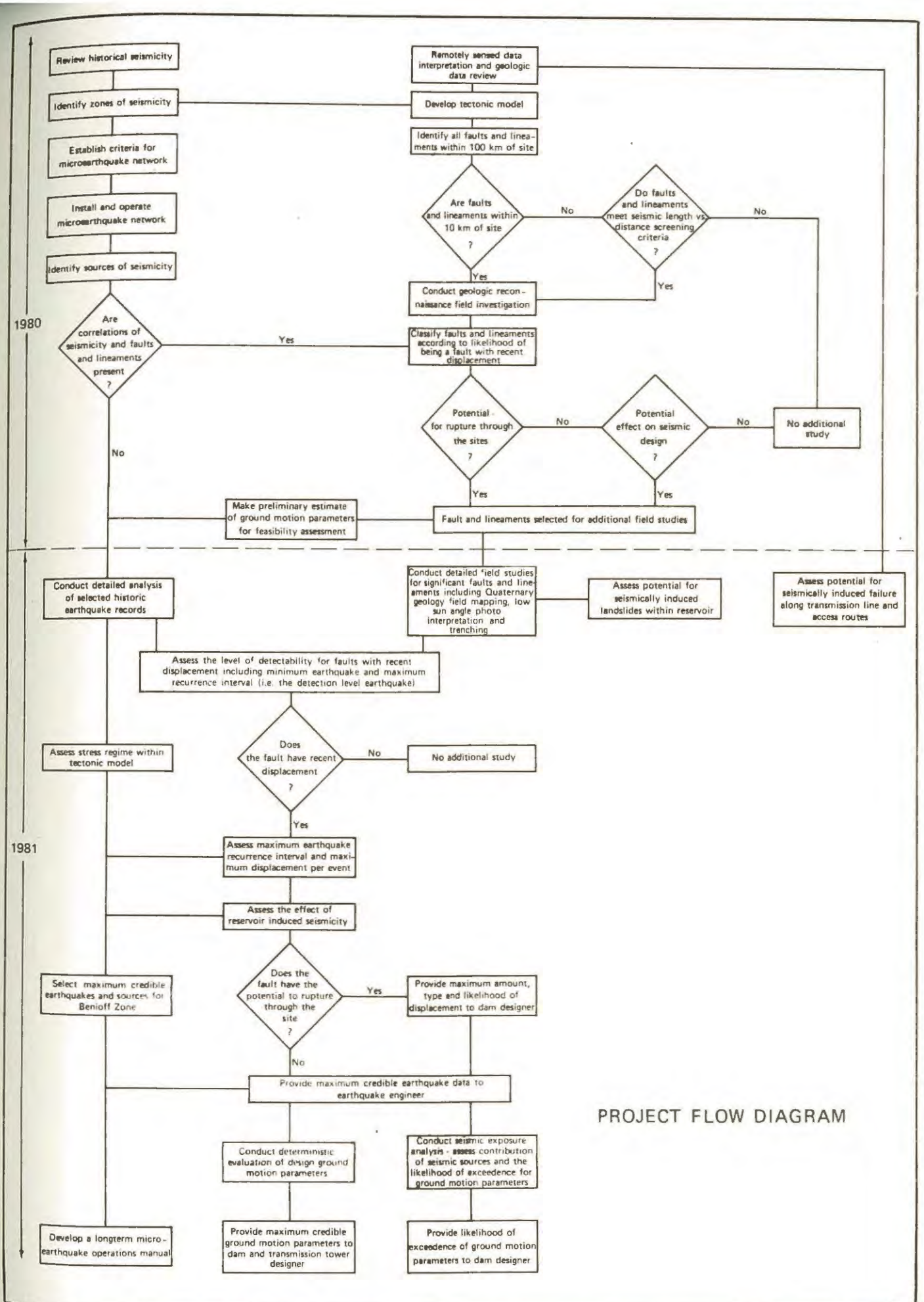

PROJECT FLOW DIAGRAM

FIGURE 2-2

3 - QUATERNARY GEOLOGY

3.1 - Introduction

Quaternary geology involves the study of geological processes in recent geologic time (i.e., the past 1.8 million years). In the site region these processes are primarily of glacial origin. As shown in Figure 3-1, the Quaternary Period includes the Holocene and Pleistocene epochs.

An understanding of the extent and age of Quaternary sediments and surfaces (collectively referred to here as surfaces) is important to seismic geology studies. This importance is related to the assessment of recency of displacement along a fault. If activity on a fault has produced surface displacement in recent geologic time, the young (Quaternary) surfaces would likely include evidence of deformation. When the age of the deformed surfaces is known, then the recency of the fault displacement and the number of displacements can be assessed.

Conversely, if a fault has not produced surface displacement in recent geologic time, then the overlying young (Quaternary) surfaces would not be deformed. When the age of the overlying surfaces is known, then the length of time during which there has been no displacement can be assessed.

Within the site region, the late Quaternary surfaces are of greatest interest to the seismic geology study. These surfaces include those of Holocene and Pleistocene age (including the Wisconsinian and Illinoian stages). This interest is due in large part to their extent and age. These surfaces are present throughout the site region, and their age ranges from a few years to approximately 120,000 years before present (y.b.p.) (Figure 3-1). One of the project objectives was to identify

faults with recent displacement. A fault with recent displacement was defined for this Project as a fault that has had surface rupture during the past 100,000 years (Section 2.4.2). Therefore, the ability to assess the presence or absence of fault displacement in the late Quaternary surfaces is pivotal to the identification of faults with recent displacement.

The approach to Quaternary geology studies used during this investigation was to develop an understanding of 1) the Pleistocene glacial geology of southern Alaska, and 2) the late Pleistocene (Wisconsinian and Illinoian) glacial geology within a region (designated as the Quaternary study region) encompassing the project sites and major segments of the 13 features identified in the Interim Report (Woodward-Clyde Consultants, 1980b). Figures 3-2 and A-1 show the Quaternary study region.

In 1980 the Quaternary geology study involved a preliminary literature review, limited aerial photography and imagery interpretation, and aerial reconnaissance of selected areas. The results of this work are summarized in Sections 6 and 7 of the Interim Report (Woodward-Clyde Consultants, 1980b). During 1981, the second year of the investigation, the Quaternary geology study involved:

a) a complete review of pertinent literature;

b) detailed interpretation of large- and small-scale aerial photography;

c) preparation of a preliminary map based on (a) and (b), prior to the field season, showing the extent and estimated age of late Quaternary surfaces;

d) field programs, including field mapping of key areas, excavation of test pits, and collection of relative age (weathering) data, and collection of material for radiocarbon age dating;

e) radiocarbon age dating of 11 samples; and

f) data synthesis and revision of the preliminary map of late Quaternary surfaces, listed in (c) above; this revised map is shown in Figure 3-2.

This section of the report presents a summary of the results of these Quaternary studies. The details of the work, including the methodology used, are presented in Appendix A. Two components of the methodology are particularly important to understanding how age determinations and correlations were made in the Quaternary study region. These are the relative age (weathering) dating technique and the correlation technique used to correlate glaciogenic features according to their relative elevation and age.

The relative age (weathering) dating technique involved the use of procedures and relationships similar to those used by Ten Brink in the Alaska Range (Ten Brink and Waythomas, in press; Werner, in press) (Appendix A.1.3.2). The technique is referred to hereafter as the relative age dating technique. It involves the measuring of weathering characteristics (such as the proportion or ratio of fresh, partially weathered, and weathered granitic boulders, or the depth of oxidation) of moraines. Differences in these characteristics, combined with radiocarbon age dates, moraine elevation, and moraine morphology were used to distinguish between the different aged surfaces (e.g., Early and Late Wisconsin surfaces) in the Quaternary study region. In addition, the relative age dating results from this study were compared with the radiometrically dated scale of Ten Brink and Waythomas (in press) developed in the Alaska Range (Table A-1).

The correlation of maximum elevations among glaciogenic features with similar morphologic characteristics was used to assess the vertical and horizontal extent of the glaciations in the Quaternary study region. (Similar morphologic characteristics are suggestive of similar age, as discussed in Appendix A.1.3.2.) To make these correlations, radiocarbon and relative age dating of glaciogenic features was conducted in key areas (such as those described in Section 3.4 below) to establish the maximum elevation of a glacier in those areas during specific glaciations. Subsequent identification of glaciogenic features with similar characteristics in other portions of the study area were used to correlate the glacial maximum throughout the Quaternary study region for each given glacial period. In this manner, the maximum elevation of ice for the various glaciations was estimated and the extent of these glaciations was assessed for the Quaternary study region (Figure 3-2).

Using the above two components of the methodology, as well as the others discussed in Appendix A.1.3, the late Quaternary geology for the Quaternary study region was accomplished.

The following discussion in this section: a) briefly reviews the regional late Quaternary setting of southern Alaska; b) summarizes the age and extent of Quaternary surfaces that were encountered in the Quaternary study region; c) briefly discusses the key areas for which Quaternary geologic relationships were used to develop the Quaternary geology map (Figure 3-2); d) summarizes the glacial geology of the Quaternary study region; and e) summarizes the relationship of Quaternary surfaces to the 13 features selected for field work during the 1981 field study (Section 4.4).

3.2 - Regional Pleistocene Geology Setting

Previous investigations of the Quaternary geology of south central Alaska have been either generalized regional studies or detailed studies

of specific areas of limited extent. Representative regional studies include those of Karlstrom and others (1964), Coulter and others (1965), Pewé and others (1965), and Pewé (1975).

Among the numerous detailed studies that have been conducted in areas near the Talkeetna Mountains are those by: Miller and Dobrovolny (1959), Karlstrom (1964), Trainer and Waller (1965), Schmoll and others (1972), for the Cook Inlet area; Wahrhaftig, (1958), Thorson and Hamilton (1977), Ten Brink and Waythomas (in press), for the central Alaska Range; and Chapin (1918) and Ferrians and Schmoll (1957), for the Copper River Basin.

Little information was available prior to this investigation regarding the Quaternary surfaces and history of the Talkeetna Mountains, although a limited amount of data pertinent to Quaternary surfaces in the Talkeetna Mountains has been presented by Bowers (1979) and by Terrestrial Environmental Specialists (1981).

The regional and detailed studies cited above provide information regarding the Quaternary geologic history of southcentral Alaska. These studies suggest that the Talkeetna Mountain region existed as an extensive mountainous to rolling upland at the beginning of the Quaternary Epoch, approximately 1.8 m.y.b.p. Subsequent to that time a series of climatic fluctuations, with conditions ranging from temperate to polar, apparently began to affect the region. The fluctuating climate, which characterized the region throughout the Quaternary Epoch, lead to several periods of extensive glaciation during polar conditions. At its Quaternary maximum, glacier ice formed an ice cap over the Talkeetna Mountains. These periods of glaciation were separated by interglacial periods with relatively temperate climatic conditions generally similar to those now found in the region.

The general regional picture of alternating glacial and interglacial periods along with specific evidence within the Talkeetna Mountains suggests that, following the Quaternary glacial maximum for the region, subsequent glacial advances were not extensive enough to produce an ice cap over the mountains. In fact, the available evidence indicates a series of glaciations of sequentially decreasing extent. It was these more recent glaciations that produced the glacial, glaciofluvial, and glaciolacustrine landforms and sediments that now dominate the Talkeetna Terrain. There is relatively little evidence, however, on which to base an interpretation of interglacial conditions.

Although glaciers covered only about 50 percent of the present area of Alaska during the Quaternary Epoch, south central Alaska, south of the crest of the Alaska Range, was nearly completely glaciated (Pewé, 1975).

Among the more recent glaciations that occurred in the Talkeetna Mountains, four were recognized during this investigation in the Quaternary study region (Figure 3-2). The glaciations and their respective ages are: pre-Wisconsin, >100,000 y.b.p.; Early Wisconsin, 75,000 to 40,000 y.b.p.; Late Wisconsin, 25,000 to 9,000 y.b.p., which included four stades, each of which was less extensive than the preceding one; and Holocene, <9,000 y.b.p. Figure 3-2 shows the surfaces of the pre-Wisconsin stage, the Early Wisconsin stage, and the first and last stade (Stades I and IV) of the Late Wisconsin stage. These are shown because of their extent in the Quaternary study region. Holocene surfaces are not shown in this figure because of their limited extent and their distance from the 13 features being studied for recency of fault displacement.

The ages for the four glaciations were assigned on the basis of radiocarbon age dates obtained for this study and generally accepted age assignments for similar glacial sequences elsewhere in Alaska (Hopkins, 1967; Flint, 1971; Pewé, 1975; Weber and others, 1980; Ten Brink and Waythomas, in press).

During the four glaciations, ice advanced from three source areas: the Alaska Range to the north of the Quaternary study region; the southern and southeastern Talkeetna Mountains; and the Talkeetna Mountains north and northwest of the Susitna River. In the Quaternary study region, the glaciers from these sources coalesced to form a piedmont glacier that flowed through the intermountain basin (shown in Figure A-1) that includes the Susitna River (near the Watana site), Watana Creek, and Stephan Lake areas. Glacial flow was dominantly to the south and southwest and left a variety of landforms, surfaces, and sediments.

The following sections summarize the results of our investigation of these landforms and sediments. They are intended to document the basis for the application of the results to the assessment of the recency of fault displacement on features near the sites.

3.3 - Age and Extent of Quaternary Surfaces in the Quaternary Study Region

The 1981 Quaternary geology study led to the identification of ten types of Quaternary glaciogenic features that were used in part to interpret the age and extent of Quaternary surfaces in the Quaternary study region. These features include: till, lacustrine deposits, outwash deposits, ice disintegration deposits, kame terrace deposits, fluvial deposits, fluting, trimlines, side glacial channels, and an assortment of glacially sculptured bedrock forms including whalebacks, stoss and lee, and grooves. The characteristics used to distinguish these glaciogenic features are summarized in Table 3-1.

The morphologic characteristics of the Quaternary glaciogenic features along with their elevation, radiocarbon age dates obtained from carbonaceous material, and relative age characteristics were used to develop an understanding of the age and extent of late Quaternary

surfaces in the Quaternary study region. The results of this interpretation are shown in Figures 3-2 and 3-3. The relationship of these surfaces to the 13 features (whose seismic source potential was studied in 1981) is summarized in Figure 3-4.

The age and extent of late Quaternary surfaces in the Quaternary study region, as summarized in Figure 3-2, are interpreted to be as follows:

a) Pre-Wisconsin surfaces are preserved at higher elevations than are Wisconsinian surfaces. Elevations range from above 4,200 feet (1,280 m) in the northern section of the Quaternary study region to 3,100 feet (945 m) in the southern portion of the region.

b) Early Wisconsin surfaces typically are preserved along the margins of topographically elevated areas (such as those on either side of Butte Lake [Figure 3-6A] and the broad upland south of the Susitna River between Kosina Creek and Oshetna River [Figure 3-2]).

c) Surfaces associated with early stades of Late Wisconsin glaciation are present on the basin and valley floors and mid to low valley walls of the Quaternary study region within the Talkeetna Mountains (Figure 3-2). The Portage Creek, Deadman Creek, and Watana Creek valleys and the Stephan Lake-Fog Lakes area are typical of the areas with Late Wisconsin glacial surfaces.

d) Surfaces associated with the last stade of Late Wisconsin glaciation (i.e., those resulting from the last advance of glacial ice in Wisconsinian time) are found in valleys leading down from the high elevations in the Talkeetna Mountains and in the basin floor areas at the mouths of some of these valleys. In addition, the Monahan Flat area (which lies between the Alaska Range and the north end of the Quaternary study region) and the Butte Creek

area have extensive surfaces from the last stade of the Late Wisconsin stage (Figure 3-2). These last stade deposits are the result of mountain glaciers which emanated from the high elevations of the Talkeetna Mountains (in the northwest corner and the southern portion of the Quaternary study region) and from glacial ice that moved southward from the Alaska Range across Monahan Flat and locally into the lower elevations of the Butte Creek area.

3.4 - Key Quaternary Study Areas

Four key areas within the Quaternary study region were studied in detail to provide a basis for interpreting the age and extent of Quaternary surfaces. These four areas have been designated as the Black River area, the Clear Valley area, the Butte Lake area, and the Deadman Creek area. The location of these areas is shown in Figure 3-2. Figures 3-5 and 3-6 show the results of the studies conducted in these areas and include the morphostratigraphic units that are present, the age of these units, the location of test pits, and radiocarbon sample locations.

In order to develop the Quaternary geology map shown in Figure 3-2 and the cross-section shown in Figure 3-3, the results of the studies in these four key areas were used along with: additional radiocarbon age dates from the Quaternary study region (the locations of the dated material are shown in Figure 3-2, and the ages are summarized in Table 3-2); the interpretation of aerial photos; and aerial reconnaissance and ground reconnaissance mapping. The following discussion summarizes the key data that were obtained from these four areas.

3.4.1 - The Black River Area

The Black River area is located south of the Susitna River near the Copper River basin in the southeastern part of the Quaternary study region, as shown in Figures 3-2 and 3-5A. The area is part of a broad undulating plain in the eastern Talkeetna Mountains that merges with the adjacent Copper River basin, as discussed in Section A.1.4.6. Three morphologically distinct, glacially scoured topographic surfaces of pre-Wisconsin, Early Wisconsin, and Late Wisconsin age have been beveled into this plain by succeeding less extensive glaciations. Two of these surfaces, those of the Early and Late Wisconsin stages, were observed in the Black River area. In addition, the last stade of the Late Wisconsin stage is represented by glacial sediments, as shown in Figures 3-2 and 3-5A.

Studies were conducted of the Late Wisconsin surfaces to assess the extent of glacial ice in the eastern Talkeetna Mountains and the adjacent Copper River basin during Early and Late Wisconsin time. At the junction of the Susitna and Oshetna Rivers, north of the Black River area (Figure 3-2), till was observed to interfinger with highly deformed lacustrine and deltaic deposits. A sample (S47-4) of wood obtained from the lacustrine sediments gave a radiocarbon age date of >37,000 y.b.p. (Table 3-3). These relationships strongly suggest that the till and lacustrine deposits are of Early Wisconsin age. Stratigraphic evidence suggests that Late Wisconsin ice did not advance into the lower reaches of the Black and Oshetna Rivers nor into the Susitna River in the eastern Talkeetna Mountains (Figure 3-5A).

Mapping, based on aerial photo interpretation, of the extent of moraines and relative age dating results corroborate the limited extent of Late Wisconsin ice in this area. As shown in Table 3-3

and Figures 3-2 and 3-5A, moraines BR-1, BR-2, and BR-3 (Late Wisconsin age) and deposits of similar age are interpreted to terminate 6 to 7 miles (10 to 11 km) south of the Susitna River.

From these data, Early Wisconsin glacial ice is inferred to have moved northward into the Black River area from southerly sources in the high elevations of the Talkeetna Mountains. This ice is believed to have coalesced with ice moving from the Copper River basin westward along the Susitna River valley. Late Wisconsin glacial ice is inferred to have moved northward, down the Black River area, from southerly sources at high elevations in the Talkeetna Mountains. The glaciers were of limited extent, and ice did not move out of the Black River area.

3.4.2 - The Clear Valley Area

The Clear Valley area lies approximately 7 miles (11 km) south of the Watana site (Figure 3-2). It is a glaciated valley that opens into the lowland area associated with Fog Lakes and Stephan Lake, as discussed in Section A.1.4.1. Twelve closely nested moraines, glacial trimlines, and ice marginal channels have been used to develop the glacial chronology in this area, as shown in Figures 3-2 and 3-5B.

Pre-Wisconsin periglacial effects are present above elevation 3,100 feet (945 m). These effects are primarily those of well developed frost-shattered boulder fields.

Studies of the 12 nested moraines were conducted to distinguish the extent and elevation of Early and Late Wisconsin glacial ice in proximity to the Watana site. Moraine morphology, relative age dating, and cross-cutting relationships were interpreted to show a distinct difference in age between the lower seven moraines

(CL-1 through CL-7 in Figure 3-6B) and the upper five moraines (CL-8 through CL-12) (Table A-1). In addition, the distal end of moraines CL-6 and CL-7 bend southwestward and lose their topographic identity in the area of ground moraines at elevation 2,500 to 2,700 feet (762 to 823 m). This deflection and loss of topographic expression suggests that Late Wisconsin ice from the Clear Valley area merged with a southwestward flowing piedmont ice sheet that flowed through the intermountain basin that is delineated in Figure A-1. It further suggests that the 2,500 to 2,700 feet (762 to 823 m) elevation represents the upper limit of Late Wisconsin ice in the basin.

The last stade (Stade IV) of Late Wisconsin ice is prominently represented in the Clear Valley area by ice disintegration features including eskers, kame deltas, and kettles. The relationship of these features to the earlier Late Wisconsin moraines suggests that glacial ice moved northward from the high areas south of the Clear Valley area. The advance, however, did not extend into the basin floor area at the mouth of Clear Valley and adjacent valleys.

A small Holocene lake was dammed by a till and bedrock ridge in the basin floor area north of the Clear Valley area (Figure 3-5B) probably beginning in the waning stages of the Late Wisconsin time and continuing into Holocene time. A radiocarbon age date of approximately 3,500 years before present was obtained from the lacustrine deposits (Sample S4-1).

The glacial chronology in the Clear Valley area (along with the results of studies conducted in the Stephen Lake and Fog Lakes areas) shows that the age of surfaces overlying the Talkeetna Thrust fault and Susitna feature south of the Susitna River are predominantly of Late Wisconsin age (Figure 3-4). This chronology

provided the basis for interpreting the age of the higher surfaces along the southwestern section of the Talkeetna thrust fault to be Early Wisconsin and pre-Wisconsin in age (Figure 3-4).

3.4.3 - The Butte Lake Area

This area lies at the north end of the Talkeetna Mountains and is separated from the Alaska Range to the north by a broad lowland called Monahan Flat (Figures 3-2 and A-1). The area includes a northeast-southwest trending linear valley, containing Butte Lake, that opens into the Monahan Flat lowland (as discussed in Section A.1.4.5). Within the broad, U-shaped valley, drainage patterns and directions have been altered by glacial erosion and deposition. The valley bottom is predominantly mantled by till while the upper valley walls are mantled by frost-shattered boulder fields.

Late Wisconsin glaciation resulted in glacial ice moving through the Butte Lake valley up to a maximum elevation of 3,900 feet (1,189 m). The elevations of Late Wisconsin end moraines suggest that as many as nine individual moraines may be present. The clustering of these moraines, the breaks in slope, and the surface morphologic contrasts led to the identification of four Late Wisconsin stades (ice pulses of glacial advance within the Late Wisconsin glacial stage). These stades appear to be similar in age and duration with those observed by Ten Brink and Waythomas (in press) in the Alaska Range.

The maximum elevation of these four stades are: Stade I is 3,900 feet (1,189 m); Stade II is 3,600 to 3,800 feet (1,098 to 1,159 m); Stade III is 3,200 to 3,300 feet (976 to 1,006 m); and Stade IV is 3,000 to 3,100 feet (915 to 945 m). Stades I and IV are shown in Figures 3-2 and 3-6A; Stades II and III are not delineated because of the limited control on their extent.

The Late Wisconsin ice in the Butte Lake valley is of pre-last stade, i.e., older than 11,000 years before present. The Stade IV glacial ice from the Alaska Range was of insufficient thickness to move into the Butte Lake valley from Monahan Flat, and the glaciers from the area to the west did not move into the valley.

These studies show that the age of the surfaces overlying the Susitna feature in the northern Talkeetna Mountains is Late Wisconsin in age.

3.4.4 - The Deadman Creek Area

This area lies north-northeast of the Watana site as shown in Figure 3-2. Deadman Creek flows southwestward in the intermountain basin at the base of the northwest section of the Talkeetna Mountains, as discussed in Section A.1.4.4. This part of the basin floor is almost entirely mantled by hummocky ice disintegration deposits and lacustrine plains (Figure 3-6B). Intervening areas are ground moraine or beveled bedrock outcrops.

Frost-shattered boulder fields above 4,100 feet (1,250 m) suggest a maximum elevation for Wisconsinian glaciations. The maximum elevation for Early Wisconsin moraines is 4,100 feet (1,250 m). The age of these moraines is based on relative age dating results (Tables 3-3 and A-1) as well as on their elevation. These deposits are interpreted to be the product of coalescing valley glaciers which merged with glacial ice emanating from the Alaska Range to produce a piedmont glacier in the intermountain basin.

Late Wisconsin glaciation resulted in a sequence of closely spaced end moraines along the base of the mountains to the west of Deadman Creek (Figure 3-6B). In early Late Wisconsin time, the glacial ice responsible for these deposits was probably a piedmont

glacier similar in nature to that of Early Wisconsin glaciers. During later stades of the Late Wisconsin stage, local valley glaciers moved from the high region in the northwestern part of the Talkeetna Mountains down into the Deadman Creek area and flowed to the northeast. The evidence for this is the northward slopes on moraines DC-1 and DC-2 (Figure 3-6B) and an arcuate moraine damming Big Lake (immediately east of the Deadman Creek area) that is concave southward.

During the last stade of the Late Wisconsin stage, a valley glacier moved out of Tsuena Creek (Figure 3-2) and into the southwestern portion of the Deadman Creek area. Subsequent stagnation of the ice produced hummocky ice disintegration deposits which locally dammed a lake, represented by the lacustrine deposits shown in Figure 3-6B. Radiocarbon age dating of a sample (S45-1) from these lake deposits gives an age of 3,450 ±170 y.b.p. (Table 3-2). This age date tends to confirm relative youthfulness of the lake and the existence of the dam until late Holocene time.

The glacial chronology of this area, as well as of the Butte Lake area, shows that the age of the surfaces overlying the Susitna feature north of the Susitna River are Late Wisconsin in age (Figure 3-4). In addition, the chronology of this area and the Clear Valley area, along with radiocarbon age dates and morphologic characteristics in the Watana Creek area, show that the surfaces overlying the Talkeetna thrust fault are also predominantly Late Wisconsin in age (Figure 3-4).

3.5 - Glacial History and Distribution of Quaternary Surfaces

The data obtained from the key areas described above, along with observations in the intervening sections of the Quaternary study region,

and radiocarbon age dates (shown in Table 3-2 and Figure 3-2) were used to develop an understanding of the glacial history and the distribution of the resulting late Quaternary glacial surfaces. The following discussion summarizes this understanding.

Evidence was found for four distinct Quaternary glacial episodes: pre-Wisconsin, >100,000 y.b.p.; Early Wisconsin, 75,000 to 40,000 y.b.p.; Late Wisconsin, 25,000 to 9,000 y.b.p.; and Holocene, <9,000 y.b.p. Each glacial episode was less extensive than the preceding one. The limits of each are defined by the elevation and geographic distribution of glacial erosional or depositional features. Glaciers advanced repeatedly from three main source areas: the Alaska Range to the north; the southern and southeastern Talkeetna Mountains; and the Talkeetna Mountains north and northwest of the Susitna River. Glacial flow was dominantly to the south and southwest, following the regional slope and structural grain. Multi-directional and convergent flow, differing glacial magnitudes, topographic influences, and other parameters make the interpretation of the glacial chronology of the Quaternary study region difficult.

Pre-Wisconsin glaciated surfaces are present at elevations above the suggested upper limit of Early Wisconsin glaciation. Bedrock scour and ice-sculptured forms (such as stoss and lee, and whalebacks) dominate the topography. The geographic extent and elevation of these surfaces suggest that ice cap conditions probably existed throughout the Talkeetna Mountains. Broad areas of the plateau south of Devil Canyon were overridden by glacial ice. Periglacial processes during later glaciations produced extensive veneers of colluvium and frost-shattered boulder fields.

A tentative age was assigned to the glaciated surfaces above the limit of the Early Wisconsin glaciation on the basis of elevation and degree of weathering. The data collected within the Quaternary study region

show only that these surfaces are older than the Early Wisconsin stage and the prior interglacial stage (120,000 to 75,000 y.b.p.), although the surfaces are probably Illinoian in age (>120,000 y.b.p.). Worldwide studies of the Illinoian glacial stage show that its youngest age is variable (Flint, 1971). However, it is generally accepted to be >120,000 y.b.p. For purposes of this study we have accepted an age of >100,000 y.b.p. to be appropriate.

Early Wisconsin glaciation was less extensive than glaciation during the preceding glacial period, and ice was present in existing valleys at lower elevations than the pre-Wisconsin ice was. Regional evidence for the maximum upper extent is limited. Prominent ice-marginal features, particularly trimlines and weathering contrasts, indicate the upper limit to be: 3,750 feet (1,143 m) in the Black River area; 3,100 feet (945 m) in the Clear Valley area; 4,200 feet (1,280 m) in the Butte Lake area; 4,100 feet (1,250 m) in the Deadman Creek area; and 3,100 feet (945 m) in the Devils Canyon area.

Glaciers from the Alaska Range and Talkeetna Mountain ice sources, described above, coalesced to form a piedmont glacier in the intermountain basin of the Susitna River (near the Watana site), Fog Lakes, and Stephan Lake; but large areas of the upland plateaus were ice-free. Successive Early Wisconsin moraines in the Clear Valley area indicate that several stades or recessional stillstands took place in Early Wisconsin time. Ice flow that emanated from the Alaska Range passed southwestward to the Talkeetna River and westward and southwestward through Devils Canyon to merge with glaciers in the Chulitna Valley.

The Late Wisconsin glaciation was composed of four distinct glacial stades. The maximum limit of Late Wisconsin ice was 2,700 feet (823 m) in the Clear Valley area; 3,900 feet (1,189 m) in the Butte Lake area; and 3,900 feet (1,189 m) in the Deadman Creek area.

The ice during each stade was less extensive than that during the preceding one. Glaciers in the first stade of Late Wisconsin time had a geographic extent similar to prior glaciations. During later stades of the Late Wisconsin stage, ice from the Alaska Range was not thick enough to advance into valley passes in Brushkana and Deadman Creeks, but it was thick enough to flow southward through the pass between Butte Creek and Watana Creek. Valley glaciers in Tsusena Creek and adjacent valley glaciers advanced into ice-free areas of the intermountain basin.

During Stades III and IV, individual valley glaciers were generally confined to valleys and the piedmont glacier had retreated north of the Susitna River. Ice from the Alaska Range continued to retreat northward up Watana Creek and supplied abundant sediment for a lacustrine environment in lower Watana Creek. Rapid regional deglaciation produced extensive hummocky ice disintegration deposits in topographic low areas. Widespread glaciation came to an end approximately 9,000 y.b.p. The Susitna and Talkeetna Rivers served as outlet channels for meltwater from the retreating glaciers, producing extensive terraced outwash gravels in the lower reaches of the rivers.

Glaciation of Holocene age is limited to cirque glaciers in the upper reaches of valleys and to the formation of glaciolacustrine lakes in lowland areas. The small cirque glaciers formed moraines within a few miles of the cirques. Rock glaciers in the upper reaches of mountain valleys are the most visible remnant of the Holocene glaciation. Glaciolacustrine lakes, such as those that formed in the Clear Valley and Deadman Creek areas (Figures 3-5B and 3-6B) were dammed by glacial units deposited by the Late Wisconsin Stade IV glacial ice. These lakes have breached their dams and are now represented by plains of lacustrine deposits.

3.6 - Quaternary Geology and Significant Features

Four features (faults and lineaments) were studied near the Watana site during this investigation to assess their significance to seismic design, as discussed in Section 4.4.1. The late Quaternary surfaces that overlie these four features are predominantly Late Wisconsin (25,000 to 9,000 y.b.p.) in age, except in the vicinity of the Talkeetna River where pre-Wisconsin (>100,000 y.b.p.) surfaces are present (Figure 3-4). For example, the Talkeetna Thrust fault from Denali to the Talkeetna River is overlain by surfaces of Late Wisconsin age along 85 percent of its length. The remaining 15 percent is Early Wisconsin and pre-Wisconsin in age, as shown in Figure 3-4.

Nine features were studied near the Devil Canyon site, as discussed in Section 4.4.2. The Quaternary surfaces that overlie these nine features are generally older than those encountered in the vicinity of the Watana site. These surfaces are of Early Wisconsin age or older (>40,000 y.b.p.), except in the vicinity of the Susitna River and its tributaries where Late Wisconsin surfaces (25,000 to 9,000 y.b.p.) are present (Figure 3-4).

The age of the Quaternary surfaces, the size of morphologic features that have been preserved on each of these surfaces, and the extent of the surfaces were evaluated and incorporated in the analysis of recent fault displacement (as discussed in Section 4.2) for the four features near the Watana site and the nine features near the Devil Canyon site. The Quaternary field study and the subsequent data analysis showed no evidence of displacement in the Quaternary surfaces overlying the the 13 features (as discussed in Section 4.4).

The evaluation of Quaternary surfaces also focused on the resolution provided by these surfaces. This resolution was used to analyze the maximum earthquake (designated the detection level earthquake) and

resultant fault displacement that could occur in the site region and still maintain the Quaternary surfaces in their observed undeformed state. This analysis of the detection level earthquake is discussed in Section 4.2.

TABLE 3-1

SUMMARY OF QUATERNARY GLACIOGENIC FEATURE CHARACTERISTICS

GLACIOGENIC FEATURE	MORPHOLOGIC CHARACTERISTICS		RELATIVE AGE CHARACTERISTICS	
Description	Photo Signature and Aerial Characteristics	Ground Characteristics	Photo Signature and Aerial Characteristics	Ground Characteristics
A. Depositional				
Till (Ground, end, and lateral moraines) nonstratified sand and cobbles within a silt and clay matrix greater than 10 ft (3 m) thick, concentrations in elongated narrow ridges called end moraines	1. Broad undulating plains, generally confined to U-shaped valleys 2. Forms blanket deposits 3. Fluting common 4. Elongated, narrow ridges built along margins of glaciers, commonly paired	1. Unsorted gravel and sand in matrix of silt and clay, unconsolidated, nonstratified	1. Geographic (spatial) position in relation to other glacial deposits 2. Topographic (elevational) relationship to adjacent deposits 3. Elevation of end moraines 4. Degree of dissection and surface modification 5. Orientation and cross cutting relationships of end moraines	1. Various quantitative soil parameters and morphologic measurements. See relative age (weathering) data Appendix A.1.2.2 and Tables 3-3 and A-1
Lacustrine Deposits Rhythmically bedded silt and/or clay with occasional ice rafted rock fragments; forms broad, flat plains	1. Nearly flat featureless plains commonly in topographic lows 2. Slumping common along margins of dissected areas 3. No fluting 4. Drainage pattern commonly contrasts with patterns on adjacent surfaces 5. Uniform vegetation type and density	1. Rhythmically bedded silt and/or clay with occasional ice rafted sand, pebbles, and gravel 2. Forms vertical cliff faces, but slumping is common 3. Grain size variations preclude loess origin 4. Sorting and stratification are common in areas of deltaic sedimentation	1. Geographic (spatial) position in relation to other glacial deposits 2. Topographic (elevational) relationship to adjacent deposits 3. Degree of stream dissection 4. Degree of surface modification	1. Soil profile development
Outwash Deposits Well-sorted and stratified rounded sand and gravel in valley bottoms, deposited by rivers draining glaciers	1. Valley trains of fluvial sediments deposited on braided floodplains headed at the terminus of glaciers	1. Well-sorted and stratified rounded sands and gravels 2. Cut and fill channels are common in cross section 3. Surface relief is less than approximately 10 ft (3 m), unless dissected or terraced by subsequent fluvial processes	1. Geographic (spatial) position in relation to other glacial deposits 2. Topographic (elevational) relationship to adjacent deposits 3. Abandonment or elevation of outwash surface above present base level 4. Degree of modification to surface morphology 5. Degree of local stream dissection	1. Soil profile development 2. Degree of cementation 3. Degree of oxidation 4. Degree of vegetation cover
Ice-Disintegration Deposits Well-sorted and stratified to unsorted and nonstratified glacial drift, stagnant ice deposits, characteristically hummocky kame and kettle topography	1. Random assemblage of hummocks, ridges, basins, and small plateaus 2. Slopes vary, but many are steep 3. Generally confined to distal end of glacier deposits 4. Slumping common 5. Generally limited to topographic lows 6. Kame and kettle, and knob and kettle topography	1. Chaotic and irregular nature of morphology 2. Kettles common 3. Gravel, sand, silt, and clay; grain size, degree sorting and stratification (structure) of sediments varies with the amount of water reworking 4. Highly deformed structure caused by slumping, settlement, and compaction are common	1. Geographic (spatial) position in relation to other glacial deposits 2. Freshness of morphology 3. Degree of slumping, infilling, and rounding 4. Degree of stream dissection	1. Soil profile development 2. Local relief 3. Degree of vegetation cover 4. Degree of roundness, infilling, and slumping infilling, and slumping
Kame Terrace Deposits Narrow constructional terrace confined between glacier and valley wall, composed of stratified rounded sands and gravels	1. Narrow, flat surfaced, constructional terrace along hillsides 2. Slopes down valley 3. May be discontinuous along valley sides 4. Surface may be pitted by kettles 5. Commonly no apparent source area for sediments 6. Parallels direction of glacial flow	1. Stratified and sorted rounded sands and gravels 2. Hillside terrace may be discontinuous and surface may contain kettles 3. Very narrow compared to fluvial terraces 4. Generally many hundreds of feet above outwash and fluvial terraces, but if long enough, can merge with outwash terraces near terminus of glaciers	1. Elevation above valley floor 2. Degree of erosional segmentation 3. Degree of surface modification and dissection 4. Geographic position in relation to other glacial deposits	1. Soil profile development 2. Degree of infilling of kettles 3. Oxidation depth 4. Modification of form by erosion (dissection or burial)
Fluvial Deposits Reworked glacial and eroded bedrock material deposited in active floodplains of major rivers	1. Confined to floodplains of active major streams and rivers 2. Broad to narrow flat floodplains 3. Commonly terraced 4. Possible meander scars 5. Stream bars common	1. Well-sorted and stratified rounded sands and gravels from reworked glacial deposits and eroded bedrock 2. Cut and fill channels are common in cross-section 3. Surface relief is minimal unless terraced	1. Deposits confined to recent age but terraces adjacent to active floodplain may be assigned age based on elevation above active floodplain 2. Degree of modification to terrace surface and scarp 3. Degree of vegetation growth	1. Soil profile development 2. Surface elevation 3. Depth of oxidation
B. Erosional				
Fluting Linear parallel to subparallel, broad topographic swales with intervening well-rounded low ridges formed in till	1. Large scale forms developed commonly on broad till plains 2. Contrast of vegetation type and density 3. Linear parallel to subparallel broad topographic swales with intervening well-rounded low ridges	1. Difficult to identify on ground because of scale 2. Relief of only a few 10's of feet (3 m) over large horizontal distances 3. Drainages differences reflected by vegetation contrasts	1. Age of fluting same as age of till on which it is developed 2. Orientation and cross-cutting relationship of linear forms	1. See criteria for till
Trimline Narrow zone along valley walls that marks former upper limit of glaciation, slope, and/or morphologic contrasts	1. Abraided rock or trimmed-off vegetation line at former ice contact, separates surface materials of differing reflectivity 2. Commonly paired on opposite valley walls 3. Slopes downvalley with same gradient as valley floor 4. Slight breaks in slope to nearly vertical planar cliffs	1. Vegetation contrast or truncation and/or contact between bedrock and unconsolidated talus 2. Change in slope grade	1. Elevation 2. Sharpness of line	1. Elevation 2. Degree of rock surface weathering
Side Glacial Channel Narrow, commonly discontinuous erosional stream channel cut between the glacier and adjacent valley wall or cut locally as bedrock gullies across hill slopes	1. Channel formed between margin of glacier and adjacent valley wall 2. Discontinuous elongated, narrow stream channel 3. Typically oblique to hillside 4. Open at both ends 5. Parallels direction of glacial flow 6. Channel that leaves ice margin cutting notch across ridge line called overflow channel 7. Channels that have no apparent source area for formation but may now be accentuated and modified by hillside runoff	1. Channels contain little or no sediment 2. Downhill side is lower than uphill side 3. Discontinuous 4. Locally open, hanging channel ends 5. No source areas for formation 6. Cut into rock with commonly no outside wall 7. Rock channel walls have steep slopes	1. Elevation of channel	1. Degree of weathering of channel rock 2. Degree of channel infilling by post-erosional sediments
Bedrock forms (Whalebacks, stoss and lee, grooves) large scale streamlined erosional bedrock forms created by ice flow, longitudinal axis approximately parallel ice flow direction	1. Polished, smooth bedrock outcrops 2. Strong preferred orientation of long axis of forms and grooves 3. Rock structural features may be differentially eroded 4. Forms with lengths greater than widths	1. Polished curved bedrock outcrops 2. Gentle slopes upstream (stoss) and steep slopes downstream (lee) 3. Smooth rock outcrops may record small-scale features of glacial abrasion, striations, polish, grooves	1. Orientation and cross-cutting relationships of longitudinal axis 2. Weather texture of rock surface 3. Degree of form modification	1. Degree of rock surface weathering 2. Degree of form modification by weathering 3. Preservation of glacial polish and small-scale abrasion features

TABLE 3-2

RADIOCARBON AGE DATES AND SAMPLE DESCRIPTIONS

Age date C^{14} years before present	Field sample number	Sample Stratum	Material dated	Site location[1]	Quadrangle	Section township & range	Lab Sample Number	Significance of date
2245 ± 140	S49-1	Frozen silty sand	Wood chips	Measured section along Watana Creek	Talk. Mtn. (D-3)	NE1/4; NW1/4; Sec. 9; T32N; R7E	GX-8056	Dates young deposits which slumped into older deposits and were subsequently frozen
2290 ± 130	S47-1	Frozen lacustrine silt with striated ice raft cobbles	Wood	Measured section at Oshetna River mouth	Talk. Mtn. (C-1)	NE1/4; NE1/4; Sec. 4; T29N; R11E	GX-8055	Anomalous date, may represent the age of wood that was incorporated into lacustrine deposits by cryoturbation
3450 ± 170	S45-1	Frozen lacustrine silt and clay	Wood	Slump exposure along Deadman Creek	Talk. Mtn. (D-3)	SW1/4; SE1/4; Sec. 32; T225; R4E	GX-8059	Minimum date of last retreat of ice from valley of Deadman Creek
3540 ± 160	S4-1	Frozen lacustrine silt and clay	Charcoal	Slump exposure at mouth of Clear Valley	Talk. Mtn. (C-4)	NW1/4; NW1/4; Sec. 34; T30N; RSE	GX-8054	Maximum age of permafrost formation (i.e., the ground froze after deposition of the charcoal); also represents time of lacustrine deposition near the north of Clear Valley
9395 ± 200	S42-1	Frozen lacustrine silt and clay	Wood	Slump exposure in upper Watana Creek valley	Talk. Mtn. (D-2)	SW1/4; NW1/4; Sec. 21; T22S; R2W	GX-8035	Dates the time of last retreat of ice from Watana Creek valley
9920 ± 265	S54-1	Fine-grained ice disintegration deposits	Peat	Slump exposure along upper Deadman Creek	Healy (A-3)	SW1/4; SE1/4; Sec. 15; T215; R4W	GX-8062	Dates the time of last retreat of ice from valley of Deadman Creek
> 27,000	S34-1	Sand matrix surrounding angular bedrock blocks, colluvial (?) deposits	Charcoal	Measured section along drainage north of Stephan Lake	Talk. Mtn. (C-4)	NE1/4; SE1/4; Sec. 29; T31N;R4E	GX-8060	Maximum date on oxidized outwash overlying the sampled stratum
> 37,000	S29-1	Interbedded lacustrine sand and silt from ice marginal lake, 12 ft (3.7 m) below outwash deposit	Wood	Measured section along Moraine Creek	Talk. Mtn. (D-4)	SW1/4; NW1/4; Sec. 24; T32N;R4E	GX-8034	Maximum date on oxidized outwash and till blanket overlying the sampled stratum
> 37,000	S12-2	Lacustrine/deltaic fine sand 51 ft (15.5 m) above till	Wood chips	Measured section along Brushkana Creek	Healy (A-3)	NE1/4; SW1/4; Sec. 8; T20S; R3W	GX-8057	Minimum date on till buried by the sampled stratum
> 37,000	S47-4	Contact of lacustrine fine sand with interfingered till	Wood	Measured section at Oshetna River mouth	Talk. Mtn. (C-1)	NE1/4; NE1/4; Sec. 4; T29N; R11E	GX-8058	Dates advance of ice into ice-marginal lake
> 37,000	S62-1	Ice marginal lacustrine silt and sand	Wood	Measured section west of Daneka Lake	Talk. Mtn. (C-5)	NE1/4; NW1/4; Sec. 22; T30N; R2E	GX-8124	Dates ice marginal deposits of the Early Wisconsin stage; limits the maximum elevation of Late Wisconsin glacial ice in the intermountain basin

Note:

1. Site locations are shown in Figure 3-2

TABLE 3-3

SUMMARY OF RELATIVE AGE DATA FOR EARLY AND LATE WISCONSIN MORAINES

Area [1]	Surface Data				Subsurface Data[3]	
	Moraine Form	Surface Morphology Modification[2]	Degree of Segmentation	Side Slopes	Average Granite Weathering Ratio[4] (%F/%PW/%W)	Oxidation Depth inches (cm)
Late Wisconsin						
Clear Valley	Fresh, prominent, moderate crest width	Slight	Slight	Moderate to steep	--	11 to 24 (3 to 7)
Butte Lake	Fresh to weathered, prominent to subdued, narrow to broad crest width	None to moderate	Slight	Gentle to steep	56/34/10	8 to 12 (2 to 4)
Deadman Creek	Fresh, prominent, moderate crest width	None to slight	Very slight	Steep	50/39/11	7 to 12 (2 to 4)
Black River	Weathered, subdued, broad crest width	Moderate to high	High	Gentle to moderate	52/40/8	11 to 17 (3 to 5)
Early Wisconsin						
Clear Valley	Weathered, subdued, broad to moderate crest width	Moderate to high	High	Gentle to moderate	--	26 to 40 (8 to 12)
Butte Lake	Weathered, prominent, moderate crest width	Moderate	Moderate	Moderate	30/46/24	14 to 29 (4 to 9)
Deadman Creek	Fresh, prominent, moderate crest width	Slight	Slight	Moderate to steep	40/40/20	17 to 18 (5 to 6)
Black River	Fresh, prominent, narrow crest width	None to slight	Very slight	Steep	42/32/26	21 to 22 (6 to 7)

Notes:

1. Areas are shown in Figures 3-5 and 3-6.
2. Surface morphology modification reflects the effect of slumping and frost heaving.
3. The subsurface data summarized here are presented for each moraine in which measurements were made and cited in Table A-1.
4. Granite weathering ratios are discussed in Appendix A.1.2.2. The numbers (e.g., 56/40/10) are the percentage of granite boulders that are fresh (%F), partially weathered (%PW), and weathered (%W), respectively.

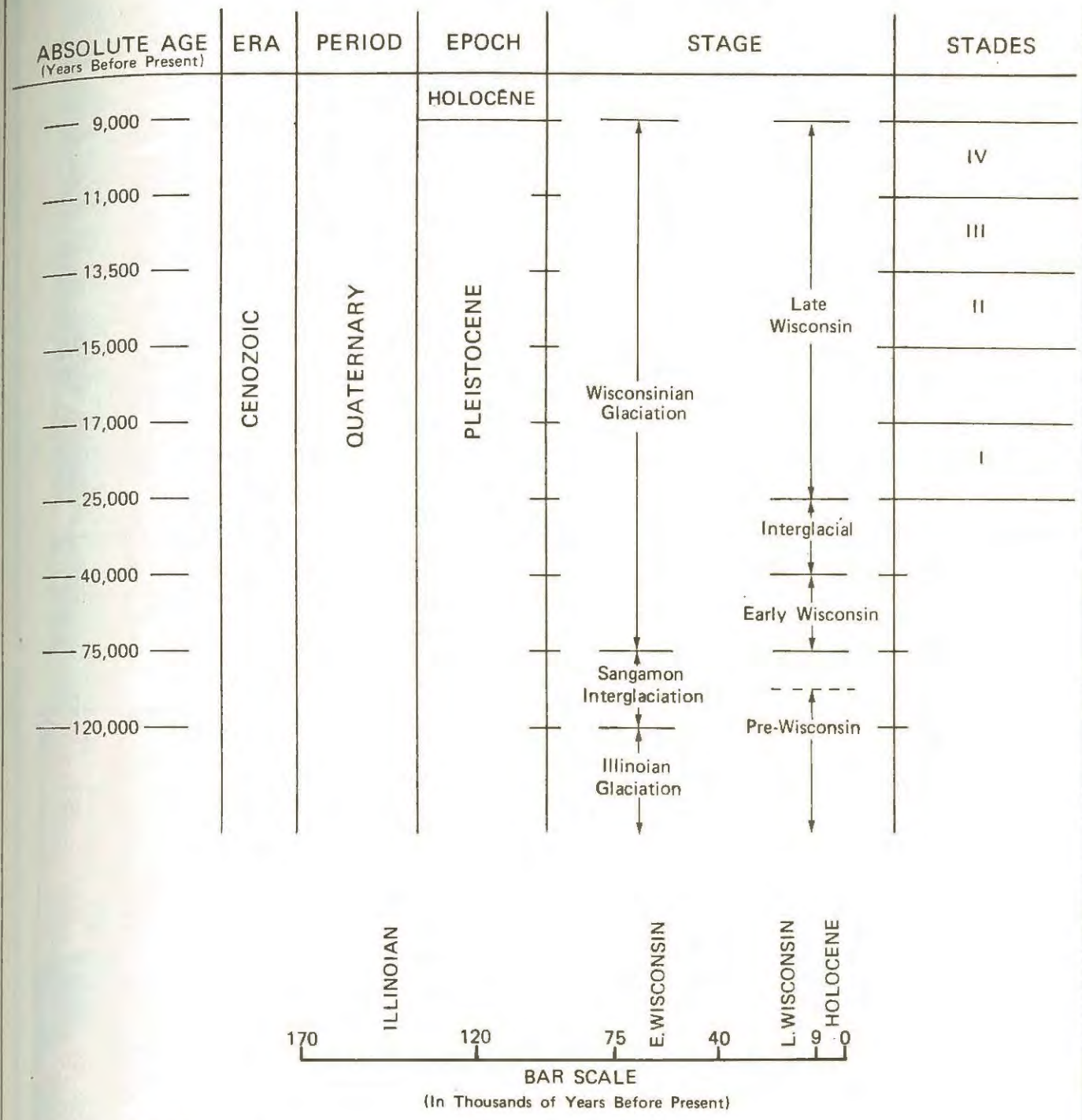

NOTES

1. Era through Epoch terminology and absolute ages are after Van Eysinga (1978).
2. Stage terminology and ages are after Pewé (1975).
3. Stade ages are modified after Ten Brink and Waythomas (in press).

QUATERNARY STUDY REGION
TIME SCALE

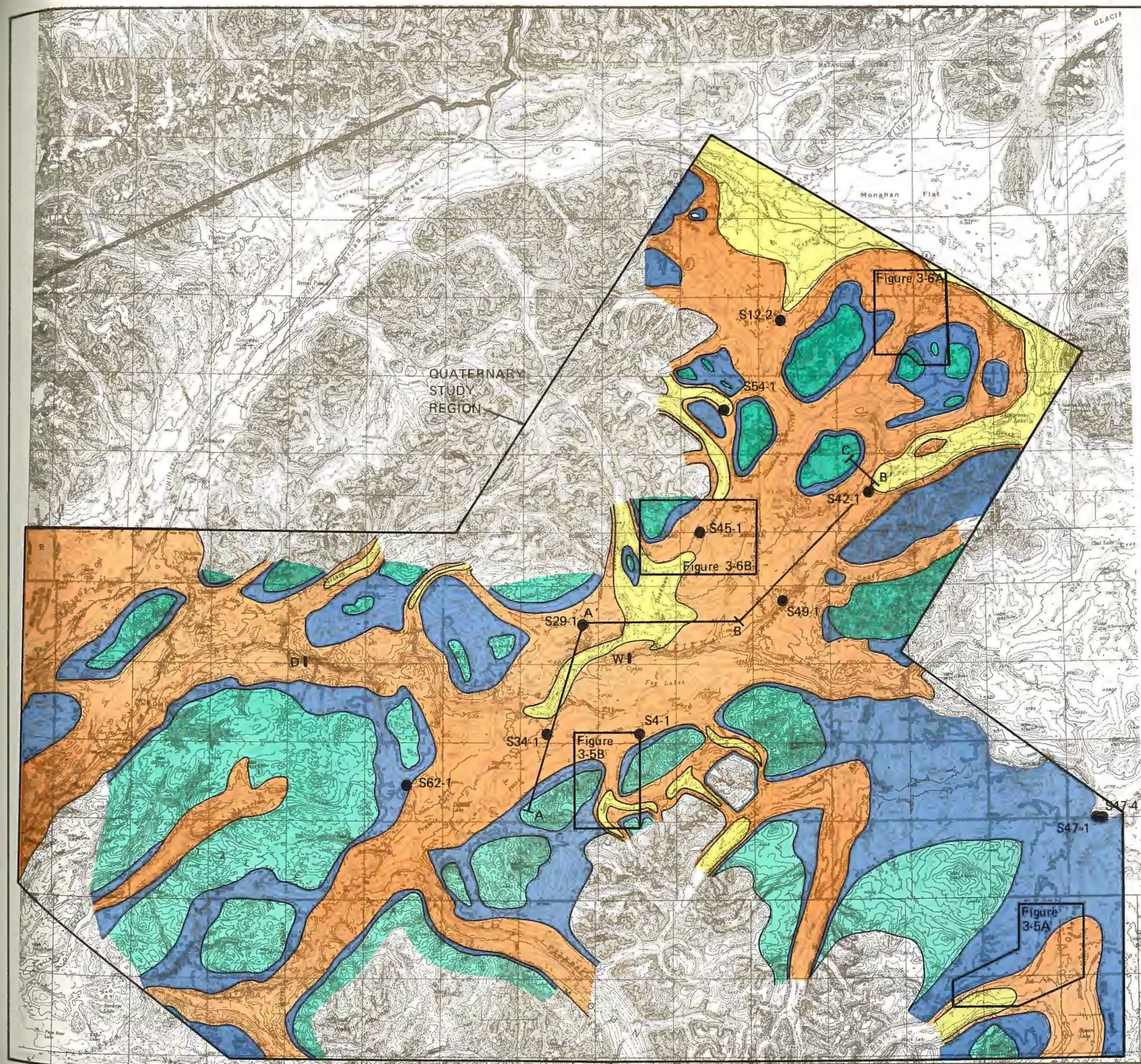

LEGEND

- Late Wisconsin surfaces 11,000 to 9,000 y.b.p.
- Late Wisconsin surfaces 25,000 to 11,000 y.b.p.
- Early Wisconsin surfaces 75,000 to 40,000 y.b.p.
- Pre-Wisconsin surfaces >100,000 y.b.p.
- S4-1 ● Radiocarbon sample locality and number
- Glacial Age Boundary
- Fig. 3-5A Detailed study areas are shown in Figures 3-5 and 3-6.
- B′ / A — Generalized projected cross section is shown in Figure 3-3.
- W I Watana Site
- D I Devil Canyon Site

NOTES

1. Figure A-1 shows the location of the Quaternary Study Region.
2. Areas with no color are bedrock and/or surfaces of undifferentiated glacial age.
3. y.b.p. is the abbreviation for years before present
4. Glacial age boundaries are interpreted from morpho-stratigraphic relationships and age dates.

-N-

QUATERNARY GEOLOGY MAP

0 10 20 Miles

0 10 20 Kilometers

WOODWARD-CLYDE CONSULTANTS 41410A February 1982

FIGURE 3-2

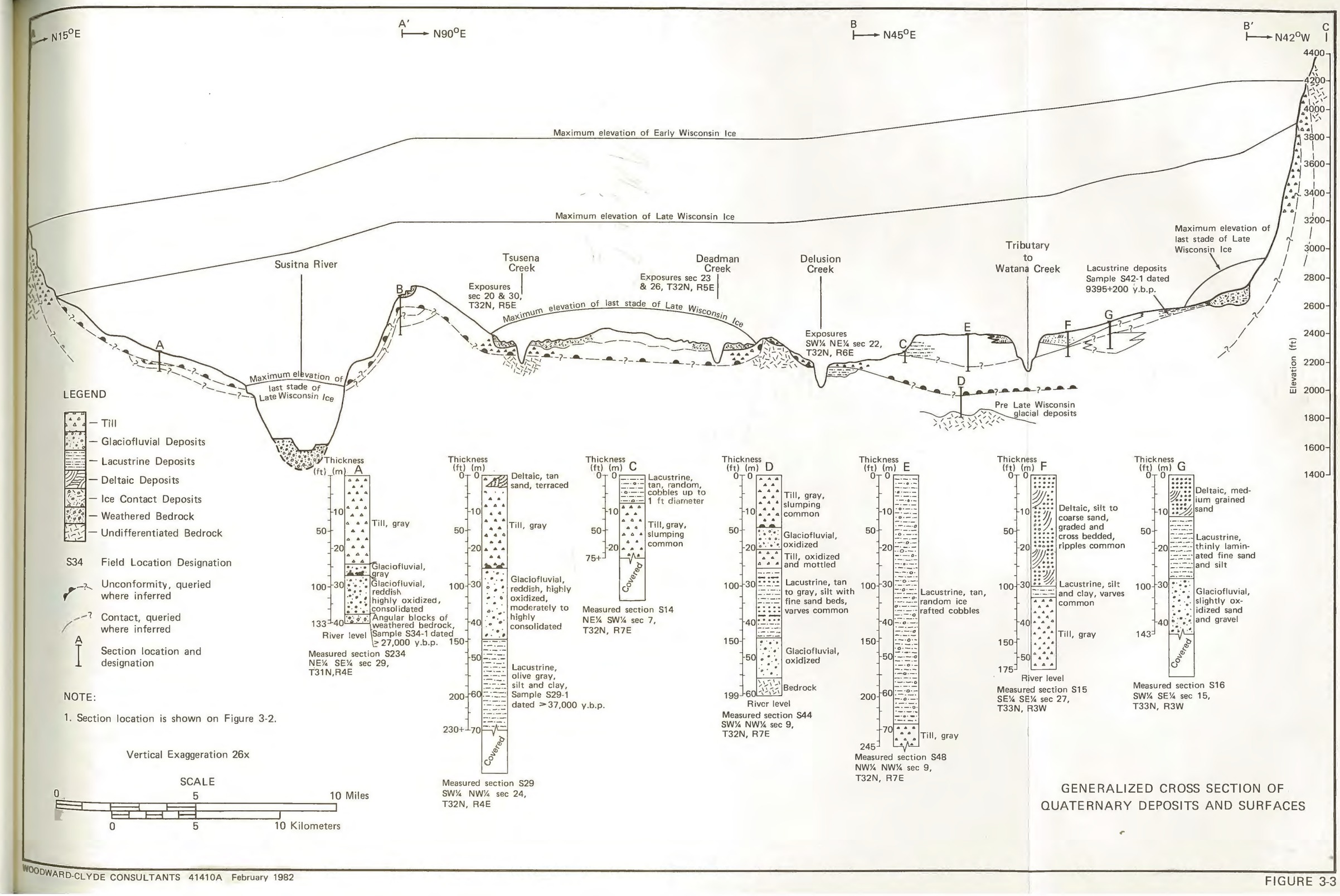

GENERALIZED CROSS SECTION OF QUATERNARY DEPOSITS AND SURFACES

QUATERNARY STUDY REGION

KD5-2
KD5-43
KD5-9
KD5-45
KD5-12
KD5-42
KD5-3
KD5-44
KC5-5
FINS FEATURE
W
WATANA FEATURE
THRUST FAULT
SUSITNA FEATURE
TALKEETNA
Monahan Flat

LEGEND

- Late Wisconsin surfaces 11,000 to 9,000 y.b.p
- Late Wisconsin surfaces 25,000 to 11,000 y.b.p.
- Early Wisconsin surfaces 75,000 to 40,000 y.b.p.
- Pre-Wisconsin surfaces >100,000 y.b.p.
- Glacial age boundary
- Thrust fault, dotted where concealed, sawteeth on upper plate
- KC5-5 — Fault and code number
- Concealed shear zone or fault
- KD5-12 — Lineament and code number
- W — Watana Site
- D — Devil Canyon Site

NOTES

1. Figure A-1 shows the location of the Quaternary Study Region.
2. Areas with no color are bedrock and/or surfaces of undifferentiated glacial age.
3. y.b.p. is the abbreviation for years before present.
4. Glacial age boundaries are interpreted from morpho-stratigraphic relationships and age dates.

N

SIGNIFICANT FEATURES AND QUATERNARY SURFACE MAP

0 10 20 Miles
0 10 20 Kilometers

WOODWARD-CLYDE CONSULTANTS 41410A February 1982

FIGURE 3-4

LEGEND

UNITS

- Lacustrine sediments
- Ice disintegration deposits
- Till
- Bedrock

AGE

- Holocene surfaces <9,000 y.b.p.
- Late Wisconsin surfaces 11,000 to 9,000 y.b.p.
- Late Wisconsin surfaces 25,000 to 11,000 y.b.p.
- Early Wisconsin surfaces 75,000 to 40,000 y.b.p.
- Pre-Wisconsin surfaces >100,000 y.b.p.

- Moraines
- Direction of meltwater flow and length of side glacial or overflow channels
- S4-1 ● Radiocarbon sample locality and number
- BR-1 ▲ Relative dating locality and number

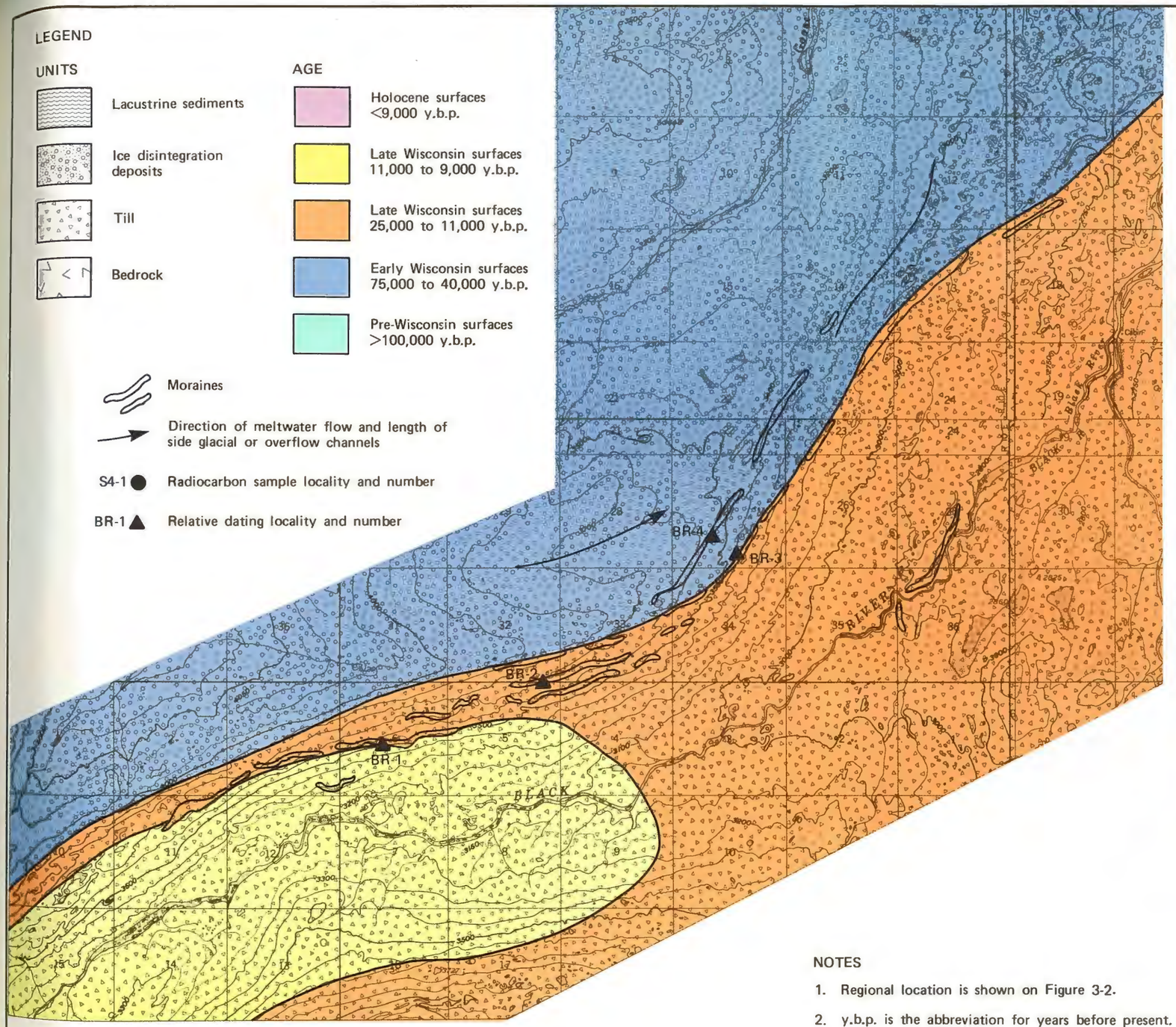

A. BLACK RIVER AREA

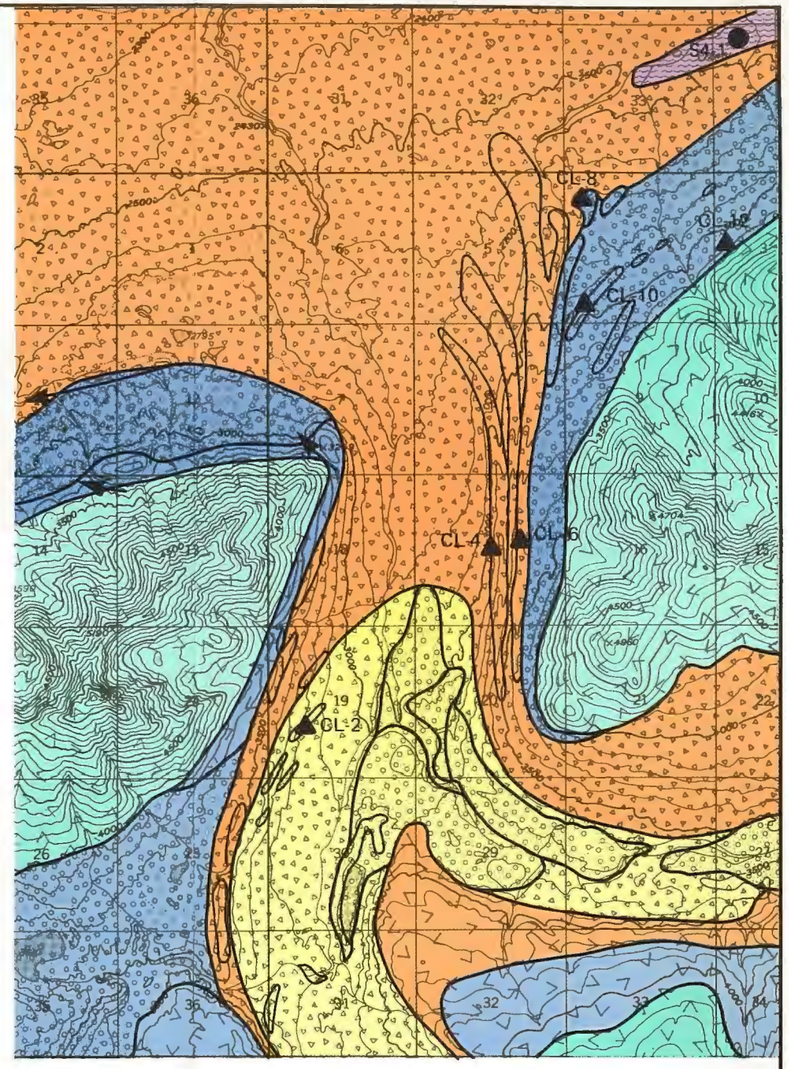

B. CLEAR VALLEY AREA

NOTES

1. Regional location is shown on Figure 3-2.
2. y.b.p. is the abbreviation for years before present.

N

QUATERNARY GEOLOGY OF THE BLACK RIVER AND CLEAR VALLEY AREAS

0 0.5 1 Mile

0 0.5 1 Kilometer

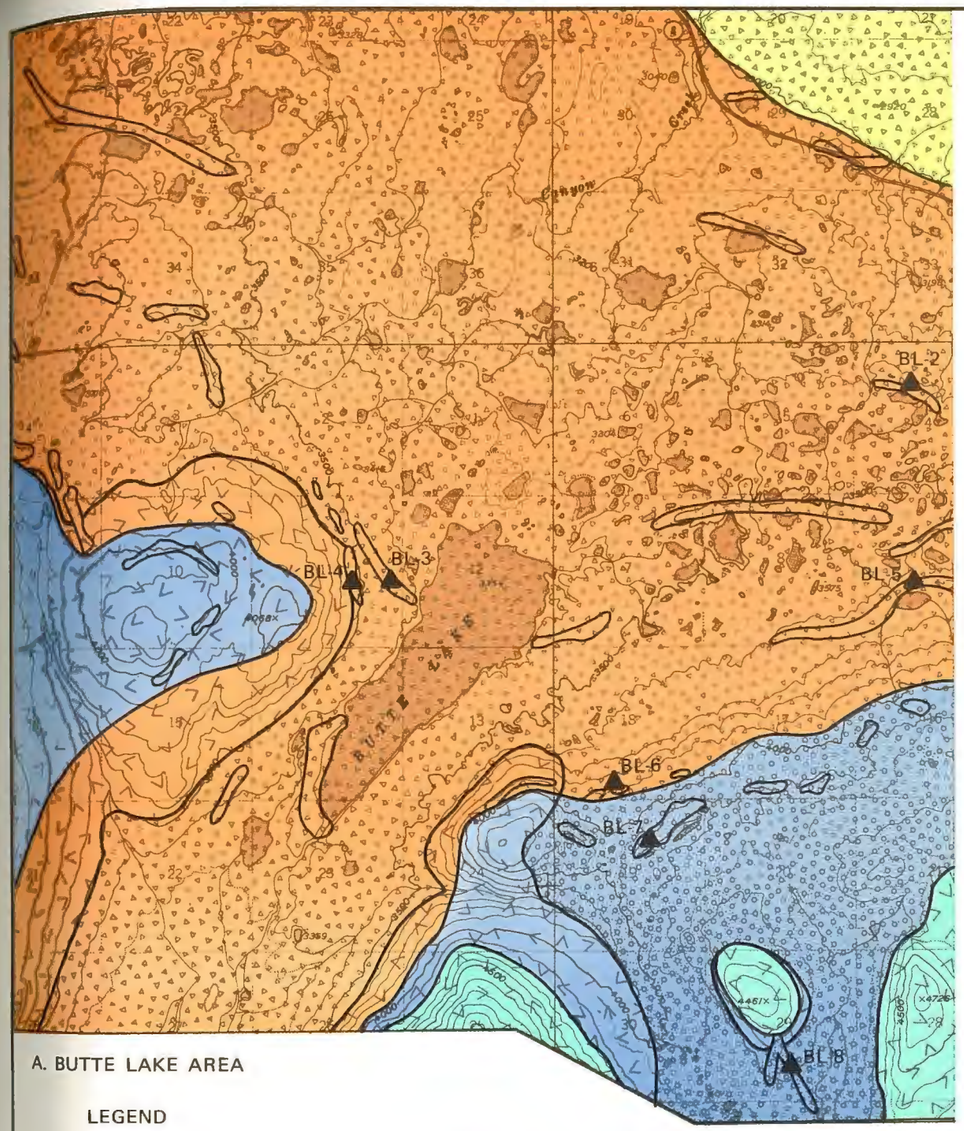

A. BUTTE LAKE AREA

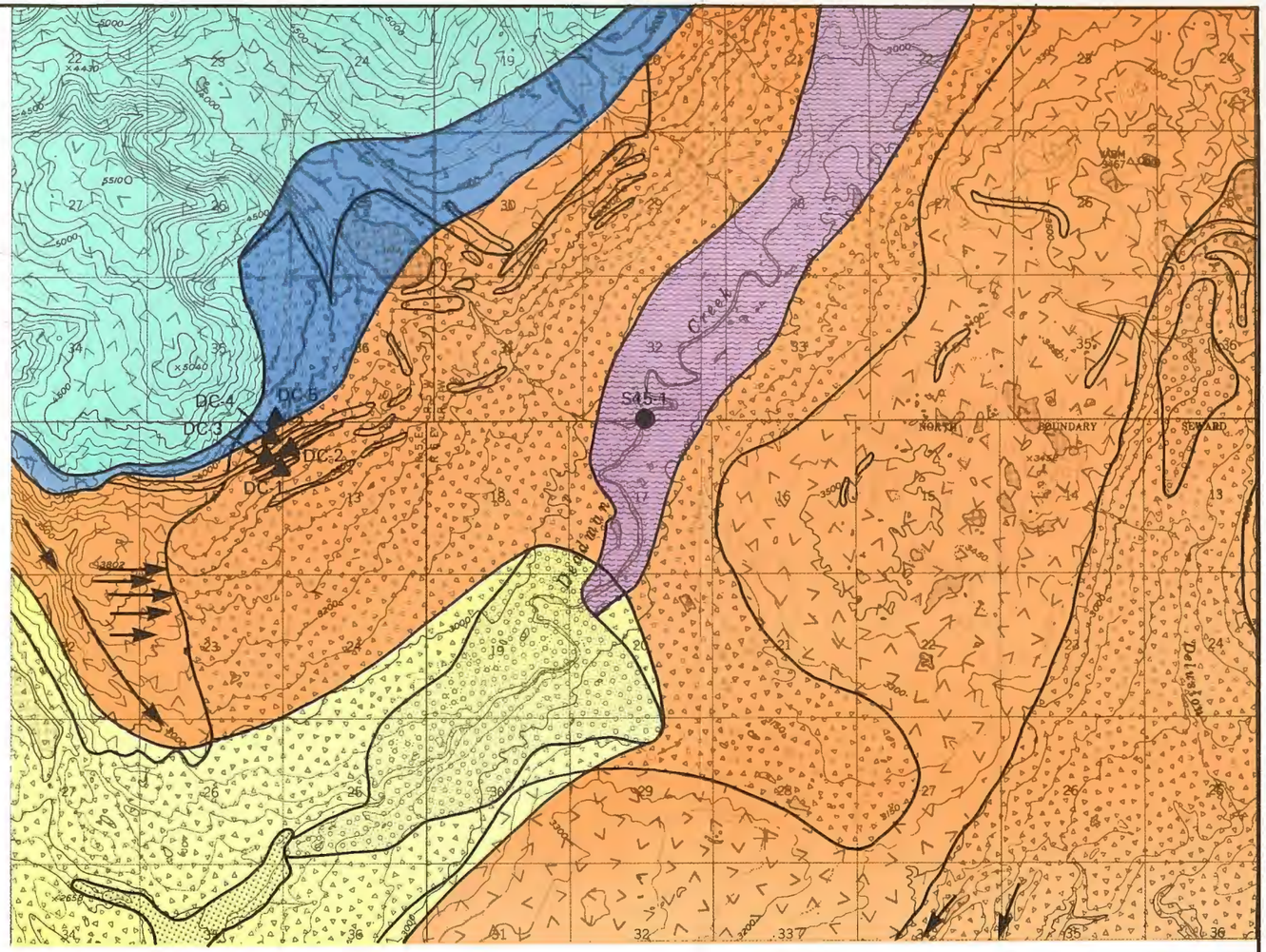

B. DEADMAN CREEK AREA

LEGEND

UNITS

- Lacustrine sediments
- Ice disintegration deposits
- Till
- Glaciofluvial sediments
- Bedrock

AGE

- Holocene surfaces <9,000 y.b.p.
- Late Wisconsin surfaces 11,000 to 9,000 y.b.p.
- Late Wisconsin surfaces 25,000 to 11,000 y.b.p.
- Early Wisconsin surfaces 75,000 to 40,000 y.b.p.
- Pre-Wisconsin surfaces >100,000 y.b.p.

- Moraines
- Direction of meltwater flow and length of side glacial or overflow channels
- S45-1 ● Radiocarbon sample locality and number
- DC-5 ▲ Relative dating locality and number

NOTES

1. Regional location is shown on Figure 3-2.
2. y.b.p. is the abbreviation for years before present.

N

QUATERNARY GEOLOGY OF THE BUTTE LAKE AND DEADMAN CREEK AREAS

0 0.5 1 Mile

0 0.5 1 Kilometer

4 - SIGNIFICANT FEATURES

4.1 - Introduction

Prior to evaluation of the faults and lineaments in the project region, a tectonic model of the region was developed as discussed in Section 1.4 and the Interim Report (Woodward-Clyde Consultants, 1980b). This model provided a conceptual framework in which the likelihood of recent fault displacement and seismic activity could be evaluated. The tectonic model applies to a region of the earth's crust that we have called the Talkeetna Terrain. This terrain is bounded by the Denali and Totschunda faults on the north and east, the Castle Mountain fault on the south, a broad zone of deformation and volcanoes to the west, and the Benioff zone and base of the crust at depth (Figure 4-1).

During the 1980 study, 216 features were studied by reconnaissance from helicopters and fixed-wing aircraft and by ground mapping at selected locations. At the conclusion of the 1980 study, the Talkeetna Terrain boundary faults were identified as being faults with recent displacement that should be considered in design. In addition, 13 significant features closer to the dam sites were selected for additional study on the basis of their potential affect on ground motion and surface rupture considerations (Woodward-Clyde Consultants, 1980b).

During the 1981 study, the boundary faults were reviewed to refine estimates of the maximum credible earthquakes (MCEs). Two of them, the Castle Mountain and Denali faults, are discussed in detail in Section 4.3; the two regions of the Benioff zone are discussed in detail in Section 5.2 and are summarized in Section 4.3.

The 13 features selected for additional study were the subject of detailed field studies in 1981 using the methodology described in

Appendix A. The approach used to guide the field studies was twofold: 1) to study the bedrock along each feature to assess whether or not the feature was a fault; and 2) to examine the surficial units along the feature to evaluate the geologic evidence for recency of displacement.

This section on significant features presents our evaluation of faults and lineaments within and bounding the Talkeetna Terrain. Section 4.2 summarizes the detectability of faults with recent displacement. Sections 4.3 and 4.4 discuss our interpretation of fault activity for the boundary faults and the features in the vicinity of the Watana and Devil Canyon sites. Our evaluation is summarized in Section 4.5.

4.2 - Detectability of Faults With Recent Displacement

The detectability of faults with recent displacement depends primarily on the following factors: 1) the age of the sediments overlying the fault; 2) the amount of displacement at the surface during earthquakes; 3) the recurrence interval of these earthquakes (i.e., how often do the earthquakes and displacements occur); 4) the type of displacement that occurs; 5) the length of the fault along which displacement occurs; and 6) the length of time that displaced features are preserved (i.e., rapidity of erosion and despositional processes relative to the rate of displacement).

Faults that generate earthquakes that are too small to rupture the surface or to cause fault scarps large enough to be preserved may not have been detected by our geologic investigation. Consequently, an estimate was made of the size of earthquake that might have occurred without leaving any detectable geologic evidence. This earthquake was designated the "detection level earthquake."

To address this question, we conducted a three-step evaluation during the 1981 study. These steps included: 1) a review of a select group

of worldwide moderate to large earthquakes (Table 4-1) to evaluate the degree of association between earthquakes and faults with recent displacement; 2) a review of moderate to large historical earthquakes in California, which has a relatively complete data base, to evaluate the threshold earthquake magnitude that results in recognizable surface displacement; and 3) a field evaluation of the Talkeetna Terrain for preservation of geological evidence of past earthquakes.

4.2.1 - Selected Worldwide Earthquakes and Faults with Recent Displacement

The primary purpose of evaluating the worldwide earthquake data base was to assess the degree of association between earthquakes and faults with recent displacement. The data analysis concentrated on the following topics: 1) assessing the threshold magnitude of earthquakes for which surface faulting was recognizable; 2) reviewing reports in the literature about large magnitude, shallow earthquakes that resulted in no surface faulting; and 3) evaluating reports of faults that had been dormant for tens of thousands of years and then were reactivated during a large earthquake. From these data and analyses, an attempt was made to estimate the threshold earthquake magnitude that would be expected to produce surface rupture.

Data were collected and analyzed for worldwide earthquakes that occurred in regions having geologic conditions similar to those of the Talkeetna Terrain. The earthquakes were selected according to the following screening criteria: tectonic setting, depth of hypocenter, geologic setting, geomorphic terrain, and style of faulting. If an earthquake occurred within the Talkeetna Terrain, it would be classified as a shallow (less than 12 miles [20 km]) intraplate earthquake associated with crustal deformation within the North American plate. However, the Talkeetna Terrain is

close to the plate boundary on a regional scale, and the Terrain may be under the influence of the North American-Pacific plate collision. Thus, an earthquake that occurred could also be classified as an interplate earthquake related to plate edge deformation on a regional scale. Both tectonic settings were considered in the selection of worldwide data because the classification of worldwide earthquakes is not standardized.

Approximately 30 earthquakes of magnitude (M_S) 5.4 to 7.8 that occurred in environments that are representative of the Talkeetna Terrain were selected from three sources: Kanamori and Anderson (1975), Slemmons (1977b), and Wyss (1979). The data reported by these three sources were reconciled and combined with data from other literature. For the earthquakes selected, available data were compiled for the following variables: date, location, magnitude, and association with faults having recent displacement. These data are presented in Table 4-1.

The most prevalent limitations in the data base are caused by differences in reporting of data. This is especially true for field reports of earthquake effects such as surface faulting. The quality of the reported data most often depends on the location and size of the earthquakes (or loss of property and lives). These limitations on quality of the worldwide earthquake data base make rigorous comparisons difficult, but conclusions can be reached and trends in the data can be described that are informative regarding the concept of the detection level earthquake.

Evaluation of the worldwide data set shows that all of the reported earthquakes occurred near a mapped fault with recent displacement or within terrains where faults with recent displacement exist (Table 4-1). Occasional reports of faults rupturing new ground or being reactivated after tens of thousands of years do exist but are

unverified. An example is the magnitude (M_S) 7.0 Inangahua, New Zealand, earthquake of 1968. During the earthquake, rupture occurred both along a pre-existing scarp and a subsidiary fault; the latter had not been previously recognized. The rupture along the subsidiary fault was called "new." However, the earthquake occurred on a recognized fault with recent displacement and the displacement along the subsidiary fault should not have been considered an unexpected event.

The results of the evaluation of this data set show that, in general, surface faulting is reported for earthquakes with magnitudes larger than magnitude (M_S) 6.5. The exceptions are mainly earthquakes in California and Japan where earthquakes are intensely studied and surface faulting has been reported for earthquakes as small as magnitude (M_S) 5. Conversely, some shallow earthquakes as large as magnitude (M_S) 7-1/4 have not had observed surface rupture; however, these earthquakes have occurred in areas where faults with recent displacement are present.

Although the quality of the worldwide earthquake data base is variable, the primary conclusions that can be drawn from the worldwide data base are: 1) moderate to large earthquakes in areas similar to the Talkeetna Terrain are consistently associated with recognizable faults with recent displacement or terrains where recognizable faults with recent displacement are present; 2) earthquakes less than magnitude (M_S) 5.5 have been observed to result in surface faulting; and 3) shallow earthquakes as large as magnitude (M_S) 7.0 or even greater have been documented with no surface faulting.

Because the worldwide data vary in quality, and trends in the data are lacking with regard to size and depth of earthquake versus occurrence of surface rupture, a more uniform data base was sought

to examine the threshold of surface faulting. The most uniform and detailed data base available is from California and is reviewed in the following paragraphs.

4.2.2 - Occurrence of Surface Faulting in California

The magnitude threshold at which shallow earthquakes result in recognizable surface faulting was estimated by evaluating earthquakes that have occurred in California. Although the historical record in California is short, a sufficiently large number of moderate to large earthquakes have been intensively investigated to estimate the threshold magnitude of surface faulting.

Data were evaluated for earthquakes that occurred between 1900 and 1980 by reviewing compilations by Slemmons (1977b), Real and others (1978), Toppozada and others (1979), and various reports of earthquakes by the California Division of Mines and Geology, U.S. Geological Survey, California Institute of Technology, and Earthquake Engineering Research Institute. These data are summarized in Table 4-2 according to periods of time from 1900 through 1969, and from 1970 through 1980. The data are for earthquakes that occurred onshore within the borders of California. Three magnitude ranges are shown to illustrate the sensitivity of recognizing surface rupture according to variation in earthquake magnitude.

Table 4-2 shows that during the first 69 years of this century surface rupture was recognized for only five of the 34 earthquakes over magnitude (M_S) 6. In contrast, from 1970 through 1980, surface rupture was documented for all three earthquakes over magnitude (M_S) 6 and for 75 percent of earthquakes over magnitude (M_S) 5.5. The reason for the difference in recognition of

surface rupture during the past eleven years is the greater interest that scientists now have in recognizing and understanding surface faulting as a phenomenon. Thus, it can be inferred that as studies of moderate to large earthquakes have become more thorough, the detection of surface faulting has increased.

From these data, it can be concluded that the threshold of surface faulting within California is on the order of magnitude (M_S) 5.5 and that for earthquakes over magnitude (M_S) 6.0 a high certainty of surface faulting is expected.

4.2.3 - Preservation of Recent Displacement

The geologic detection of faults with recent displacement depends on preservation of geologic evidence of past earthquakes. Earthquakes over the threshold magnitude of (M_S) 5.5 to 6.0 rupture the sediments overlying the fault and rupture the ground surface, thus creating a fault scarp. The ruptured sediments may be detected if they are not buried by younger sediments. Detection of the fault scarp depends on: 1) the height and length of the original fault scarp, and 2) the degree of degradation of the scarp between the time it was created and the present.

Faults with recent displacement may be detected if the sediments and geomorphic surfaces present along the trace of the fault were in existence prior to the last earthquake that produced surface rupture. For example, the Talkeetna thrust fault has sediments from the earlier part of the Late Wisconsin epoch (25,000 to 15,000 y.b.p.) along 85 percent of its length (Figure 3-4). Consequently, single fault displacements from earlier than 25,000 y.b.p. cannot be detected by surface geologic studies along 85 percent of the fault. Erosion of a new geomorphic surface may not preclude

detection of the fault. Geologic evidence for recency of displacement may be destroyed, but the fault should still be detectable as a lineament.

The initial height and length of a fault scarp depends on the magnitude and depth of the earthquake. The degree of degradation depends on the type of geomorphic surfaces and Quaternary sediments present in the Talkeetna Terrain and the geologic processes, such as annual freeze and thaw, slumping, and solifluction, that reduce the sharpness of small topographic features such as fault scarps. Glacial scarps of varying heights and lengths that were similar in form to fault scarps were examined in the project region to establish the detection limit for preserved scarps in the Talkeetna Terrain. On the basis of this examination, the detection limit for initial surface rupture is a rupture length of approximately 9 miles (15 km) and a scarp height of approximately 1.7 to 3.3 feet (1/2 to 1 m). Geologic evidence of this initial surface rupture would be recognizable for thousands of years. Surface ruptures of these dimensions are associated with earthquakes of magnitude (M_S) 6 to 6-1/2 (Slemmons, 1977b).

Since most faults with recent displacement have many magnitude (M_S) 6 to 6-1/2 or greater earthquakes during any 25,000-year period, detectable evidence usually remains somewhere along the length of the fault. However, it is theoretically possible for a fault to have a single displacement associated with a magnitude (M_S) 6 to 6-1/2 earthquake that occurred between 25,000 and 100,000 years ago. Such cases of long recurrence intervals of displacement with surface rupture dimensions near the limits of detection present the most difficulty in identifying faults with recent displacement.

Again using the example of the Talkeetna thrust fault, 62 miles (100 km) of the total fault length of 78 miles (126 km) are covered by sediments that are only 15,000 to 25,000 years old (as shown in Figure 3-4). It is hypothetically possible, though geologically unlikely, that eight single ruptures with lengths that are smaller than the detection limit of our investigation (rupture length of 9 miles [15 km]) could be fit within the 78-mile (126-km) fault length. However, even if earthquakes occurred on each of the eight sections of the fault only once every 100,000 years, it is highly unlikely that all eight earthquakes would have occurred before 25,000 y.b.p. Our investigation should have detected evidence of one of the ruptures somewhere along the fault. Therefore, faults with recent displacement having surface ruptures associated with earthquakes smaller than magnitude 6 to 6-1/2 are likely to have been detected by our field studies.

4.2.4 - Detection Level Earthquake

Evaluation of worldwide data for moderate to large earthquakes in areas similar to the Talkeetna Terrain shows that recognizable faults with recent displacement occurred in close proximity to or were directly associated with the earthquakes.

On the basis of the review of the worldwide and California data on surface faulting associated with earthquakes, it is reasonable to assume that the threshold of surface faulting within the Talkeetna Terrain is on the same order of magnitude, that is, magnitude (M_S) 5.5 to 6.0. On the basis of the study of scarp preservation, we consider it likely that scarps that were originally 1.7 to 3.3 ft (0.5 to 1.0 m) high would be detectable today. Scarps of these dimensions would result from earthquakes of magnitude (M_S) 6.0 to 6.5 (Slemmons, 1977b). Thus, faults with recent displacement associated with magnitude (M_S) 6.5 or greater earthquakes may be directly detected by observing the individual fault scarps.

Faults with recent displacement that are associated with earthquakes of magnitude as low as (M_S) 6.0 are also considered likely to have been detected by our geologic investigation for four reasons: 1) there are no confirmed cases of faults that have been dormant for tens-of-thousands of years being the source of a moderate to large earthquake; 2) a fault characterized by many short ruptures along its length would probably have been detected; 3) lineaments on geomorphic surfaces or in sediments often make a fault detectable even if the fault scarp is not preserved; and 4) terrains with moderate to large shallow earthquakes also have clearly recognizable faults with recent displacement, and, within the Talkeetna Terrain, no faults with recent displacement are apparent.

Because no fault-related scarps were detected in the Talkeetna Terrain, we concluded that the magnitude of the detection level earthquake is (M_S) 6.0. This is the largest earthquake that could theoretically occur on a fault that might not have been detected by our geologic investigation. Such an earthquake could occur on a source anywhere within the Talkeetna Terrain to the depth of the crust, which is approximately 12 miles (20 km) as discussed in Section 5. The recurrence interval for such an earthquake is low, as shown in Figure 5-9. Consequently, the likelihood of this earthquake occurring within 6 miles (10 km) of either of the sites is considered to be low. This low likelihood incorporates the size of the rupture plane that can be estimated for a magnitude (M_S) 6 earthquake and the variety of orientations (from horizontal to vertical) that the rupture plane could have within the crust. As shown in Figure 8-8, the rupture plane associated with a magnitude (M_S) 6 earthquake is 27 square miles (71 km^2) with a length and width of 5.2 miles by 5.2 miles (8.4 km by 8.4 km).

4.3 - Talkeetna Terrain Boundary Faults

4.3.1 - Castle Mountain Fault

The Castle Mountain fault is predominantly a strike-slip fault that dips steeply to the north. The fault is approximately 295 miles (475 km) long and trends east-northeast/west-southwest about 71 miles (115 km) south of the Devil Canyon site and 65 miles (105 km) south of the Watana site (Figure 4-1). It is nearly vertical or steeply dipping to the north (Detterman and others, 1974, 1976).

The fault is present as a single trace along its mapped western section. Along the eastern section of the fault, in the Matanuska Valley, the fault consists of the main trace and a major splay, which is known as the Caribou fault (Grantz, 1966; Detterman and others, 1974, 1976). Detterman and others (1976) propose that the main trace represents the older and more fundamental break of the two traces, while the Caribou fault is the trace along which late Cenozoic displacement has occurred. As is reported for the Denali fault, the Castle Mountain fault is generally regarded as a major suture zone within the earth's crust.

Displacement along the fault has been occurring since about the end of Mesozoic time (Grantz, 1966), approximately 60 to 70 m.y.b.p. (Figure 4-2). The fault incorporates a combination of right-lateral and reverse motions with the north side up relative to the south side (Grantz, 1966; Detterman and others, 1974, 1976). The maximum amount of vertical displacement is approximately 1.9 miles (3 km) or more (Kelley, 1963; Grantz, 1966); the maximum amount of strike-slip displacement is estimated by Grantz (1966) to have been several tens of kilometers, although Detterman and others (1976) cite 10 miles (16 km) as the total displacement that has occurred along the eastern traces of the fault.

During aerial reconnaissance for this study, the fault was observed to be expressed as a series of linear scarps and prominent vegetation alignments in the Susitna Lowland. Along its eastern portion in the Talkeetna Mountains, a lithologic contrast and possible offset of the Little Susitna River and other streams provide evidence for the location and recent age of the fault.

Evidence of Holocene displacement is observed only in the western segment of the fault in the Susitna Lowland (Detterman and others, 1974, 1976). To date, no evidence of Holocene displacement has been reported in the Matanuska Valley, although Barnes and Payne (1956) propose that up to 0.8 mile (1.2 km) of vertical displacement has occurred in the Matanuska Valley in Cenozoic time.

Slip on the Castle Mountain fault during Holocene time (<9,000 y.b.p.) continues to be predominantly strike-slip with a component of dip slip as indicated by displacement of undated Holocene features. In the Susitna Lowland horizontal displacement of a sand ridge has involved 23 feet (7 m) of right-lateral displacement; near-surface sediments have been displaced vertically 7.5 feet (2.3 m) (Detterman and others, 1974). Bruhn (1979) excavated two additional trenches across the fault. A river terrace near one of two trenches has been right-laterally displaced approximately 7.9 feet (2.4 m), and one of the trenches across the fault revealed 3.0 to 3.6 feet (90 to 110 cm) of dip-slip displacement of sediments. At this location, the north side is up relative to the south side along predominantly steeply south-dipping fault traces. This reversal of dip in faulted youthful sediments is commonly caused by curving of the fault plane near the surface. The dominance of right-lateral over vertical displacement appears to be continuing in a similar proportion to that which occurred earlier during Cenozoic time.

Detterman and others (1974) found evidence suggesting that the 7.5 feet (2.3 m) of dip-slip movement they observed has occurred within the past 225 to 1,700 years, and Bruhn (1979) estimates that the displacements he observed are similar in age, 222 to 1,860 y.b.p. Detterman's age estimate was interpreted from Carbon-14 age dates obtained from the soil horizons displaced by the fault and tree-ring counts from trees growing on the scarp. From the available data, the rate of strike-slip displacement cannot be calculated directly; however, the data imply a strike-slip rate of displacement of 0.05 to 0.4 inches/year (0.13 to 1 cm/year). A value of 0.2 inches/year (0.5 cm/year) is used to estimate the average recurrence of the MCE. Considering this slip rate and the earthquake recurrence relationship for the Castle Mountain fault (Figure 5-9), and applying the model for the proportion of slip caused by the maximum credible earthquake (Appendix A.7), we have estimated that a magnitude (M_S) 7.5 earthquake can occur on the Castle Mountain fault with an average recurrence of 235 years.

There is no documented displacement along the Castle Mountain fault in historic time. Plafker (1969) reports no observed displacement during the 1964 Prince William Sound earthquake. A magnitude (M_S) 7.0 earthquake occurred in the vicinity of the Castle Mountain fault west of Anchorage in 1933. It is not known if the earthquake was related to the Castle Mountain fault, and no investigations to look for surface displacements have been reported (Page and Lahr, 1971).

Detterman and others (1976) have reviewed historical seismicity in the vicinity of the fault for the time period 1934 through October 1974. Most of the events in the vicinity of the fault have reported focal depths of more than 19 miles (30 km) with the precision in hypocenter depths estimated by the authors to be up to

±12 miles (20 km). The depth of these earthquakes suggests that the events may be occurring at depth below the crust. In summary, there has been seismic activity in the vicinity of the fault but no reported correlation of earthquakes with the fault.

The Castle Mountain fault was classified during this investigation as being a fault with recent displacement. The effect of potential seismic ground motions from the Castle Mountain fault is considered to be significantly less than that of the Denali fault because the Denali fault has the potential for a larger earthquake and is closer to the sites (as discussed in Sections 7 and 8). The Castle Mountain fault is too far from the sites to affect potential surface rupture considerations.

4.3.2 - Denali Fault

The Denali fault is predominantly a right-lateral strike-slip fault that is approximately 1,358 miles (2,190 km) long (Richter and Matson, 1971). The fault consists of a number of segments and has an arcuate east-west trend in the site region as shown by Grantz (1966) and Richter and Matson (1971), among others. North of the site, the fault divides into two traces or strands. The northerly segment is the Hines Creek strand, as shown in Figure 8-2 of the Interim Report (Woodward-Clyde Consultants, 1980b). The southerly strand is the part of the McKinley strand that passes within 43 miles (70 km) north of the Watana site and 40 miles (64 km) north of the Devil Canyon site.

The fault has been the subject of numerous studies and is generally agreed to represent a major suture zone within the earth's crust as discussed by St. Amand (1957), Grantz (1966), Cady and others (1955), Richter and Matson (1971), Page and Lahr (1971), Stout and others (1973), Forbes and others (1973), Wahrhaftig and others

(1975), Hickman and others (1978), and Stout and Chase (1980), among others. The total amount of displacement along the fault is the subject of continuing discussion. Some investigators suggest the amount of strike-slip displacement is relatively small (Csejtey, 1980), while others cite evidence supporting total displacements of up to 155 miles (250 km) (St. Amand, 1957).

The Hines Creek strand of the Denali fault is believed to be the older of the two strands with strike-slip displacement ceasing by approximately 95 million years before present (m.y.b.p.) (Wahrhaftig and others, 1975; Hickman and others, 1976). Subsequent strike-slip displacement has principally occurred along the McKinley strand of the Denali fault (Wahrhaftig, 1958; Grantz, 1966; Hickman and Craddock, 1973; Stout and others, 1973). Because the McKinley strand is the closer of the two strands to the sites, and because most of the major strike-slip displacement is thought to be occurring along this strand (rather than along the Hines Creek strand), the Denali fault (in the site region) was considered for the purposes of this investigation to consist of the McKinley strand along with the Togiak-Tikchik fault segment, the Holitna fault segment, the Farewell fault segment, and the Shakwak valley fault segment (west of the Totschunda fault), as described by Grantz (1966). These segments and the McKinley strand comprise the Denali fault as cited in this report. The Denali fault is shown in Figures 1-1 and 4-1.

Aerial reconnaissance of the fault in the vicinity of Cantwell during this study revealed strong morphologic expressions of recent displacement, such as fault scarps, offset ridges, linear valleys, and sag ponds in bedrock or surficial sediments of undefined age. The linearity of these features across the topography suggests that the fault plane is close to vertical in this area.

Holocene age displacements along the southern segment have been studied by several investigators. In the Nenana River area, Hickman and Craddock (1973) found evidence for as much as 443 feet (135 m) of right-lateral displacement and 10 to 13 feet (3 to 4 m) of dip-slip offset, with the south side up relative to the north side, in Holocene time. These data suggest a displacement rate of approximately 0.53 inches/year (1.3 cm/year). Stout and others (1973) measured right-lateral offsets as great as 197 feet (60 m) and as much as 33 feet (10 m) of dip-slip displacement, with the north side up relative to the south side, in Holocene units east of the Black Rapids Glacier (northeast of the site region); on the basis of these data, they estimated the displacement rate to be between 0.20 and 0.24 inches/year (0.5 and 0.6 cm/year) of right-lateral motion and less than 0.06 inches/year (0.15 cm/year) of dip-slip motion during Holocene time. Other studies, including Plafker and others (1977), Hickman and others (1977; 1978), and Richter and Matson (1971), found evidence supporting a displacement rate between 0.4 to 1.4 inches/year (1.0 to 3.5 cm/year) on the southern segment in Holocene time.

In summary, displacement rates in Holocene time along the Denali fault locally range from approximately 0.2 to 1.4 inches/year (0.5 to 3.5 cm/year). Considering this slip rate and the earthquake recurrence relationship for the Denali fault (Figure 5-9), and applying the model for proportion of slip caused by the maximum credible earthquake (Appendix A.7), we have estimated that a magnitude (M_S) 8 earthquake can occur on the Denali fault with an average recurrence of 290 years. There is no documentation of displacement on the fault in historic time. Hickman and others (1978) suggest that the latest movement was several hundred to several thousand years ago.

Review of historic seismicity during this investigation, including review of other published historical seismicity studies (e.g., Tobin and Sykes, 1966; Boucher and Fitch, 1969; Page and Lahr, 1971), suggests that seismic activity has occurred in the vicinity of the Denali fault. This seismicity includes microseismicity reported by Boucher and Fitch (1969) and macroseismicity, i.e., events of up to magnitude (M_S) 5 to 6 (Tobin and Sykes, 1966). As discussed in Section 5.1, two large earthquakes (magnitude greater than 7) have occurred in the general vicinity of the Denali fault. However, uncertainties in the location and focal depth of these events preclude their correlation with the Denali fault.

The Denali fault was classified during this investigation as being a fault with recent displacement. The fault affects consideration of the potential for seismic ground motions at both sites. However, the fault does not affect consideration of surface rupture potential through either site because of the distance of the fault from the sites.

4.3.3 - Benioff Zone

The Pacific plate is moving northwestward at a relatively faster rate than the North American plate. Along the Aleutian Trench in the Gulf of Alaska, the differential rate of movement is accommodated by subduction or underthrusting of the Pacific plate beneath the North American plate, as shown in Figure 4-1. The subducting Pacific plate dips beneath Alaska to a depth of approximately 93 miles (150 km), as discussed by Packer and others (1975), Davies and House (1979), Agnew (1980), and Lahr and Plafker (1980).

Evidence for the subducting Pacific plate is the zone of seismicity associated with the plate. This zone of seismicity, the Benioff

zone, has been observed in the site region by Davies (1975) and Agnew (1980) and is discussed in Section 5 and shown in Figure 5-7. Southeast of the site (beneath the Matanuska Valley region), the Benioff zone becomes decoupled from the North American plate and increases in dip. Hypocentral data obtained during this investigation show the Benioff zone to be at depths of 31 miles (50 km) and 38 miles (61 km) at its closest distance to the Watana and Devil Canyon sites, respectively (Figure 5-7).

The Benioff zone is considered to consist of two subzones or regions separated by a transition zone, as discussed in Section 5.2.1 and shown in Figure 5-7. The two regions are referred to as the interplate region and the intraplate region. The interplate region includes earthquakes along the interface between the crustal plate and the subducting plate. The intraplate region is that portion of the Benioff zone that is detached from and dips beneath the crustal plate. This region includes earthquakes that occur within the subducting plate.

Both regions of the Benioff zone are considered to be a source of seismicity for the sites. This judgment is based on the association of earthquakes with the downgoing slab and the proximity of the slab to the sites. The zone is not considered to affect consideration of surface rupture potential through the sites because of the depth of the zone at the sites and the decoupling from the crust.

4.4 - Features Within the Talkeetna Terrain

4.4.1 - Watana Site

Talkeetna Thrust Fault

The Talkeetna thrust fault is a reverse or thrust fault that was active during Cretaceous and early Cenozoic time, more than 50 million years ago (Figure 4-2). Although it is apparently very old, it is the largest identifiable fault that passes near the dam sites; therefore, field studies were conducted to detect any evidence for recent fault displacement.

The Talkeetna thrust fault generally trends N50°E and passes 4 miles (6.5 km) southeast of the Watana site and 16 miles (25 km) southeast of the Devil Canyon site. The fault is approximately 78 miles (126 km) long and is part of a longer zone of deformation that includes the Broxson Gulch fault to the northeast (Beikman, 1974a) and an inferred extension beneath the Susitna lowland to the southwest (Csejtey and others, 1980).

The Talkeetna thrust fault is recognized primarily as a lithologic contrast of regional extent between early Cretaceous or Jurassic and older volcanic and sedimentary rocks of the Wrangellia terrane to the southeast, and Lower Cretaceous sedimentary rocks of the Maclaren terrane to the northwest (Figure 4-3) (Csejtey and St. Aubin, 1981). Adjacent to the fault within the site region, the Wrangellia terrane includes interfingered subaerial and submarine basalt, argillite, sandstone, and limestone (Silberling and others, 1981). The Maclaren terrane includes argillite and greywacke sandstone (Csejtey and St. Aubin, 1981). Both terranes have been metamorphosed.

Csejtey and others (1978) suggest that the Talkeetna thrust fault is associated with large-scale thrust faulting along the continental margin that juxtaposed the Maclaren and Wrangellia terranes in late Mesozoic to Tertiary time, 50 to 100 m.y.b.p. Faults of this type have been found throughout southcentral Alaska; they are the result of accretion of parts of the Pacific plate onto the North American plate during Cretaceous and early Tertiary time (Jones and Silberling, 1979).

This accretionary process initially started in the Fairbanks area in Jurassic time approximately 141 to 195 m.y.b.p. As accretion continued through geologic time, the faulting associated with it shifted southward from the Tintina fault near Fairbanks, through the area of the Talkeetna thrust fault, and is currently occurring in the Gulf of Alaska along the Aleutian trench. Thus, the tectonic environment in which the Talkeetna thrust fault is believed to have been active is no longer present in the Talkeetna Terrain. Faulting is now occurring along the Aleutian trench.

The location of the fault is imprecisely known along major sections of its length because it is covered by relatively young (Cenozoic) deposits except in the headwaters of Windy Creek (east of Location W1), and at Locations W9 and W10 near the Talkeetna River (Figure 4-4). Between these locations, the fault is inferred to be located between outcrops of the Maclaren and Wrangellia terranes that are widely separated by areas covered by younger Cenozoic sediments. The location of the fault can be inferred to be within a three-mile- (4.8-km-) wide band along most of its length and within a one-mile- (1.6-km-) wide band at the Susitna River (near location W5 in Figure 4-4).

The Talkeetna thrust fault dips steeply to the southeast according to: geologic mapping conducted during this study; the work of Turner and Smith (1974) and Csejtey and others (1978); and aeromagnetic surveys of the Talkeetna Mountains quadrangle (Csejtey and Griscom, 1978). Southwest of Denali to the town of Talkeetna, the aeromagnetic surveys and geologic mapping suggest a southeastward to near vertical dip of the fault. The southeastward dip is the original dip from early Cenozoic formation of the fault (Csejtey and St. Aubin, 1981).

Northeast of Denali, the lithologic contrast between the Wrangellia and Maclaren terranes can be recognized across northwest-dipping thrust faults. Outside the project region to the northeast, Stout and Chase (1980) and Chase (1980) have observed Oligocene dikes and sediments that are offset by the northwest-dipping Broxson Gulch thrust fault. Nokleberg (1981) has extended the Broxson Gulch fault into the project region on the basis of detailed mapping of the Mount Hayes quadrangle. Detailed geologic mapping of the adjacent Healy quadrangle by Smith (1981) shows the same lithologic contrast and northwestward fault dip east of Denali. Because of these similarities, we applied the name Broxson Gulch to the zone of deformation east of Denali.

West of the Susitna River at Talkeetna, the aeromagnetic data across the lithologic contrast were interpreted by Griscom (1979) to suggest an unconformity that dips to the northwest rather than a fault. The unconformity is also broken by later northwest-trending faults (Griscom, 1979). Displacement by later faulting and loss of character as a fault begin at the Talkeetna River (near location W10 in Figure 4-4).

Although they may be part of the same long zone of deformation, each part of the zone may be a different tectonic boundary. The different segments may have developed as separate faults having an opposite sense of underthrusting in Cretaceous and early Tertiary time. Alternatively, the Talkeetna thrust fault may represent the original dip of the zone of deformation to the southeast, with the Broxson Gulch thrust fault and inferred southwestward extension having been rotated to a northwestward dip by later deformation.

Field studies were conducted along the Talkeetna and Broxson Gulch thrust faults during 1981 to: 1) confirm the basis for differentiating the two faults, 2) refine knowledge of the nature of the Talkeetna thrust fault, and 3) assess whether the fault has been subject to recent displacement (i.e., displacement within the past 100,000 years). During these studies, a number of key locations were mapped or logged that contributed significantly to our understanding about the nature and age of the Talkeetna thrust fault. The key locations are shown in Figure 4-4.

The Windy Creek cross-section at location W1 is representative of the Broxson Gulch trust fault. The fault dips to the north, and the lithologic contrast is between metasedimentary rocks of the Maclaren terrane and volcanic rocks of the Wrangellia Terrane (Figure 4-5). The northward dip is inferrred from the northwestward dip of overturned drag folds in Windy Creek, which is consistent with the dip inferred from mapping by Smith (1981) and Nokleberg (1981). Smith (1981) suggests that the Maclaren terrane was thrust over the Wrangellia terrane in the same direction as on the Broxson Gulch thrust fault in the Mount Hayes quadrangle.

The cross-section of the fault near Butte Creek at location W2 is believed to be typical of the Talkeetna thrust fault in the vicinity of the dam sites (Figure 4-6). However, the Talkeetna thrust fault itself is covered by Quaternary glacial sediments in Butte Creek valley and in the vicinity of the sites. Its location in Butte Creek valley is inferred from the presence of Maclaren terrane rocks within and to the northwest of the valley and Wrangellia terrane rocks to the southeast of the valley. Good exposures in the Clearwater Mountains indicate that the two subsidiary thrust faults shown in Figure 4-6 dip southeastward and have thrust progressively older rocks northwestward over younger rocks. The dip of the Talkeetna thrust fault is inferred to be southeastward, similar to the better exposed subsidiary thrust faults. Aeromagnetic data for the area of Location W2 show a low gradient that was interpreted to suggest a northwestward dip (Csejtey and Griscom, 1978); however, the observed low gradient may well be caused by the intervening fault slices of nonmagnetic sedimentary rock (KJs and TrPs shown in Figure 4-6). The steep gradients of narrow, elongate magnetic highs (southeast of the trace of the fault) appear to be more suggestive of a southeastward dip.

The Talkeetna thrust fault is exposed in the bedrock near the Talkeetna River at Location W9, on Talkeetna Hill (Figure 4-7). Here the fault traverses an area of low relief and is marked by a sharp differential erosion contrast between the argillite on the northwest and basalt on the southeast. The fault is inferred to extend southwest from this area of low relief, down a steep canyon. The slightly sinuous trace and steeply northwestward dipping axial planes of folds indicate that the fault dips steeply to the northwest or is vertical (Figure 4-8).

The detailed variation in lithology within the fault zone at Location W9 is shown in Figure 4-9. The zone is approximately

180 feet (55 m) wide between competent argillite on the northwest and competent basalt on the southeast. The rock units in between are slightly to extremely sheared.

Tertiary age rocks near the fault at Watana Creek, Fog Creek, and Talkeetna Hill were evaluated for the presence of deformation that would be related to displacement on the Talkeetna thrust fault during or after the Tertiary period.

At Watana Creek, the inferred trace of the Talkeetna thrust fault is less than one mile (1.6 km) from 15 good exposures of Oligocene deltaic and marine sediments distributed along a 7-1/2-mile- (12-km-) long stretch of Watana Creek (Figure 4-10). The sediments have been folded (with minor faulting) into northwest trending anticlines and synclines. The orientation of these folds strongly suggests that they are related to a northeast-southwest compressional stress regime that has existed since deposition of the sediments approximately 22.5 to 38 m.y.b.p. The northeast-southwest compression is inconsistent with significant thrust or lateral faulting along the Talkeetna thrust fault.

At Fog Creek (Location W6 in Figure 4-4), undated Tertiary volcanic rocks overlie approximately one-third of a three-mile- (4.8-km-) wide area across the inferred trace of the fault. Although undated, these volcanic rocks are probably similar in age (50 m.y.b.p.) to the volcanic rocks at Talkeetna Hill (Location W8, Figure 4-4). The Tertiary volcanic rocks are flat-lying to gently tilted. Deformation of the volcanic rocks would be expected to be more extensive if the Talkeetna thrust fault had been active at a low level during the past 50 million years.

The absence of recent displacement on the Talkeetna thrust fault is supported by overlying volcanic rocks and later faulting that displaces the Susitna segment. At Location W8, the Talkeetna thrust fault projects beneath Tertiary andesite and basalt (Figures 4-7 and 4-8). The volcanic rocks are not displaced by the fault; thus, this part of the Talkeetna thrust fault has not been active since the volcanic rocks were deposited. The age of these rocks has been estimated from a potassium-argon age date (Csejtey and others, 1978) as 50 m.y.b.p. Because this part of the fault has not been subject to displacement for at least 50 million years, it provides strong circumstantial evidence that the Talkeetna thrust fault has not had recent displacement near the dam sites 20 miles (32 km) to the northeast. The Talkeetna thrust fault is also displaced by later faulting at the Talkeetna River (Figure 4-7). Several miles (several kilometers) of displacement have occurred on this and similar faults since the Talkeetna thrust fault had displacement along it.

Low-sun-angle aerial photographs were interpreted for the Talkeetna thrust fault between Location W2 and the intersection with the Susitna feature near the Talkeetna River (Figure 4-4). Seven linear features were observed that were considered to have a low to moderate likelihood of being fault related. These seven features were then field checked to evaluate their origin. Of the seven features, six were found to be clearly of glacial origin. One of the seven features, at location W7 (Figure 4-4) was considered to have a moderate likelihood of being fault related.

The feature at location W7 is a N68°E trending linear scarp (Figure 4-11) that is approximately 1,700 feet (518 m) long and 7 feet (2.1 m) high and has a northwest facing slope of 26 degrees (Figure 4-11). The feature is located within 0.5 miles

(0.8 km) of the inferred location of the Talkeetna thrust fault. Tertiary and Quaternary cover in this area precludes precise location of the fault trace. The scarp at location W7 is similar in form to a fault-related scarp.

Trench T-1 was excavated across the scarp in sediments that are glacial in origin and of probable Late Wisconsin (25,000 to 15,000 y.b.p.) age; this age estimate was based on the elevation and surface morphology (Figure 3-4). Examination of the exposures in the trench showed that the sediments are not faulted at the base of the scarp or northwest of the scarp within the trench (Figures 4-12 and 4-13).

On the basis of the logging of the trench and detailed mapping of nearby glacial deposits, the scarp is interpreted to mark the edge of the Late Wisconsin ice sheet. At the margin of this ice sheet a large ice-marginal river flowed parallel to the scarp and nearly perpendicular to the trench. The direction of flow is indicated by the orientation of channel banks across the trench at three locations. The river flowed across lodgement till (Unit 6 in Figure 4-12) and the ice sheet to the northwest of the scarp. The river carried a heavy bedload of gravel (Unit 5). When the ice sheet melted, the gravel collapsed onto the lodgement till (Unit 6) northwest of the scarp. As evidence of this collapse, bedding and clast orientations appear to have been slightly disrupted within the trench in the interval 95 to 105 feet (29 to 32 m).

Trench T-2 was excavated at Talkeetna Hill, Location W10 (Figure 4-4). The trench site was selected because it is on a clear trace of the Talkeetna thrust fault, and because the low swale along the fault may have preserved Early Wisconsin sediments. At this location, the fault is a zone of deformation approximately

180 feet (55 m) wide. Logging of the trench showed that the Wisconsin glacial sediments had been flushed from the swale and replaced by colluvium and loess of probable Holocene age (Figure 4-12 and 4-14). No fault displacement was observed in these Holocene sediments. However, the youth of these sediments makes this observation relatively insignificant. Bedrock within the trench was observed to be locally highly sheared (Figures 4-9 and 4-12).

The Talkeetna thrust fault is judged to be a fault without recent displacement for the following reasons:

1) Tertiary volcanic rocks with a potassium-argon age date as being 50 m.y.b.p. (Csejtey and others, 1978) in age overlie the fault near the southwest end of the fault (Location W8). These volcanic rocks have not been displaced.

2) There is no evidence of faulting in surficial units whose age is 15,000 to 25,000 y.b.p. (Location W7).

3) Folding of Oligocene strata in Watana Creek (Location W3) suggest that deformation is being accommodated in a fashion that is inconsistent with fault displacement along the Talkeetna thrust fault.

4) The Talkeetna thrust fault is offset at least six miles by younger faulting at the Talkeetna River south of Location W10.

5) The Talkeetna thrust fault is the result of continental accretion during late Cretaceous and early Tertiary time. The present site of continental accretion is 350 miles (564 km) to the south-southeast.

Therefore, the Talkeetna thrust fault does not affect consideration of seismic ground motion or surface rupture potential at either the Devil Canyon or Watana Dam sites.

Susitna Feature (KD3-3)

The Susitna feature is a northeast-southwest trending lineament that is 95 miles (153 km) long and approaches to within 2 miles (3.2 km) of the Watana site (Figure 4-4). The feature was first described by Gedney and Shapiro (1975) as a prominent topographic lineament, which they observed on LANDSAT imagery. These authors postulated that the lineament was a fault, in part on the basis of data assembled by Turner and Smith (1974), which is described below, and also on the basis of their interpretation of seismic activity in the vicinity of the southern end of the feature.

Evidence that the feature is a fault has been inferred by Turner and Smith (1974) in the Susitna Glacier area of the south flank of the Alaska Range. The inference is based on K-Ar dates on plutonic bodies and interpreted cool-down rates associated with these plutons (Smith, 1980). According to this hypothesis, the plutonic units on the east side of the Susitna feature cooled down more rapidly than those on the west side of the feature, suggesting that the west side was at greater depth than the east and, subsequently, was faulted up into contact with the units that cooled down more rapidly.

Gedney and Shapiro (1975) report that the Susitna feature corresponds to the eastern boundary of the metasedimentary units in the project area; however, mapping by Turner and Smith (1974) and Csejtey and others (1978) shows metasedimentary rocks extending east of the Susitna feature several miles (several

kilometers) to the Talkeetna thrust fault. Csejtey and others (1978) report finding no evidence for the postulated Susitna feature.

Gedney and Shapiro (1975) also suggest that there is seismic activity associated with the Susitna feature. In particular, they cite a magnitude (m_b) 4.7 event that occurred on 1 October 1972 and a magnitude (m_b) 5.0 event that occurred on 5 February 1974. The location given by Gedney and Shapiro (1975) shows the earthquakes to be spatially close to the surface trace of the Susitna feature. They hypothesize that the focal mechanisms suggest a right-lateral strike-slip sense of displacement.

Review of the 1972 and 1974 earthquakes during this investigation showed that, with the error in location reported by Gedney and Shapiro (1975), the two epicenters could be more than 8 miles (13 km) from the feature and that the focal depths put the events at depths of 46 to 47 miles (75 to 76 km). Even with the imprecision associated with focal depth determinations, it is reasonable to associate these two earthquakes with the Benioff zone. The correlation of these events with the Susitna feature appears to be unwarranted because the Susitna feature lies in the crust and the maximum thickness of crust is approximately 12 miles (20 km) as shown in Figure 5-7.

Field studies were conducted during 1981 to: 1) locate any evidence that the Susitna feature is a fault; and 2) evaluate the likelihood that the feature is a fault with recent displacement. Figure 4-4 shows field locations where interpretation of rock exposures and surficial deposits contributed important knowledge about the nature or age of the Susitna feature.

Bedrock was mapped at five key locations to assess whether or not the Susitna feature is a bedrock fault. These locations, shown in Figure 4-4, are the Butte Lake area (Location W11), outcrops between Butte Lake and Deadman Lake (Location W13), an outcrop near Deadman Lake (Location W14), Tsusena Creek (Location W15), and the Talkeetna River south of the confluence with Prairie Creek (Location W16). Each of these locations is discussed below.

The Butte Lake area has been mapped by Smith (1973). Some of the results of this mapping are summarized on a map by Turner and Smith (1974). As a result of their mapping, Turner and Smith (1974) inferred that the Susitna feature may be a fault because of relationships of crystalline units on either side of the valley in which the Susitna feature is located. They observed no evidence of a fault in the lowland where bedrock is covered by glacial deposits.

During the 1981 study, mapping was conducted by Woodward-Clyde Consultants in the Butte Lake area (Figure 4-15, Location W11). The lithologic units shown by Turner and Smith (1974) were confirmed; however, the relationship of these units can be explained by several reasonable alternatives (including the presence of a fault). No direct or indirect evidence of a fault was observed, and there is circumstantial evidence of no faulting on the basis of the geophysical data described below. Smith (1980) has re-examined his mapping of the Butte Lake area and did not find evidence of a fault. In addition, he has not observed evidence of the Susitna feature being a fault at any location other than the Susitna Glacier area.

Three magnetometer traverses were conducted at Location W11 (Figure 4-16). One of the traverses was run across the lowland

in which the Susitna feature is located. Two of the traverses were run across mapped contacts between lithologic units; these traverses served to calibrate the magnetic signature between units where no fault was inferred. As shown in Figure 4-16, the traverse across the Susitna feature (profile 2A) shows no change in magnetic signature across the Susitna feature (shown by Turner and Smith [1974] as a mapped contact between the paragneiss and the migmatitic intrusive rocks). The magnetic signature is nearly identical with that observed in profile 1 which crosses the contact between the same two rock units where no fault is inferred. Although the absence of a magnetic anomaly is not conclusive evidence of no faulting along the Susitna feature, it does provide circumstantial evidence that a fault is not present.

No evidence of a bedrock fault was observed at Location W14 between Deadman and Butte Lakes. At Location W13 near Deadman Lake, minor faulting and a bedrock shear zone was observed within one mile (1.6 km) of the trace of the Susitna feature. The orientation of the shear zone is subparallel to that of the Susitna feature. This faulting and shear zone are similar to that observed elsewhere in the site region and are not considered to be related to a throughgoing fault zone.

Tsusena Creek (Location W15) is the one location in the site region that has exposed bedrock where the Susitna feature is mapped. Turner and Smith (1974) show the Susitna feature as a fault that cuts across meanders in the creek. Mapping in 1980 and 1981 showed no evidence of a fault in the canyon walls of Tsusena Creek. A prominent oxidized zone with shearing and faulting is present in the creek. However, mapping at this exposure showed the oxidation to be related to a secondary intrusion within the host granitic rocks. The faulting and shearing within the oxidized zone is oriented northwest-south-

east, at right angles to the Susitna feature. This structural orientation appears to be related to the Fins feature (as discussed below in this section), not to the Susitna feature. Therefore, we have concluded that there is no evidence of a major fault passing through Tsusena Creek with an orientation parallel to that of the Susitna feature.

At Location W16 on the Talkeetna River, joint orientations were measured to make an assessment as to whether the Susitna feature could be related to joint control. No evidence of a fault was observed at this location and the joint orientations are at right angles to the trend of the Susitna feature.

Low-sun-angle aerial photographs were interpreted for the Susitna feature between Location W16 and the Denali Highway near Location W11 (Figure 4-4). Twenty-eight lineaments were marked for consideration of their possible relation to faulting. On the basis of interpretation of the aerial photographs, all but 10 of the lineaments were explained by glacial processes or were not part of a pattern of lineaments that might be related to faulting. These ten remaining lineaments were field checked and, on this basis, assigned to a glacial origin or very low likelihood of relation to surface rupture by faulting.

One lineament at Location W12 was trenched in order to confirm our interpretation of glacial origin for the lineaments. For this purpose, a prominent scarp was selected that is oriented parallel to and within 500 to 2,500 ft (152 to 762 m) of the Susitna feature (Figure 4-17). The scarp is approximately 18 feet (5.5 m) high and 8,000 ft (2.4 km) long.

The slope of the scarp is approximately 22° and faces eastward. Examination of exposures in the trench (Figures 4-18 and 4-19)

showed that the scarp is the product of glacial processes, probably an ice contact process. No faults were observed in the trench and the glacial sediments are continuous across the base of the scarp and 90 feet (27 m) to the southeast. On this basis, we have concluded that the scarp is not related to faulting and that the other morphologically similar scarps are also not related to faulting.

The Susitna feature is judged to be a lineament that is not related to faulting, except for possible consequent erosion along some bedrock faults at Location W13. This judgment is based on the following reasons:

1) Bedrock exposures at three locations within the topographic valley forming the Susitna lineament show no evidence of faulting or subparallel joints.

2) The outcrop pattern of late Mesozoic and early Tertiary bedrock at Butte Lake does not support the existence of a fault. Although it is possible to hypothesize the existence of a fault, a fault is not required to explain the outcrop pattern.

3) No evidence of a fault was observed in Tsusena Creek where the Susitna feature crosses exposed rock in canyon walls.

4) Glacial sediments that overlie the fault along most of its length do not have any surface geomorphic features related to fault rupture of the ground surface. The age of these glacial sediments is primarily 25,000 to 9,000 y.b.p.

5) A trench excavated across a prominent scarp located along the Susitna lineament revealed that the scarp is not related to faulting and is of glacial origin.

We classified the Susitna feature as being a lineament; therefore, it does not affect consideration of seismic ground motion or surface rupture potential at either site.

Watana Lineament (KD3-7)

The Watana lineament trends approximately east-west along the Susitna River for a distance of 31 miles (50 km). At its western end, the lineament passes through the Watana site (Figure 4-20). The lineament was identified by Gedney and Shapiro (1975) on LANDSAT and SLAR imagery; they reported no fault control was reported. At the scale of the imagery, the lineament approximately corresponds to a series of somewhat linear sections of the Susitna River between approximately the confluences of Tsusena Creek on the west and Jay Creek on the east.

Field studies were conducted in 1981 to: 1) search for bedrock outcrops across or near the plotted location of the lineament, and 2) search for any evidence of Quaternary faulting.

Locations along the Watana lineament where exposures of Mesozoic bedrock occur near the lineament were checked for the presence of direct or indirect evidence of faulting (Figure 4-20). Exposures of bedrock were observed by aerial reconnaissance or ground investigation at Locations W17, W19, W20, and W22. Color aerial photographs (at a scale of 1:24,000) of bedrock outcrops at Locations W24 and W25 were interpreted for linear features that might be related to faulting.

Approximately six miles (10 km) upstream of the Watana site, the lineament cuts across the south bank of the Susitna River and trends across the low plateau northwest of Mount Watana (Figure 4-20). No evidence of faulting was observed at Location

W19 or at a small outcrop in a canyon at Location W22. A large hill of argillite that is separated from the canyon wall of the Susitna River is located at Location W20. A zone of sheared rock in the east side of the hill trends approximately N65°E. Joints at Location W20 trend approximately N45°E. The zone of sheared rock and joints are representative of the small-scale faults and joints found throughout the Talkeetna Terrain and are not considered indicative of fault control for the Watana River lineament.

Bedrock exposures along the east and west projection of the lineament (Locations W17, W24, and W25) show no evidence of faulting. Angle borings DH-21 and BH-6 drilled at the Watana site by Acres American Inc. and the U.S. Army Corps of Engineers, respectively, show no evidence of a throughgoing structural zone, although there is a remote possibility that such a zone could be present that would not have been encountered by the borings across the Susitna River at the Watana site.

Low-sun-angle color infrared and color aerial photographs were interpreted for the Watana lineament. The color aerial photographs cover the entire lineament as far east as Location W24, and the color infrared photographs cover the lineament as far east as Location W22. No lineaments or patterns of lineaments suggestive of youthful faulting were observed on the photographs; however, several short, isolated lineaments were field checked. All of these lineaments were interpreted to have glacial origin or to be related to surface processes such as slumping. The triangular areas on the west end (Location W18, Figure 4-20) and the east end (Location W23, Figure 4-20) were intensively checked for subparallel or splay lineaments. These two areas, like Location W21, are on plateau areas where some surface morphologic

expression should reveal the presence of a fault. No surface morphology was observed that might be related to a fault along the Watana lineament.

The Watana lineament is judged to be a series of disconnected short lineaments that are not related to youthful faulting. Therefore, it does not affect consideration of seismic ground motion or surface rupture potential at either site.

Fins Feature (KD4-27)

The Fins feature is a shear zone or fault that trends northwest-southeast between the Susitna River and Tsusena Creek and is nearly vertical (Figure 4-21). The feature is 2 miles (3.2 km) long and is shown as a shear zone or fault dipping 70° to 75° to the northeast on an undated U.S. Army Corps of Engineers Alaska District map (Plate D5 entitled "Watana Reservoir Surficial Geology"). The Fins feature is prominently exposed on the north side of the Susitna River (Location W27) as a series of vertical shear zones, which has a total width of approximately 400 feet (122 m). The shear zone is approximately 2,500 feet (762 m) upstream from the proposed Watana dam axis and is in a dioritic unit mapped as being Paleocene in age by Csejtey and others (1978).

Evidence of the feature has not been observed on the south side of the Susitna River (Location W28). However, the south bank does not have the prominent bedrock exposures that are present on the north bank in this area.

The Fins feature observed on the north bank of the Susitna River appears to correlate with a moderately to highly weathered, oxidized shear zone present on the northeast bank of Tsusena

Creek approximately 2 miles (3.2 km) upstream from the confluence with the Susitna River at Location W15.

Joint measurements were obtained during the 1980 field season by Acres American Inc. and Woodward-Clyde Consultants in Tsusena Creek (Location W15 and other locations). These measurements show a prominent northwest-southeast trending set of joints that dip steeply northeast to southwest.

Observations during this investigation at Tsusena Creek included that of a 6.5-foot- (2-m-) wide fault zone (within the oxidized zone) that is oriented N30°W and dips 72°NE. The fault zone is in granitic units of reported Paleocene age and contains mylonite and possibly pseudotachylite. Elsewhere in the oxidized zone, small-scale faults oriented northwest-southeast with a northeast dip and slickensides were observed. The faulting and shearing at Location W15 appears to be related to shearing associated with the intrusive events rather than due to displacement along a fault zone.

No evidence of the feature was observed northwest of the Tsusena Creek exposure. However, prominent exposures similar to that at Tsusena Creek are lacking.

The Fins feature appears to underlie a morphologic depression in surficial units between the Susitna River and Tsusena Creek. It is also coincident, in part, with a buried paleochannel, which is filled with glacial deposits. Evidence for the paleochannel is based on seismic refraction studies conducted by Dames and Moore (1975) and Woodward-Clyde Consultants (1980a; 1982).

The approximately triangular areas at W26 and W29 (Figure 4-21) were investigated for surface morphology that might be related to

an extension of the Fins feature to the northwest or southeast. Low-sun-angle color infrared and color aerial photographs at a scale of 1:24,000 were interpreted for subparallel and splay lineaments. No lineaments were found. Several lineaments trending at a high angle to the Fins feature were checked to confirm their relation to glacial processes.

The Fins feature is judged to be a fault at the Susitna River, but its relation to faulting at Tsusena Creek is questionable. No Quaternary expression of the feature was found between the Susitna River and Tsusena Creek or along the two projections of the feature.

The Fins feature was classified as a fault without recent displacement; therefore, it does not affect consideration of seismic ground motion or surface rupture potential at either site.

This judgment is supported by the extremely short length of the feature and the tectonic setting of the region. Experience in other parts of Alaska and other areas of the world, including California, Japan, and South America, suggests that short faults with recent displacement exist in association with other longer faults whose recency of displacement is clearly recognizable. That is, if a region is being subjected to stresses that are of sufficient magnitude to cause surface faulting, it is extremely unlikely that strain release in the region would produce no surface rupture longer than along one fault a few miles (a few kilometers) in length. Rather, it is logical to expect that the strain release would cause extensive rupture during some earthquakes and smaller amounts of rupture on both the main faults and shorter subsidiary faults.

4.4.2 - Devil Canyon Site

Feature KC5-5

Feature KC5-5 trends N15°W for a distance of 12 miles (19 km) and approaches within 4.5 miles (7 km) east of the Devil Canyon site (Figure 4-22). The feature was originally identified as a lineament, in part, by Gedney and Shapiro (1975) on LANDSAT imagery. Subsequent examination of U-2 photography and aerial reconnaissance during the 1980 field study resulted in the extension of the lineament at its northern and southern ends. North of the river the lineament is a linear stream drainage. South of the river the morphologic expression is that of a prominent linear canyon that becomes a shallow linear depression (Figure 4-22).

Review of the feature in 1980 and 1981 showed clear evidence of fault control in the canyon south of the Susitna River (Segment 2 in Figure 4-22) as well as possible fault control along a scarp at the southern end of the feature (Segment 4 in Figure 4-22). For the purposes of this investigation, the feature was considered to be a fault along its entire length; it is referred to in this report as Fault KC5-5.

Four segments of the fault are discussed below; each segment has characteristics which bear on the consideration of whether or not the original lineament is a fault and/or on the recency of displacement. Segment 1 is the section north of the Susitna River; Segment 2 is the 6-mile- (10-km-) long section south of the Susitna River which is marked by a prominent canyon; Segment 3 is the upland plateau south of the canyon section; and Segment 4 is the low, curvilinear scarp at the southern end of the fault, which was shown in Figure 8-12 of the Interim Report (Woodward-Clyde Consultants, 1980b).

Segment 1 is a linear stream drainage north of the Susitna River which has no observed outcrops and no evidence which conclusively confirms or precludes a fault origin. Joint measurements taken on the north side of the Susitna River, approximately 656 feet (200 m) up river from Segment 1, have a subparallel orientation suggesting possible joint control of this segment of Fault KC5-5.

Segment 2 is a prominent canyon which is approximately 6 miles (10 km) long and has a maximum relief of 1,000 feet (305 m). Rugged terrain and limited access at the bottom of the canyon precluded ground observations. However, detailed aerial review of the canyon by helicopter showed clear evidence of faulting in the canyon at three locations (summarized as Location D1 in Figure 4-22). The observed fault zones are parallel to the axis of the canyon and are observable in three ridges which jut into the canyon.

The zones are aligned, have orientations of N15°W to N20°W, and are near vertical. The zones form sharp, distinct boundaries between what appear to be intrusive rocks. They may also locally separate intrusive rocks from metamorphic rocks. The width of the fault zone varies from a few inches (few centimeters) in width to a few feet (few meters). Locally there is discoloration of the fault zone to a light gray color. No direct evidence of the sense of displacement was observed.

The linear trace of the fault and the canyon suggest that the fault may be predominantly a strike-slip fault; however, a substantial oblique component to the sense of displacement cannot be precluded. If the orientation of the fault zone (approximately N15°W) relative to the generally northwest orientation of the regional maximum compressive stress direction is considered, a strike-slip sense of displacement is reasonable

(assuming that the Mesozoic stress regime associated with accretion of this land mass to the North American craton was responsible for origin of the bedrock fault).

On the basis of observations to date, the amount of displacement along the fault zone cannot be estimated. The prominence of the zone suggests that substantial displacement has taken place, but it isn't clear if this involves several tens of feet (tens of meters) or hundreds of feet (hundreds of meters) of displacement.

This segment of the fault lies within Tertiary intrusive rock units (Figure 4-22) whose age is inferred to be 50 to 60 m.y.b.p. (Csejtey and others, 1978). There are no recent geologic units in this segment of Fault KC5-5 which provide direct evidence about the recency of displacement. However, the faulting is in bedrock, and morphologic relationships in Segment 3, discussed below, strongly suggest that the fault has not been subject to displacement in the last 100,000 years, and probably not in the last several million to several tens of millions of years. The development of the canyon appears to be related to differential erosion along the fault zone. There may be other factors which also contributed to development of the canyon, such as additional faults and/or joints along which differential erosion occurred. The entire canyon shows evidence of both brittle and ductile deformation. Taking into consideration this deformation and the prominent bedrock fault observed in the bottom of the canyon, we have concluded that this segment of Fault KC5-5 is clearly fault controlled.

Segment 3 is a shallow, broad curvilinear depression on the upland plateau which lies south of Segment 2 and the Susitna River (Figure 4-22). Regional mapping by Csejtey and others

(1978) originally suggested that this segment of the feature could be related to a lithologic contact between the Cretaceous argillite and greywacke metasedimentary sequence on the east and the Tertiary intrusive sequence on the west. However, mapping conducted during this investigation shows clearly that the metasediment-intrusive contact is irregular, and it clearly does not coincide with Segment 3 of the fault. The fault lies entirely within the Tertiary intrusive rocks in this segment.

A shear zone is exposed in close proximity to the fault at Location D2 and may be related to the fault. The shear zone consists of highly altered, locally decomposed rock, which may be the result of fault displacement, hydrothermal alteration, or a combination of both processes. The shear zone appears to be related to intrusion of a Tertiary pluton, but conclusive evidence to support this conclusion was not obtained.

Southeast of Location D2 is a broad depression in which meandering streams and marshlike conditions exist. No bedrock exposures are present in this area. The sediments which are present are interpreted to be of Early Wisconsin age (approximately 40,000 to 75,000 years in age) as discussed in Section 3.4. Detailed aerial reconnaissance of this area showed no morphologic features suggestive of fault displacement in the Early Wisconsin sediments. It is, therefore, concluded that there clearly has not been displacement along this fault in the last 40,000 years.

Segment 4 consists of an alignment of linear scarps in bedrock which face northeast on the northeast side of a series of low rises. These scarps can be followed for a distance of 3.2 miles (2 km); the longest scarp is approximately 3,280 feet (1,000 m). The maximum height of the scarp is approximately 3 ft (1 m), and it has a rounded, subdued expression. The terrain is one of

subdued relief with a thaw in the mantle of glacial sediments and in situ soil. Bedrock is exposed intermittently in the area and is rarely exposed at the scarp or near it.

Reconnaissance mapping conducted in 1980 suggested that the scarp could be related to joint control or to slumping. Additional mapping in 1981 suggested that slumping is not a likely cause of the scarp, as there is no morphologic evidence for slumping besides the presence of the scarp itself. The scarp may be joint controlled. Joint orientations near Location D3 (Figure 4-22) are N11°W to N39°W, parallel to subparallel to the N15°W trend that Fault KC5-5 has in this segment. The scarp could, therefore, be related to differential erosion controlled by jointing.

During the 1981 field studies, we examined the possibility that the scarp was controlled by the lithologic contact between the Cretaceous metasedimentary strata to the southwest and the Tertiary intrusive rocks to the northeast. Mapping in and near Location D3 showed that the contact between the two units is irregular, as is typical of such contacts, and that the contact, in general, lies up to a half mile (800 m) northeast of the scarp (Figure 4-22). The scarp, therefore, does not appear to be controlled by a lithologic contact.

A number of springs were observed to emanate from the base of the scarp in or near Location D3. Hand excavation of two of these springs suggested that they emanated from bedrock, but the controlling mechanism within the bedrock was not directly observable. The springs may simply be related to "daylighting" of the groundwater table at the scarp or a decrease in permeability between weathered rock and fresh rock. The springs could also be related to a groundwater barrier imposed by a fault zone.

Our assessment of this segment of the feature is that it could be fault controlled. No direct evidence of faulting was observed; however, circumstantial evidence of faulting (e.g., the springs and the scarp itself) was present, and no compelling alternate explanation for its presence has been found.

Feature KC5-5 was classified during this investigation as being a fault without recent displacement; therefore, it does not affect consideration of seismic ground motion or surface rupture potential at either site. The judgment about fault inactivity is based on the absence of morphologic features in 40,000- to 75,000-year-old sediments which overlie part of the fault, and the absence of any compelling evidence of recent fault displacement (e.g., systematic stream drainage offsets, scarps in recent sediments, or offset of youthful geomorphic units). As discussed in Section 4.2, we believe the level of detectability of surface rupture in this region is approximately 2 to 3 feet (0.5 to 1.0 m) of vertical displacement over a distance of 9 miles (15 km). That is, rupture greater than this would be detectable. We feel that such a displacement has not occurred along this feature during the last 100,000 years.

Feature KD5-2

Feature KD5-2 trends N55°E for a distance of 0.8 miles (1.3 km) and approaches within 3.5 miles (5.6 km) northwest of the Devil Canyon site (Figure 4-22). The feature is a fault mapped by Richter (1967). The fault is described by Richter (1967) as having a strike of N70°E and a dip of 30° to the northwest, although his map shows a strike of N20°E to N60°E for various segments of the fault. Richter (1967) mapped the fault as having normal displacement which downdropped Cretaceous metasedimentary rocks (argillite) on the northwest relative to Tertiary intrusive

rocks (quartz monzonite) on the southeast. The amount of displacement is not reported. The fault zone is exposed in and near Treasure Creek (Figure 4-22) and is described by Richter (1967) as having clay gouge, slickensides, and limonite staining.

Richter (1967) describes the structural setting of the fault to be generally northeast-southwest trending, e.g., fold axes have a strike parallel to the fault strike. From these relationships he concludes that the fault and the other structural features were formed during intrusion of the quartz monzonite. The quartz monzonite was intruded approximately 50 to 60 m.y.b.p., assuming the intrusive is of an age similar to that reported by Csejtey and others (1978) for nearby intrusives.

During the 1980 study, an indistinct linear depression was observed on U-2 photography, which appeared to represent a possible extension of this fault to the northwest. Feature KD5-2 was, therefore, considered to include both the fault and the lineament with a total length of 3.5 miles (5.6 km) as reported in the Interim Report (Woodward-Clyde Consultants, 1980b).

During the 1981 study, large scale (1:24,000 scale) low-sun-angle photography and color photography were reviewed for Feature KD5-2. The indistinct linear depression showed no evidence of fault morphology and no evidence suggesting that it should be considered as part of the fault mapped by Richter (1967). Detailed aerial review during the 1981 study supported this conclusion.

We classified Feature KD5-2 as being a lineament with a short bedrock fault along part of its length; therefore, it does not affect consideration of seismic ground motion or surface rupture potential at either site. Based on the work conducted on this

fault, our conclusion is that a short bedrock fault is present. There is no evidence to suggest that the fault has had recent displacement. The lineament does not now represent a possible extension of the fault (in our judgment). These conclusions are based on Richter's (1967) suggestion that the fault is Mesozoic in age, the absence of any evidence suggestive of a fault with recent displacement, and the extremely short length of the fault.

Feature KD5-3

Feature KD5-3 trends N45°E to N55°E for a distance of 51 miles (82 km) and approaches within 3.6 miles (5.8 km) northwest of the Devil Canyon site (Figure 4-22). Part of the lineament is identified as a fault by Kachadoorian and Moore (1979) on the basis of mapping by Csejtey and others (1978). The remainder of the lineament was identified by Gedney and Shapiro (1975) on SLAR and LANDSAT imagery. Subsequent examination of U-2 photography (Woodward-Clyde Consultants, 1980b) showed the lineament to be expressed morphologically as a prominent linear segment of Portage Creek and as a prominent linear bench along the south bank of the Susitna River southwest of Portage Creek.

Ground and aerial reconnaissance studies conducted in 1980 along Portage Creek showed the lineament to consist of an elevated prominent linear depression along the northwest bank of Portage Creek (Woodward-Clyde Consultants, 1980b). At the northeast end of the lineament, mineralized zones were observed in Portage Creek. Further to the south, along the northwest side of the creek, an apparent shear zone was observed which could not be reached on the ground. It was concluded in 1980 that the shear zone could be related to the lineament (Woodward-Clyde

Consultants, 1980b). Elsewhere along this linear depression, the depression appeared to be underlain by bedrock and to represent a glacial meltwater side channel.

In 1981, evidence strongly indicative of no fault control of the lineament was observed where the lineament trends across a low plateau in the southwest quadrant of the confluence of the Portage Creek and the Susitna River. This area is designated Segment 1 in Figure 4-22 and is referred to here as the Portage Creek plateau.

The Mint Mine is located at the northeast margin of the Portage Creek plateau (Location D4; Figure 4-22). Review of State of Alaska claims records and discussions with miners show that the claims were staked in 1922 and some silver has been mined from the property intermittently. Bedrock in the mine is Cretaceous slate. These slates have been intruded by andesite dikes along a shear zone. The dikes are accompanied by extensive brecciation and silicification. The mineralization appears then to be related to the intrusive and/or shearing episodes. These episodes can be inferred to have occurred in Tertiary time, approximately 50 to 60 m.y.b.p., if they are assumed to be related to the same tectonic activity as the Tertiary volcanic rocks and/or intrusive rocks in the region, as dated by Csejtey and others (1978).

Immediately northeast of the mine is a northeast-southwest trending tributary to Portage Creek. On the southwest wall of this tributary is an exposure of bedded metasedimentary rocks (Location D5; Figure 4-22). Feature KD5-3 projects directly through this exposure. Detailed aerial examination of this exposure was made from a helicopter (limited access and the

steepness of the tributary walls precluded ground examination). The beds were observed to dip southward into the tributary wall. No displacement of these beds was observed (the resolution was judged to be 12 to 20 inches (5 to 8 cm).

Southeast of the Mint Mine, on the Portage Creek Plateau, two magnetic profiles were conducted across the feature during the 1981 study at Location D6 (Figure 4-22). The traverses were conducted using the procedures described in Appendix A, Section A.5. The magnetic signature across the zone where the fault is projected was absolutely flat. No deviation in magnetic signature was observed. From these data, it was concluded that no magnetic anomalies are associated with this segment of the feature. The absence of an anomaly is circumstantial evidence that no fault is present.

Northeast of the Mint Mine, Csejtey and others (1978) shows a 14-mile (23-km) long inferred thrust fault segment near Thoroughfare Creek (Figure 4-22). This fault segment coincides with the Feature at this location. This fault segment is related to late Mesozoic-early Tertiary tectonism (at least 60 to 70 m.y.b.p.). No evidence was observed during this field investigation to suggest that the fault has been subject to displacement since that time.

Southeast of the Portage Creek plateau, the feature coincides with either a glacial meltwater side channel along the south bank of the Susitna River or with the margin of the Susitna River floodplain. (The uncertainty results from the width of the trace when it is transferred from the scale of Gedney and Shapiro [1975] to a scale of 1:24,000.)

On the basis of work conducted in 1981, we believe the floodplain margin of the Susitna River is the best location of the lineament drawn by Gedney and Shapiro (1975). No evidence was observed along this floodplain to suggest that a fault is present or that it has been subject to recent displacement. There are no prominent scarps, there is no consistent offset of tributary drainages to the Susitna River, nor is there any other morphologic evidence of a fault.

The pronounced change in lithologic texture and color and possible structural fabric in the vicinity of Curry reported in the Interim Report (Woodward-Clyde Consultants, 1980b) was not re-examined during the 1981 study. The clear evidence of no fault control elsewhere along the feature from the Portage Creek plateau renders this relationship inconsequential to the evaluation of active fault potential.

A possible zone of sheared rock was reported in the Interim Report (Woodward-Clyde Consultants, 1980b) to be present northeast of the Portage Creek plateau. The exposure which contained this zone of sheared rock was not observed in 1981. It apparently had been covered by slumped material or sediment deposited by the tributary.

Feature KD5-3 was classified during this investigation as being a lineament; therefore, it does not affect consideration of seismic ground motion or surface rupture potential at either dam site. The origin of the lineament is related to an alignment of the Portage Creek and Susitna River drainages which locally have linear glacial features. The lineament was judged not to be a fault and is, therefore, not a fault with recent displacement. This judgment concurs with that of Kachadoorian and Moore (1979) who concluded that there was no evidence of active faulting along Portage Creek.

Feature KD5-9

Feature KD5-9 trends N55°W to N70°W for a distance of 2.5 miles (4 km) and approaches within one mile (1.6 km) south of the Devil Canyon site (Figure 4-22). The lineament initially was identified on SLAR imagery by Gedney and Shapiro (1975). Subsequent examination of U-2 photography during the 1980 study showed the lineament to be expressed morphologically as a linear alignment of a stream drainage, several small lakes, and marshland. This feature consists of three segments, which are discussed below. Due to the short length, the segments are not labelled in Figure 4-22.

The eastern segment of the feature is a ravine with approximately 200 ft (60 m) of relief. Where the ravine intersects the west bank of Cheechako Creek, exposures of Tertiary intrusive rocks were examined during the 1981 field study. No evidence of a fault was observed; however, the exposure is not continuous across the projection of the lineament. Therefore, there is some possibility of a fault being present but concealed beneath vegetation and/or colluvium.

Joint measurements were taken in the eastern segment. Stereonet plots of the joint orientation show dominant orientations of N25°W, N55°W, and N65°W. The latter two orientations and the advance of glacial ice through this region strongly suggest that this segment of the lineament is the result of glacial fluting, the orientation of the fluting being controlled by the ice flow direction and the joint orientations.

Woodward-Clyde Consultants (1980b) reported a knickpoint in Cheechako Creek which aligned with the feature. Detailed review of the knickpoint (with waterfalls) during the 1981 study showed

that the knickpoint is not aligned with feature KD5-9. It is concluded, therefore, that the knickpoint is not related to the feature.

The central segment of the feature is the northeastern shoreline of two small lakes which lie in a depression whose northwest margin is linear. The area is generally marshy with standing water. No evidence of fault control was observed during either the 1980 or 1981 studies.

West of the intersection of feature KD5-9 with feature KD5-45 (Figure 4-22), a small outcrop is present which is overlain by glacial deposits. The orientation of the schistosity within the outcrop is parallel to the alignment of the feature. No evidence of a fault was observed in the outcrop nor in the glacial sediments overlying this area.

The western end of the lineament is a broad, shallow depression on top of an elongate, broad rise. The depression is marked by standing water and marsh. The margins of the depression are bordered by spruce forest on the slightly higher ground. No evidence of fault control was observed. The depression is considered to be the result of glacial fluting.

Feature KD5-9 was classified during this investigation to be an unrelated series of linear features whose origin is related to glacial processes and to control by dominant joint and foliation orientation. The feature is considered to be a lineament; therefore, it does not affect consideration of seismic ground motion or surface rupture potential at either site.

Feature KD5-12

Feature KD5-12 trends N50°E for a distance of 14.5 miles (24 km) and approaches within 1.5 miles (2.4 km) upstream of the Devil Canyon site (Figure 4-22). The lineament initially was identified, in part, on SLAR imagery by Gedney and Shapiro (1975) as a linear stretch of Cheechako Creek south of the Susitna River. The lineament was extended northward across the Susitna River; this judgment was based on morphologic relationships observed on U-2 photography during the 1980 study by Woodward-Clyde Consultants (1980b). North of the Susitna River, the lineament is expressed in part as a linear depression in which lie several small lakes, and in part as a linear stream drainage. This depression cuts across the predominant structural grain of this area.

Five locations (Figure 4-22) examined during the 1981 field season clearly demonstrate that feature KD5-12 is not a fault, and these five locations locally provide alternate explanations for its origin. The segment of the feature northeast of the Susitna River corresponds to the contact between the Tertiary intrusive unit to the southeast and the Cretaceous metasediments to the northwest (Figure 4-22). At location D7, Cretaceous argillite has been intruded by the Tertiary pluton. There is no evidence of faulting along this contact.

No morphologic evidence of a fault or structural control was observed where the feature crosses the Susitna River (Figure 4-22, Location D8). Vegetation and soil cover the river banks at the projection of the feature, so observations in bedrock could not be made at the river crossing.

The northeast wall of Cheechako Creek, at the projection of the feature (Figure 4-22, Location D9), was examined on the ground from a distance of 1,000 feet (305 m). No evidence of fault control was observed in the Tertiary intrusive rocks; however, the resolution of this observation is limited by the distance of the observation and access limitations imposed by the canyon walls.

At location D10 (Figure 4-22) in Cheechako Creek, the east bank juts westward into the creek and has deflected the creek into a horseshoe-shaped bend. Rock is continuously exposed on the promontory and the west wall here where the feature is projected to lie within Cheechako Creek. Examination of the east promontory on the ground and the east wall, using binoculars, provided evidence of no faulting through the exposure. The resolution of this observation was judged to be 4 to 9 inches (10 to 15 cm).

During the 1980 field study, a prominent shear zone was observed from the air near the southwestern end of the feature at Location D11 (Figure 4-22). Mapping was conducted at the shear zone during the 1981 field study. The results of the mapping confirm that a 23-foot- (7-m-) wide shear zone is present in the Tertiary intrusive rocks. The zone consists of highly altered and decomposed rock which has been sheared and faulted along a N35°W to N40°W trend. This trend is perpendicular to the N50°E orientation of Feature KD5-12. From this orientation of the shear zone, we concluded that it is not related to the feature, and that there is no evidence of structural control at this location.

The observations made at the five locations described above provide the basis for our judgment that Feature KD5-12 is not a fault. It is, rather, a series of unrelated linear features

whose origin is related to a lithologic contact, or to the alignment of discontinuous stream drainages. No evidence of a bedrock fault was observed, nor was any morphologic evidence of recent displacement observed. We classified Feature KD5-12 as being a lineament; therefore, it does not affect consideration of seismic ground motion or surface rupture potential at either dam site.

Feature KD5-42

Feature KD5-42 trends N50°W to N65°W for a distance of 3 miles (5 km) and approaches within 0.5 miles (0.8 km) south of the Devil Canyon site (Figure 4-22). The feature was originally identified as a lineament on U-2 photography by Woodward-Clyde Consultants during the 1980 field study. The lineament is comprised of two aligned stream drainages. The eastern drainage trends N65°W and the western drainage trends N50°W.

Information from three locations was used to evaluate this feature. The eastern location, D12 (Figure 4-22), is an exposure of argillite within the Cretaceous metasedimentary sequence. The outcrop showed no evidence of faulting with the resolution described below. A foliation or indistinct bedding trend was observed in the argillite. The orientation was uniformly N20°E to N60°E. The presence of this foliation or bedding trend provided a high degree of resolution in assessing the absence of a fault. Tempering this resolution was an intermittent cover of vegetation and surficial materials which provided an overall resolution at the outcrop of at least 6 feet (2 m).

Location D13 (Figure 4-22) is a linear trough several hundred feet (200 m) long and 200 feet (60 m) wide, which has been cut into the Tertiary intrusive rock. The feature lies in the middle

of this trough. A dike has been intruded into the Tertiary intrusive in this trough. The dike is oriented approximately perpendicular to the axis of the trough, but it is not exposed on the bottom of the trough. Measurements taken on the dike show it to have a uniform strike of N50°E. This strike can be projected across the trough and shows evidence that it has not been displaced. The accuracy of the alignment was judged to be 2°; so the resolution in the absence of displacement is approximately 6 feet (2 m).

The feature projects across Cheechako Creek, and there are limited exposures in the vicinity of that projection. Steep canyon walls and limited access in the creek bottom precluded ground examination of the exposures. From the air, however, there appeared to be a contact between the Cretaceous metasedimentary sequence on the north and the Tertiary intrusive unit to the south. The orientation of the contact was not visible. Consequently, the contact may coincide with the feature, but this interpretation remains to be confirmed.

No evidence of a fault was observed in the walls of Cheechako Creek. However, the limited extent of exposures and the inability to review the available exposures on the ground limit the confidence in this observation.

The feature projects into the south wall of Devils Canyon at location D15 (Figure 4-22). These walls have been examined from the air by geologists for both Woodward-Clyde Consultants and Acres. In addition, Acres' geologists mapped the walls using rock-climbing methods. No evidence of a fault was observed in the canyon walls. A near vertical joint was observed in the wall, which is infilled with what appeared to be a dike that is 1 foot (30 cm) wide.

Feature KD5-42 was classified during this investigation as being a series of short lineaments which originated from glacial enhancement of surface morphology and stream drainages. The feature was judged to be a lineament; therefore, it does not affect consideration of seismic ground motion or surface rupture potential at either site.

Feature KD5-43

Feature KD5-43 trends N80°E for a distance of 1.5 miles (2.4 km) and passes through the left abutment of the Devil Canyon site (Figure 4-22). The lineament is expressed morphologically as a short, prominent depression, approximately 300 feet (91 m) wide, which is oriented parallel to the Susitna River. Within the depression are two small lakes with a low saddle of glacial material between them.

The depression associated with the lineament was considered to be a potential spillway during initial feasibility studies conducted by the U.S. Bureau of Reclamation (USBR) in 1957 and 1958 (U.S. Bureau of Reclamation, 1960). During the USBR study, five borings were drilled across the depression on the saddle between the two lakes. An additional boring was drilled on the southwest shore of the eastern lake, and a test pit was excavated in the saddle near the northwest shore of the eastern lake during this study.

During the 1980 feasibility study, Acres drilled an angle boring (BH-4) southward from the north shore of the eastern lake. The boring was drilled beneath the lake for a distance of 501 feet (153 m) across the axis of the depression. In 1981, Acres drilled an angle boring (BH-7) northward from the south shore of the eastern lake. The boring was drilled beneath the lake for a distance of 498.3 feet (151.9 m).

The results of this drilling program were that no significant fault zone or shear zone was encountered in boring BH-4. In Boring BH-7, a zone of brecciated rock with zones of clay (gouge?) and slickensided surfaces was encountered beneath the eastern lake. One of the borings drilled in the center of the buried valley during the USBR study (DR-6) encountered "sheared rock" for the 20-foot (6-m) distance that the boring was drilled in rock.

In 1978, Shannon and Wilson conducted a seismic refraction traverse (along the saddle between the two lakes) across the feature for the U.S. Army Corps of Engineers (1979). As part of this feasibility study, Woodward-Clyde Consultants (1980a) conducted two north-south seismic refraction traverses across the eastern lake and a northwest-southeast traverse at an oblique angle to the north-south traverses and the axis of the depression.

The data obtained from these studies show that a buried bedrock channel is present beneath the eastern part of the depression. The channel has a maximum depth of approximately 90 feet (27 m) and is filled with 80 feet (24 m) of sand and gravel (glacial outwash) which is overlain by approximately 10 feet (3 m) of silt, sand, gravel, and cobbles (glacial till).

The faulted or sheared rock encountered in Boring BH-7 (and to a lesser extent in DR-6) suggests that a fault or shear zone may underlie the feature. However, review of the core obtained from BH-7 suggests that it does not necessarily represent a major throughgoing structure. The shearing and fault-related features are not dissimilar from those which would be expected in rocks which have been subjected to several periods of tectonic activity. They could represent a throughgoing fault; although it is not clear that they do.

If the sheared zone encountered in boring BH-7 does represent a fault which controls feature KD5-43, the fault dips southward. The absence of the shear zone in boring BH-4 precludes its dipping northward toward the river.

Ground reconnaissance studies conducted along the feature during this investigation in 1980 included fracture analyses in bedrock on both sides of the depression and ground traverses of the saddle between the two lakes. The fracture analyses showed that fractures on both sides of the depression have similar orientations. The dominant orientation is N35°W with a steep northeast to southwest dip. Thus, there is no major disruption of joint attitudes from one side of the feature to the other.

The canyon wall of Cheechako Creek at the east end of the lineament was examined from the air. No evidence of faulting was observed. No evidence of displacement was observed from the air on the Susitna River canyon wall at the west end of the lineament. However, access limitations and vegetation cover limit the confidence in the interpretations on both canyon walls.

Considering the above information and data, the depression associated with lineament KD5-43 appears to be a meltwater side-channel that may be structurally controlled. According to this interpretation, the depression may have developed from differential erosion along a prominent structure such as a fracture zone or bedrock fault. Subsequent glacial and/or meltwater processes served to enhance and probably deepen the depression, and it was later filled with sediments during a late glacial episode (perhaps in Late Wisconsin time).

If it is conservatively assumed that the feature is a fault, then the question about the recency of displacement needs to be addressed. Given the short length of the feature and the tectonic setting of the region (the only observed faults with recent displacement in the site region were the Talkeetna Terrain boundary faults, as discussed in Section 4.5), we consider it unlikely that Feature KD5-43 is the only fault with recent displacement in the region. We, therefore, consider it to be extremely unlikely that Feature KD5-43 is a fault with recent displacement.

This judgment is based on the extremely short length of the feature and the tectonic setting of the region. Experience in other parts of Alaska and other areas of the world, including California, Japan, and South America, suggests that short faults with recent displacement exist in association with other longer faults for which recency of displacement is clearly recognizable. That is, if a region is being subjected to stresses that are of sufficient magnitude to cause surface faulting, it is extremely unlikely that strain release in the region would produce no surface rupture longer than along one fault a few miles (a few kilometers) in length. Rather, it is logical to expect that the strain release would cause extensive rupture during some earthquakes and smaller amounts of rupture on both the main faults and shorter subsidiary faults.

Feature KD5-43 has been classified as being a possible fault. There is circumstantial evidence of a fault zone in the subsurface; however, there is no evidence of a fault on the canyon walls along the projection of the feature. We have concluded that the feature is a fault without recent displacement; therefore, Feature KD5-43 does not affect consideration of seismic ground motion or surface rupture potential at either site.

Feature KD5-44

Feature KD5-44 trends N15°W for a distance of 21 miles (34 km) and approaches within 0.3 miles (0.5 km) upstream of the Devil Canyon site (Figure 4-22). The feature initially was identified south of the Susitna River as two discontinuous lineaments on SLAR imagery by Gedney and Shapiro (1975). One of the lineaments followed, in part, the northern end of Cheechako Creek, whose confluence with the Susitna River is immediately upstream from the Devil Canyon site. Air photo interpretation conducted during the 1980 investigation identified a lineament with a similar alignment along a stream drainage whose confluence with the Susitna River is opposite that of Cheechako Creek.

During the 1980 field study, it was the opinion of the Woodward-Clyde Consultants geologists that the two lineaments identified by Gedney and Shapiro (1975) and the lineament identified by Woodward-Clyde Consultants should be considered as a single feature (Woodward-Clyde Consultants, 1980b). The 1981 field study and the subsequent analysis of the feature considered the feature to be a single lineament, 21 miles (34 km) long.

The feature is expressed morphologically as a linear stream drainage north of the Susitna River. On the south side of the Susitna River, the feature is the northern segment of Cheechako Creek and a tributary to Cheechako Creek. South of this tributary, the feature is a shallow, broad, linear depression on the upland plateau which lies south of the Susitna River (Figure 4-22).

Three locations were studied in detail in 1981 to determine if Feature KD5-44 is a fault and whether it is a fault with recent displacement. Location D15 (Figure 4-22) is on the north side of

the Susitna River opposite the confluence of Cheechako Creek. Here an oxidized mafic dike is exposed in the canyon wall.

Aerial measurements made during the 1981 field investigation show that the dike has a northwest strike and an apparent dip of 70° to 80° NE. The dike can be traced for a distance of approximately 300 feet (91 m) and has an apparent maximum width of approximately 20 feet (6 m). The dike was inaccessible on the ground during the 1981 field study. Observations made from the helicopter strongly suggest that the dike dies out at its eastern end. At its western end, it may die out, or it may continue on strike across the drainage associated with Feature KD5-44. The reason for the apparent ambiguity is due to the orientation of the exposure relative to the dike and the inaccessibility of the exposure. The dike visually appears to wedge out, or die out on the east bank of the drainage. However, during aerial examination of the west bank, a dike was observed on strike with the main dike. It is not clear if the two dikes are segments of a single dike or if they are completely separate.

Whether or not the dike dies out on the east bank of the tributary or continues across the tributary is not significant to the evaluation of Feature KD5-44. Either relationship provides circumstantial evidence that the dike is not truncated by a fault associated with Feature KD5-44.

Location D16 is the large point bar which juts into the Susitna River upstream from Devil Canyon (Figure 4-22). Seismic refraction studies were conducted across the point bar by Shannon and Wilson in 1978 for the U. S. Army Corps of Engineers (1979). The results of the study suggest that a buried step or scarp in bedrock steps from a depth of approximately 100 feet (30 m) below the point bar (on the downstream side) to a depth of 300 to

330 feet (91 to 100 m) on the upstream side. On the basis of these two seismic refraction lines, the buried step can be inferred to have a buried relief of approximately 200 to 230 feet (61 to 70 m). Its base is oriented N10°W, subparallel to the trend of Feature KD5-44. The slope dip is approximately 20°NE. The southwest side of the step is up relative to the northeast side.

The presence of the buried bedrock step beneath the point bar is an anomaly. Its origin is open to question at this point. It could represent a fault scarp which was modified by glacial and fluvial processes prior to burial. However, the absence of a fault northwest and southeast of Location D15 strongly suggests that it is not part of a throughgoing fault. It may be the product of differential erosion along a joint system. Evaluation of the glacial history of the region (Section 3) has provided no compelling explanation to date.

In summary, the origin of the buried bedrock step at Location D15 remains an enigma. It does not, however, represent a throughgoing fault scarp, in our opinion, because there is no evidence observed of faulting northwest and southeast of this location.

In the Interim Report (Woodward-Clyde Consultants, 1980b), zones of light-colored, fractured, and highly weathered rock in Cheechako Creek were described. The origin of the zones was suggested to be possibly related to faulting. The walls of Cheechako Creek were mapped under the direction of Acres during the winter of 1980-1981, and no evidence of a throughgoing fault system was observed (Bruen, 1981). We conclude then that these zones of rock are not related to a throughgoing fault.

The location with the most compelling evidence that Feature KD5-44 is not fault-controlled is Location D17 (Figure 4-22). Here, Tertiary intrusive rock is exposed across the entire zone in which the feature is projected. The rock is exposed on the banks and in the channel of a tributary to Cheechako Creek. There is clearly evidence of no fault displacement in the exposure with the resolution being approximately one inch (2 to 3 cm).

In the Interim Report (Woodward-Clyde Consultants, 1980b) an apparent morphologic anomaly was reported along Feature KD5-44. A linear shallow depression, approximately 500 feet (152 m) long was observed in a terrace. During the 1981 field study, the origin of the terrace was reviewed as a part of the Quaternary geology studies. It has been judged to be a glaciofluvial deposit associated with a glacial stade following early Late Wisconsin time. The linear depression is a drainage channel which was subsequently cut into the terrace.

Feature KD5-44 was classified during this investigation as being a series of unrelated lineaments whose origin is related to the alignment of stream drainages. The feature is a lineament; therefore, it does not affect consideration of seismic ground motion or surface rupture potential at either site.

Feature KD5-45

Feature KD5-45 trends N80°E to N85°E for a distance of 19.5 miles (31 km) and approaches within 0.8 miles (1.3 km) of the left abutment of the Devil Canyon site (Figure 4-22). The lineament was identified during the 1980 field investigation as a prominent north-facing linear bluff along the south bank of the Susitna River. Aligned with this bluff is a small, linear stream

drainage at the west end of the lineament, a linear topographic depression along the eastern portion of the lineament, and several small lakes along the lineament.

Ground and aerial reconnaissance conducted during the 1980 field study showed that the lineament corresponds primarily to the front of the hills (i.e., range-front) along the south bank of the Susitna River and locally is expressed as a linear trough approximately 150 feet (46 m) wide and 10 feet (3 m) deep. The linear trough is underlain by argillite and glacial till. Water was observed flowing at a rate of approximately 3 to 5 gallons per minute (11 to 19 liters per minute) out of the till at the base of the trough. Reexamination of the till during the 1981 field study showed that the flowing water was emanating from the contact between the till and the underlying argillite. Thus, the water is flowing locally along the top of the bedrock surface.

Detailed aerial reconnaissance during the 1981 field study disclosed no anomalous morphologic relationships that required ground-checking. There are no exposures along the base of the range front which could be examined for information on the origin of the feature.

The origin of Feature KD5-45 is that of a range front which has been modified by glacial processes. There is a conspicuous absence of faceted spurs, scarps, and other morphologic features representative of a fault origin. We have concluded that the feature is a lineament; therefore, it does not affect consideration of ground motion or surface rupture potential at either site.

4.5 - Assessment of Recent Displacement

Faults for which evidence of recent displacement was found were considered to be potential seismic sources. Each potential seismic source was evaluated during this study to estimate its potential seismic ground motions at the Watana and Devil Canyon sites and its potential for surface rupture within 6 miles (10 km) of the sites.

On the basis of the 1980 study, the Talkeetna Terrain boundary faults were identified as seismic sources that need to be considered as potential sources of seismic ground motion at the dam sites. These include: the Castle Mountain fault, the Denali fault, the Benioff interplate region, and the Benioff intraplate region (Figure 1-1). These faults are considered to be or to contain faults with recent displacement that could cause seismic ground motions at the dam sites; however, because of their distance from the sites, these faults do not have the potential for rupture through the sites (Table 4-3). The 1980 study also identified 13 features nearer the dam sites that required detailed evaluation during the 1981 study to assess their importance for seismic design.

On the basis of the 1981 study, no evidence for faults with recent displacement other than the Talkeetna Terrain boundary faults has been observed to date within 62 miles (100 km) of either dam site and none of the 13 features near the dam sites are faults with recent displacement. Therefore, the 13 features are not considered to be potential seismic sources that could cause seismic ground motions at the sites or surface rupture through the sites (Table 4-3).

Our interpretation that none of the 13 features are faults with recent displacement is based on data collected during our investigation. The data are limited in the sense that a continuous 100,000 year-old

stratum or surface was not found along the entire length of each of the features. For this reason, the available data were analyzed and professional judgment was applied to reach conclusions concerning the recency of displacement on each of the 13 features.

E 4-1

ARY OF SELECTED WORLDWIDE EARTHQUAKES

Earthquake	Location	Magnitude[1] (M_S)	Active[2] Tectonic Terrain	Distance to Fault with Late Quaternary Displacement (km)	Documented Surface Faulting	References
ne 1929	W. Nelson, New Zealand	7.6	Yes	0	Yes	Slemmons (1977b)
v 1930	Izu, Japan	7.0	Yes	0	Yes	Slemmons (1977b); Kuno (1936); Matsuda (1977)
n 1931	Hawkes Bay, New Zealand	7.8	Yes	0	Yes	Adams and others (1933); Wyss (1979); Slemmons (1977b)
p 1931	Nishi-Saitama, Japan	6.75 7.0	Yes	0	No	Kanamori and Anderson (1975) Matsuda (1977); Abe (1974)
p 1932	Wairoa, New Zealand	6.8	Yes	0	Yes	Iida (1965); Richter (1958)
r 1935	Taiwan	7.1	Yes	0	Yes	Slemmons (1977b)
p 1935	Ituango, Columbia	6.25	Yes	(?)	(?)	Woodward-Clyde Consultants (1979)
p 1943	Tottori, Japan	7.4	Yes	0	Yes	Kanamori (1972); Iida (1965)
n 1944	San Juan, Argentina	7.6	Yes	0	Yes	Slemmons (1977b); Iida (1965)
n 1945	Mikawa, Japan	7.1	Yes	0	Yes	Ando (1974); Iida (1965)
ne 1946	British Columbia, Vancouver Island	7.2	Yes	0(?)	(?)	Rogers and Hasegawa (1978); Slauson and Savage (1979)
l 1952	Kern, California	7.7 M_L 7.2	Yes	0	Yes	Gutenberg (1955); Dibblee (1955); Dunbar and others (1980)
t 1955	Japan	5.7	Yes	0	No	Okada and Ando (1979)
1958	Central Alaska	M_b 7.3	Yes(?)	(?)	No	Davis (1960); Sykes (1971)
g 1961	Kita Mino, Japan	7.0	Yes	0	No	Bonilla (1979); Kawasaki (1975)
1962	Buyin-Zara, Iran	7.25	Yes	0	Yes	Ambraseys (1965); Slemmons (1977b)
p 1966	Truckee, California	M_L 5.75	Yes	0	Yes	Ryall and others (1968); Tsai and Aki (1970)
1968	Saitama, Japan	5.8	Yes	(?)	No(?)	Kanamori and Anderson (1975); Abe (1975)
t 1968	Meckering, Australia	7.0	Yes	0	Yes	Everingham and others (1969)
t 1968	Rampart, Alaska	6.5	(?)	0(?)	No	Lander (ed.) (1969); Gedney and others (1969); Huang (1981)
l 1969	Pariahuanca, Peru	5.7 M_b 5.9	Yes	0	Yes	Lander (ed.) (1970)
1969	Pariahuanca, Peru	6.4 6.2	Yes	0	Yes	Lander (ed.) (1970)
1971	Sylmar, California	6.6 M_L 6.4	Yes	0	Yes	Singh and others (1980); Langston (1978); Yerkes (1973)
b 1973	Point Mugu, California	M_L 5.75 6.0	Yes	0	No	Castle and others (1977); Boore and Stierman (1976)
1976	Friuli, Italy	6.4	Yes	0	Yes	Cagnetti and Pasquale (1979); Cipar 1980); Cipar (1981); Finetti and others (1979)
v 1977	San Juan, Argentina	7.4	Yes	0-5(?)	No	Rojan and others (1977)
n 1978	Izu-Oshima, Japan	6.8	Yes	0	Yes	Shimazaki and Somerville (1978)
1979	Coyote Lake, California	5.7 M_L 5.9	Yes	0	Yes	Lee and others (1979); Urhammer (1980)
n 1980	Livermore, California	M_L 5.5	Yes	0	Yes	Bolt and others (1981)
t 1980	El Asnam, Algeria	7.3	Yes	0	Yes	Burford and others (1981)

[1] Magnitude is expressed as M_S unless otherwise indicated. Some earthquakes are assigned more than one M_S value in the literature by different authors.
[2] Active tectonic terrain is discussed in Section 4.2.1.

TABLE 4-2

SUMMARY OF SURFACE FAULTING IN CALIFORNIA

Earthquake Magnitude Range	Total Number of Events	Number of Events With Surface Faulting	ercent of Events with Surface Faulting (%)
A. 1900 through 1969			
≥ 5.0	287	8	3
≥ 6.0	34	5	15
B. 1970 through 1980			
≥ 5.0	24	8	33
≥ 5.5	8	6	75
≥ 6.0	3	3	100

TABLE 4-3

SUMMARY OF BOUNDARY FAULTS AND SIGNIFICANT FEATURES

Feature[1,2] No.	Feature Name[3]	Fault (F) or Lineament (L)	Length[4] miles(km)	Distance[5] miles(km) from Devil Canyon	Distance[5] miles(km) from Watana	Fault with Recent Displacement
BOUNDARY FAULTS						
AD5-1	Castle Mountain Fault	F	295 (475)	71 (115)	65 (105)	Yes
HB4-1	Denali Fault	F	1,358 (2,190)	40 (64)	43 (70)	Yes
-	Benioff Zone (Interplate)	F	434 (700)	56 (91)	40 (64)	Yes
	Benioff Zone (Intraplate)	F	46 (75)	38 (61)	31 (50)	Yes
WATANA SIGNIFICANT FEATURES						
KC4-1	Talkeetna Thrust	F	78 (126)	16 (25)	4 (6.5)	No
KD3-3	Susitna Feature	L	95 (153)	16 (25)	2 (3.2)	No
KD3-7	Watana River	L	31 (50)	22 (35)	0 (0)	No
KD4-27	Fins Feature	F	2 (3.2)	23 (37)	0 (0)	No
DEVIL CANYON SIGNIFICANT FEATURES						
KC5-5	-	L	12 (19)	4.5 (7)	19 (31)	No
KD5-2	-	F	0.8 (1.3)	3.5 (5.6)	24 (38)	No
KD5-3	-	L	51 (82)	3.6 (5.8)	14 (23)	No
KD5-9	-	L	2.5 (4)	1 (1.6)	24 (39)	No
KD5-12	-	L	14.5 (24)	1.5 (2.4)	17 (28)	No
KD5-42	-	L	3 (5)	0.5 (0.8)	22 (35)	No
KD5-43	-	L	1.5 (2.4)	0 (0)	24 (38)	No
KD5-44	-	L	21 (34)	0.3 (0.5)	23 (37)	No
KD5-45	-	L	19.5 (31)	0.8 (1.3)	35 (41)	No

Notes:

1. Alpha-numeric code number is based on: a) a first letter designation for the 1:250,000 quadrangle where the feature is located (A = Anchorage, H = Healy, K = Talkeetna Mountains); b) the letter and number of the 1:63,380 quadrangle at the midpoint of the feature; and c) a number designating the order of the feature's recognition.
2. Feature locations are shown in Figures 4-3, and 4-18 through 4-20.
3. Feature name is given where assigned.
4. Length is from the text.
5. Distance is the closest approach of the surface trace of the fault or lineament as measured on the base maps referred to in Note 2.

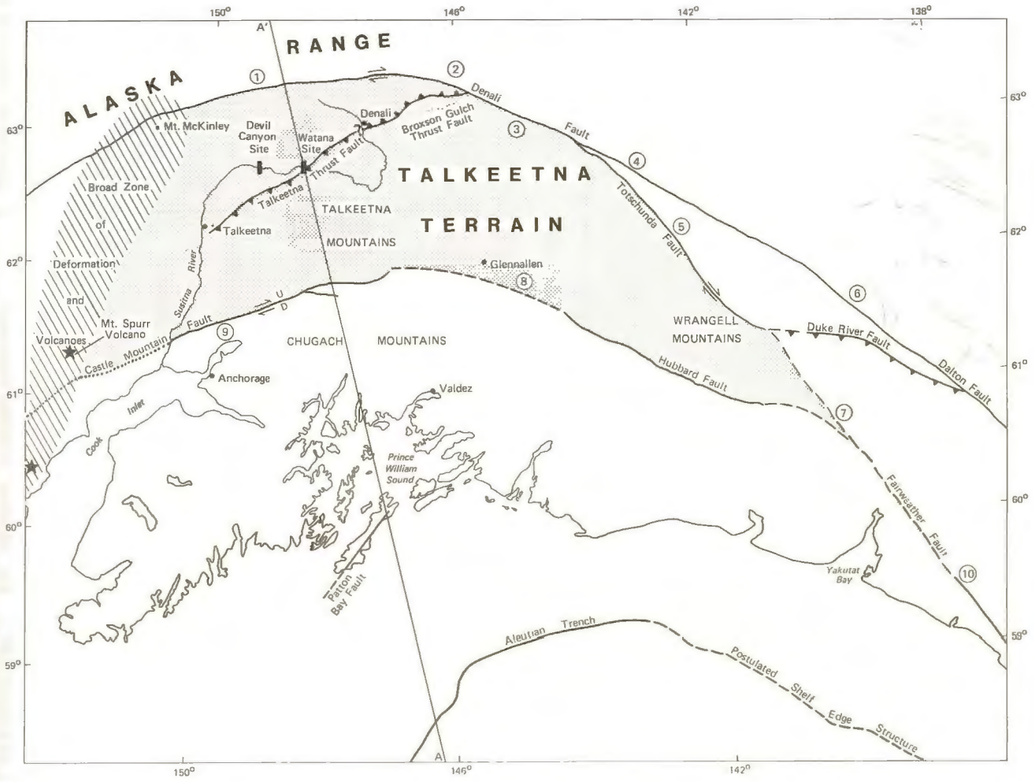

A. TALKEETNA TERRAIN MODEL

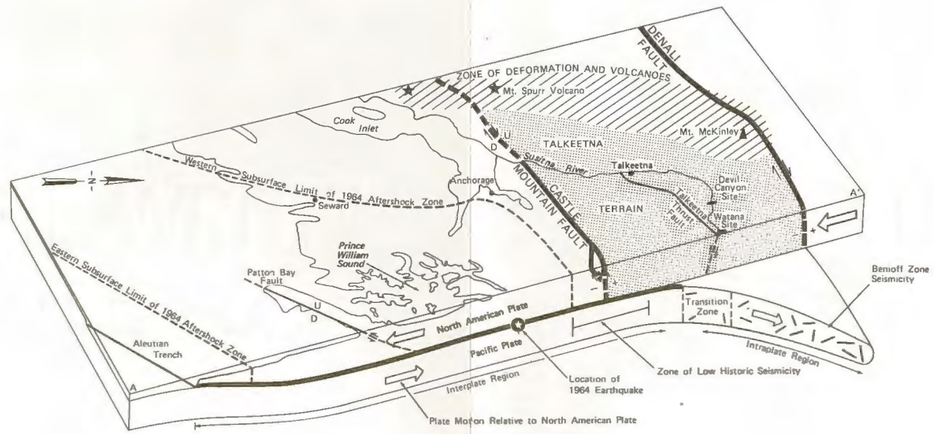

B. SCHEMATIC TALKEETNA TERRAIN SECTION

LEGEND

- Mapped strike-slip fault, arrows show sense of horizontal displacement
- Mapped strike-slip fault with dip slip component, letters show sense of vertical displacement: U is up; D is down.
- Mapped fault, sense of horizontal displacement not defined
- Inferred strike-slip fault
- Mapped thrust fault, sawteeth on upper plate

NOTES

① 0.9 – 2.0 cm/yr Hickman and Campbell (1973); and Page (1972).
② 0.5 – 0.6 cm/yr Stout and others (1973).
③ 3.5 cm/yr Richter and Matson (1971).
④ 1.1 cm/yr, no Holocene activity farther east, Richter and Matson (1971).
⑤ 0.9 – 3.3 cm/yr Richter and Matson (1971).
⑥ Inferred connection with Dalton fault; Plafker and others (1978).
⑦ Inferred connection with Fairweather fault; Lahr and Plafker (1980).
⑧ Connection inferred for this report.
⑨ 0.1 – 1.1 cm/yr Detterman and others (1974); Bruhn (1979).
⑩ 5.8 cm/yr Lahr and Plafker (1980).
⑪ Aleutian Trench and Postulated Shelf Edge Structure after Guptill and others (1981).
⑫ Slip rates cited in notes ① through ⑩ are Holocene slip rates.
⑬ All fault locations and sense of movement obtained from Beikman (1978; 1980).

TALKEETNA TERRAIN MODEL AND SECTION

0 100 200 Miles
0 100 200 Kilometers

FIGURE 4-1

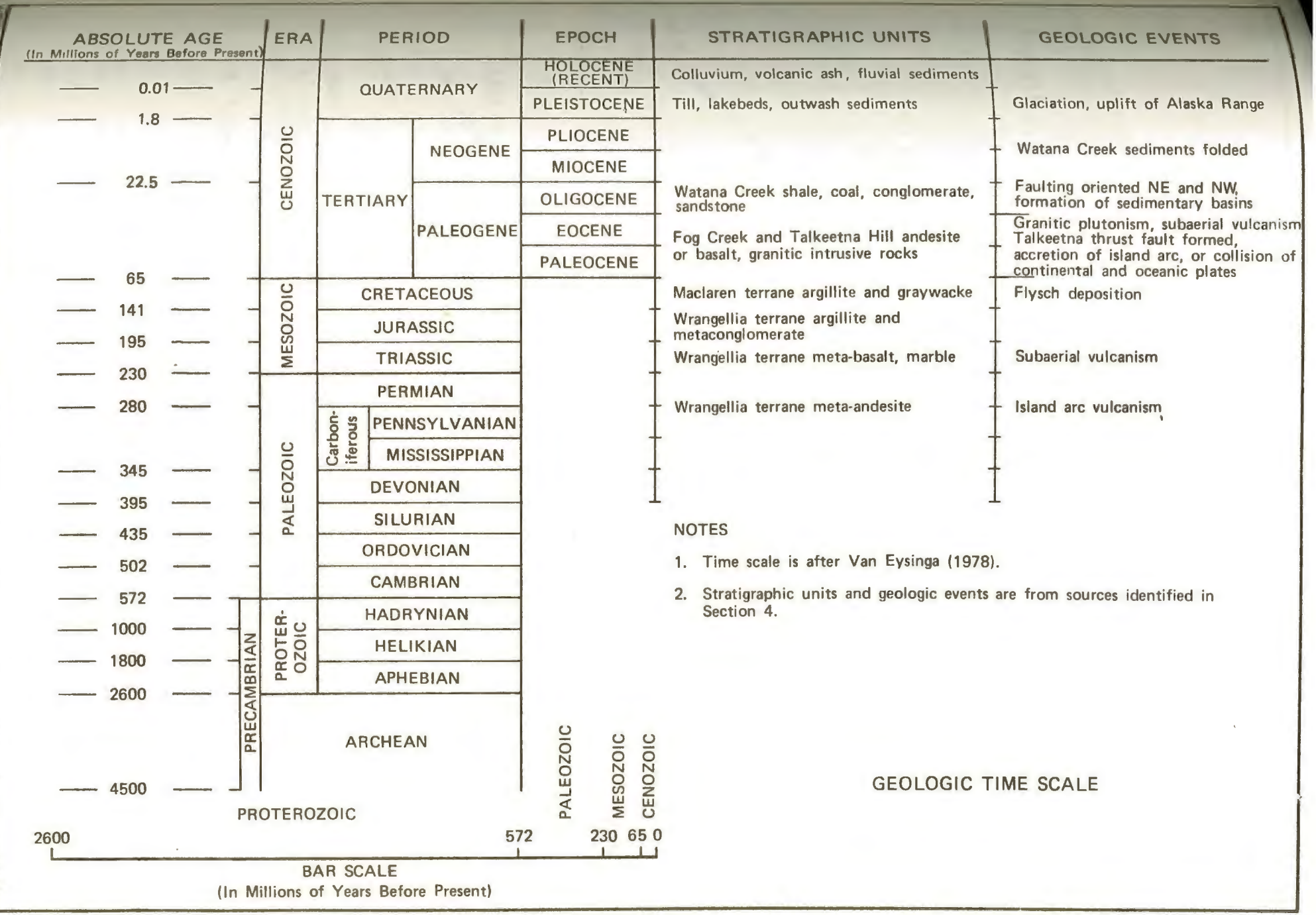

NOTES

1. Time scale is after Van Eysinga (1978).
2. Stratigraphic units and geologic events are from sources identified in Section 4.

GEOLOGIC TIME SCALE

FIGURE 4-2

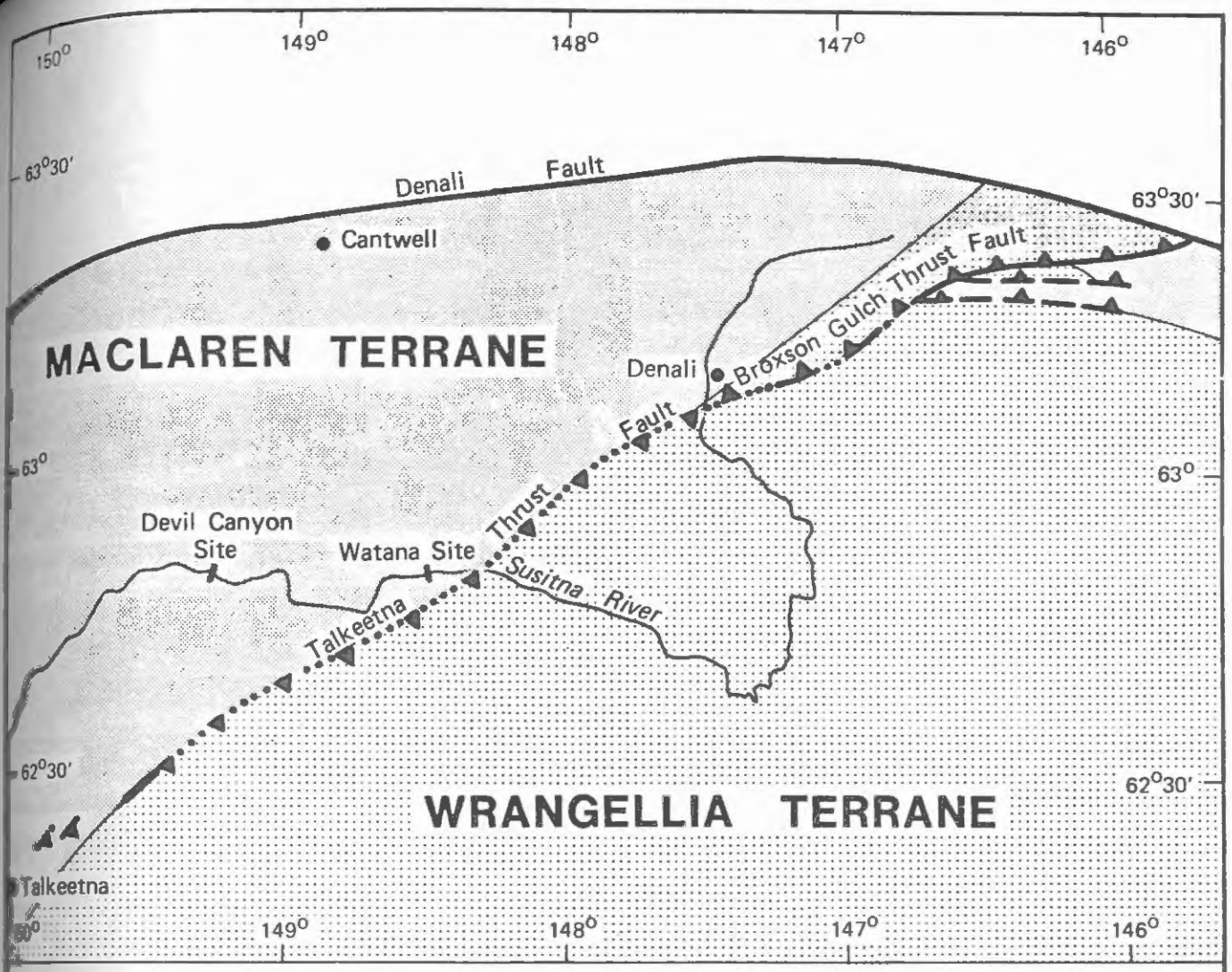

LEGEND

Thrust fault, dashed where inferred, dotted where concealed, sawteeth on upper plate

Inferred terrane boundary

N

NOTE

1. Geology is from Csejtey and others (1978), Nokleberg and others (1981), and Turner and Smith (1974).
2. Terranes are described in Section 4.4.1

REGIONAL TECTONIC TERRANE MAP

0 10 20 30 40 Miles

0 10 20 30 40 Kilometers

LEGEND

W4 ■ Location and age designation of Quaternary units (0 to 1.8 m.y.b.p.)

W3 ▲ Location and age designation of Tertiary units (1.8 to 65 m.y.b.p.)

W2 ● Location and age designation of Mesozoic and Paleozoic units (65 to 570 m.y.b.p.)

Thrust fault, dotted where concealed, sawteeth on upper plate

Lineament

NOTES

1. m.y.b.p. is the abbreviation for million years before present.
2. Geologic relations at locations W2, W3, etc. are discussed in Section 4.4.1.
3. Lineament and fault locations are modified from Csejtey and others (1978), and Turner and Smith (1974).

-N-

TALKEETNA THRUST FAULT AND SUSITNA FEATURE LOCATION MAP

0 10 20 40 Miles

0 20 40 Kilometers

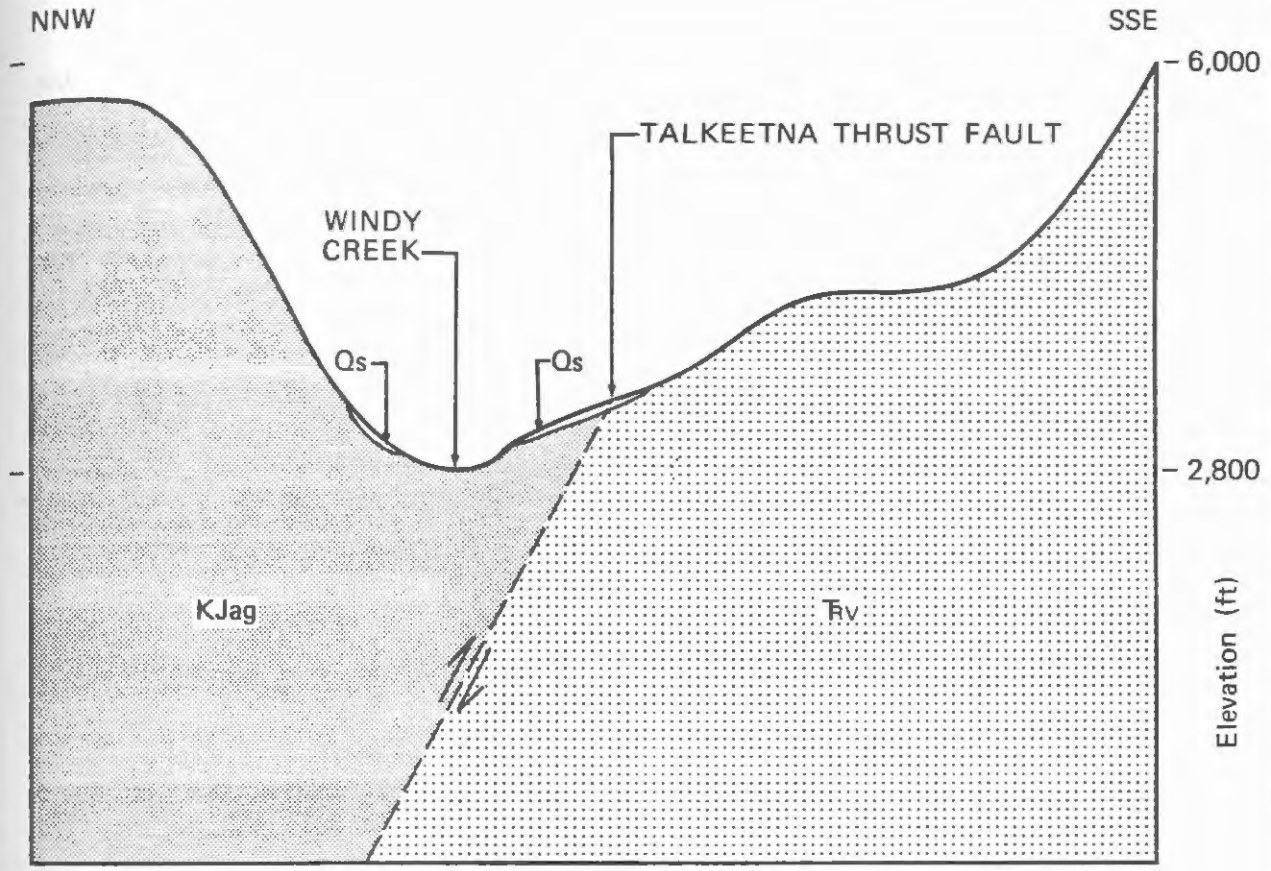

LEGEND

Qs	Quaternary glacial sediments
KJag	Cretaceous and Jurassic meta-sedimentary rocks
TRv	Triassic volcanic rocks
	Thrust fault, inferred from lithologic contrast, arrows show sense of dip slip displacement

NOTES

1. Section location is shown in Figure 4-4.
2. Geology is from Woodward-Clyde Consultants' 1981 field study and Smith (1981).

DIAGRAMMATIC CROSS-SECTION OF THE BROXSON GULCH THRUST FAULT AT WINDY CREEK (LOCATION W1)

FIGURE 4-5

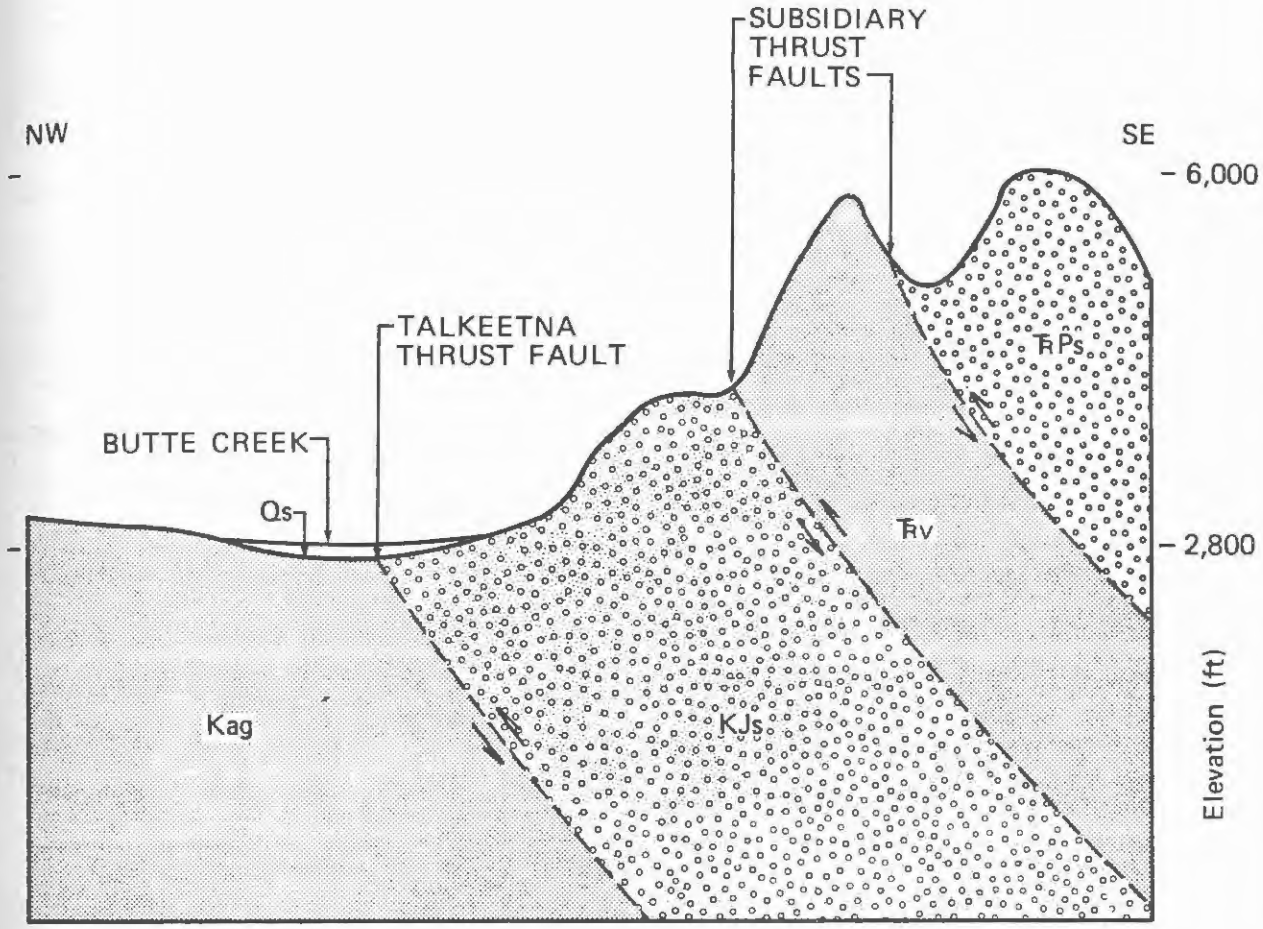

LEGEND

Qs	Quaternary glacial sediments
Kag	Cretaceous metasedimentary rocks
KJs	Cretaceous and Jurassic meta-sedimentary rocks
TRv	Triassic volcanic rocks
TR Ps	Triassic and Permian sedimentary rocks
	Thrust fault, inferred from lithologic contrast, arrows show sense of dip slip displacement

NOTES

1. Section location is shown in *Figure* 4-4.
2. Geology is from Woodward-Clyde Consultants' 1981 field study and Csejtey (1981).

DIAGRAMMATIC CROSS-SECTION OF THE TALKEETNA THRUST FAULT NEAR BUTTE CREEK (LOCATION W2)

FIGURE 4-6

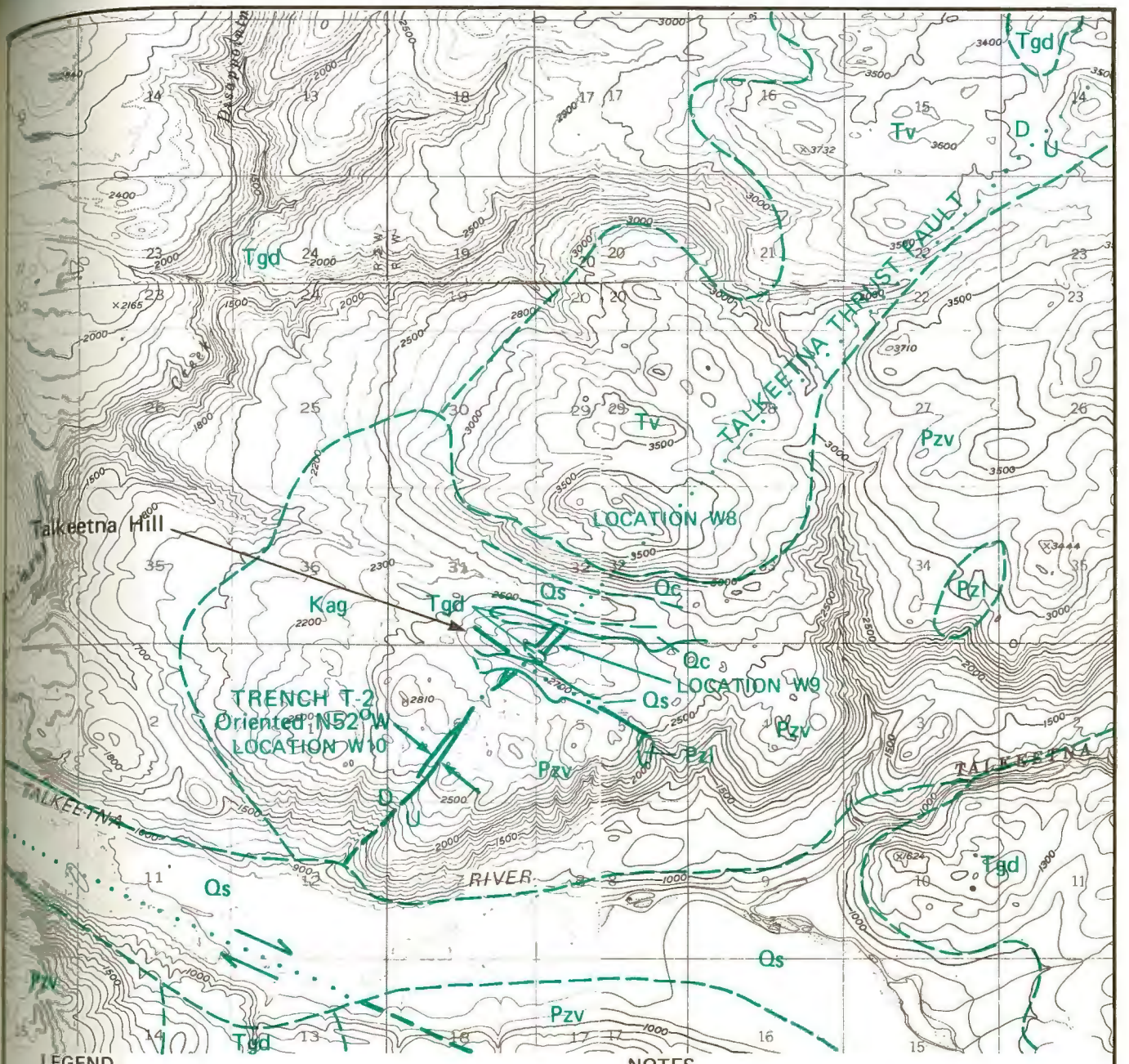

LEGEND

Qs	Quaternary glacial sediments
Qc	Quaternary colluvium and talus
Tgd	Tertiary granodiorite
Tv	Tertiary andesite or basalt
Kag	Cretaceous argillite
Pzv	Paleozoic basalt, greenstone
Pzl	Paleozoic limestone

Lithologic contact, dashed where approximately located

D / U — Fault, dashed where approximately located, dotted where concealed; arrows show sense of horizontal displacement, letters show sense of vertical displacement: U is up; D is down.

Trench located between arrows

NOTES

1. Geology is from Woodward-Clyde Consultants, 1981 field studies and photogeology, and Csejtey and others (1978).
2. Geologic relations shown in this figure are discussed in Section 4.4.1.

N

GEOLOGIC MAP OF LOCATIONS
W8, W9, AND W10 NEAR TALKEETNA HILL

0 1 2 Miles

0 1 2 Kilometers

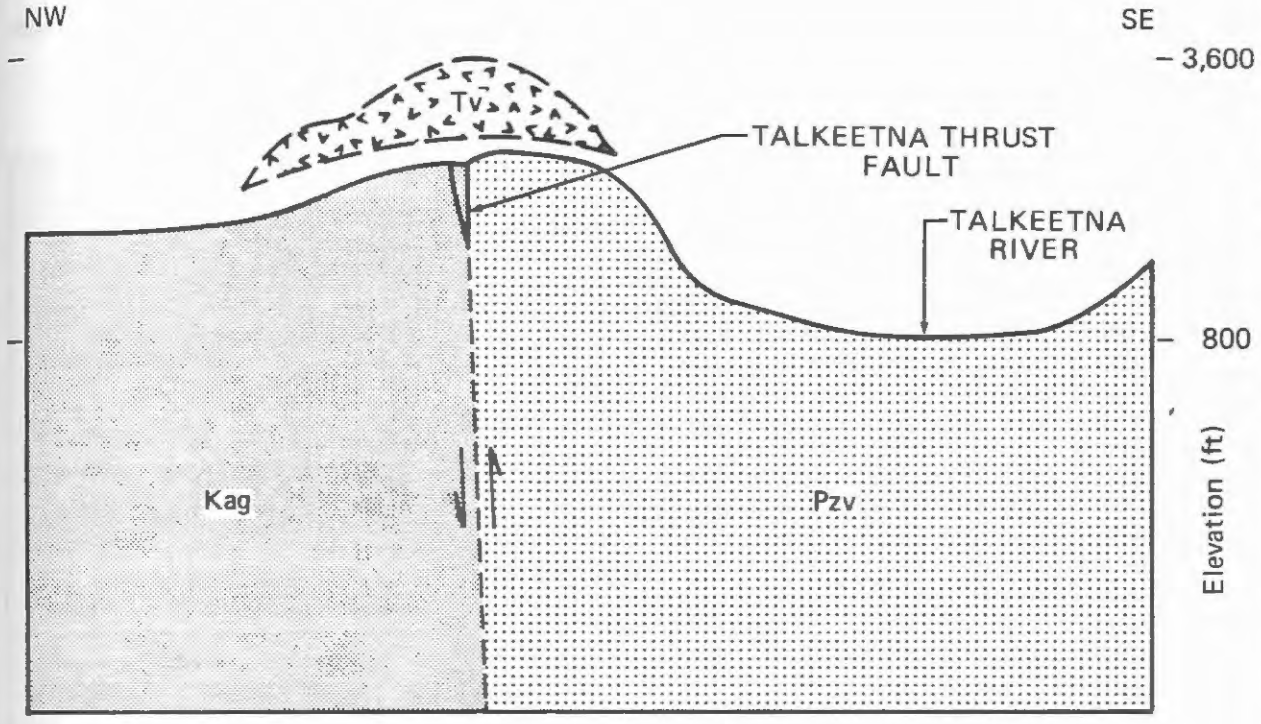

LEGEND

Tv	Tertiary volcanic rocks
Kag	Cretaceous metasedimentary rocks
Pzv	Paleozoic volcanic rocks
	Thrust fault, inferred from lithologic contrast, arrows show sense of vertical displacement

NOTES

1. Section location is shown in Figures 4-4 and 4-7.
2. Area labeled "Tv" represents a hill of Tertiary volcanic rock into which the Talkeetna thrust fault projects. The hill (Location W8 in Figure 4-4) is separated from Talkeetna Hill by a narrow valley represented in the figure as a space.
3. Geology is from Woodward-Clyde Consultants' 1981 field study and Csejtey (1981).

DIAGRAMMATIC CROSS-SECTION OF THE TALKEETNA THRUST FAULT AT TALKEETNA HILL (LOCATION W9)

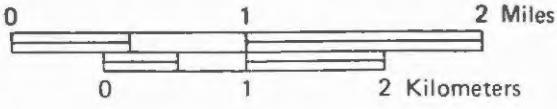

FIGURE 4-8

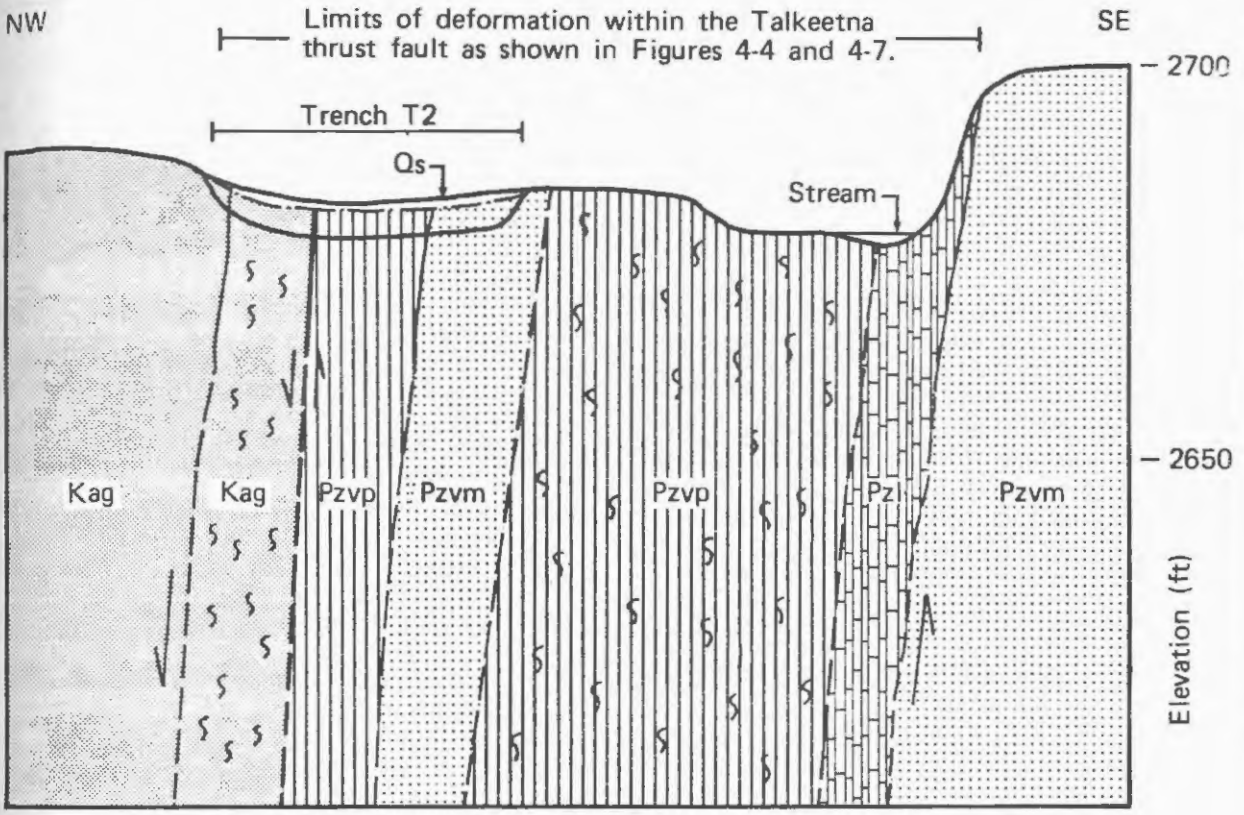

LEGEND

Qs	Quaternary sediments
Kag	Cretaceous argillite
Pzvp	Paleozoic phyllitic greenstone, originally basalt
Pzvm	Paleozoic massive greenstone, originally basalt
Pzl	Paleozoic limestone with argillite inclusions
ʃʃ	Sheared rock
	Fault with gouge, dashed where inferred, arrows show sense of vertical displacement
	Lithologic contact, dashed where inferred
	Sense of vertical displacement from regional geologic relationships, Csejtey (1981).

NOTES

1. Section location is shown in Figures 4-4 and 4-7.
2. Geology is from Woodward-Clyde Consultants 1981 field study.

DIAGRAMMATIC CROSS-SECTION OF THE TALKEETNA THRUST FAULT AT TRENCH T-2 (LOCATION W10)

0 50 100 Feet

0 10 20 30 Meters

FIGURE 4-9

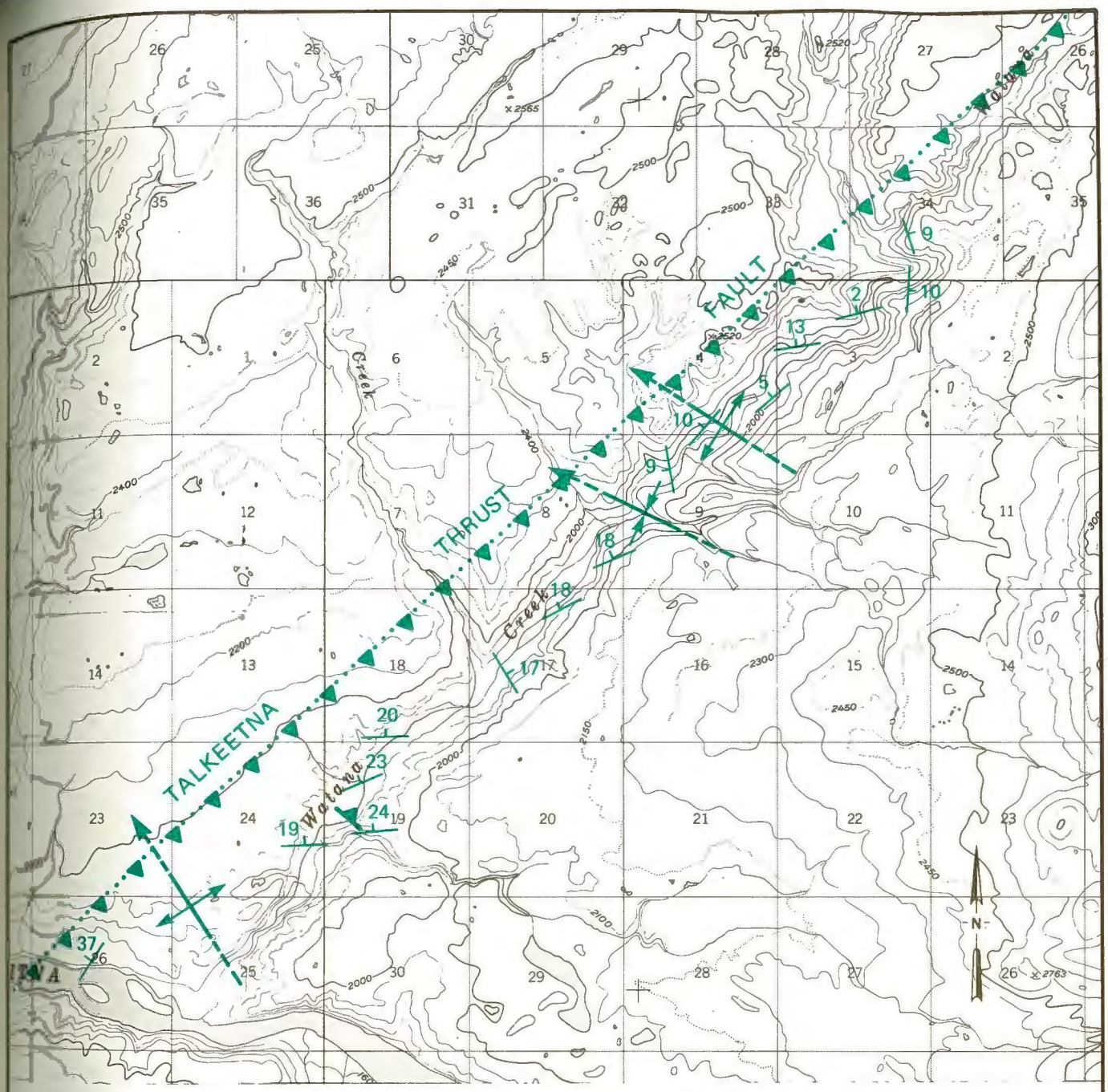

LEGEND

- Strike and dip of bedding
- Plunging syncline, dashed where inferred
- Plunging anticline, dashed where inferred
- Thrust fault, dotted where concealed, sawteeth on upper plate

NOTES

1. Orientations were measured in Tertiary strata. Fold axes are inferred from the bedding orientations.
2. Geology is from Woodward-Clyde Consultants 1981 field studies.
3. Geologic relations shown in this figure are discussed in Section 4.4.1.

ORIENTATION OF FOLDED STRATA IN WATANA CREEK (LOCATION W3)

0 1 2 Miles

0 1 2 Kilometers

FIGURE 4-10

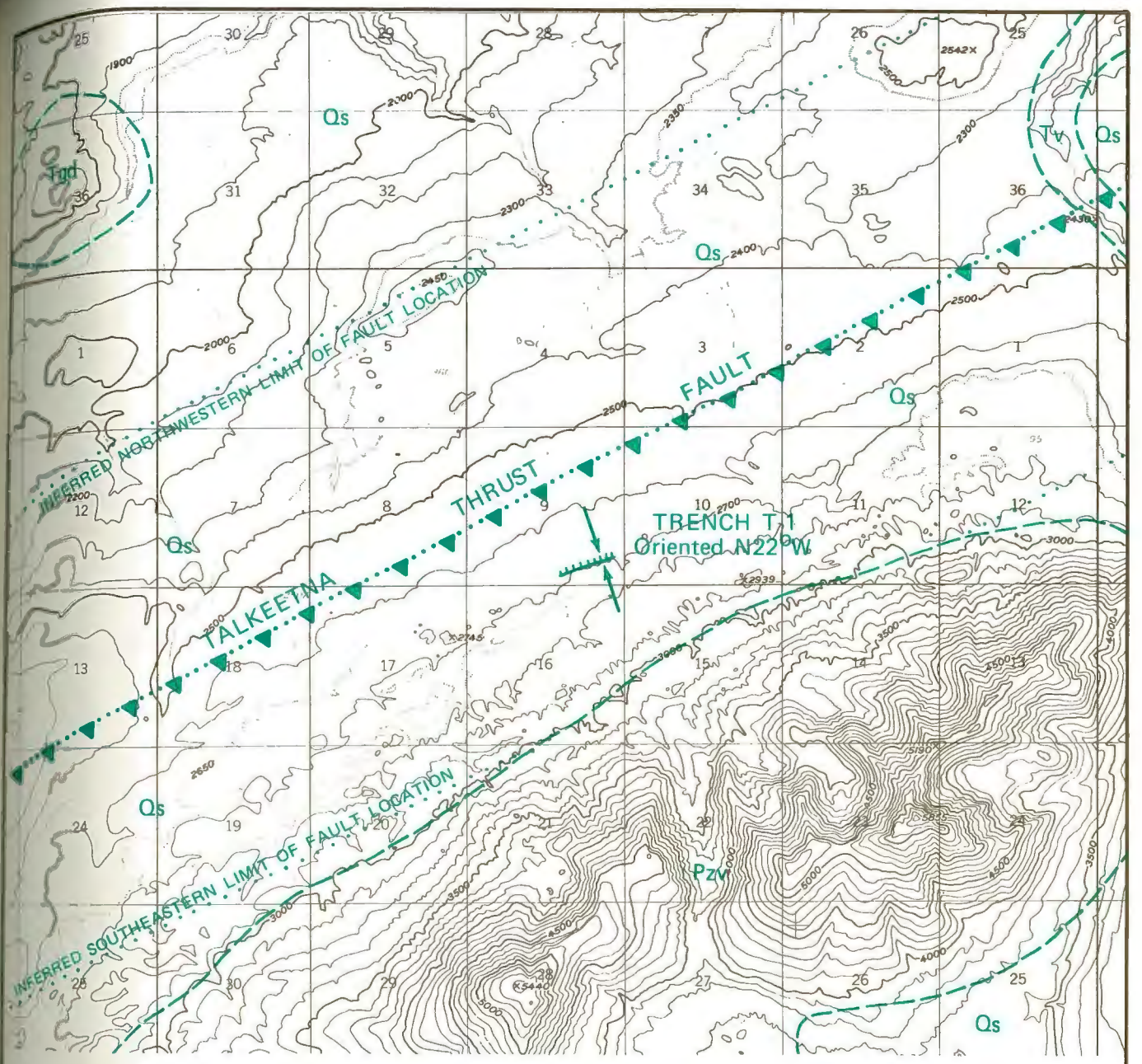

LEGEND

Qs	Quaternary glacial deposits
Tgd	Tertiary granodiorite
Tv	Tertiary volcanic rocks
Pzv	Paleozoic volcanic rocks
- - -	Lithologic contact, approximately located
	Linear scarp, line at top of slope, hachures on slope
	Concealed thrust fault, sawteeth on upper plate
	Trench located between arrows

NOTES

1. Geology is from Csejtey and others (1978).
2. Geologic relations shown in this figure are discussed in Section 4.4.1.

N

LOCATION OF TRENCH T-1
AT LOCATION W7

0 1 2 Miles

0 1 2 Kilometers

FIGURE 4-11

LEGEND

Lithologic Contacts, Description, Width

- Abrupt, <0.1 ft (<3 cm)
- Gradational, 0.1 to 0.5 ft (3 to 15 cm)
- Very gradational, >0.5 ft (>15 cm)

Soil Boundaries, Description, Width

- Abrupt, <0.1 ft (<3 cm)
- Gradational, 0.1 to 0.5 ft (3 to 15 cm)
- Very gradational, >0.5 ft (>15 cm)

Other Symbols

- ≡ or ≡ — Laterally gradational or interfingering contact
- ▽ — Water table at time of excavation
- ✔ — Boulder
- ..... — Gravel layer
- ..... — Sand layer
- ---------- — Original surface disturbed by excavation
- ʃ — Fracture due to shear
- ▾ — Sample location

NOTES

1. Trench data:

	T–1	T–2
Length:	205 ft (62.5 cm)	78 ft (24 m)
Maximum Depth:	10.5 ft (3.2 m)	6 ft (1.8 m)
Excavated:	4 to 13 August 1981	26 August 1981
Geologists:	Phillip C. Birkhahn Edward H. Sabins Kerry E. Sieh	Phillip C. Birkhahn Robert G. Goodwin Edward H. Sabins
Logging Scale:	1 in. = 5 ft	1 in. = 5 ft

2. Description of units is according to Compton (1962), and Pettijohn (1949).
3. Trench T–1 and T–2 locations are shown in Figures 4-11 and 4-7, respectively.

DESCRIPTION OF UNITS

TRENCH T–1

1. Organic soil horizon. Fibrous, peaty mat of muskeg with silt and pebbles, alive at top, very dark brown (10YR 2/2, moist).
   A. Buried organic soil horizon.
2. Mixed loess and colluvium. Silt: Pebbly and sandy, poorly to well sorted, subrounded, porous, yellowish brown (10YR 5/4, moist), mottled with very dusky red (2.5YR 2.5/2, moist), massive except for faint, very pale brown (10YR 7/4, moist) and dark brown (7.5YR 3.5/3, moist) horizontal bands that may represent bedding.
3. Loess. Silt: Local patches of 5% very fine sand, well sorted, porous, yellowish brown (10YR 5/4, moist) with faint horizontal strong brown (10YR 5/6, moist) bands, massive, moist.
4. Volcanic ash. Grayish brown (10YR 6/2, moist) to light brownish gray (10YR 5/2).
5. Glaciofluvial gravel. 35% pebbles and cobbles, sandy matrix except locally clast supported, some boulders up to 2 ft (61 cm) in diameter, poorly sorted, subangular to subrounded, very dark brown (10YR 2/2, moist) with patchy stains of very dusky red (2.5YR 2.5/2, moist) or dark reddish brown (5YR 2.5/2, moist), poorly bedded, clasts of greenstone with less than 1% granitoid rocks.
   A. Less than 5% cobbles, pebbles weathered to clayey silt, loose, clast supported.
   B. Pebbles with no cobbles or boulders, very loose, clast supported.
   C. Sandy pebble gravel, <5% cobbles and boulders near base, locally bedded.
6. Lodgement till. Clay: Sandy and gravelly with boulders up to 3 ft (91 cm) in diameter, very poorly sorted, subrounded to subangular, dark grayish brown (2,5Y 4/2, moist), massive, very hard greenstone clasts.

TRENCH T–2

1. Organic soil horizon. Fibrous, peaty mat of muskeg with silt and pebbles, alive at top, very dark brown (10YR 2/2, moist).
2. Colluvium. Silt with sand, clay, pebbles, and cobbles, poorly sorted, angular, porous, olive brown (2.5Y 4/4, moist) to olive (5Y 4/4, moist), massive, argillite and greenstone clasts, gradational contact over weathered bedrock and abrupt contact over fresh bedrock.
3. Loess. Silt with very fine sand, light yellowish brown (10YR 6/4, moist), locally weathered to dark brown (7.5YR 3/4, moist), massive, partly mixed with colluvium, 1-in.-(2.5-cm-) thick, discontinuous paleosol at base, very dark brown (10YR 2/2, moist).
4. Weathered bedrock. Sand, silt, and clay, decomposed argillite and greenstone.
5. Argillite (Kag). Medium light gray (N6, moist), weathered light brownish gray (10YR 6/2, moist) to brownish yellow (10YR 6/6, moist), thin bedded, bedding plane cleavage.
   A. Hard.
   B. Hard, moderately sheared.
   C. Intensely sheared.
   D. Closely sheared, grayish black (N2, moist).
   E. Closely sheared, red (10R 4/6, moist).
   F. Gouge of crushed argillite and argillite flakes.
   G. Closely sheared.
6. Greenstone (Pzv). Basalt metamorphosed to pumpellyite-prehnite grade of metamorphism.
   A. Dark gray (N3, moist) to dark greenish gray (5GY 4/1, moist), subophitic and finely granular, traces of pyrite and quartz.
   B. Phyllitic with interbeds of Unit 6A, dusky yellow green (5GY 5/2, moist) and grayish olive green (5GY 4/2, moist).
7. Fault gouge. Clay, red (2.5YR 5/8, moist).

FIGURE 4-12 (SHEET 1 OF 2)

TRENCH T–1, TRENCH LOG

TRENCH T–2, TRENCH LOG

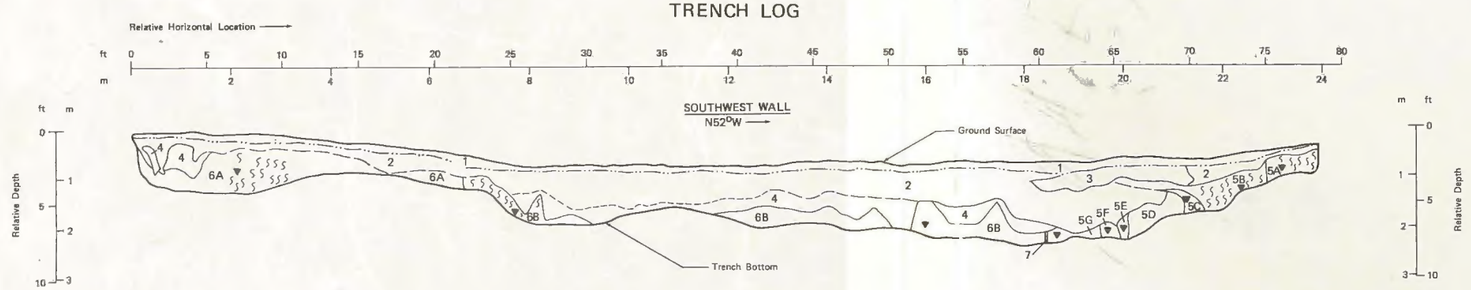

TRENCHES T–1 AND T–2, TRENCH LOGS

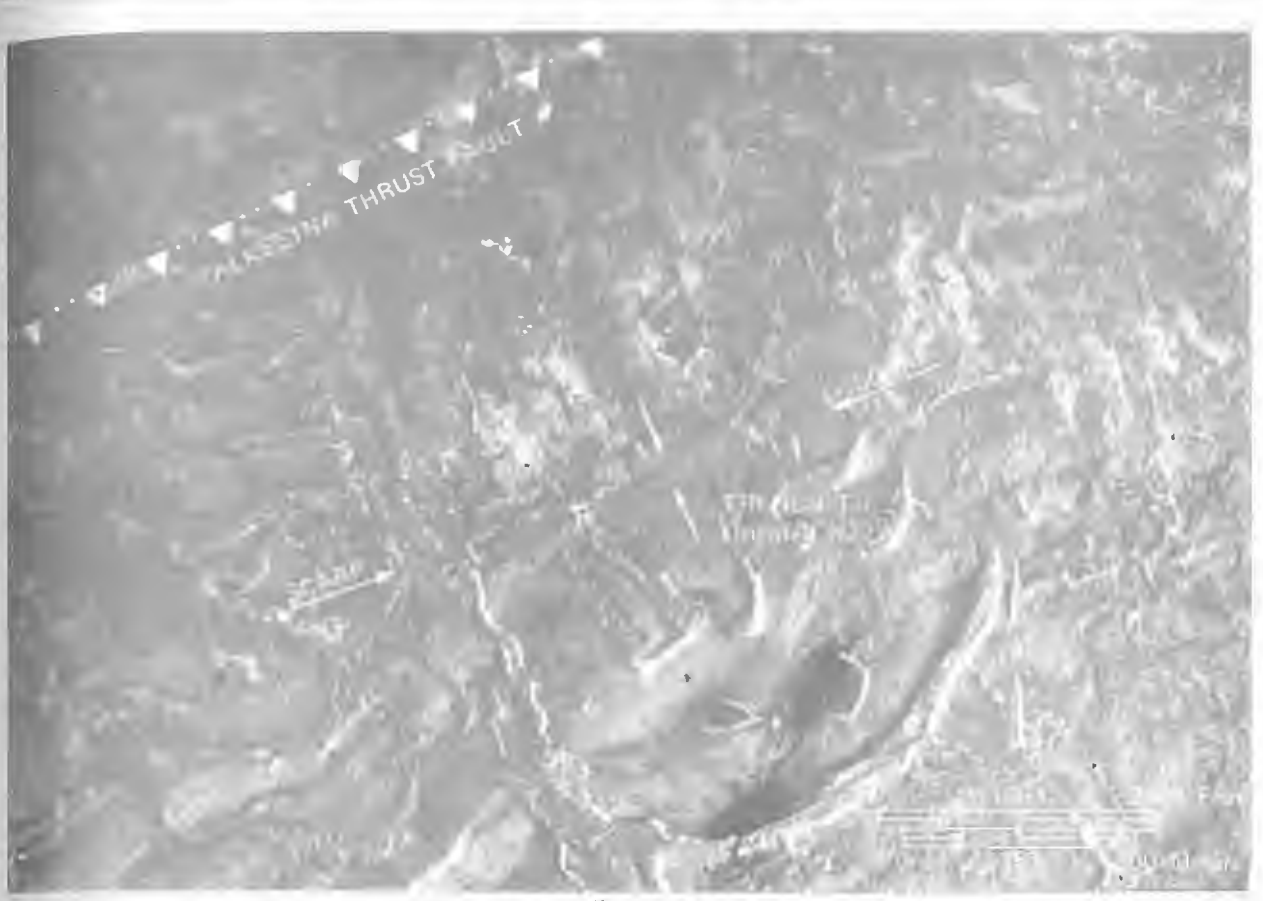

A. Low sun-angle aerial photograph of the Trench T-1 location.

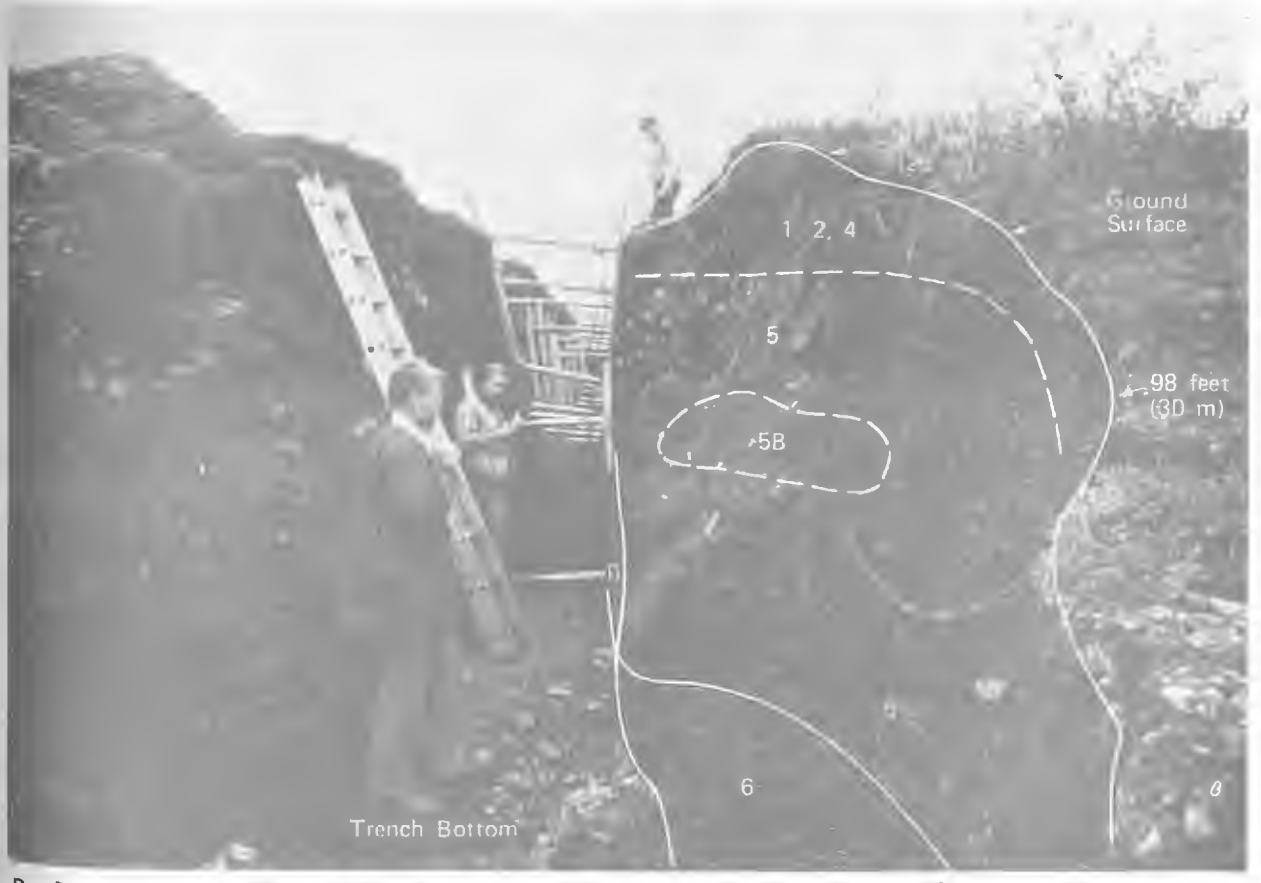

B. Southeast view of Trench T-1 at the scarp. Units are described in Figure 4-12.

PHOTOGRAPHS OF TRENCH T-1

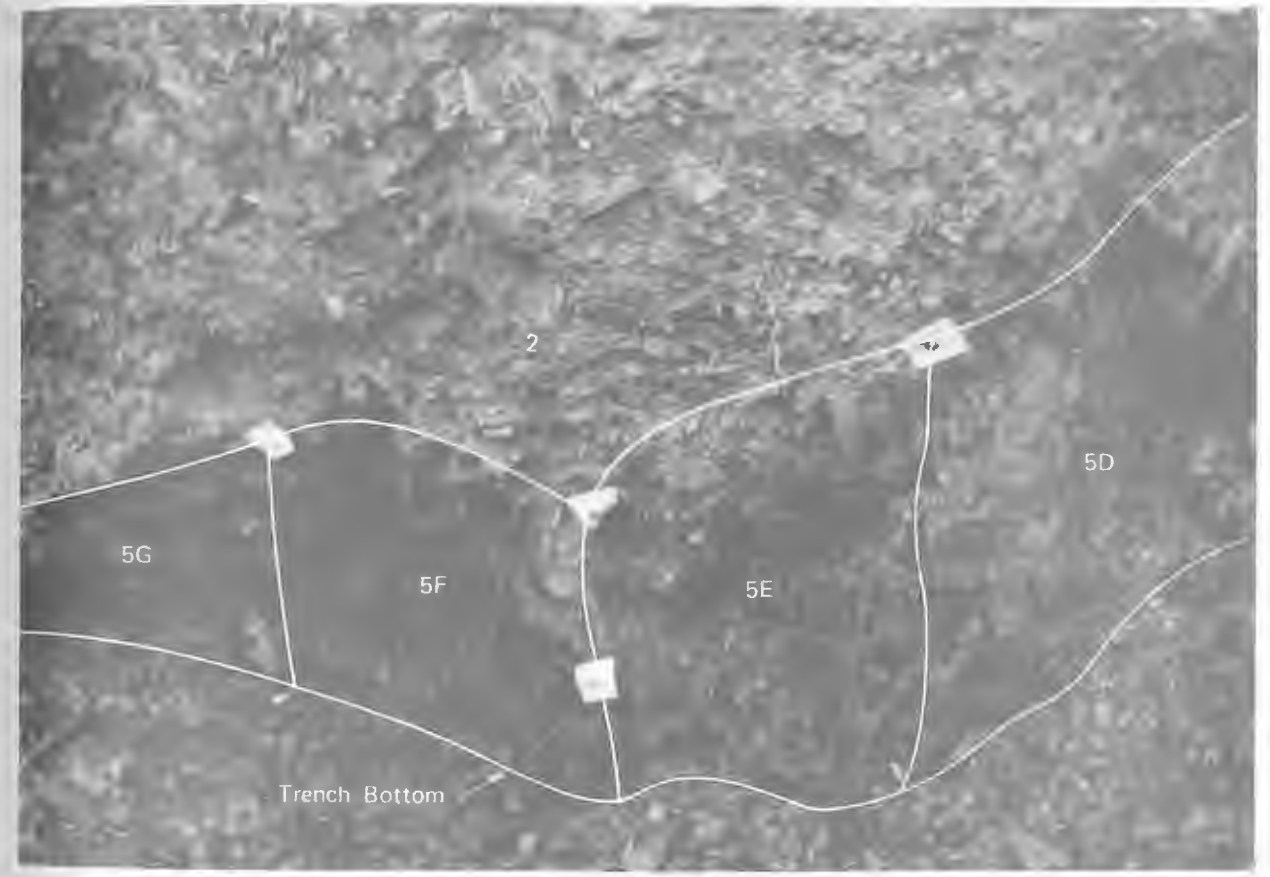

Southwest wall of Trench T-2 between 63 and 67 feet (20.7 and 22.0m). Units are described in Figure 4-12.

PHOTOGRAPH OF TRENCH T-2

FIGURE 4-14

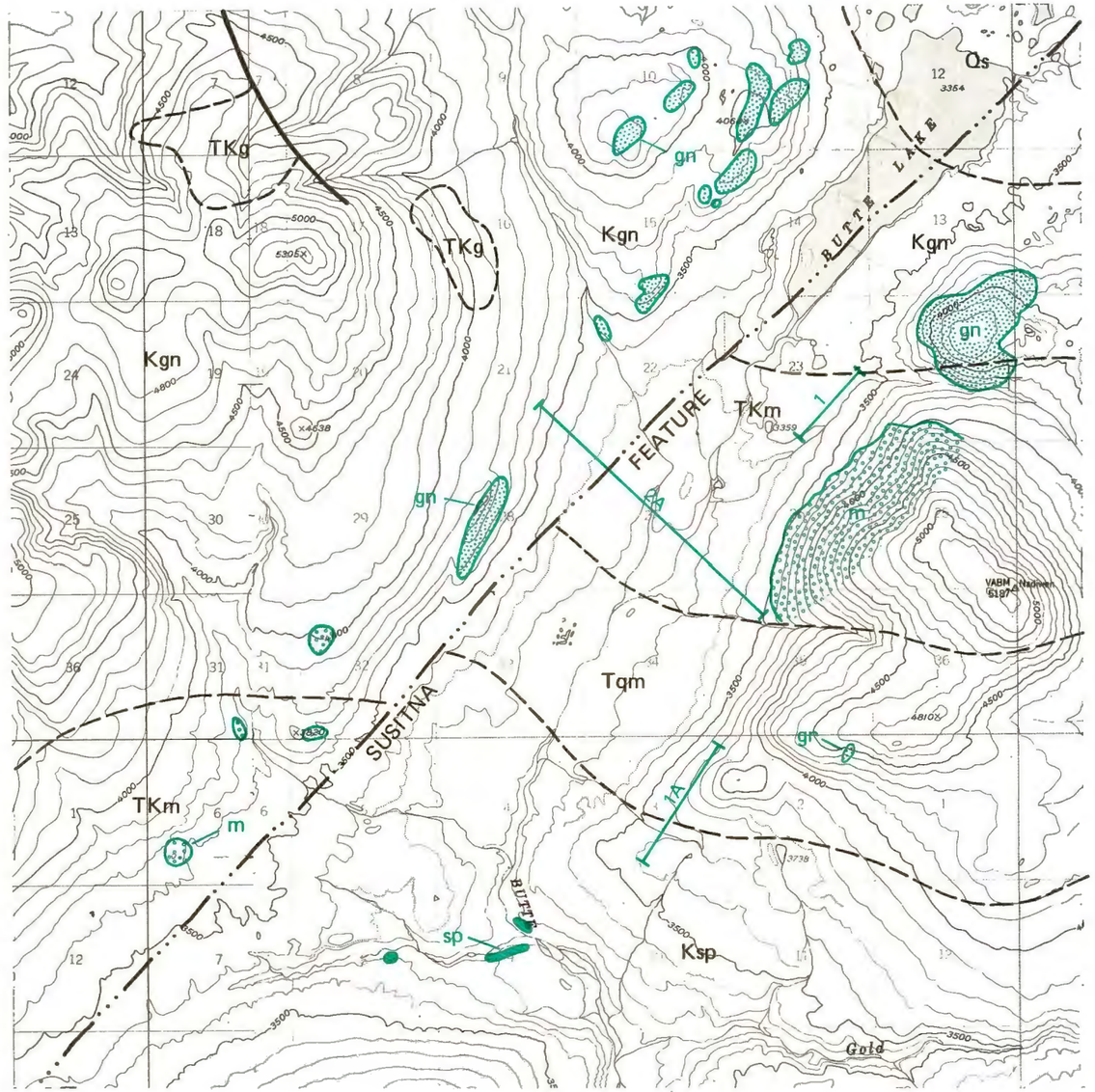

LEGEND

Turner and Smith (1974)

Qs	Quaternary surficial deposits
Tqm	Tertiary quartz monzonite
TKm	Tertiary or Cretaceous migmatitic intrusive rocks
TKg	Tertiary or Cretaceous granodiorite and quartz diorite
Kgn	Cretaceous paragneiss
Ksp	Cretaceous pelitic schist

Lithologic contact

Lineament

Woodward-Clyde Consultants 1981 Field Studies

m	Quartz monzonite and equivalent gneiss
gn	Biotite schist and gneiss
sp	Pelitic schist
1	Location and number of magnetic profile

NOTES

1. Geologic relations shown in this figure are discussed in Section 4.4.1.
2. Magnetic profiles are shown in Figure 4-16.

N

GEOLOGIC MAP OF
LOCATION W11 NEAR BUTTE LAKE

0 1 2 Miles

0 1 2 Kilometers

FIGURE 4-15

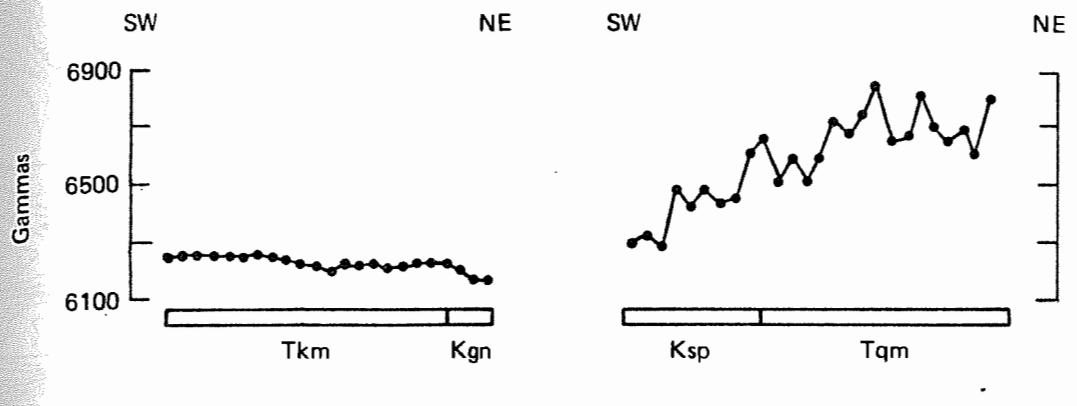

A. MAGNETIC PROFILE 1

B. MAGNETIC PROFILE 1A

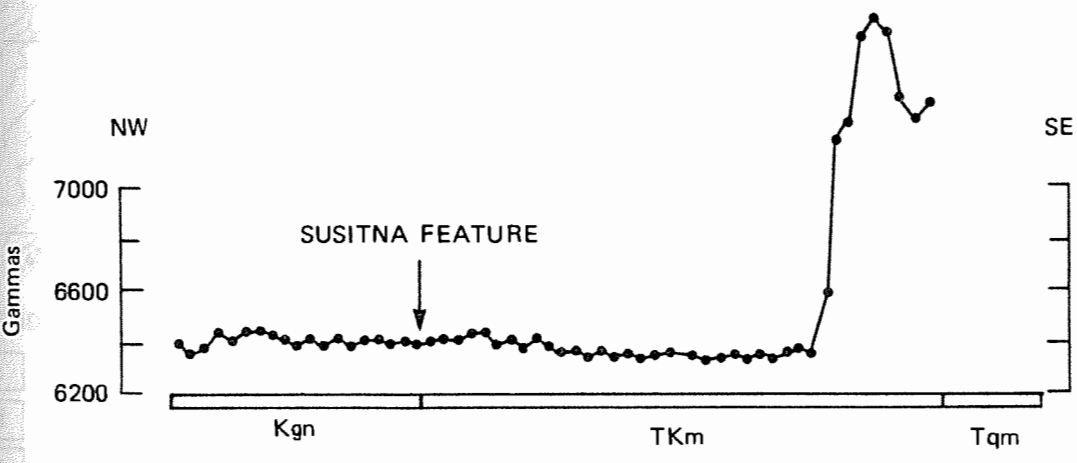

C. MAGNETIC PROFILE 2A

LEGEND

- • Station reading
- Tqm Tertiary quartz monzonite
- TKm Tertiary or Cretaceous migmatitic intrusive rocks
- Kgn Cretaceous paragneiss
- Ksp Cretaceous pelitic schist

NOTES

1. Susitna feature location and bedrock geology is from Turner and Smith (1974).
2. Magnetic profile 1 is a calibration line across rock units similar to those in magnetic profile 2A across the Susitna feature.
3. Magnetic profile locations are shown in Figure 4-14.
4. Magnetic data acquisition methodology is described in Section A.5.

BUTTE LAKE
MAGNETIC PROFILES

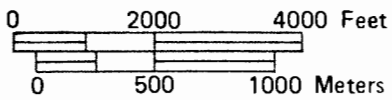

FIGURE 4-16

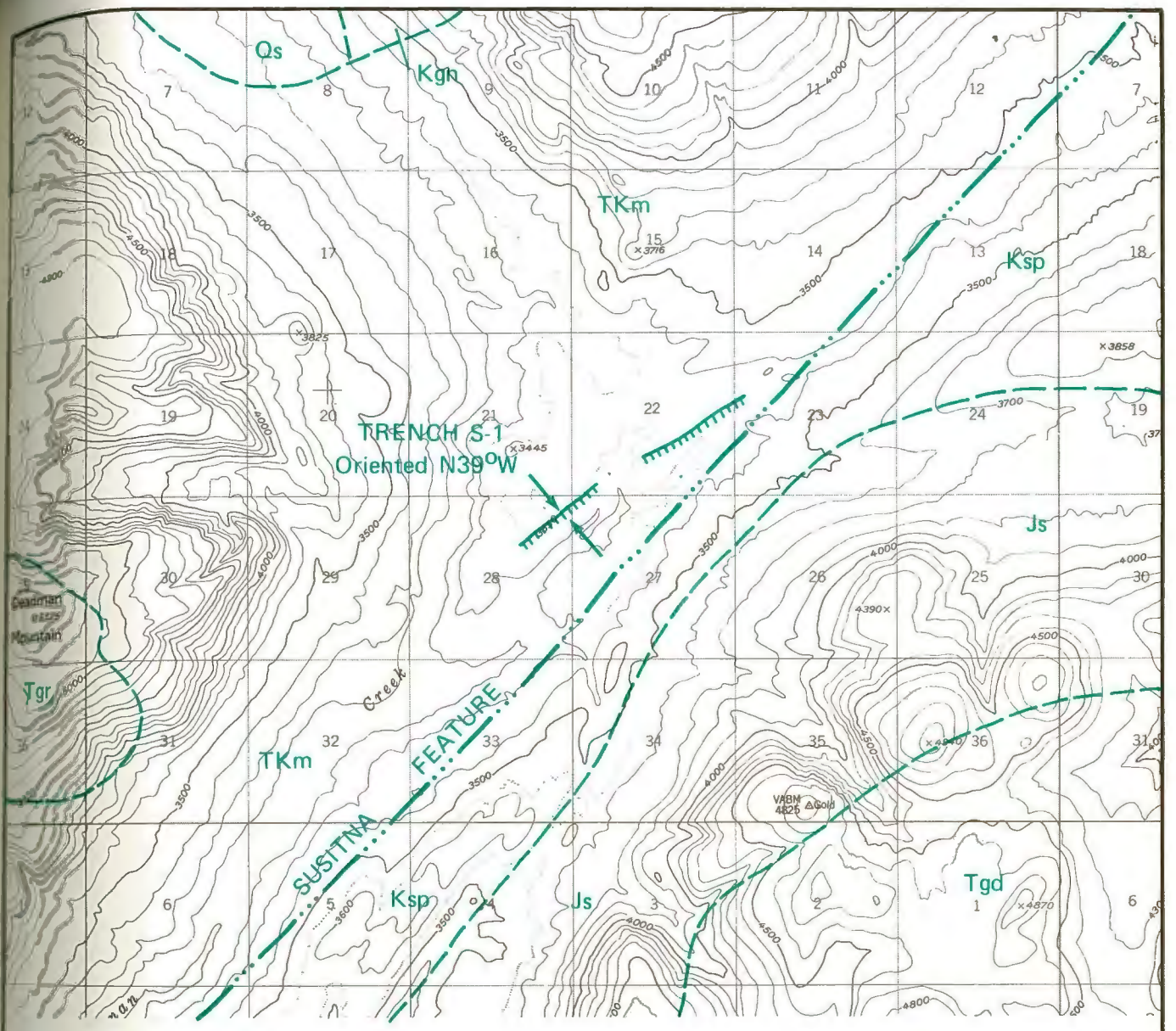

LEGEND

Qs	Quaternary glacial sediments
Tgd	Tertiary granodiorite
Tgr	Tertiary felsic intrusive rock
TKm	Tertiary and Cretaceous migmatitic instrusive rocks
Kgn	Cretaceous paragneiss
Ksp	Cretaceous pelitic schist
Js	Jurassic flysch
— — —	Inferred lithologic contact
	Linear scarp, line at top of slope, hachures on slope
— ··· —	Lineament
	Trench located between arrows

NOTES

1. Geology is from Turner and Smith (1974).
2. Geologic relations shown in this figure are discussed in Section 4.4.1.

N

LOCATION OF TRENCH S-1
AT LOCATION W12

0 1 2 Miles

0 1 2 Kilometers

FIGURE 4-17

LEGEND

Lithologic Contacts, Description, Width

Abrupt, <0.1 ft (<3 cm)

Gradational, 0.1 to 0.5 ft (3 to 15 cm)

Very gradational, >0.5 ft (>15 cm)

Soil Boundaries, Description, Width

Abrupt, <0.1 ft (<3 cm)

Gradational, 0.1 to 0.5 ft (3 to 15 cm)

Very gradational, >0.5 ft (>15 cm)

Other Symbols

≡ or ≋ Laterally gradational or interfingering contact

⊻ Water table at time of excavation

✔ Boulder

Gravel layer

Sand layer

Original surface disturbed by excavation

ʃ Fracture due to shear

▼ Sample location

NOTES

1. Trench Data: S–1

   Length: 228 ft (69.5 m)

   Maximum Depth: 9 ft (2.7 m)

   Excavated: 23 to 24 August 1981

   Geologists: Phillip C. Birkhahn
   Robert G. Goodwin
   Kerry E. Sieh

   Logging Scale: 1 in. = 5 ft

2. Description of units is according to Compton (1962), and Pettijohn (1949).

DESCRIPTION OF UNITS

TRENCH S–1

1. Organic soil horizon. Fibrous, peaty mat of muskeg with silt and pebbles, alive at top, very dark brown (10YR 2/2, moist), massive.

2. Colluvium. Silt, sand, pebbles, and boulders, poorly sorted, angular, strong brown (7.5YR 4/6, moist) with streaks of yellowish brown (10YR 3/4, moist), massive.

3. Clay. Silty with some pebbles, sticky and plastic, stiff, olive gray (5Y 4/2, moist), massive, weak horizontal platey partings, wet.

4. Sandy loam to sandy clay. 5% angular pebbles with clay coatings, slightly sticky and slightly plastic, crumbles, very dark brown (10YR 2/2, moist) with patches of brown (10YR 4/3, 4/3, moist) silt, massive.

5. Lodgement till. Olive gray (5Y 4/2, moist).
   A. Sand: Trace of clay, massive, weak horizontal platey partings.
   B. Clay: Sandy and silty, sticky and plastic, olive gray (5Y 4/2, moist), massive, strong horizontal platy fabric.
   C. Clay: Silty, sticky and slightly plastic to plastic, dark olive gray (5Y 3/2, moist), massive.

6. Ablation till. Sand and gravel with boulders.
   A. Sand: fine to medium with <5% pebbles and cobbles, moderately sorted, subangular to subrounded, massive to poorly bedded; with gravel lenses: 50% pebbles and cobbles, poorly sorted, subangular, 4° to 6° in-to-slope dip.
   B. Gravel: Coarse sand and pebbles with cobbles and boulders, moderately sorted, subangular, dark grayish brown (10YR 3.5/2, moist) to very dark grayish brown (2.5Y 3.5/2, moist), weak fabric parallel to slope, clast supported.
   C. Silt: Sandy and pebbly, poorly sorted, subrounded, very dark grayish brown (2.5Y 3/2, moist), massive, friable.
   D. Sand: Very fine with <10% coarse sand and pebbles with cobbles and boulders, moderately sorted, subrounded, olive gray (5Y 4/2, moist), massive, friable, faint platy fabric subparallel to slope.
   E. Gravel: Sandy and silty, moderately sorted, angular to subangular, dark olive gray (5Y 3/2, moist), moderately bedded, quartz and lithic clasts, silt and sand interbeds.
   F. Sand: Very fine, well sorted, subangular, dark grayish brown (10YR 3.5/2, moist) to very dark grayish bronw (2.5Y 3.5/2, moist), massive.
   G. Sand: Medium to coarse, gravelly, moderately sorted, angular to subangular, olive gray (5Y 4/2, moist), massive quartz, granitoid, and argillite clasts, weak fabric subparallel to slope.

FIGURE 4-18 (SHEET 1 OF 2)

TRENCH S–1,
TRENCH LOG

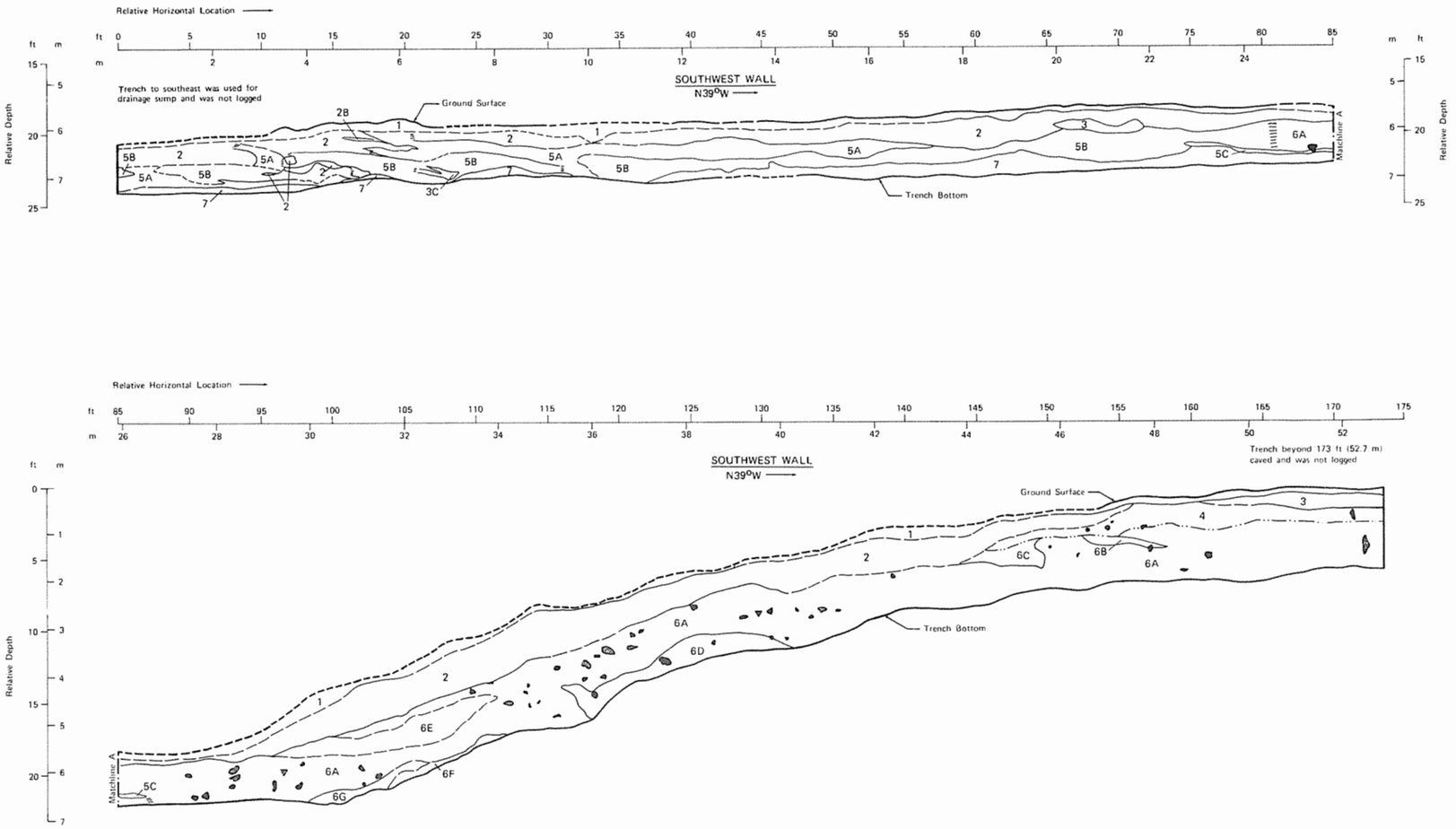

TRENCH S–1,
TRENCH LOG

FIGURE 4-18 (SHEET 2 OF 2)

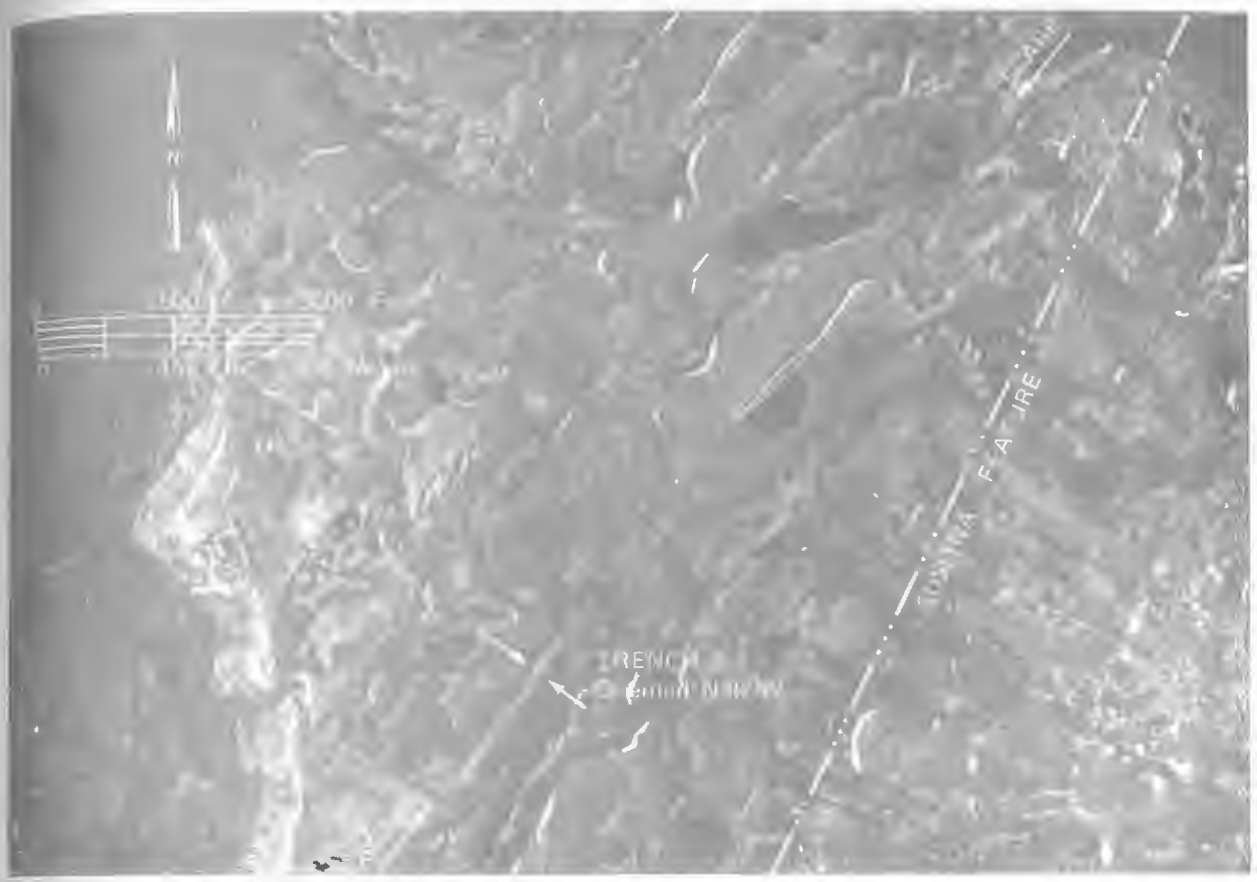

A. Low sun-angle aerial photograph of the Trench S-1 location.

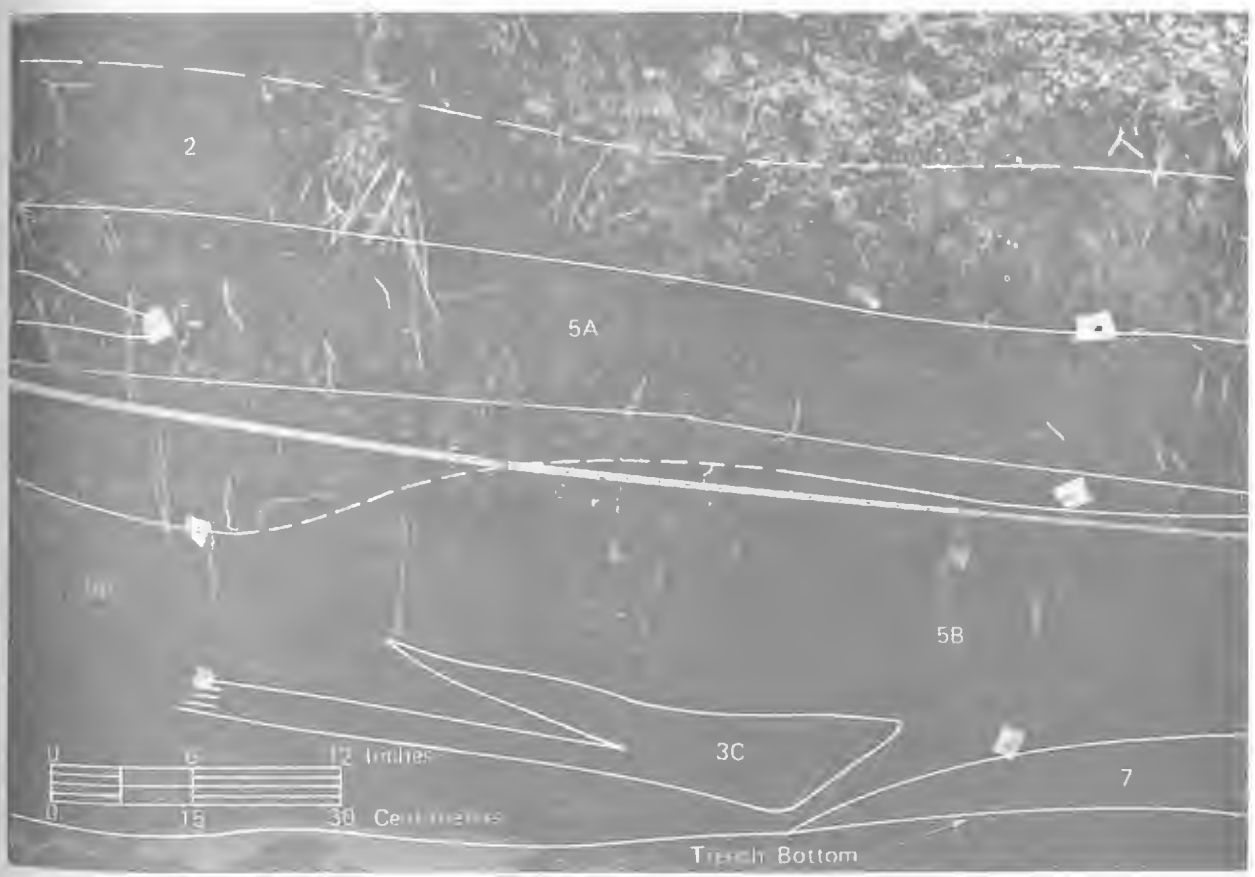

B. Southwest wall of Trench S-1 between 20.5 and 24.7 feet (6.3 and 7.5 m). Units are described in Figure 4-18.

PHOTOGRAPHS OF TRENCH S-1

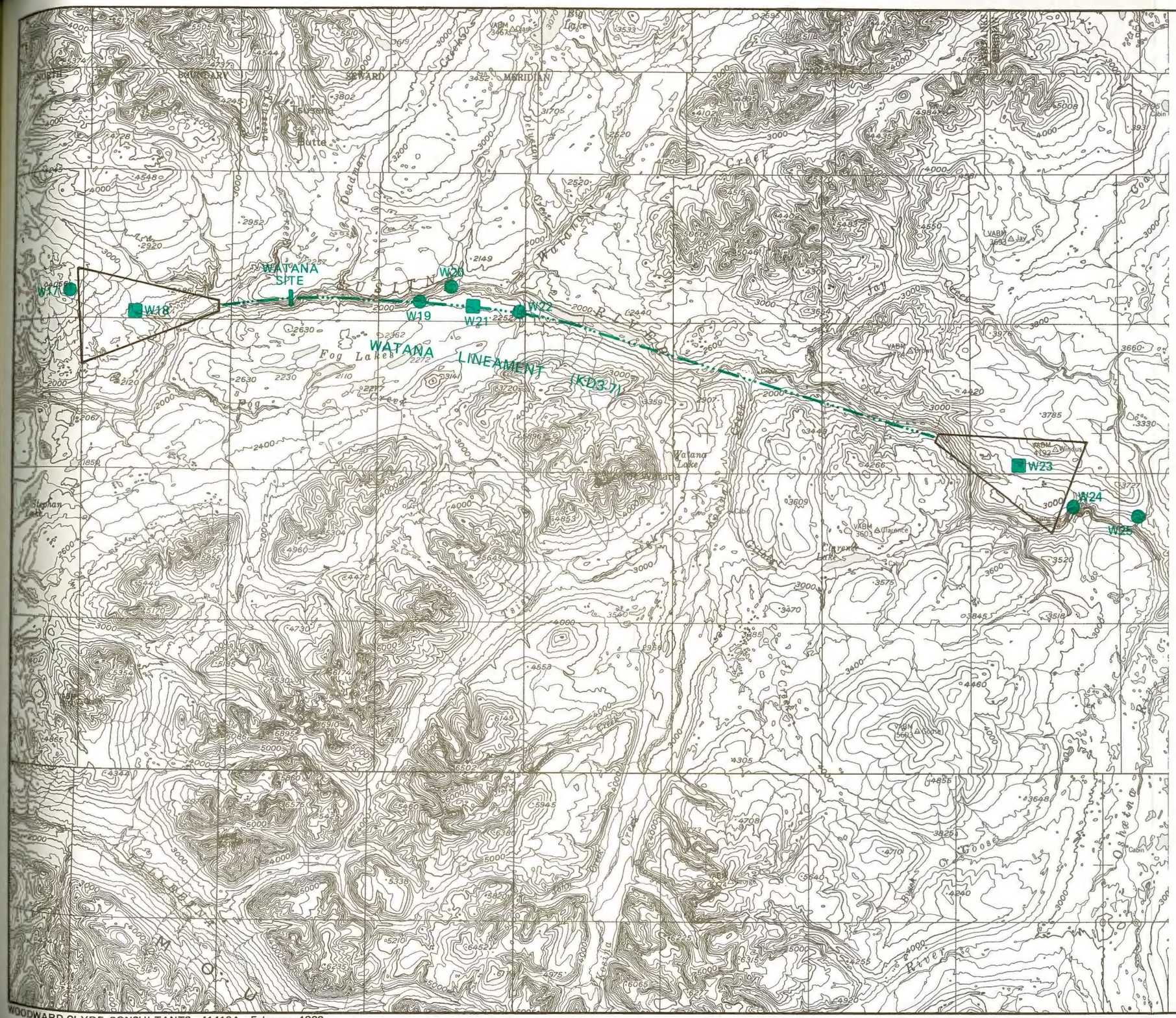

LEGEND

- Lineament
- Location and age designation of Quaternary units (0 to 1.8 m.y.b.p.)
- Location and age designation of Mesozoic and Paleozoic units (65 to 570 m.y.b.p.)
- Area checked for features related to the Watana lineament.

NOTES

1. m.y.b.p. is the abbreviation for million years before present.
2. Geologic relations at locations W17 through W25 are discussed in Section 4.4.1.

WATANA LINEAMENT (KD3-7)
LOCATION MAP

0 5 10 Miles
0 5 10 Kilometers

FIGURE 4-20

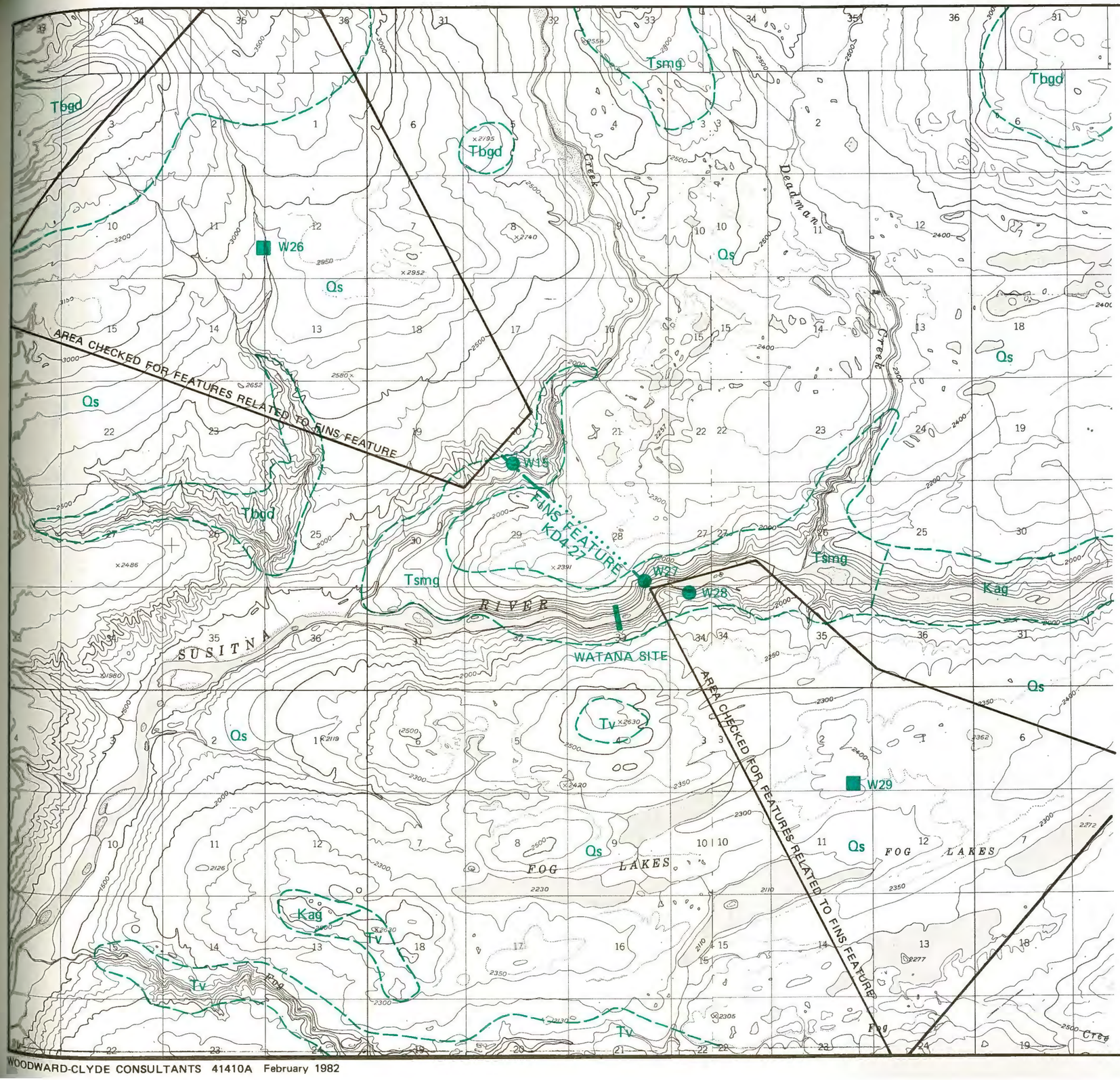

LEGEND

Qs	Quaternary glacial sediments
Tv	Tertiary volcanic rocks
Tbgd	Tertiary granodiorite
Tsmg	Tertiary schist, migmatite, granite
Kag	Cretaceous argillite and graywacke
— — —	Inferred lithologic contact
— — ·	Shear zone or fault, dashed where inferred, dotted where concealed
W26 ■	Location and age designation of Quaternary units (0 to 1.8 m.y.b.p.)
W27 ●	Location and age designation of Mesozoic and Paleozoic units (65 to 570 m.y.b.p.)

NOTES

1. m.y.b.p. is the abbreviation for million years before present.
2. Geologic relations at these locations are discussed in Section 4.4.1
3. The location of the Fins Feature is from U.S. Army Corps of Engineers, Alaska District (undated).
4. Geology is from Csejtey and others (1978).

N

FINS FEATURE (KD4-27)
LOCATION MAP

0 1 2 Miles
0 1 2 Kilometers

FIGURE 4-21

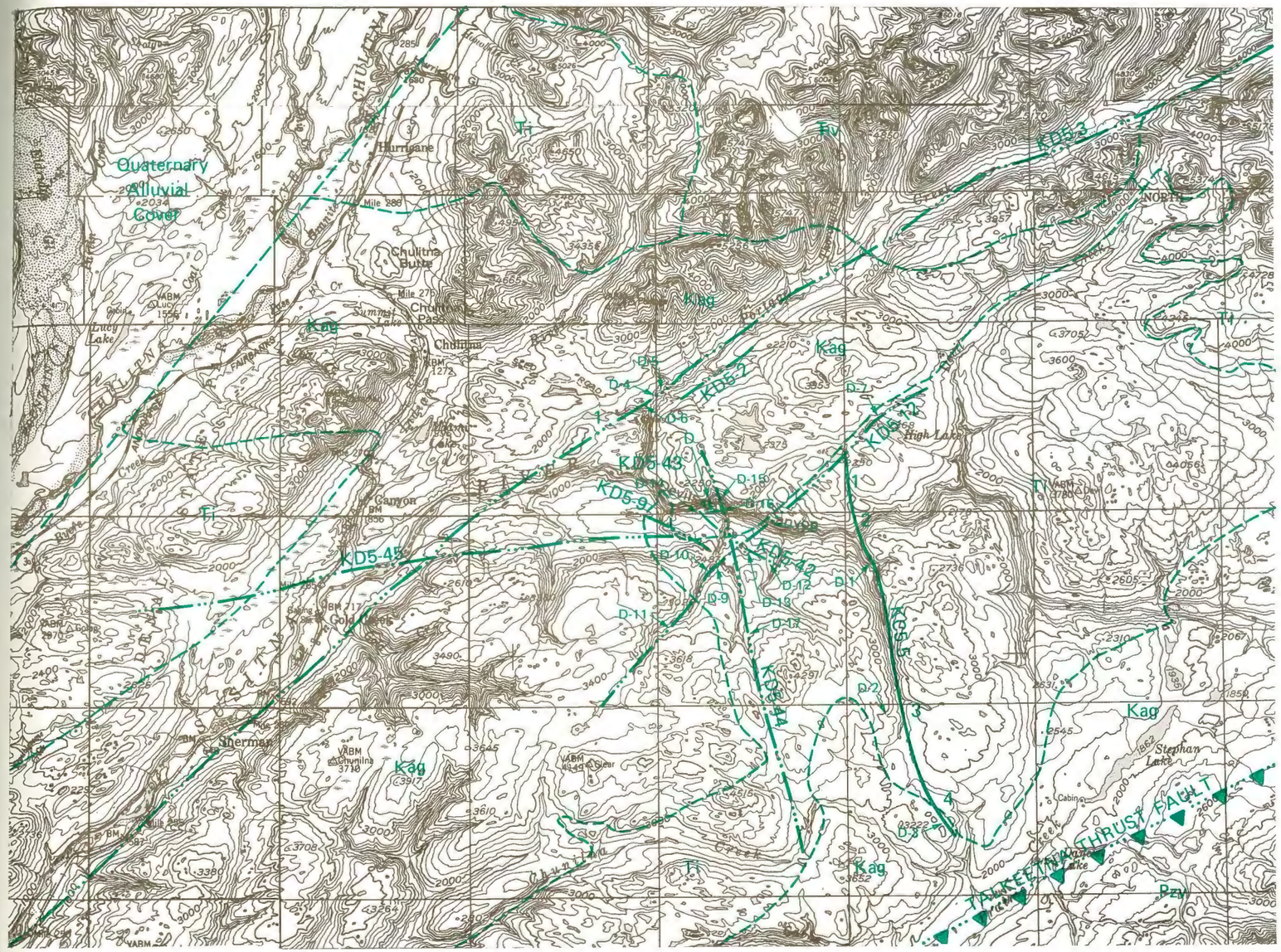

LEGEND

Tv	Tertiary volcanic rocks
Ti	Tertiary intrusive rocks
Kag	Cretaceous argillite and graywacke
Trv	Triassic volcanic rocks
Pzv	Paleozoic volcanic rocks
	Inferred lithologic contact
KD5-3	Lineament and Code No.
KC5-5	Fault and Code No.
	Concealed thrust fault, sawteeth on upper plate
3 / D-3	3 is the segment number discussed in Section 4.4.2 D-3 is the location number discussed in Section 4.4.2.
D	Devil Canyon Site

NOTES

1. Geology is modified after Csejtey and others (1978).
2. Geologic relations shown in this figure are discussed in Section 4.4.2.
3. The Talkeetna thrust fault is concealed by Quaternary sediments.

N

DEVIL CANYON FEATURES
LOCATION MAP

0 5 10 Miles
0 5 10 Kilometers

FIGURE 4-22

5 - SEISMICITY AND STRESS REGIME

This section summarizes the regional historical seismicity study and the results of the microearthquake network operation that were conducted in 1980 (Woodward-Clyde Consultants, 1980b). The results of the work conducted in 1981 are also presented. The overall objective of these studies was to increase the understanding of earthquake potential within the Benioff zone of the subducted Pacific plate and within the Talkeetna Terrain. The results of these studies have were used primarily to refine our understanding of the location, size, and focal mechanism of possible maximum credible earthquakes associated with these regions.

The 1981 seismicity study included: an evaluation of the tectonic associations of moderate to large earthquakes in or adjacent to the Talkeetna Terrain; a review of the Benioff zone seismicity (to refine the assessment of the size and location of the largest earthquake that could be expected to occur on the Benioff zone); a review of small earthquakes in the Talkeetna Terrain to refine the assessment of the nature of the stress regime; development of recurrence relationships for the crustal zone seismicity and seismic sources within the Benioff zone; and preparation of a manual for a long-term seismic monitoring network. The first four topics are discussed below. The manual is presented as a separate document from this report.

To assess the maximum credible earthquake in the Talkeetna Terrain and the Benioff zone, historical earthquakes of about magnitude (M_S) 6 or larger (that occurred within or beneath the Talkeetna Terrain) were re-examined in terms of location, focal depth, focal mechanism, and tectonic association. To augment this work, an additional literature review and an analysis of worldwide historical earthquake data were conducted to refine the earthquake potential of the Benioff zone. The stress regime within the Talkeetna Mountains portion of the Talkeetna

Terrain was also studied further by analyzing records from the 1980 network (Woodward-Clyde Consultants, 1980b) and from the University of Alaska Geophysical Institute (UAGI).

The following discussion presents: a) the regional historical seismicity, including the analysis of moderate to large historical earthquakes; b) the results of the Benioff zone seismicity review; c) a summary of the results of the microearthquake network operation in 1980; d) a discussion of the regional stress regime in the Talkeetna Terrain, including the analysis of focal mechanisms for selected events; and e) recurrence relationships developed for the crustal zone seismicity and the Benioff zone.

5.1 - Regional Seismicity

5.1.1 - Tectonic Setting

Recent concepts of plate tectonics have had a major influence on interpretations of the contemporary tectonics of Alaska. According to these concepts, the underlying cause of the geologic and seismic activity in central and southern Alaska is the subduction of the Pacific plate at the Aleutian Trench as the plate spreads northward from the east Pacific Rise (Isacks and others, 1968; Tobin and Sykes, 1968). This northward movement occurs at a rate of approximately 2.4 inches/yr (6 cm/yr) relative to the North American plate and is illustrated in Figure 4-1. As the Pacific plate reaches the Aleutian Trench, it is thrust under the portion of the North American plate that includes Alaska and the Aleutian Islands.

In the Gulf of Alaska area, the interplate movement is expressed as three styles of deformation: right-lateral slip along the Queen

Charlotte and Fairweather faults; underthrusting of the oceanic Pacific plate beneath the continental block of Alaska; and a complex transition zone of oblique thrust faulting near the eastern end of the Aleutian Trench (Figure 4-1). The Trench represents the ground surface expression of the initial bending of the oceanic plate as it moves downward beneath the North American plate.

The regional earthquake activity is closely related to the plate tectonics of Alaska. Figure 4-1 shows an oblique schematic view of the major geologic and tectonic features of the regional plate tectonics. The subducting plate is shown moving to the northwest away from the Aleutian Trench and dipping gently underneath the upper Susitna River region. The subducted material is located at depth on the basis of the hypocenter distribution of instrumentally located earthquake activity. This kind of subcrustal seismic zone is called a Benioff zone. In some areas, such as to the southwest of the site region along the Alaska Peninsula, the presence of subducted oceanic crust is inferred from the presence at the ground surface of andesitic volcanic rocks.

The Benioff zone in the site region is characterized by earthquake activity extending to a depth of about 93 miles (150 km) (Agnew, 1980). No autochthonous andesitic volcanic rocks or volcanoes currently are known to be present at the ground surface in the site region above the Benioff zone.

Beneath the Prince William Sound area, which is on the North American plate, the subducted plate moves nearly horizontally. The two plates appear to be closely coupled in this region and have the capacity to accumulate and release very large amounts of elastic strain energy. The most recent example of this process was the 28 March 1964 earthquake of magnitude (M_S) 8.4 (M_W 9.2). Part of the rupture zone of this earthquake near the sites, as evidenced by aftershocks, is shown in Figures 4-1 and 5-7.

The overlying North American plate is also disrupted by intraplate deformation that is related to the interplate motion. Evidence for tectonic deformation is found in the Alaska Range more than 279 miles (450 km) northwest of the surface interplate boundary at the Aleutian Trench in the Gulf of Alaska. Much of this deformation is the composite expression of the plate interaction process over millions of years and of the seaward migration of the subducting zone, which has periodically accreted additional crust to the continental land mass.

The historical seismicity within 200 miles (322 km) of the Project is associated with three general source areas: the crustal seismic zone within the North American plate; the intraplate region of the Benioff zone; and the interplate region of the Benioff zone. The seismicity of these three source areas is reviewed in this section following a discussion of the record of historical seismicity in the Talkeetna Terrain and adjacent areas.

5.1.2 - Historical Seismicity Record

Prior to the installation in 1935 of a seismograph near Fairbanks at College, Alaska (CMO), only local felt reports or seismograph recordings made at distant stations were available to determine epicenters and focal depths of earthquakes in south central Alaska. Among these distant stations were: one at Sitka, Alaska, installed in April 1904, consisting of two Bosch-Omori horizontal seismometers; one each at Berkeley and at Lick Observatory in California, installed in 1887 (published readings began in 1910 and 1911, respectively); and some Japanese stations developed in 1879. Davis and Echols (1962), Davis (1964), and Meyers (1976) have published lists of felt earthquakes for Alaska dating from the 18th century, although the very low-population density in Alaska prior to 1900 has precluded historical felt reports of earthquakes in the interior of Alaska earlier than the large event of 1904.

Davis (1964) and Meyers (1976) have published lists of felt earthquakes for Alaska dating from the 18th century, although the very low-population density in Alaska prior to 1900 precluded historical felt reports of earthquakes in the interior of Alaska earlier than the large event of 1904.

During the early and middle portion of the twentieth century, prior to 1964, epicenters and focal depths of earthquakes in Alaska were computed primarily from teleseismic data. Location uncertainty varied greatly and depended on the specific combination of earthquake size and source region depth. For example, larger earthquakes (magnitude [M_S] greater than 6) that occurred within the shallow Benioff zone may have been well-recorded worldwide, but may not have had clear pP phases to constrain depth estimates and may have been located using travel time curves that did not account for local tectonic structure. Uncertainties in location and depth could be as large as 62 miles (100 km) or more. For earthquakes of uncertain focal depth, the focal depth is often constrained to a depth of 20 miles (33 km) to compute the epicentral location. In addition, recomputations of some earlier earthquake locations, such as those published by Sykes (1971), have reduced some of the original catalog errors.

The accuracy of epicentral locations improved slightly with the installation of the seismograph at College, Alaska (CMO), (near Fairbanks) in 1935, but it was not until the mid 1960s, after the devastating Prince William Sound earthquake of 28 March 1964, that earthquake monitoring was significantly improved in central and southern Alaska. After the 1964 earthquake, epicentral and focal depth accuracy improved with the installation of seismic networks operated by the University of Alaska Geophysical Institute (UAGI), the National Oceanographic and Atmospheric Administration (NOAA),

and the U.S. Geological Survey during the period 1964 to 1967, and with the preparation of a velocity model for the area by Biswas and Battacharya (1974).

Since 1974, the focal depths of earthquakes recorded and located by the UAGI are accurate to approximately plus or minus 9 miles (15 km) with the epicentral accuracy generally being better than the depth accuracy. Location accuracy and magnitude detection levels have varied due to the number of stations in operation at a given time and changes in data handling procedures and priorities, so the above values may be too small for some poorly recorded events. From 1967 to 1974, the focal depth error estimates are approximately plus or minus 12 to 19 miles (20 to 30 km), with epicentral uncertainty of plus or minus 12 to 16 miles (20 to 25 km). The accuracy of focal depth estimation within the U.S. Geological Survey seismograph network is very good, probably plus or minus 6 miles (10 km) or less. However, this network is south of the Project and generally outside of the site region.

5.1.3 - Analysis of Large Historical Earthquakes

Within the tectonic setting of the site region (Section 5.1.1) the Benioff zone has a substantially higher level of seismicity than the crust, which includes the Talkeetna Terrain (as shown in Figures 5-1 and 5-2 and discussed in Section 4.3 of the Interim Report [Woodward-Clyde Consultants, 1980b]). This observation implies that most large historical earthquakes of magnitude (M_S) 6 or larger have occurred in the Benioff zone rather than in the crust. To obtain a better understanding of this concept and to ascertain its validity, we reviewed available records for these events using the computational seismology techniques of Helmberger (1968) and others cited below. The earthquakes that were studied

are listed in Table 5-1 and shown in Figures 5-1 and 5-2, which are revised from Figure 4-6 of the Interim Report (Woodward-Clyde Consultants, 1980b).

In carrying out this study, seismograms of the selected events were acquired from data sources in the United States and Europe. The seismograms were used to evaluate focal parameters such as location and depth of the earthquake, orientation of the fault plane, and sense of displacement. The focal parameters were then determined or estimated by using waveform analysis based on synthetic seismograms (e.g., Helmberger, 1968; Langston and Helmberger, 1975; Rial, 1978) and first-motion polarities of body waves. For events prior to 1960, only two or three seismograms of the events were usually available, so some of the determinations are necessarily more uncertain and a greater level of judgment was used. In order to calibrate the judgments of waveform interpretation, two more recent earthquakes were analyzed, the 1964 and 1975 earthquakes listed in Table 5-1.

1 January 1975

The focal depth of this m_b 5.9 earthquake, as listed in Appendix C of the Interim Report (Woodward-Clyde Consultants, 1980b), is 41 miles (66 km), suggesting its association with the subducting plate. Examination of the available World-Wide Standardized Seismographic Network (WWSSN) records shows clear depth phases (pP) that allowed the focal depth estimate to be revised to 34 miles (55 km). The first-motion directions of P-waves read from nine of these records do not provide much constraint on the focal mechanism, but examination of the waveforms suggest the occurrence of normal faulting. The first-motion observations and the assumed normal fault mechanism are shown in Figure 5-3A. This mechanism and focal depth are consistent with earthquake sources occurring within the subducted plate.

29 June 1964

The first-motion plot for this magnitude (m_b) 5.6 event is shown in Figure 5-3B. Data from stations Apatity, U.S.S.R. (APA), Nurmijarvi, Finland (NUR), and Köngsberg, Norway (KON), were taken from the International Seismological Centre (ISC) bulletin; other readings were taken from the WWSSN seismograms. Examination of the available WWSSN records shows waveform characteristics typical of a shallow crustal event (depth = 9 to 12 miles [15 to 20 km]). This earthquake was clearly not associated with the Benioff zone which lies at a depth of about 80 miles (125 km) beneath the epicenter. It is concluded that this event occurred in the crust and is assumed to have a pure thrust solution (as shown in Figure 5-3B); however, a substantial amount of oblique slip is possible. The strike of the nodal planes is N55°E with dips of 10°NW and 80°SE.

19 August 1948

This magnitude (M_S) 6-1/4 earthquake was examined to verify its focal depth, which was estimated as 62 miles (100 km) in Appendix C of the Interim Report (Woodward-Clyde Consultants, 1980b). The records at Pasadena, California (PAS), and several other southern California stations show clear depth phases indicating a focal depth of 55 miles (90 km). Thus, this event is associated with the Benioff zone. The wave form characteristics suggest a thrust mechanism.

3 November 1943

This earthquake of magnitude M_S 7.3 is the largest historical earthquake that has been located within the Talkeetna Terrain. It has, therefore, been studied in greater detail during this study than the other events.

Good seismograms showing clear body and surface waves were obtained from Kew, England (KEW), Ottawa, Canada (OTT), College, Alaska (CMO), Honolulu, Hawaii (HON), Puerto Rico (SJG), Pasadena, California (PAS), and additional stations in the southern California network. Synthetic seismograms were constructed to match the observed records, as shown for the long-period record at PAS in Figure 5-4. The shape and complexity of the P-wave form indicates the presence of two sources separated in time by 1.7 seconds and occurring at nearly the same location. A focal depth of 11 miles (17 km) gives the best fit of the synthetic record to the observed records for the phases pP and sP (with an accuracy of $\pm$1 mile [2 km]). The source model for both sources is a high-angle, nearly pure reverse mechanism (dip and rake of 80° to 90°) with strike of N45°E. The second source is slightly larger, with relative seismic moment of 5.5×10^{26} dyne-cm compared to 5.0×10^{26} dyne-cm for the first source. The source time-functions for both sources indicate a relatively high stress drop; this interpretation is consistent with the interpretation that this double event is an intraplate earthquake (Kanamori and Anderson, 1975).

The observed polarities of the body waves are consistent with the theoretical radiation pattern of the NE-striking reverse-slip model. Figure 5-5 shows the theoretical radiation patterns for P, SV, and SH for epicentral distance greater than 30°. Stations and polarities are plotted at their azimuths from the epicenter. P-wave polarities at OTT, KEW, PAS, and CMO allow for up to 15° uncertainty in the fault orientation and dip.

With the focal depth accurately estimated at 11 miles (17 km), the epicenter of the earthquake (as listed in Appendix C of Woodward-Clyde Consultants, 1980b) can also be refined. To analyze the epicenter, the residuals at stations reported in the

ISC Bulletin were minimized using a trial and error approach that took into account the 11 mile (17 km) focal depth. The revised location of 61.9°N latitude and 151.3°W longitude is 19 miles (30 km) northwest of the NOAA location. The uncertainty of the revised location is 6 to 12 miles (10 to 20 km). This location is approximately 90 miles (145 km) southwest of the Project (Figure 5-1) and lies along the transitional western boundary of the Talkeetna Terrain.

Geological Association

The seismological analysis of the 1943 earthquake places it in the crust along the western boundary of the Talkeetna Terrain (Figure 5-6). For an earthquake of this size and focal depth, we would expect it to have occurred on an identifiable source (e.g., a fault with recent displacement) as discussed in Section 4.2. No faults with recent displacement had been reported in this region, so a limited literature review and remotely sensed data interpretation program was conducted during this study. The literature review involved the review of geophysical studies and field mapping, primarily by Griscom (1979), Csejtey and Griscom (1978), and Csejtey and others (1978) and evaluation of the tectonic model (including the Talkeetna Terrain); the review led to the following observations:

a) The earthquake occurred along the western boundary of the Talkeetna Terrain. As discussed in Section 4.1, this boundary is a broad zone of deformation and volcanoes.

b) A prominent northeast-southwest trending aeromagnetic anomaly (separating aeromagnetically dissimilar terrain) was identified within 15 miles (25 km) north of the epicenter by

Griscom (1979), as shown in Figure 5-6. This anomaly corresponds in part (such as near Mount Yenlo [Figure 5-6]) to what Griscom (1979) refers to as an unconformable contact between the Mesozoic metasedimentary sequence of the Maclaren Terrane to the northwest and the Paleozoic and Mesozoic volcanic sequence of the Wrangellia Terrane to the southeast (these terranes are discussion in Section 4.4.1). In the project site region, this contact was mapped as the Talkeetna thrust fault (Csejtey and others, 1978).

c) The Talkeetna thrust fault is offset near the town of Talkeetna by a series of strike-slip faults, as shown in Figure 5-6. This offset presents convincing evidence that this segment of the Talkeetna thrust fault has not been subject to recent displacement (i.e., if the Talkeetna thrust fault had had youthful displacement, it would have displaced these strike-slip faults rather than having been displaced by them). It also shows that the contact described in (b) above is not part of the same fault system.

d) The Mount Yenlo contact dips to the northwest as shown in Figure 5-6. This dip is in the opposite direction from that of the Talkeetna thrust fault described in Section 4.4.1 and shown in Figure 5-6.

e) The southwestern end of the Talkeetna thrust fault is capped by Tertiary volcanic units that have no observed displacement.

f) The aeromagnetic anomaly described in (b) above does not correlate with the mapped trace of the Talkeetna thrust fault southwest of Stephan Lake. A number of causes could have produced this deviation, for example, the presence of intrusive bodies with a high percentage of minerals with magnetic properties.

In addition to the above geophysical and geologic data review, interpretations were made of LANDSAT imagery for a 705-square-mile (1,960-km^2) area encompassing the epicentral region. Available U-2 photography at a scale of 1:60,000, which covered approximatelty 60% of the region, was also interpreted, and a winter overflight was made of the epicenter region. The purpose of the overflight made on 16 December 1981 was to review the lineaments identified on the remotely sensed data and to assess if any clearly identifiable faults with recent displacement were present in the epicentral region. Lighting and weather conditions during the overflight were poor, the cloud ceiling was at 2,500 feet to 3,000 feet (762 m to 915 m), and light was diffuse, with approximately three hours of usable daylight.

The results of the remotely sensed data analysis and overflight led to the following observations:

a) A number of lineaments are possible candidate sources for this earthquake. These lineaments are shown in Figure 5-6.

b) The observed lineaments predominantly trend northwest-southeast perpendicular to the northeast-southwest trend obtained from the focal mechanism studies.

c) The observed lineaments are parallel to the range front (and the Talkeetna Terrain boundary) and the direction of glacial ice.

d) Many of the lineaments are of glacial origin. Some of the lineaments may be of tectonic origin.

From the geophysical, geological, and remote sensing observations described above, it was concluded that:

a) Potential sources for the 1943 earthquake are present in the epicentral region (e.g., the source of the aeromagnetic anomaly; or one of the lineaments observed in the epicentral area).

b) Among the potential sources for the 1943 earthquake, no obvious faults with recent displacement were observed.

c) The 1943 earthquake did not occur on a fault that is part of the Talkeetna thrust fault.

27 April 1933

This magnitude (M_S) 7 earthquake was reported by NOAA (Appendix C in Woodward-Clyde Consultants, 1980b) with an assigned focal depth of 0 miles (0 km). Available records from Tucson, Arizona (TUC), Berkeley, California (BKS), and Pasadena, California (PAS), and additional southern California stations show clear evidence that a multiple event occurred in the crust at an approximate depth of 9 miles (15 km). Comparisons with waveforms for earthquakes with thrust mechanisms, presented by Langston and Helmberger (1975), indicate that waveforms for P and S arrivals

are typical of a thrust mechanism. This earthquake occurred outside of the Talkeetna Terrain. It may have been associated with the Castle Mountain fault.

4 July 1929

This magnitude (M_S) 6-1/2 earthquake was reported by NOAA (Appendix C in Woodward-Clyde Consultants, 1980b) to have the same epicenter as the 21 January 1929 event of M_S 6-1/4. No focal depth was reported for either event. A record from TUC, was the only one obtained for this event during this investigation. A qualitative interpretation of this record suggested that the earthquake occurred in the crust. Its epicentral location north of the the Denali fault (Figure 5-1) appears to be justified, on the basis of work by Sykes (1981); therefore, it occurred outside of the Talkeetna Terrain.

3 July 1929

This earthquake had a magnitude of (M_S) 6-1/4 and no reported focal depth, according to NOAA (Appendix C in Woodward-Clyde Consultants, 1980b). The only record available for this earthquake is TUC. The focal depth appears to have been below the crust, possibly in the depth range 25 to 31 miles (40 to 50 km). This estimate is based on a subjective assessment of the waveforms and the general aspect of the record. This event appears to have occurred in the Benioff zone below the Talkeetna Terrain. Sykes (1981) has relocated the event to 62.3°N and 149.3°W (Figure 5-2), about 12 miles (20 km) south of the NOAA location.

21 January 1929

The 21 January 1929 earthquake had a reported magnitude (M_S) of 6-1/4 and was located north of the Denali fault (Appendix C in

Woodward-Clyde Consultants, 1980b). No reported focal depth was given. Review of the TUC record suggested that this event occurred in the crust, as shown in Figure 5-1, and that its epicentral location north of the Denali fault appears to be justified, considering the work of Sykes (1981). Therefore, it occurred outside the Talkeetna Terrain.

7 July 1912

This earthquake had a reported magnitude of M_S 7.4 and an original location north of the Denali fault (Appendix C in Woodward-Clyde Consultants, 1980b). Review of felt reports during the 1980 study were used to relocate the event to a location near the Hines Creek strand of the Denali fault (Figures 4-6 and 4-8 in Woodward-Clyde Consultants, 1980b, and Figure 5-1 in this report). Evaluation of the available Honolulu (HON) record for this event suggests that it is crustal. The location along or north of the Denali fault lies outside of the Talkeetna Terrain.

27 August 1904

This earthquake of magnitude (M_S) 7-3/4 was reported by NOAA to have a location north of the Denali fault (Appendix C in Woodward-Clyde Consultants, 1980b). Review of felt reports during the 1980 study, and data obtained from Sykes (1981) have resulted in the relocation of the earthquake 53 miles (85 km) northwest of the NOAA location. Review of the available HON record for this event suggested that it is crustal. The crustal location appears to lie substantially north of the Talkeetna Terrain.

Summary

This additional analysis of historical earthquakes provides significant confirmation of the low level of crustal deformation occurring within the Talkeetna Terrain. As shown in Figure 5-1, the largest earthquakes with reported locations within the Talkeetna Terrain are the M_S 5.6 earthquakes of 17 July 1923, 29 May 1931, 17 October 1931, and 26 July 1933. These are too small to be analyzed by the procedures used above, but they may in fact have occurred in the Benioff zone, as the 3 July 1929 event apparently did. The 3 November 1943 earthquake occurred in the crust along the western margin of the Talkeetna Terrain.

5.2 - Benioff Zone Seismicity

In the Interim Report (Woodward-Clyde Consultants, 1980b), the Benioff zone beneath the Talkeetna Terrain was clearly identified and exhibited several detailed features of Benioff zones that have been defined in Japan. In order to assess more fully the impact of potential future earthquakes occurring in the subcrustal region, additional comparative analyses were used to characterize the subduction process in central Alaska. These characteristics were used to distinguish the intraplate and interplate regions more accurately than was done for the 1980 report and to refine further the estimates of maximum earthquakes for these regions.

5.2.1 - Benioff Zone Zonation

The Benioff zone shown in profile in Figure 5-7 was interpreted in the Interim Report (Woodward-Clyde Consultants, 1980b) on the basis of Yoshii's "aseismic front" model (Yoshii, 1975, 1979) and the model of Davies and House (1979). The principal element of

Yoshii's model is the aseismic front, which is a vertical plane separating seismic (trenchward) from aseismic (landward) portions of the mantle above the subducting plate. The front also separates the trenchward portion of the plate interface, which is subject to interplate earthquakes, from the landward portion of the plate interface, which is aseismic but below which intraplate earthquakes occur within the subducting plate.

The physical interpretation of the aseismic front is that it marks the lower boundary of coupling between the two plates on the shallow portion of this interface. This coupling is reflected in interplate earthquakes on the interface and in the earthquakes in the mantle of the overriding plate above the plate interface. The latter earthquakes are believed to be caused by stress transmitted across the interface from below by the subducting slab. Landward of the aseismic front, there is no coupling across the plate interface and thus interplate earthquakes on the interface and earthquakes above the interface are absent.

The aseismic front shown in Figure 5-7 was located on the basis of mantle earthquake locations. It intersects the plate interface at a depth of 29 miles (47 km). The apparent absence of mantle seismicity in the adjacent region to the southwest (Lahr, 1975) prevents the identification of the aseismic front using this method in that locality.

According to Yoshii's model, it should be possible to locate the aseismic front by finding the point of transition from interplate to intraplate earthquake mechanisms. On re-examination of the 1980 microearthquake data combined with the UAGI data, two additional focal mechanisms in the region to the southeast of the area were covered by the network. These two mechanisms are plotted in Figures 5-8A and 5-8B, and their locations in cross-section are shown in Figure 5-7. Event A is the only apparent thrust mechanism

found in the interplate region of the Benioff zone, and this mechanism is somewhat uncertain. The horizontal axis of maximum compression (P) is not well-aligned with the northwest plate motion vector, and the inferred fault planes are too steep to represent interplate slip. This event (A) lies southeast of the aseismic front and the transition zone (discussed shortly) and is located approximately along the plate interface.

Events within the intraplate region of the Benioff zone (Figure 5-7) generally show down-dip tensional axes, indicating intraplate mechanisms, and their depths range from 23 to 54 miles (37 to 89 km). This suggests that the aseismic front may lie farther east than shown in Figure 5-7, because the aseismic front occurs at a depth of 29 miles (47 km) on the plate interface.

Earthquake mechanisms in an adjacent region southwest of the study area were studied by Lahr (1975). He found a composite solution for events in the depth range 26 to 34 miles (42-55 km), with an average depth of 30 miles (48 km), that indicated interplate faulting. Intraplate earthquake mechanisms were generally at depths greater than 26 miles (42 km), although a composite intraplate solution was found for a group of earthquakes in the depth range 18 to 26 miles (29 to 43 km), with an average depth of 23 miles (38 km). These results suggest that the transition occurs in the depth range 21 to 31 miles (35 to 50 km) and may not necessarily be sharply defined. Since Yoshii's study, Seno and Pongsawat (1981) have found that the interplate and intraplate regions in a limited segment of the northern Honshu Benioff zone may overlap over an interval of approximately 31 miles (50 km) trenchward of the aseismic front, with intraplate events occurring just below the interplate ones. This area of overlap is in the location identified by Lahr (1975) as the transition zone.

There is a distinct change in the level of seismicity in the Benioff zone at a depth of about 21 miles (35 km). It is possible that the interval from this depth to the aseismic front represents overlapping of interplate and intraplate zones as found by Seno and Pongsawat (1981). This possibility is compatible with the apparent existence of a transition zone in focal mechanisms as discussed previously.

Davies and House (1979) distinguish between the "main thrust" zone (which is termed the "interplate region of the Benioff zone" in this report) and the "Benioff" zone (which is termed the "intraplate region of the Benioff zone" in this report). Davies and House (1979) provide three lines of evidence that argue for a distinction between the "main thrust" (shallower, interplate) zone and the "Benioff" (deeper, intraplate) zone. These are the change in dip of the subducting plate, the transition from interplate to intraplate earthquake mechanisms in the vicinity of this bend, and the occurrence in the "main thrust zone" (shallow plate interface) of great thrust-type earthquakes followed by periods of quiescence (Mogi, 1969; Kelleher and others, 1974; Kelleher and Savino, 1975) as compared to the relatively uniform seismicity in the "Benioff zone" (deeper intraplate zone).

Davies and House (1979) find a change in dip at a depth of approximately 24 miles (40 km) in a seismicity profile across the subduction zone in the vicinity of Skwentna, south of the site region. Although the seismicity in Figure 5-7 does not extend very far trenchward, it is clear that a change in dip must occur at about a depth of 21 miles (35 km) in order that the projected plate interface intersect the surface at the Alaska trench. This projected interface has a dip of approximately 8° and has a depth of 15 miles (25 km) at the northern limit of the aftershock zone of the 1964 Prince William Sound, Alaska, earthquake (Figure 5-7).

The distinct change in level of seismicity in the subduction zone that occurs at a depth of 21 miles (35 km) has already been noted. This change is interpreted to be the boundary of the "Benioff" and the "main thrust" zones of Davies and House (1979), since it satisfies all three of their criteria. There is a change in dip, the beginning of a transition in earthquake mechanisms, and a change in seismicity level.

No synthesis of Yoshii's (1975; 1979) "aseismic front" model and the "Benioff - main thrust" model of Davies and House (1979) has been published. However, it would appear that these two boundaries define lower and upper depth limits of a transition zone from seismic to aseismic behavior of the plate interface.

It is concluded from the "Benioff - main thrust" model for Alaska that great shallow interplate earthquakes do not rupture down-dip beyond the transition at a depth of 21 miles (35 km). The aftershock zone of the 1964 Prince William Sound earthquake suggests that rupture terminated at a shallower depth, approximately 15 miles (25 km) deep, at a distance of 43 miles (70 km) trenchward of the transition. It is not clear that this 43-mile (70-km) interval ever ruptures seismically in great interplate earthquakes. Instead, it is likely that this interval undergoes plastic deformation after great interplate earthquakes or undergoes steady creep during the interseismic period of the earthquake cycle (Thatcher and Rundle, 1979).

5.2.2 - Magnitude Estimates of Benioff Zone Earthquakes

The Benioff zone earthquakes fall into two categories: interplate earthquakes (which represent the relative motion of plates) and intraplate earthquakes (which represent the internal deformation of the subducting plate). The maximum magnitudes of interplate earthquakes were evaluated from estimated rupture dimensions and

from a comparative study of worldwide seismicity. Intraplate earthquakes have much smaller dimensions than large interplate earthquakes, but these dimensions are usually not precisely determined because aftershocks are scarce. For this reason, the maximum magnitude of intraplate earthquakes was estimated from a comparative study of worldwide seismicity.

Prior to assessing the maximum magnitude values, a relationship between magnitude scales and rupture dimension is needed. Kanamori (1977) has suggested that magnitude scales for large earthquakes should be based on seismic moment. This is because surface wave magnitude M_S begins to saturate above M_S = 7.5. Seismic moment M_O is defined by the relationship:

$$M_O = \mu AD \quad \text{. . . . . Equation 5-1}$$

were μ = the rigidity,
D = the average displacement on a fault, and
A = the area of the fault surface.

Kanamori (1977) defines a magnitude scale M_W based on seismic moment which does not saturate at the upper end and is equivalent to surface-wave magnitude in the range 6.0 and 8.0. M_W can therefore be considered as a continuation of the M_S scale for large earthquakes. Relationships between seismic moment and magnitude have been derived from worldwide earthquake data. For M_W greater than 7-1/2 and M_S greater than 5 and less than 7-1/2, Hanks and Kanamori (1979) define a moment magnitude scale M, which is related to seismic moment by the relation:

$$M = 2/3 \log M_O - 10.7 \quad \text{. . . . . Equation 5-2}$$

Direct determination of M_O is made by using long-period body waves, surface waves, free oscillations, and geodetic data.

Indirect estimates of M_o can be made from measured surface displacements, rupture lengths, and estimated fault width. For faults that have not been subject to historical rupture, geologic and seismic studies may provide information on these parameters; seismic moment can then be calculated, and a moment magnitude can be derived from the equation given above.

An assumption made in the derivation of the moment magnitude relationship is constant stress drop for large earthquakes (Kanamori, 1977). Some error may be introduced into moment magnitude calculations because of temporal on regional variations in stress drop. In addition, uncertainties in the estimation of displacement, rupture length, and fault width may lead to errors in the estimation of seismic moment. However, we shall now see that the uncertainties involved in the estimation of future large earthquake moments or magnitudes may be quite small if the fault area can be accurately estimated.

Estimating Magnitude of Benioff Zone Earthquakes from Fault Area

Abe (1975) showed that a remarkably linear relationship exists between fault area and seismic moment of large earthquakes. This relationship is given by:

$$M_o = 1.23 \times 10^{22} S^{3/2} \text{ dyne/cm} \quad \text{Equation 5-3}$$

where S is the fault area in km^2. The measured moment values for this data set deviate from this equation within a factor of 1.3 for M_o larger than 10^{27} dyne/cm, i.e., for M_s larger than 7.3.

We may convert from moment M_o to moment magnitude M using the relation of Hanks and Kanamori (1979):

$$M = 2/3 \log M_o - 10.7 \quad \text{Equation 5-4}$$

This moment magnitude is equivalent to M_S in the range $5 \leq M_S \leq 7\text{-}1/2$. Then Abe's equation becomes:

$$M = \log A + 4.03 \quad \text{Equation 5-5}$$

This equation is very similar to an equation obtained by Wyss (1979):

$$M = \log A + 4.15 \quad \text{Equation 5-6}$$

Abe's equation (Equation 5-5) is preferred for our purposes because it is based on a data set for which all earthquakes larger than 7.5 are subduction zone earthquakes, whereas Wyss' equation (Equation 5-6) is based on a global set of data.

5.2.3 - Maximum Earthquakes from Significant Benioff Zone Sources

There are two significant subduction zone sources to be considered at the sites:

- Source 1 is an interplate earthquake on the shallow portion of the plate interface southeast of the sites.
- Source 2 is an intraplate earthquake within the subducting plate beneath the sites.

Maximum Magnitude of Interplate Earthquakes (Source 1)

The source 1 interplate earthquakes can be very large because of the large dimensions of plate interfaces. The length of the zone that ruptured in the 1964 Prince William Sound earthquake is

approximately 525 miles (750 km) (Sykes and Quittmeyer, 1981). The width that ruptured is variously estimated, for example from 112 miles (180 km) (Sykes and Quittmeyer, 1981) to 223 miles (360 km) (Davies and House, 1979). The width of the aftershock zone (Page, 1968) appears to increase from approximately 124 miles (200 km) in the southwest to approximately 217 miles (350 km) in the northwest. Using the dimensions assumed by Sykes and Quittmeyer, we obtain a magnitude (moment magnitude) of 9.2, which agrees with the value measured by Kanamori (M_W = 9.2).

As discussed previously, the plate interface appears to have ruptured to a depth of approximately 15 miles (25 km) during the 1964 Prince William Sound earthquake. If we assume that it is possible for rupture to extend to a depth of 23 miles (35 km), an additional strip 43 miles (70 km) wide is added at the lower edge of the 1964 fault plane, giving a magnitude (moment magnitude) of 9.35.

Maximum Magnitude of Intraplate Earthquakes (Source 2)

A search of the NOAA worldwide earthquake catalog in the depth range 22 to 43 miles (35 to 70 km) was conducted in order to find the largest historic intraplate earthquakes in the Benioff zone in that depth interval. All of the earthquakes having catalog magnitudes greater than (M_S) 7.5 are listed in Table 5-3. Of these earthquakes, all but six were excluded from the prescribed category for reasons given in the "comment" column. These reasons include more precise magnitude or depth determinations, the focal mechanism determinations, and the hypocentral locations that indicate interplate faulting or other dissimilarities in tectonic setting. Four of the remaining six earthquakes have unknown mechanisms; thus, it is not known whether they are

intraplate events. These earthquakes, for which the magnitudes (M_S) are all 7.6, are the 1933 Peru, 1935 Kuril, 1943 Kermadec, and 1953 Chile events.

The two remaining earthquakes are known to be intraplate events. They are the 1970 Peru earthquake (M_S = 7.6, M_W = 7.9) and the 1959 Kamchatka earthquake (M_S = 7.7, M_W = 8.2). These are the only two earthquakes having down-dip tension axes within the Benioff zone that are believed to have ruptured a large fraction of the descending lithosphere at depths shallower than 100 km (Abe, 1972; Seno, 1981). The estimates of M_W (Abe and Kanamori, 1980) are based on the dimensions of the aftershock zones.

Isacks and Barazangi (1977) showed that although the 1970 Peru mainshock had a down-dip tensional mechanism, its aftershocks included events having both down-dip tensional and down-dip compressional mechanisms, which were spatially separated into lower and upper regions within the subducting plate. By comparing this distribution of mechanisms with that found in Kamchatka by Vieth (1974), they inferred the existence of upper and lower seismic planes within the descending lithosphere. This phenomenon is now widely recognized, although Fujita and Kanamori (1981) do not include Peru in their worldwide list of double seismic zones.

The presence of a double-planed seismic zone beneath the Shumagin Islands, Alaska, has recently been reported by Reyners and Coles (1982). However, no evidence for the lower plane is found beneath south-central Alaska (Figure 5-7).

Both of the large intraplate earthquakes occurred in double-planed seismic zones and appear to have ruptured the interval

between the two planes. Beneath the Susitna site, the absence of a lower plane implies the absence of seismogenic stress in the lower region of the plate and, thus, the absence of large (M_S > 7-1/2) intraplate earthquakes. Therefore, it is concluded that the maximum magnitude intraplate earthquake that can occur in the intraplate region of the Benioff zone beneath the site is magnitude (M_S) 7-1/2.

5.3 - Local Microearthquake Activity

During the three-month period 28 June to 28 September 1980, Woodward-Clyde Consultants conducted microearthquake recording and analysis to study seismicity in the vicinity of the proposed Devil Canyon and Watana sites. The objective of the study was to collect microearthquake data of value in assessing earthquake sources within approximately 30 miles (48 km) of the sites. The data were used to calculate earthquake locations, focal depths, local Richter magnitudes (M_L), and first-motion plots that could be interpreted with respect to regional and local geologic features, tectonic models, and historical seismicity. These results have been combined with seismic geology results to assess the seismic design bases for the Project. These results have also been used to plan a program of long-term seismic monitoring.

This section summarizes the monitored activity and presents the results of additional focal mechanism studies that were conducted to refine the 1980 focal mechanism analysis.

5.3.1 - Network Operation

During the period 25 June to 4 July 1980, ten seismograph stations were installed around the Watana and Devil Canyon sites at the locations shown in Figures 9-1 and B-1 of the Interim Report

(Woodward-Clyde Consultants, 1980b). Data from eight of the ten stations were telemetered into the Watana Base Camp, where seismographs continuously recorded data on smoked drum recorders. Two of the ten stations recorded data at their respective field sites and required servicing every other day by helicopter. This station configuration and instrumentation provided a reliable field operation and produced a high-quality data set. The seismic records were read at the field camp, and local earthquakes were located with a portable microcomputer. The field data analyses provided the latitude, longitude, depth of the focus, and local Richter magnitude (M_L) of each processed earthquake.

After the field season, the earthquakes were reprocessed by Woodward-Clyde Consultants using data analysis procedures described in Appendix B of the Interim Report; final locations were cataloged in Appendix D of the Interim Report (Woodward-Clyde Consultants, 1980b).

5.3.2 - Recorded Earthquakes

Between 28 June and 28 September 1980, a total of 268 earthquakes were located within an area bounded by 62.3° to 63.3° north latitude, 147.5° to 150.4° west longitude, designated the microearthquake study area. Of these 268 earthquakes, 98 occurred below a depth of 19 miles (30 km) in the dipping Benioff zone, and 170 occurred in the crust above 19 miles (30 km), primarily in the depth range of 5 to 12 miles (8 to 20 km) as shown in Figure 5-7. These earthquakes are shown in Figures 9-1 and 9-2 of the Interim Report (Woodward-Clyde Consultants, 1980b). The accuracy of the earthquake locations is considered to be very good (within a few kilometers) for those events that occurred within the network, but the accuracy of the location of earthquakes outside the network decreases as the distance from the network increases.

Among the crustal events, the largest earthquake was of magnitude (M_L) 2.8 and occurred approximately 7 miles (11 km) northwest of the Watana site on 2 July 1980. Five smaller events have also been located within 6 miles (10 km) of the Watana site. A magnitude (M_L) 1.66 earthquake occurred within 3 miles (5 km) of the Devil Canyon site on 12 September 1980 at 0428 Universal Coordinated Time (UCT). In addition, six smaller events occurred in the Devil Canyon area.

In addition to the crustal zone of seismicity, the existence of a subcrustal zone of seismicity is clearly demonstrated in Figure 5-7. The deeper zone dips in the direction of approximately N45°W at an angle of 20°. The depth of 19 miles (30 km) separates the crustal zone from the deeper seismicity.

It is clear by inspection of Figure 5-7 that the Benioff zone is characterized by having more frequent larger earthquakes than does the shallow crustal zone. Thirteen Benioff zone earthquakes were assigned a magnitude (M_L) of 3.0 or larger, the largest of which had a magnitude (M_L) of 3.68 and occurred on 13 July 1980. The contrast in level of seismicity in the crustal and Benioff zones is consistent with the Benioff zone being about an order of magnitude more active than the crustal zone.

5.3.3 - Talkeetna Terrain Stress Regime

In the Interim Report (Woodward-Clyde Consultants, 1980b), composite focal mechanisms were prepared using data obtained during the 1980 microearthquake monitoring study. In order to refine and extend this analysis, additional data were obtained from the University of Alaska Geophysical Institute (UAGI) by reading the original film records for the three-month time period of the microearthquake study. Eleven earthquakes were large enough to

record on both networks during July, August, and September 1980. These earthquakes include the events listed in Table 5-2.

Of the 11 events, three occurred in a cluster, designated as Cluster #1 in the southern portion of the network (shown in Figures 9-6 and 9-7 of the Interim Report [Woodward-Clyde Consultants, 1980b]). Four of the events (including catalog numbers 49, 116, and 197) are applicable to the focal mechanism shown in Figure 9-8 of Woodward-Clyde Consultants (1980b). The remaining four events did not provide well-constrained focal mechanisms and have not been considered further.

The additional first motion data obtained from the UAGI stations did not alter or improve the mechanism shown in Figure 9-7 of the Interim Report (Woodward-Clyde Consultants, 1980b). That mechanism, using the first motion data and the geologic structural trends, was judged to be a N23°E plane dipping 50°NW, with maximum compression oriented northwest-southeast.

The additional four events associated with the mechanism shown in Figure 9-8 of Woodward-Clyde Consultants (1980b) did not change the reported composite mechanism, which indicates northwest-southeast compression.

5.4 - Recurrence

Earthquake magnitude-frequency relationships (recurrence models) were developed for this investigation to be used as part of the input for the seismic exposure analysis discussed in Section 8. The recurrence parameters a and b in the relation Log N = a - bM for the Talkeetna Terrain, the intraplate Benioff zone, and the interplate zone are listed in Table 8-2. The recurrence relations are plotted in Figure 5-9 for a

unit area of 386 square miles (1,000 km^2) per 100 years along with the data points that are discussed below. The data were taken from the study area of the 1980 microearthquake network, an area of 6,564 square miles (17,000 km^2), as shown in Figure 5-1.

The recurrence relationships shown in Figure 5-9 are intended to represent the seismicity of the three zones shown. However, the data used to develop or constrain these relations are subject to several sources of uncertainty. A primary uncertainty is due to the limited time periods of observation at various magnitude completeness levels. Earthquakes of magnitude (M_L) 2 and larger were observed for three months (Woodward-Clyde Consultants, 1980b); earthquakes of magnitude (M_L) 4 and larger were observed for about 15 years (Agnew, 1980); and earthquakes of magnitude 5-1/2 and larger, for about 55 years (Woodward-Clyde Consultants, 1980b). Secondly, the magnitude scales used by the various data sources are not necessarily compatible and have varied over time. Finally, the form of the frequency-magnitude relationship for the larger events in the zones is not constrained to be linear by the few data points, but is only assumed to behave so. Some zones, such as interplate regions, may rupture in "characteristic" large earthquakes (the 1964 earthquake, for example) that recur in a periodic fashion and are not necessarily accompanied by a suite of smaller earthquakes that fit a linear relation as shown in Figure 5-9. Additional aspects of uncertainty and constraints of the individual recurrence relations are discussed in the following sections.

5.4.1 The Interplate Region

The slope of the interplate relationship is assumed to be 0.85 (Woodward-Clyde Consultants, 1978). The position of the curve (a-value) is determined so as to allow the recurrence of a magnitude 8-1/2 earthquake in 160 years, consistent with the repeat time

of the 1964 earthquake as estimated by Davies and others (1981). The area assumed for such an event is 69,498 square miles (180,000 km^2). Because this source is at a large distance from the sites, only the larger earthquakes would generate ground motions of possible engineering significance. Thus, the distribution of smaller earthquakes is not particularly important here.

5.4.2 - The Intraplate Region

The recurrence relationship for the intraplate region was taken from Woodward-Clyde Consultants (1978). In that study, recurrence was estimated for a large section of the Benioff zone and was based on earthquakes in the magnitude range of 5 to 6 and larger. To test the applicability of this relation to the 6,564 square-mile (17,000-km^2) area considered here, two additional data points were used, as shown in Figure 5-9. The first data point was for magnitude ≥ 4 (using earthquakes with focal depths greater than 19 miles [30 km]), and the second was for magnitude (M_S) ≥ 6. These two data points were derived from Agnew (1980). Recurrence data obtained from the 1980 microearthquake study (Woodward-Clyde Consultants, 1980b) were extrapolated to magnitude ≥ 4 and plotted in Figure 5-9. These points suggest that the b-value should be higher (perhaps as high as near 1.0) than that obtained from Woodward-Clyde Consultants (1978). The Woodward-Clyde Consultants' (1978) relationship, therefore, may somewhat overpredict the events of magnitude ≥ 7.

5.4.3 - The Talkeetna Terrain

The frequency-magnitude relationship for the Talkeetna Terrain is based upon the three data points shown in Figure 5-9. The point for earthquakes of magnitude M_L ≥ 2 is taken from the seismicity data recorded during the summer of 1980 (Woodward-Clyde

Consultants, 1980b). The b-value observed for this data set, 1.48, is very high as a representation of large-earthquake crustal seismicity in other worldwide areas. Thus, only the number of events of magnitude (M_L) $\geq$2 was used here, not the b-value. As was noted in the Interim Report (Woodward-Clyde Consultants, 1980b), this data set was strongly influenced by several clusters of earthquakes, which may have resulted in the large b-value.

The data point for events of magnitude $\geq$4 represents the number of events reported by Agnew (1980) for the 6,564 square-mile (17,000 km^2) study area with focal depths of <19 miles (<30 km). This sample is assumed to be complete for the 15-1/2 year period analyzed by Agnew (1980), but it may in fact be missing some events of approximately magnitude 4 because of inadequate detection. Also, the focal depths for these events are not necessarily accurate, and events may be improperly included or excluded from this data set.

One earthquake (of magnitude [M_S] 5-1/2 on 24 May 1931) has been reported in the study area, as shown in Figure 5-1. This earthquake was used to obtain the data point for events of magnitude $\geq$5-1/2 (Figure 5-9). The 3 July 1929 earthquake (magnitude [M_S] 6-1/4) was assigned to the Benioff zone (Section 5-1) and is not included in this frequency-magnitude relationship.

Five events are shown in Figure 5-1 to lie immediately east of the study area. Three of these (the events of 1923, 1931, and 1933) have magnitude (M_S) 5.6 and the same location, while the two events of 1958 and 1963, reported by Tobin and Sykes (1966), are assumed in this study to have magnitudes less than 5-1/2. As was discussed in the Interim Report (Woodward-Clyde Consultants, 1980b) and as can be seen by comparing the seismicity patterns of Figures 5-1 and 5-2, the likelihood is high that several if not

most of these events should be associated with the Benioff zone at a depth of about 25 miles (40 km) rather than with the crust at a depth of 12 miles (20 km). Focal depths that would be sufficiently accurate to resolve the structural association of these earthquakes have not been determined or reported. However, the higher rate of earthquake occurrence in the Benioff zone (relative to the crust) favors their occurrence at depth.

If the earthquakes to the east of the study area were included in an analysis and if the area were expanded to include much more of the Talkeetna Terrain, the recurrence of magnitude (M_S) 5-1/2 and larger earthquakes could increase by up to a factor of about two. This would not significantly affect the results of the seismic exposure analysis presented in Section 8.4.3. Such an increase (by a factor of approximately two) in recurrence of larger events for the Talkeetna Terrain would suggest that the rate of seismicity in the Terrain is close to that of the Benioff zone within the subducted Pacific plate. This suggested similarity is clearly not correct. The 3 November 1943 earthquake (magnitude [M_S] 7.3) was not included in recurrence considerations for the Talkeetna Terrain. As discussed in Section 5.1.3, it occurred along the western boundary of the Terrain and is not considered to represent the earthquake potential within the interior of the Terrain, which includes the Project sites.

5.4.4 - Summary

The frequency-magnitude relationships shown in Figure 5-9, and for which parameters are listed in Table 8-2, were developed as inputs to the seismic exposure analysis discussed in Section 8.4. These relationships are considered to represent the average seismicity of the regions discussed and do not reflect conservative or upper

bound recurrence estimates, except in that the relationships are limited by the maximum earthquake magnitude values selected for each region. Further data analysis and a more detailed evaluation of uncertainties in these relationships would be needed if these relationships were to be used for purposes other than the seismic exposure anlaysis described in Section 8.

TABLE 5-1

METERS OF SELECTED HISTORICAL EARTHQUAKES

Date	Location		Magnitude[1] (M_S)	Depth (miles)	Depth (km)	Mechanism
1 January 1975	61.9°N,	149.7°W	5.9 m_b	34	55	Normal
29 June 1964	62.7°N,	152.0°W	5.6 m_b	9-12	15-20	Thrust-oblique
19 August 1948	63.0°N,	105.5°W	6-1/4	55	90	Thrust[2]
3 November 1943	61.9°N,	151.3°W	7.3	10	17	Thrust
27 April 1933	61.3°N,	150.8°W	7	9	15	Thrust
4 July 1929[3]	64.2°N,	147.9°W	6-1/2	crustal		Strike-Slip[2]
3 July 1929[3]	62.3°N,	149.3°W	6-1/4	25-31	40-50	Not Known
21 January 1929[3]	64.2°N,	148.0°W	6-1/4	crustal		Strike-Slip[2]
7 July 1912	63.8°N,	147.5°W	7.4	crustal		Strike-Slip[2]
27 August 1904[3]	64.8°N,	151.5°W	7-3/4	crustal		Strike-Slip[2]

Notes:

1. Magnitude is M_S except where otherwise noted.
2. Focal Mechanism is not well constrained.
3. Location is from Sykes (1981).

TABLE 5-2

EARTHQUAKES ANALYZED IN THE STRESS REGIME STUDY

Catalog No.[1]	Date	Time (GMT) Hr Min Sec	Latitude °N	Longitude °W	Magnitude (M_L)	Hypocenter Depth (km)
14	8 Jul 1980	01:22:08	63.1	149.2	1.40	15
25	13 Jul 1980	10:17:45	63.2	148.8	2.53	9
49	19 Jul 1980	06:12:04	62.9	149.1	1.79	6
103	6 Aug 1980	16:15:14	62.6	148.9	1.12	14
105	6 Aug 1980	11:36:51	62.6	148.9	1.07	15
116	9 Aug 1980	01:27:12	61.9	149.0	1.46	16
171	25 Aug 1980	16:17:09	63.1	149.3	1.31	17
172	25 Aug 1980	20:10:07	63.1	149.2	1.40	8
187	30 Aug 1980	06:33:17	62.6	148.9	1.70	16
197	1 Sep 1980	01:49:30	62.9	149.0	0.85	12
199	2 Sep 1980	05:18:11	62.5	149.0	1.23	15

Note:

1. Catalog number is listed in Appendix C of the Interim Report (Woodward-Clyde Consultants, 1980b).

TABLE 5-3

Woodward-Clyde Consultants

[redacted]ARY OF SELECTED BENIOFF ZONE EARTHQUAKES

[redacted]	Latitude[2,3] (°N)	Longitude[3,4] (°E)	Magnitude[5] (Ms)		Focal Depth[6]		Region	Comment[7]	Reference
19 Nov 1906	-22.0	109.0	7.75	(7.5)	60		Java	Ms=7.5, not 7.75	Geller and Kanamori (1977)
22 Mar 1925	-18.5	168.5	7.6		50		New Hebrides	Inferred to be interplate from aftershock zone	McCann (1981)
7 Mar 1929	51.0	-170.0	8.6	(7.5)	50		Aleutians	Ms=7.5, not 8.6	Geller and others (1978)
23 Feb 1933	-20.0	-71.0	7.6		40		Peru	Focal mechanism unknown	NOAA[8]
11 Sep 1935	43.0	146.5	7.6		60		Kurils	Focal mechanism unknown	NOAA[8]
5 Nov 1938	36.8	141.8	7.7	(7.7)	60	(30)	Japan	Interplate	Abe (1977)
5 Nov 1938	37.2	141.8	7.7	(7.8)	60	(45)	Japan	Interplate	Abe (1977)
6 Nov 1938	37.2	142.2	7.6	(7.7)	60	(17)	Japan	Normal fault beneath trench	Abe (1977)
14 Sep 1943	-30.0	-177.0	7.6		60		Kermadecs	Focal mechanism unknown	NOAA[8]
2 Aug 1946	-26.5	-70.5	7.9	(7-1/2)	50		Chile	Ms=7-1/2, not 7.9; inferred to be interplate	Gutenberg and Richter (1954); Kelleher (1972)
1 Mar 1948	-3.0	127.5	7.9	(7-1/2)	50		Banda Sea	Ms=7-1/2, not 7.9; geometrically complex arc	Cardwell and Isacks (1978); Gutenberg and Richter (1954)
2 Nov 1950	-6.5	129.5	8.1		50	(220)	Banda Sea	Focal Depth = 220 km	Abe and Kanamori (1979)
6 May 1953	-36.5	-73.0	7.6		60		Chile	Focal mechanism unknown	NOAA[8]
4 May 1959	52.5	159.5	8.0	(7.7)	60	(74)	Kamchatka	Ms=7.7; Mw=8.2	Abe and Kanamori (1980); Seno (1981)
4 Feb 1965	51.3	178.6	7.75		40		Aleutians	Interplate	Stauder (1968)
12 Mar 1966	24.2	122.6	7.6		48		Taiwan	Strike slip	Sudo (1972)
31 May 1970	-9.2	-78.8	7.8	(7.6)	43		Peru	Ms=7.6; Mw=7.9	Abe and Kanamori (1980); Abe (1972); Stauder (1975)
14 Jul 1971	-5.5	153.9	7.9	(7.8)	47	(65)	Solomons	Interplate	Magnitudes: Abe and Kanamori (1980) Focal Depth: Pascal (1979) Tectonic Interpretation: McCann (1981)
26 Jul 1971	-4.9	153.2	7.9	(7.7)	48	(53)	Solomons	Interplate	Magnitudes: Abe and Kanamori (1980) Focal Depth: Pascal (1979) Tectonic Interpretation: McCann (1981)
17 Jun 1973	43.2	145.8	7.7		48		Japan	Interplate	Shimazaki (1975)
20 Jul 1975	-6.6	155.1	7.9		49		Solomons	Inferred to be interplate from aftershock zone	McCann (1981)
20 Jul 1975	-7.1	155.2	7.7		44		Solomons	Inferred to be interplate from aftershock zone	McCann (1981)
31 Oct 1975	12.6	126.0	7.2	(7.6)	50		Philippines	Normal fault beneath trench	Cardwell and others (1980)
14 Jan 1976	-29.2	177.9	7.7		69		Kermadecs	Inferred to be interplate from aftershock zone	McCann (1981)
12 Jun 1978	38.2	142.0	7.7		44		Japan	Interplate	Seno and others (1980)
14 Mar 1979	17.8	-101.3	7.6		49		Mexico	Interplate	Gettrust and others (1981)

Notes:

1. These earthquakes are of M_s >7.5 with focal depths between 35 and 70 km.
2. Latitude is °S when given in negative degrees (e.g., -9.2 is 9.2°S latitude).
3. Latitude and longitude are from the National Oceanographic and Atmospheric Administration (NOAA) locations.
4. Longitude is °W when given in negative degrees (e.g., -78.8 is 78.8°W longitude).
5. Magnitude is from NOAA. Alternate magnitude values are cited as (7.6). The source of the alternate magnitude value is cited as a reference.
6. Focal depth is from NOAA. Alternate focal depths are cited as (65). The source of the alternate focal depth is cited as a reference.
7. The comments summarize Woodward-Clyde Consultants' conclusions after reviewing the NOAA data and the sources cited as references.
8. This reference is the NOAA worldwide earthquake catalog available from NOAA in Boulder, Colorado.

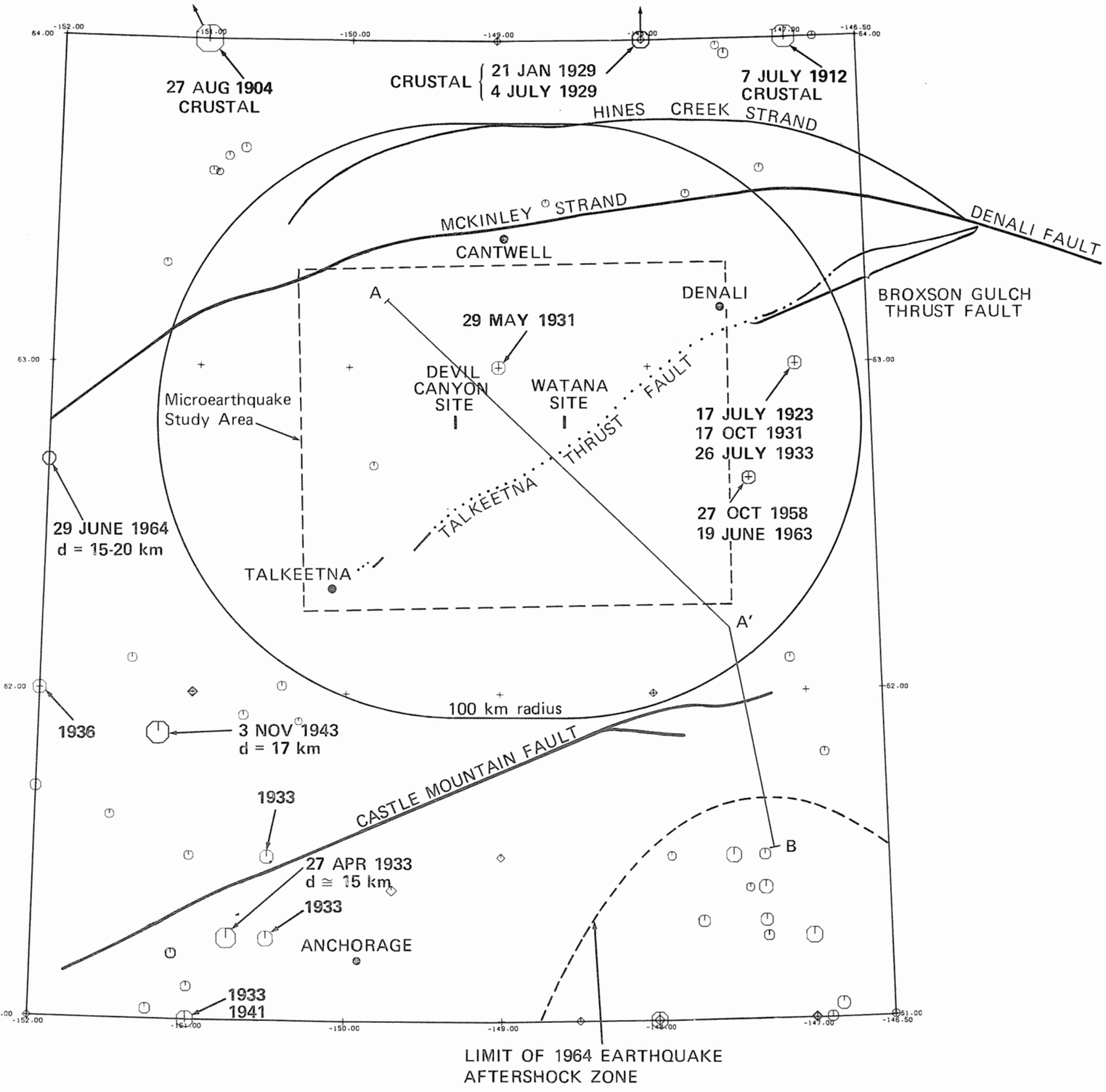

LEGEND

REPORTED MAGNITUDE

8.0
7.0
6.0
5.0
4.0

INTENSITY

XII
XI
X
IX
VIII
VII
VI
V

1936 or 3 NOV 1943	Earthquake date of occurrence
d = 17 km	Hypocenter depth
d ≅ 17 km	Approximate hypocenter depth
CRUSTAL	Crustal — hypocenter depth not known
———	Faults with recent displacement
———·····	Faults with no observed evidence of recent displacement, dotted where concealed

NOTES

1. Earthquakes of magnitude greater than 4 or intensity greater than MM V are shown.
2. Magnitude symbol sizes are shown on a continuous nonlinear scale.
3. Earthquakes are listed in Appendix C of Woodward-Clyde Consultants (1980b).
4. Epicenter locations and hypocenter depths, where revised from Woodward-Clyde Consultants (1980b), are summarized in Table 5-1.
5. Section A–A'–B is shown in Figure 5-7.

N

HISTORICAL EARTHQUAKES OF FOCAL DEPTH LESS THAN 30 km IN THE SITE REGION FROM 1904 THROUGH 1978

0 10 20 30 40 50 Miles

0 10 20 30 40 50 Kilometers

FIGURE 5-1

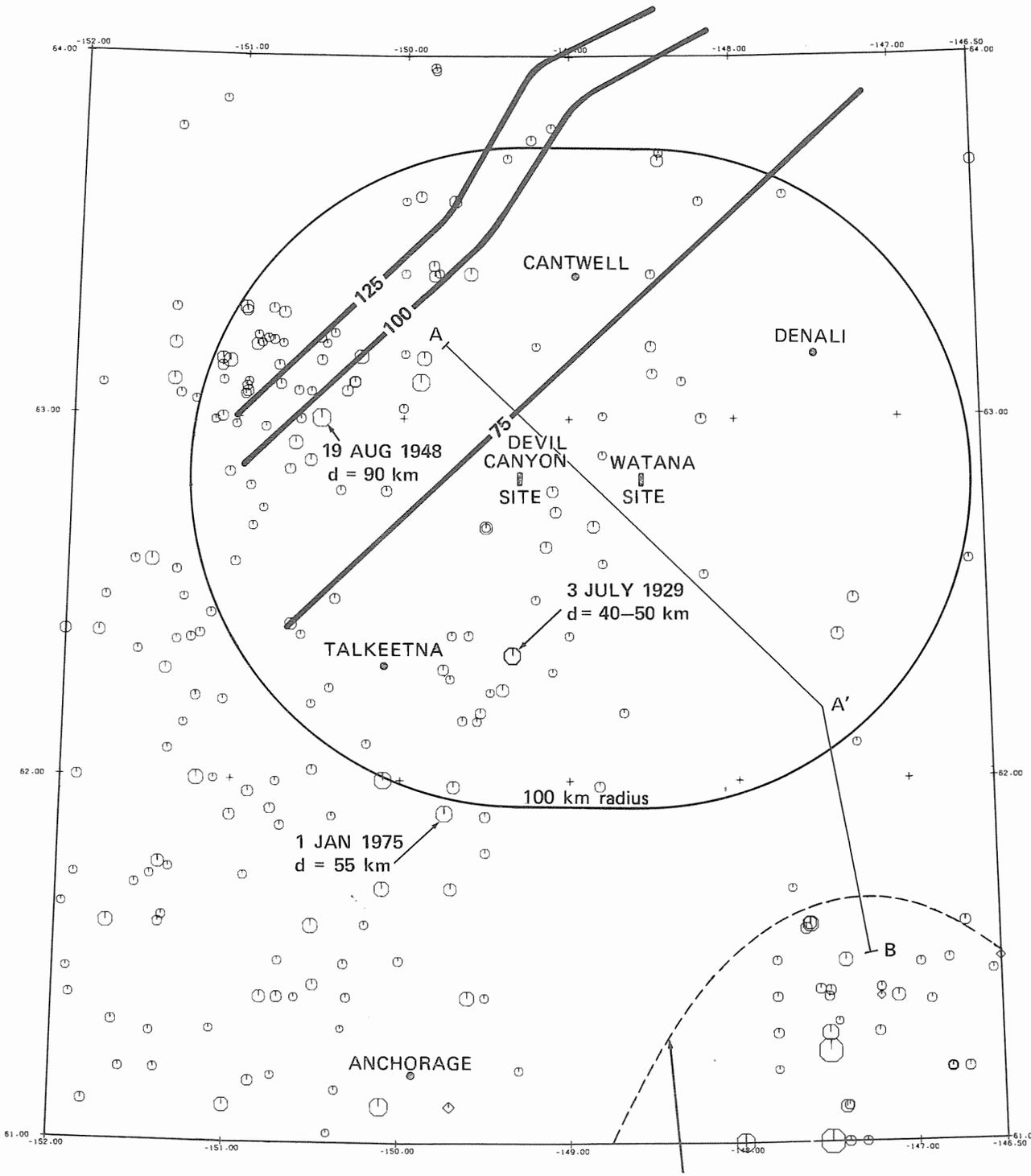

LEGEND

REPORTED MAGNITUDE

8.0
7.0
6.0
5.0
4.0

INTENSITY

XII
XI
X
IX
VIII
VII
VI
V

75 — Depth to Benioff zone in kilometers after Agnew (1980).

19 AUG 1948 — Earthquake date of occurrence

d = 55 km — Hypocenter depth

NOTES

1. Earthquakes of magnitude greater than 4 or intensity greater than MM V are shown.
2. Magnitude symbol sizes are shown on a continuous nonlinear scale.
3. Earthquakes are listed in Appendix C of Woodward-Clyde Consultants (1980b).
4. Epicenter locations and hypocenter depths, where revised from Woodward-Clyde Consultants (1980b), are summarized in Table 5-1.
5. Section A–A'–B is shown in Figure 5-7.

N

HISTORICAL EARTHQUAKES OF FOCAL DEPTH GREATER THAN 35 km IN THE SITE REGION FROM 1904 THROUGH 1978

0 10 20 30 40 50 Miles

0 10 20 30 40 50 Kilometers

FIGURE 5-2

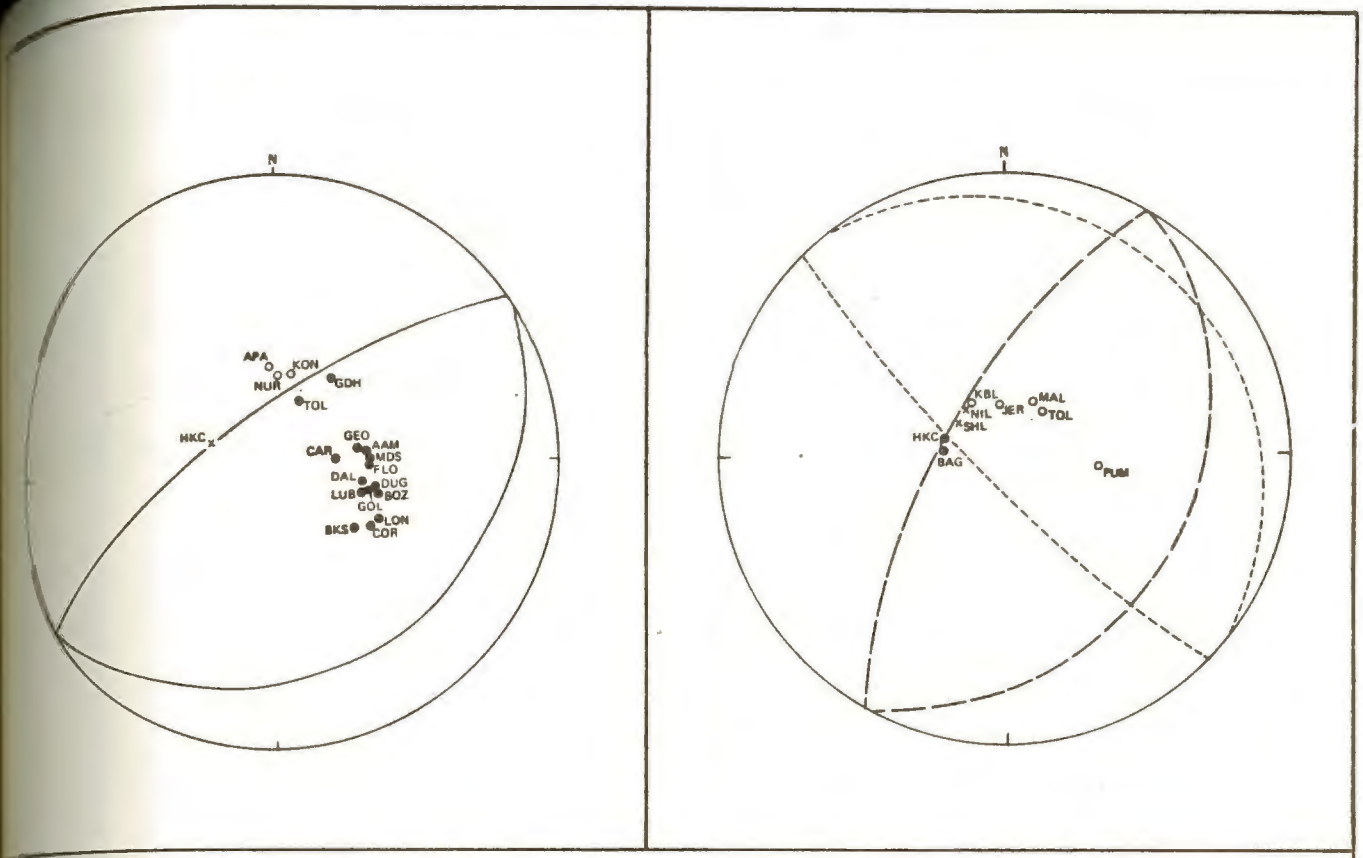

A. 29 JUNE 1964 EARTHQUAKE

Origin Time:	0721 hr.
Location:	62.7°N latitude 152.0°W longitude
Magnitude (m_b):	5.6
Depth:	5 to 20 km

B. 1 JANUARY 1975 EARTHQUAKE

Origin Time:	0355 hr.
Location:	61.9°N latitude 149.7°W longitude
Magnitude (m_b):	5.9
Depth:	55 km

LEGEND

- • Compression
- ○ Dilatation
- × Nodal
- Fault or Nodal Plane, long dashes indicates low reliability, short dashes indicate very low reliability

NOTES

1. Lower hemisphere plots.
2. Equal area projection.

FOCAL MECHANISMS FOR 29 JUNE 1964 AND 1 JANUARY 1975 EARTHQUAKES

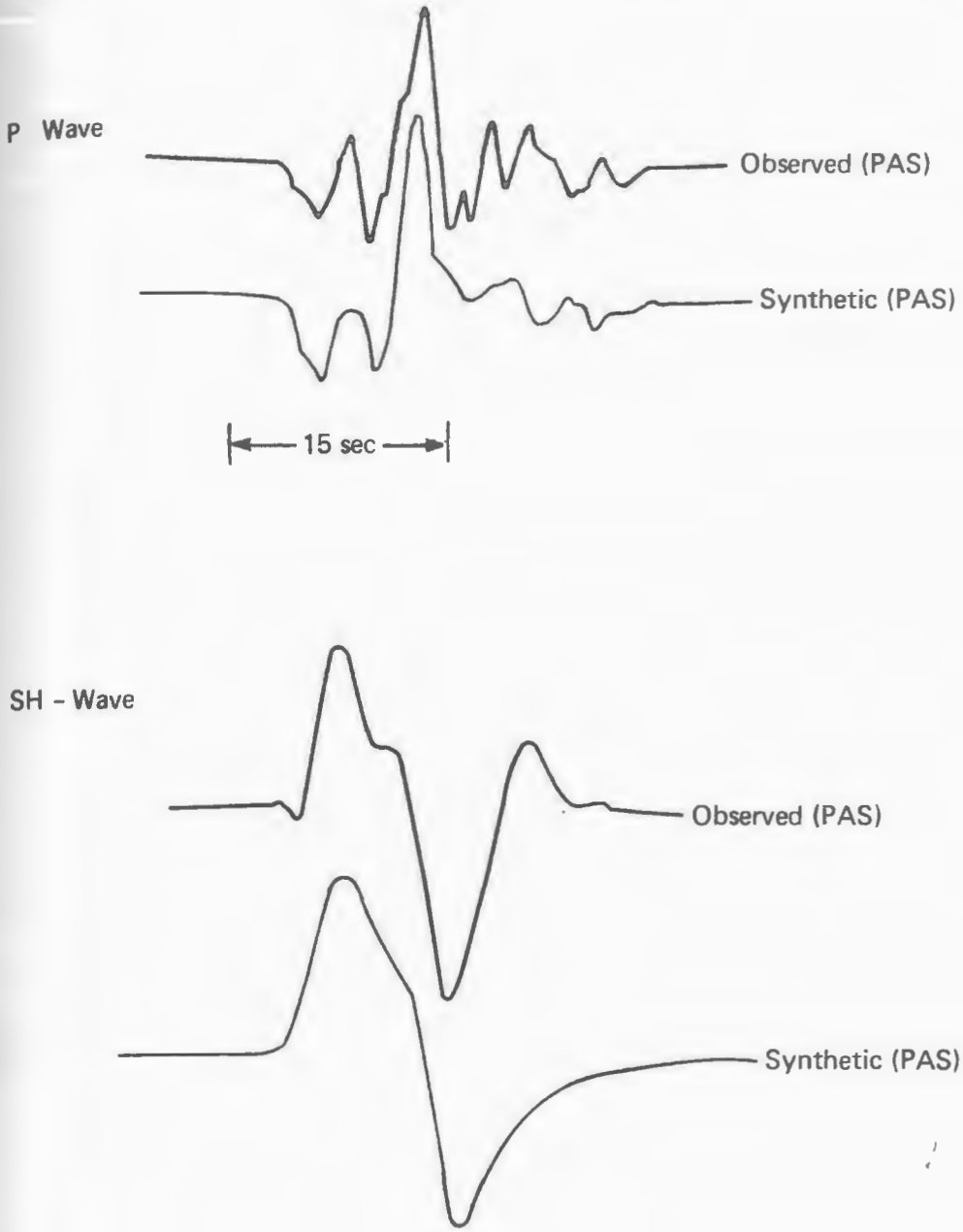

OBSERVED AND SYNTHETIC SEISMOGRAMS FOR
P AND SH WAVES AT PAS FOR THE
3 NOVEMBER 1943 EARTHQUAKE

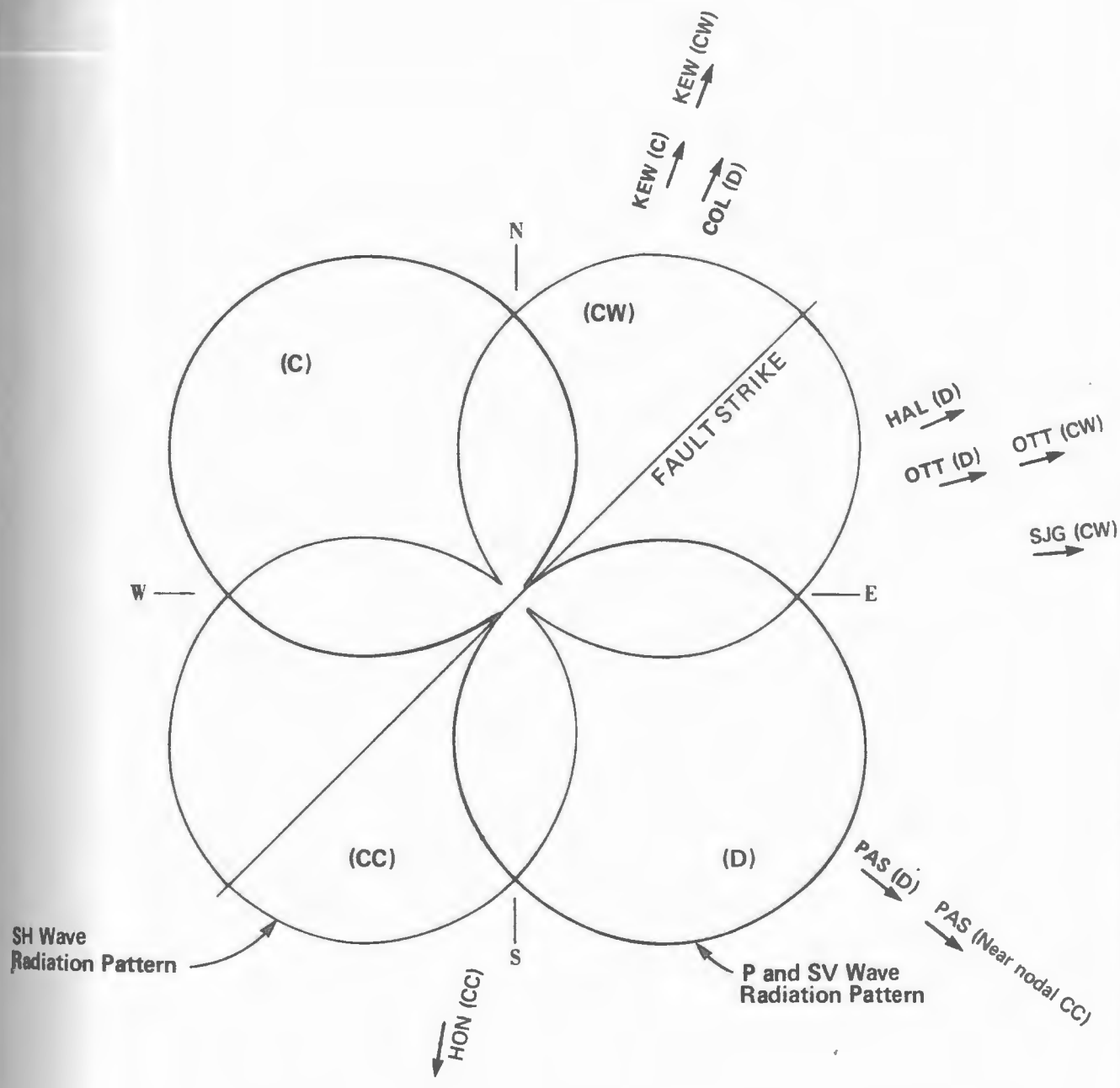

LEGEND

(D)	Dilatation
(C)	Compression
(CC)	Clockwise from above
(CW)	Counter clockwise from above
KEW →	Azimuth to Station

OBSERVED POLARITIES AND
THEORETICAL RADIATION PATTERN FOR
THE 3 NOVEMBER 1943 EARTHQUAKE

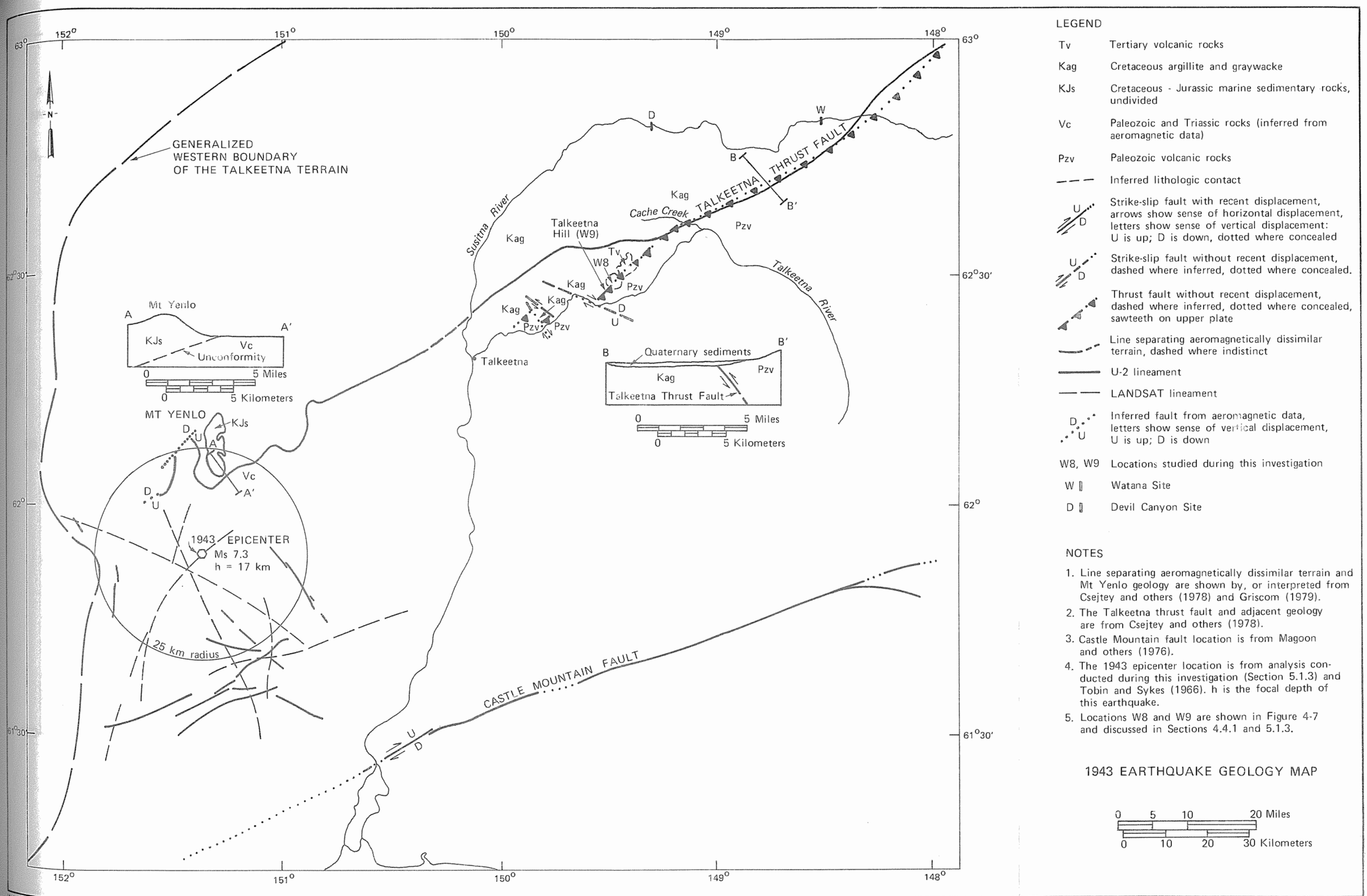

LEGEND

Tv	Tertiary volcanic rocks
Kag	Cretaceous argillite and graywacke
KJs	Cretaceous - Jurassic marine sedimentary rocks, undivided
Vc	Paleozoic and Triassic rocks (inferred from aeromagnetic data)
Pzv	Paleozoic volcanic rocks
— —	Inferred lithologic contact
U D	Strike-slip fault with recent displacement, arrows show sense of horizontal displacement, letters show sense of vertical displacement: U is up; D is down, dotted where concealed
U D	Strike-slip fault without recent displacement, dashed where inferred, dotted where concealed.
	Thrust fault without recent displacement, dashed where inferred, dotted where concealed, sawteeth on upper plate
	Line separating aeromagnetically dissimilar terrain, dashed where indistinct
	U-2 lineament
	LANDSAT lineament
D U	Inferred fault from aeromagnetic data, letters show sense of vertical displacement, U is up; D is down
W8, W9	Locations studied during this investigation
W	Watana Site
D	Devil Canyon Site

NOTES

1. Line separating aeromagnetically dissimilar terrain and Mt Yenlo geology are shown by, or interpreted from Csejtey and others (1978) and Griscom (1979).
2. The Talkeetna thrust fault and adjacent geology are from Csejtey and others (1978).
3. Castle Mountain fault location is from Magoon and others (1976).
4. The 1943 epicenter location is from analysis conducted during this investigation (Section 5.1.3) and Tobin and Sykes (1966). h is the focal depth of this earthquake.
5. Locations W8 and W9 are shown in Figure 4-7 and discussed in Sections 4.4.1 and 5.1.3.

1943 EARTHQUAKE GEOLOGY MAP

0 5 10 20 Miles
0 10 20 30 Kilometers

FIGURE 5-6

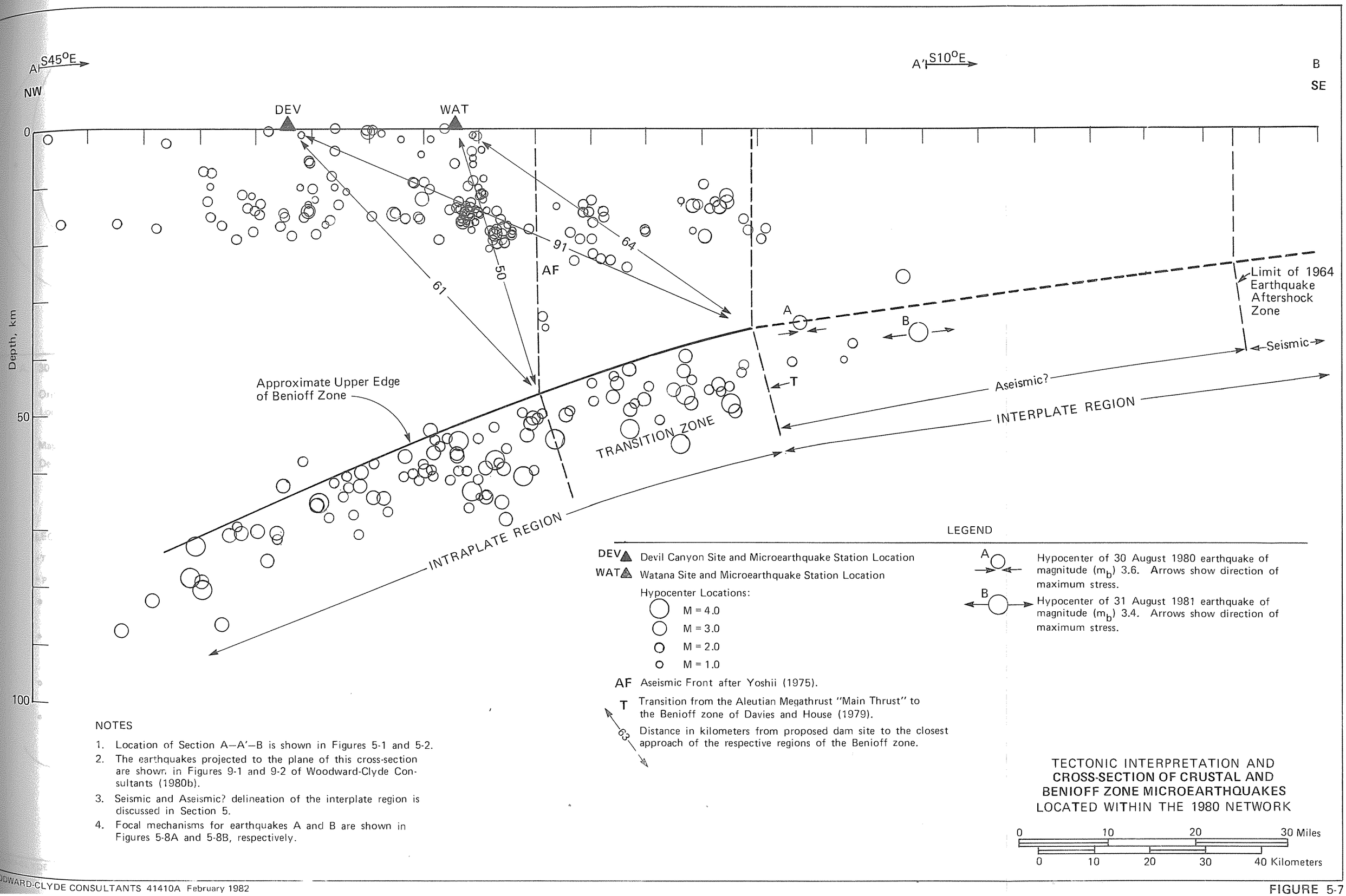

LEGEND

DEV ▲ Devil Canyon Site and Microearthquake Station Location

WAT ▲ Watana Site and Microearthquake Station Location

Hypocenter Locations:

- ◯ M = 4.0
- ◯ M = 3.0
- O M = 2.0
- o M = 1.0

AF Aseismic Front after Yoshii (1975).

T Transition from the Aleutian Megathrust "Main Thrust" to the Benioff zone of Davies and House (1979).

63 Distance in kilometers from proposed dam site to the closest approach of the respective regions of the Benioff zone.

A ◯→ Hypocenter of 30 August 1980 earthquake of magnitude (m_b) 3.6. Arrows show direction of maximum stress.

B ←◯→ Hypocenter of 31 August 1981 earthquake of magnitude (m_b) 3.4. Arrows show direction of maximum stress.

NOTES

1. Location of Section A–A'–B is shown in Figures 5-1 and 5-2.
2. The earthquakes projected to the plane of this cross-section are shown in Figures 9-1 and 9-2 of Woodward-Clyde Consultants (1980b).
3. Seismic and Aseismic? delineation of the interplate region is discussed in Section 5.
4. Focal mechanisms for earthquakes A and B are shown in Figures 5-8A and 5-8B, respectively.

TECTONIC INTERPRETATION AND
CROSS-SECTION OF CRUSTAL AND
BENIOFF ZONE MICROEARTHQUAKES
LOCATED WITHIN THE 1980 NETWORK

0 10 20 30 Miles

0 10 20 30 40 Kilometers

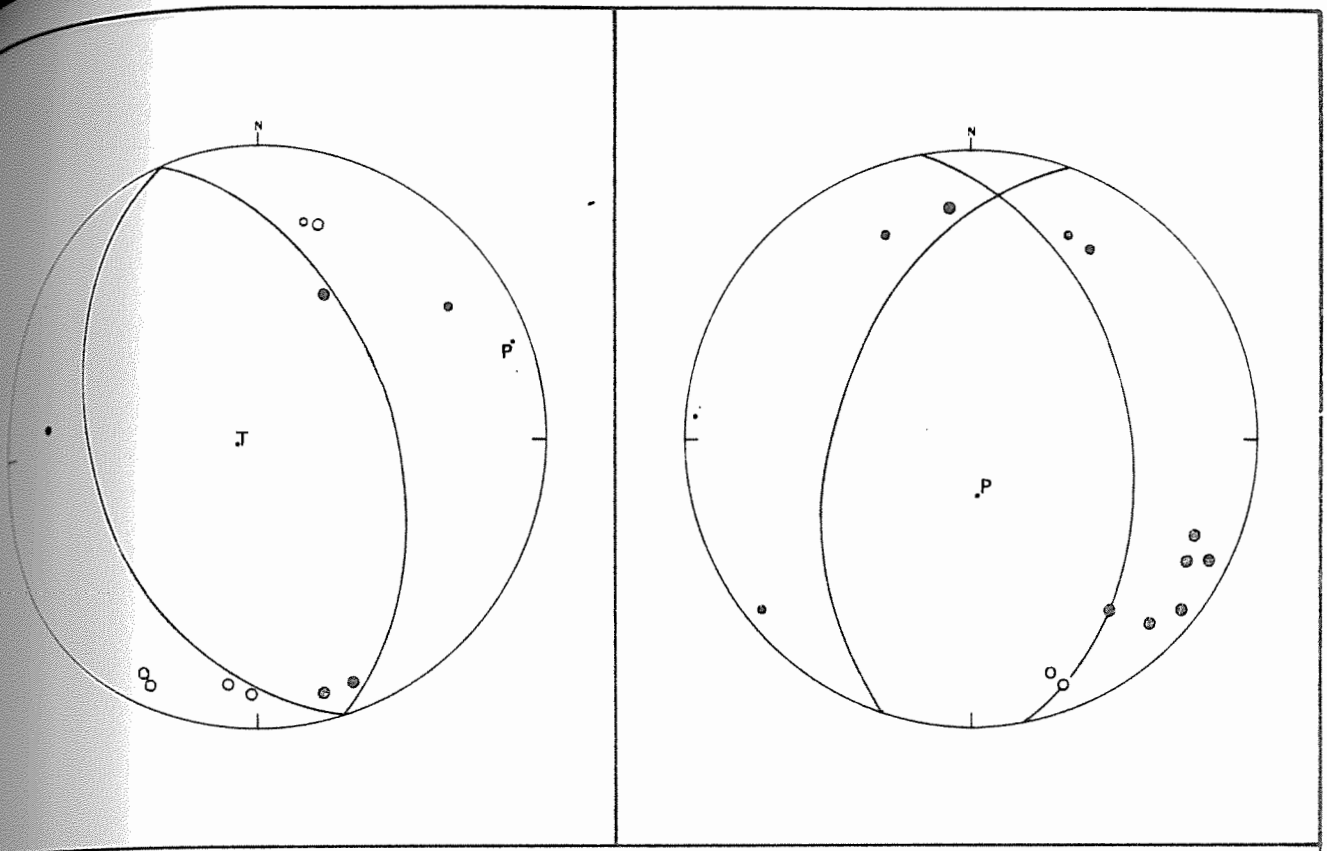

A. 30 AUGUST 1980 EARTHQUAKE

Origin Time:	1732 hr.
Location :	61.8°N latitude 148.9°W longitude
Magnitude (m_b):	3.6
Depth:	35 km

B. 31 AUGUST 1980 EARTHQUAKE

Origin Time:	1552 hr.
Location:	62.2°N latitude 147.5°W longitude
Magnitude (m_b):	3.4
Depth:	35 km

LEGEND

- T Minimum Compressive Stress Axis
- P Maximum Compressive Stress Axis
- Compression— high confidence in interpretation
- Compression— low to moderate confidence in interpretation
- Dilatation— high confidence in interpretation
- Dilatation— low to moderate confidence in interpretation
- Fault or Nodal Plane

NOTES

1. Lower hemisphere plots.
2. Equal area projection.

FOCAL MECHANISMS FOR 30 AUGUST 1980 AND 31 AUGUST 1980 EARTHQUAKES

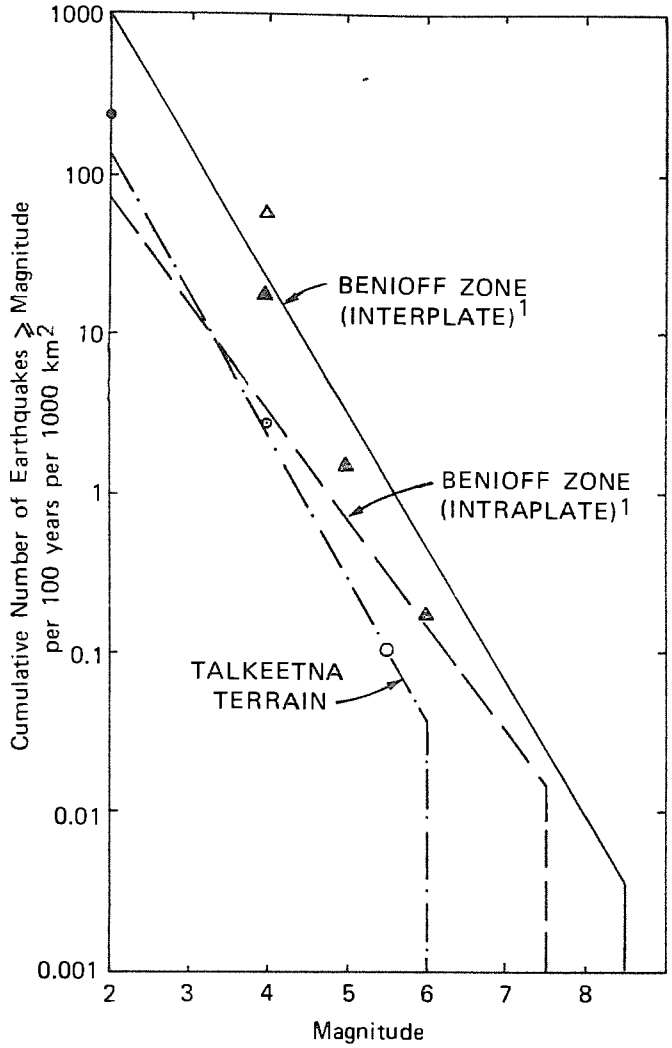

LEGEND

Benioff Zone Intraplate Region

- ▲ Calculated from Agnew (1980) data
- △ Calculated from Woodward-Clyde Consultants' (1980b) data.

Talkeetna Terrain

- ● Calculated from Woodward-Clyde Consultants' (1980b) data
- ⊙ Calculated from data reviewed during this 1981 study [2]
- ○ Calculated from Agnew (1980) data

NOTES

1. Benioff zone interplate and intraplate frequency-magnitude curves are from Woodward-Clyde Consultants (1978).
2. Earthquakes reviewed for the Talkeetna Terrain during this 1981 study are shown in Figure 5-1.

FREQUENCY-MAGNITUDE RELATIONSHIPS

6 - RESERVOIR-INDUCED SEISMICITY (RIS)

The objective of this part of the investigation was to evaluate the potential for the possible future occurrence of reservoir-induced seismicity (RIS) in the vicinity of the proposed reservoirs. Reservoir-induced seismicity is defined here as: the phenomenon of earth movement and resultant seismicity that has a spatial and temporal relationship to a reservoir and is triggered by nontectonic stress.

In the early 1940s in a study of Hoover Dam in the United States (Carder, 1945), a relationship was first recognized between the level of water impounded by a dam and the rate of occurrence of local earthquakes. Since that time, similar relationships have been reported for 99 other reservoirs around the world. A review of these reported cases (Packer and others, 1977; Packer and others, 1979; Perman and others, 1981) resulted in 55 cases being classified as either accepted or questionable cases of RIS (Table 6-1, Figure 6-1). A later reanalysis of these cases resulted in 68 cases being classified as accepted cases of RIS (Perman and others, 1981).

Several reservoir-induced seismic events (at Kremasta, Greece; Koyna, India; Kariba, Zambia-Rhodesia; and Xinfengjiang, China) have exceeded magnitude (M_S) 6. Damage occurred to the dams at Koyna and Xinfengjiang, and additional property damage occurred at Koyna and Kremasta.

Studies of the occurrence of RIS (Simpson, 1976; Packer and others, 1977; Withers, 1977; Packer and others, 1979) have shown that RIS is influenced by the depth and volume of the reservoir, the filling history of the reservoir, the state of tectonic stress in the shallow crust beneath the reservoir, and the existing pore pressures and permeability of the rock under the reservoir. Although direct measurements

are difficult to obtain for some of these factors, indirect geologic and seismologic data, together with observations about the occurrence of RIS at other reservoirs, can be used to assess the potential for and the possible effects of the occurrence of RIS at the proposed Project reservoirs.

The scope of this study included: a) a comparison of the depth, volume, regional stress, geologic setting, and faulting at the Devil Canyon and Watana sites with the same parameters at comparable reservoirs worldwide (discussed in Woodward-Clyde Consultants, 1980b); b) an assessment of the likelihood of RIS at the sites based on the above comparison; c) a review of the relationship between reservoir filling and the length of time to the onset of induced events and the length of time to the maximum earthquake; d) an evaluation of the significance of these time periods for the sites; e) the development of a model to assess the impact of RIS on ground-motion parameters; f) a review of the relationship between RIS and method of reservoir filling; and g) an assessment of the potential for landslides resulting from RIS. Items (a) through (d) were discussed in Woodward-Clyde Consultants (1980b) and are updated in Section 6.1 of this report to reflect a recent addition to the data base by Perman and others (1981). Items (e) through (g) are discussed in Sections 6.2 through 6.4, respectively.

For this study, the two proposed reservoirs were considered to be one hydrologic entity (designated the proposed Devil Canyon-Watana reservoir) because the hydrologic influence of the two proposed reservoirs is expected to overlap in the area between the Watana site and the upstream end of the Devil Canyon reservoir. The proposed Devil Canyon-Watana reservoir will be approximately 87 miles (140 km) long. Based on Acres American Inc. (in press) data, the predicted parameters for the reservoir will be the following:

	Devil Canyon	Watana	Combined
Max. Water Depth	551 ft (168m)	725 feet (221m)	725 ft (221m)
Max. Water Volume	1.09×10^6 acre-feet ($1,348 \times 10^6 m^3$)	9.52×10^6 acre-feet ($11,741 \times 10^6 m^3$)	10.61×10^6 acre-feet ($13,089 \times 10^6 m^3$)
Stress Regime	Compressional	Compressional	Compressional
Bedrock	Metamorphic	Igneous	Igneous

The combined hydrologic body of water, as proposed, would constitute a very deep, very large reservoir within a primarily igneous bedrock terrain that is undergoing compressional tectonic stress.

6.1 - Evaluation of Potential Occurrence

6.1.1 - Likelihood of Occurrence

For comparative purposes, a deep reservoir has a maximum water depth of 300 feet (92 m) or deeper; a very deep reservoir is 492 feet (150 m) deep or deeper; a large reservoir has a maximum water volume greater than 1×10^6 acre feet ($1,234 \times 10^6 m^3$); and a very large reservoir has a volume greater than 8.1×10^6 acre feet ($10,000 \times 10^6 m^3$) as discussed in Packer and others (1977). Twenty-one percent of all deep, very deep, or very large reservoirs have been subject to RIS. Thus, the likelihood that any deep, very deep, or very large reservoir will experience RIS is 0.21. However, the tectonic and geologic conditions at any specific reservoir may be more or less conducive to RIS occurrence.

Models have been developed by Baecher and Keeney in Packer and others (1979) to estimate the likelihood of RIS at a reservoir, characterized by its depth, volume, faulting, geology, and stress regime. The models from which the likelihoods are calculated are

sensitive to changes in data classification for the geologic and stress regime (Packer and others, 1979; Perman and others, 1981). The calculations from models, however, do not significantly influence the basic relatively high likelihood of RIS at the Devil Canyon-Watana reservoir considering its depth and volume. The calculation of the likelihood of occurrence of RIS at the Devil Canyon-Watana reservoir is presented in Section 6.2.2.

6.1.2 - Location and Maximum Magnitude

Packer and others (1979) and Woodward-Clyde Consultants (1980b), among others, have discussed the concept, based on theoretical considerations and existing cases of RIS, that an RIS event is a naturally occurring event triggered by the impoundment of a reservoir. That is, reservoirs are believed to provide an incremental increase in stress that is large enough to trigger strain release in the form of an earthquake. In this manner, reservoirs are considered capable of triggering an earlier occurrence of an earthquake (i.e., of decreasing the recurrence interval of the event) than would have occurred if the reservoir had not been filled. In this regard, reservoirs are not considered capable of triggering an earthquake larger than that which would have occurred "naturally."

The portion of crust that a reservoir may influence is limited to the area affected by its mass and pore pressure influences. This area of influence is often referred to as a reservoir's hydrologic regime. Defining the precise extent of the hydrologic regime of a reservoir is a complicated task and is the subject of numerous studies (e.g., Withers, 1977; Withers and Nyland, 1978). However, documented cases of RIS (Packer and others, 1979) indicate that the RIS epicenters occur within an area that is related to the surface area that the reservoir covers. For the purposes of this study,

the hydrologic regime of the proposed reservoir has been described as an envelope with a 19-mile (30-km) radius that encompasses the reservoir area, as discussed in Woodward-Clyde Consultants (1980b).

Previous studies (e.g., Packer and others, 1979) present evidence that strongly suggests that moderate to large RIS events are expected only to occur along faults with recent displacement. Among the reported cases of RIS, at least 10 have had magnitudes of (M_S) $\geq$5 (Table 6-2). Field reconnaissance and information available in the literature indicate that Quaternary or late Cenozoic surface fault rupture (i.e., rupture on faults with recent displacement) occurred within the hydrologic regime of eight of these ten reservoirs (Packer and others, 1979).

On the basis of this investigation, it has been concluded that there are no faults with recent displacement within the hydrologic regime of the proposed reservoir (Section 4.5). Therefore, the maximum earthquake which could be triggered by the reservoir is an earthquake with a magnitude below the detection level of currently available techniques (i.e., the detection level earthquake discussed in Section 4.2.4). Thus, the magnitude of the largest earthquake that could be triggered by the proposed reservoir is judged to be (M_S) 6, which is the maximum magnitude of the detection level earthquake.

6.2 - Effect of RIS on Earthquake Occurrence Likelihood

A probabilistic seismic exposure analysis was performed during this investigation to evaluate the likelihood of exceeding design levels of ground motion at the Devil Canyon and Watana sites (Section 8). An important input to such an analysis is the rate (or recurrence) of earthquake activity on potential seismic sources in the vicinity of the

sites. As discussed in Section 6.1, the impoundment of a very deep and very large reservoir may trigger the occurrence of earthquakes that would not have occurred otherwise within the design life of a dam. The objective of the model described below is to characterize the likelihood of occurrence of RIS events given the specific seismologic and tectonic setting of the Devil Canyon and Watana sites. The information developed from this model has been included in the seismic exposure analysis in Section 8. A description of the overall model and the implementation of various components of the model are discussed in Sections 6.2.1 and 6.2.2.

6.2.1 - Description of the Model

The basic approach consists of:

1) calculating the likelihood of occurrence of earthquakes within an area and within a time period affected by RIS;

2) converting the likelihood of occurrence of earthquakes into the mean number of earthquakes within the specified area and time;

3) distributing the mean number of earthquakes among faults with recent displacement (if present) within the specified area or distributing the earthquakes randomly throughout the specified area if faults with recent displacement are not present; and

4) using the expected number of earthquakes on each fault or within the specified area in the seismic exposure analysis to obtain the contribution of that fault or the specified area (when faults with recent displacement are not present) to the probability of exceeding a given level of ground motion.

A brief description of each step in the approach follows.

1. Calculation of Likelihood of Occurrence of RIS Events

The likelihood of occurrence of earthquakes triggered by the impoundment of reservoirs can be calculated from a prediction model developed by Baecher and Keeney in Packer and others (1979). The prediction model is based on statistical discriminant analysis and is calibrated by the data to provide an approximate estimate of the likelihood of RIS events for specific sites. The model incorporates the worldwide RIS data base and the historical seismicity of the site region (Section 5); it is designed to predict the likelihood of occurrence of an RIS event with magnitude (M_S) ≥ 4. Events of lesser magnitude were deleted because they are considered to be too small to have a significant contribution to seismic design.

2. Calculation of Mean Number of RIS Events

From the likelihood of occurrence of RIS events, one can calculate the mean number of RIS events by assuming a Poisson model. The following equation can be used:

$$\lambda = -\ln (1 - p) \quad \text{. . . . . Equation 6-1}$$

where λ = mean number of RIS events within an area and time period affected by reservoir impoundment.

and p = probability of occurrence of RIS events within the assumed area and time period.

Estimates of the time period and area within which RIS events would generally occur can be obtained from the analysis of a

large data base of characteristics of the major reservoirs of the world (Packer and others, 1979; Perman and others, 1981). The time between reservoir impoundment and the largest suspected RIS event ranges from 0 to 25 years, with most of such events occurring within 5 to 10 years.

For long, thin reservoirs (such as the proposed Devil Canyon-Watana reservoir) most of the RIS events (80 to 90 percent) are located within a three-dimensional space that has the configuration of a half-pipe (the bottom half). This half-pipe space encompasses the hydrologic influence of the reservoir and typically has a radius equal to three times the width of the reservoir (Withers, 1977).

For this study, the maximum width of the proposed reservoir was defined as 6 miles (10 km) at Watana Creek. The radius of the half-pipe space then is 19 miles (30 km).

For the purposes of model calculations, the half-pipe space was converted to a rectangular three-dimensional space. The length and width of the rectangular space is 37 miles by 37 miles (60 km by 60 km) which is twice the 19-mile (30-km) distance cited above. The depth of the rectangular space is 19 miles (30 km) corresponding to the half-pipe radius of 19 miles (30 km). This rectangular space was centered about each site, such that the distance from the site to the edge of the space in all three dimensions was 19 miles (30 km). This configuration was used to facilitate model calculations because a rectangular space is easier to model than a cylindrical space and because the effect of ground motions from a RIS event that might occur more than 19 miles (30 km) from either site would be negligible.

3. Distribution of Mean Number of RIS Events

It is generally believed that stresses resulting from reservoir impoundment can affect the timing of earthquakes. An earthquake that would have occurred in the vicinity of a reservoir because of natural seismicity may be triggered sooner because of RIS (i.e., its recurrence interval may be reduced). Because there are no faults with recent displacement within the hydrologic regime of the reservoir, it would seem appropriate to assign the mean number of RIS events to discrete units of volume within the hydrologic regime of the reservoir. For the present study, the extent of the hydrologic regime in which RIS events are expected to occur is defined by the rectangular space described in (2) above. An earthquake with a magnitude up to that of the detection level earthquake is assumed to be able to occur on a source anywhere within this three-dimensional space.

Given the above guidelines, the volume units within which RIS events are to be distributed are defined. Then the seismicity may actually be distributed by proportioning the number of events according to the mean number of events that would have occurred naturally. Since RIS would be expected to decrease the recurrence interval between earthquakes, the mean number of RIS events for a given area would generally be greater than the mean number of naturally occurring events for the same area.

4. Use of RIS Events in the Seismic Exposure Analysis

In order to perform the seismic exposure analysis, it is necessary to know not only the mean number of RIS events greater than some minimum magnitude of interest but also

the distribution of these events over the appropriate magnitude range (defined by the b-slope), and the size of the maximum credible earthquake (MCE) at which the earthquake recurrence curve would be truncated. The values of both of these parameters for RIS events (b-slope and the size of the MCE) are assumed to be equal to the values of the same parameters for naturally occurring earthquakes. This is consistent with the hypothesis that RIS only shifts the timing of earthquakes and does not have a significant effect on the magnitude distribution or the magnitude of a maximum credible earthquake.

6.2.2 - Implementation of the Model for the Susitna Project

The implementation of the four steps of the model for the Susitna project is discussed in this section. Since the potential earthquake sources were at different distances from the two sites (Devil Canyon and Watana), the analysis using these sources was performed separately for each site.

1. Calculation of Likelihood of Occurrence of RIS Events

Baecher and Keeney (in Packer and others, 1979) have discussed two models for calculating the likelihood of occurrence of RIS events: in one model, reservoir characteristics (depth, volume, stress state, and geology) are assumed to be independent; in the other, dependence between reservoir depth and volume is assumed. For the Devil Canyon-Watana reservoir, the first model produced an expected likelihood of 0.37 for a RIS event (of any magnitude) with a standard deviation of 0.13, while the second produced an expected likelihood of 0.46 with a standard deviation of 0.22. Since some dependence between reservoir depth and volume would be

expected and since the assumption of dependence produces a more conservative result (i.e., a higher likelihood for a RIS event to occur), the results of the second model were used for this study.

The worldwide RIS data base on which the Baecher and Keeney in Packer and others (1979) model was developed is limited. To accommodate the uncertainties associated with the limited data base, the likelihood of occurrence of RIS events was assumed to be the mean plus one standard deviation value (i.e., 0.46 + 0.22 = 0.68). In order to examine the sensitivity of results to this assumption, a mean plus two standard deviation value (0.46 + 2 x 0.22 = 0.90) was also analyzed.

2. Calculation of Mean Number of RIS Events

From equation 6-1, the mean plus one standard deviation number of RIS events with magnitude ≥ 4 was calculated to be 1.14; for M ≥ 5, it was calculated to be 0.93. It was assumed that these events would be expected to occur within 10 years after the reservoir was impounded and that they would occur within the three-dimensional rectangular space described in Section 6.2.1, Item 2. After the first 10 years, only the naturally occurring seismicity was assumed to occur during the remaining design life of the dam.

3. Distribution of Mean Number of RIS Events

As there are no known faults with recent displacement within an area of 37 miles by 37 miles (60 km by 60 km) around each site (Section 4.5), the mean number of RIS events for use in the seismic exposure analysis was distributed as a random source over a rectangular space of 37 miles by 37 miles by 19 miles (60 km by 60 km by 30 km).

4. Use of RIS Events in Seismic Exposure Analysis

The mean number of events was calculated for ground motions that exceeded a given level of peak ground acceleration in the first 10 years. The rate of naturally occurring seismicity was used to calculate the mean number of events (for which ground motions exceeded the given level of peak ground acceleration) during the design life of the proposed dams after the first 10 years. The sum of the mean number of incremental events resulting from RIS during the first 10 years and the mean number of events due to natural seismicity during the remainder of the proposed dam design life yields the total mean number of events for which ground motions are expected to exceed a given level during the design life of the Project. The results of these calculations are included in the analysis presented in Section 8.

6.3 - RIS and Method of Reservoir Filling

The occurrence of RIS events has often been correlated with rapid initial filling of a reservoir, especially with irregular filling histories or rapid reservoir refill following major drawdowns (Packer and others, 1979). The precise relationship between irregularities in the filling cycle and the occurrence of RIS events is not well-documented in most cases. Furthermore, no controlled experiments have been performed at reservoirs to vary filling rates and examine the effect on seismicity. However, detailed information is available on the correlation between seismicity and filling rates for at least one reservoir--Nurek, U.S.S.R.

Although impoundment at Nurek began in 1968, the first significant impoundment (328 feet [100 m]) took place between late August and early

November 1972. A step was made in the filling curve late in September; following this step, seismicity increased. Upon completion of the first stage filling cycle, seismicity reached a peak with maximum magnitudes (M_S) of 4.6 and 4.3. Seismicity between November 1972 and June 1976 broadly paralleled changes in water level (Simpson and Negnatullaiv, 1978).

On the basis of this experience, it was recommended that second-stage filling of the Nurek reservoir, resulting in a water depth of 656 feet (200 m), be accomplished by a smooth filling cycle with no abrupt slowdowns in filling rate. Seismicity remained low during this filling until a minor but rapid fluctuation in filling rate occurred in August 1976. Following this fluctuation, there was a pronounced increase in seismicity, along with the occurrence of the largest earthquake reported to that time, a magnitude (M_S) 4.1 earthquake. It has been implied that the increase in seismicity during this second filling cycle may have been directly related to the sudden change in rate of filling (Simpson and Negnatullaiv, 1978; Keith and others, 1979).

From this experience at Nurek, and from consideration of the correlations between filling curves and seismicity for other cases of RIS, it appears that sudden changes in water level and sudden deviations in rate of water level change can be triggers of induced seismicity. A controlled, smooth filling curve, with no sudden changes in filling rate, should be less likely to be accompanied by induced seismicity than rapid, highly fluctuating filling rates.

6.4 - Potential for Landslides in the Devil Canyon-Watana Reservoir Area Resulting from RIS

Any assessment of the potential landslides in the Devil Canyon-Watana reservoir (this area is considered to include the banks of the present

course of the Susitna River) resulting from RIS should be considered within the context of the overall potential for landslides and rockfalls in the reservoir area. That is, the potential for landslides which can be triggered by impoundment of the reservoir by natural processes (such as freeze-thaw conditions) as well as by RIS should be considered. Within this context, we have considered the potential for landslides triggered by RIS by making a preliminary assessment of whether in situ conditions suitable for landslides exist in the proposed reservoir area, and whether earthquakes are likely to release enough energy to trigger landslides. Detailed studies of potential landslide-prone areas were outside the scope of this investigation and therefore, were not conducted. Consequently, the judgment presented below represents a very preliminary assessment of the potential for RIS induced landslides.

During this investigation, a very preliminary assessment of landslide potential was made from remotely-sensed data interpretation, review of previous studies conducted for the project, and limited aerial reconnaissance. On the basis of this assessment, it is concluded that the potential exists for landslides to occur in the reservoir area.

A RIS event occurring within the hydrologic regime of the reservoir could trigger landslides if the earthquake occurred close enough to a potential slide area and if it released sufficient energy to trigger a slide. Within the scope of this investigation, the location of a RIS event within the hydrologic regime of the combined reservoir cannot be estimated with sufficient precision to provide a meaningful assessment of where in the reservoir area a landslide could occur, how large the landslide would be, and how large an earthquake would be necessary to trigger a landslide. Given these constraints and the configuration of the Susitna River valley, the likelihood of a large landslide in the proposed reservoir during a reservoir-induced earthquake appears to be low. This judgment should be reviewed when final dam design is considered.

TABLE 6-1

REPORTED CASES OF RESERVOIR-INDUCED SEISMICITY (RIS) [1]

No.[2]	Dam Name, Reservoir Name[3]	Country	Classification of RIS	Magnitude of Largest[4] RIS Event
1	Akosombo Main, Lake Volta	Ghana	Accepted, macro	Intensity V
2	Almendra, Tormes Reservoir	Spain	Accepted, micro	Less than 2
3	Bajina Basta	Yugoslavia	Accepted, micro	Less than 3
4	Benmore	New Zealand	Accepted, macro and micro	5 (?)
5	Blowering	Australia	Accepted, macro and micro	3.5
6	Cabin Creek	USA	Not RIS	---
7	Cajuru	Brazil	Questionable	Approx. 4
8	Camarillas	Spain	Accepted, macro	4.1
9	Canelles	Spain	Accepted, macro	4.7
10	Clark Hill	USA	Accepted, micro (macro?)	4.3 (?)
11	Contra, Lake Vogorno	Switzerland	Accepted, micro	Less than 3
12	Coyote Valley, Lake Mendocino	USA	Accepted, macro	5.2
13	El Grado	Spain	Not RIS	---
14	Emosson	Switzerland	Accepted, micro	Less than 3
15	Eucumbene	Australia	Accepted, macro	5 (?)
16	Fairfield, Lake Monticello	USA	Accepted, micro	2.8
17	Ghirni	India	Questionable	---
18	Grancarevo	Yugoslavia	Accepted, micro	Less than 3
19	Grandval	France	Accepted, macro and micro	Intensity V
20	Hendrik Verwoerd	South Africa	Accepted, micro	Less than 2
21	Hoover, Lake Mead	USA	Accepted, macro and micro	5.0
22	Itezhitezhi	Zambia	Accepted, macro	4 or less (?)
23	Jocassee	USA	Accepted, macro and micro	3.2
24	Kamafusa	Japan	Accepted, micro	Less than 3
25	Kariba	Zambia/Rhodesia	Accepted, macro and micro	6.25
26	Kastraki	Greece	Accepted, macro	4.6
27	Keban	Turkey	Accepted, micro	Less than 3
28	Kerr, Flathead Lake	USA	Accepted, macro	4.9
	Kinarsani	India	Questionable	---
29	Koyna, Shivaji Sagar Lake	India	Accepted, macro and micro	6.5
30	Kremasta	Greece	Accepted, macro and micro	6.3
31	Kurobe	Japan	Accepted, macro and micro	4.9
32	La Cohilla	Spain	Questionable	---
33	La Fuensanta	Spain	Questionable	---
34	Mangalam	India	Questionable	---
35	Mangla	Pakistan	Not RIS	---
36	Manicougan 3	Canada	Accepted, macro and micro	4.1
37	Marathon	Greece	Accepted, macro	5.75
38	Mica	Canada	Not RIS	---
39	Monteynard	France	Accepted, macro	Intensity VII
40	Mula	India	Accepted, micro	Less than 1
41	Nurek	USSR	Accepted, macro and micro	4.5
42	Oroville	USA	Accepted, macro	5.7
43	Oued Fodda	Algeria	Accepted, micro	Less than 3
44	Palisades	USA	Accepted, micro	3.7 (?)
45	Parambikulam	India	Questionable	---
46	Piastra	Italy	Accepted, macro and micro	4.4
47	Pieve di Cadore	Italy	Accepted, macro and micro	Intensity V
48	Porto Colombia	Brazil	Accepted, macro	Intensity VI to VII
49	Rocky Reach	USA	Not RIS	---
50	San Luis	USA	Not RIS	---
51	Sanford	USA	Not RIS	---
52	Schlegeis	Austria	Accepted, micro	Less than 2
53	Sefid Rud	Iran	Questionable	4.7
	Sharavathi	India	Questionable	---
54	Shasta	USA	Accepted, micro	Less than 3
55	Sholayar	India	Questionable	---
56	Talbingo	Australia	Accepted, macro and micro	3.5
57	Ukai	India	Questionable	---
58	Vajont	Italy	Accepted, micro	Less than 3
59	Volta Grande	Brazil	Accepted, macro	Less than 4
60	Vouglans	France	Accepted, macro	4.4
61	Warragamba, Lake Burragorang	Australia	Questionable	5.4
62	Xinfengjiang	China	Accepted, macro and micro	6

Notes:

1. Data source: Packer and others (1979).
2. Numbers correspond to numbers in Figure 6-1; Kinarsani and Sharavathi are unplotted because of insufficient data.
3. Where only one name is given, either the reservoir name is the same as the dam name or only the dam name is known.
4. A dash indicates the magnitude was not obtained. Intensities are given in the Modified Mercalli Scale of Wood and Neumann (1931) for cases in which this value was given in lieu of the Richter magnitude.

TABLE 6-2

RESERVOIR-INDUCED SEISMIC EVENTS WITH MAXIMUM MAGNITUDE OF 5 OR GREATER[1]

Dam	Reservoir	Magnitude	Active Fault[2] Present
Koyna	Shivaji Sagar Lake	6.5	Yes[3]
Kariba	Lake Kariba	6.25	Not obtained[4]
Kremasta	Lake Kremasta	6.3	Yes[3]
Xinfengjiang	Xinfengjiang	6.0	Yes
Marathon	Lake Marathon	5.75	Not obtained[4]
Oroville	Oroville Reservoir	5.7	Yes
Coyote Valley	Lake Mendocino	5.3	Yes
Benmore	Lake Benmore	5.0	Yes[3]
Eucembene	Lake Eucembene	5.0	Yes[3]
Hoover	Lake Mead	5.0	Yes[3]

Notes:

1. Data Source: Packer and others (1979).
2. Active faults are those defined as having displacement in the present tectonic stress regime.
3. Determination is based on field reconnaissance studies.
4. The presence of an active fault has not been obtained but is considered probable because of the tectonic setting.

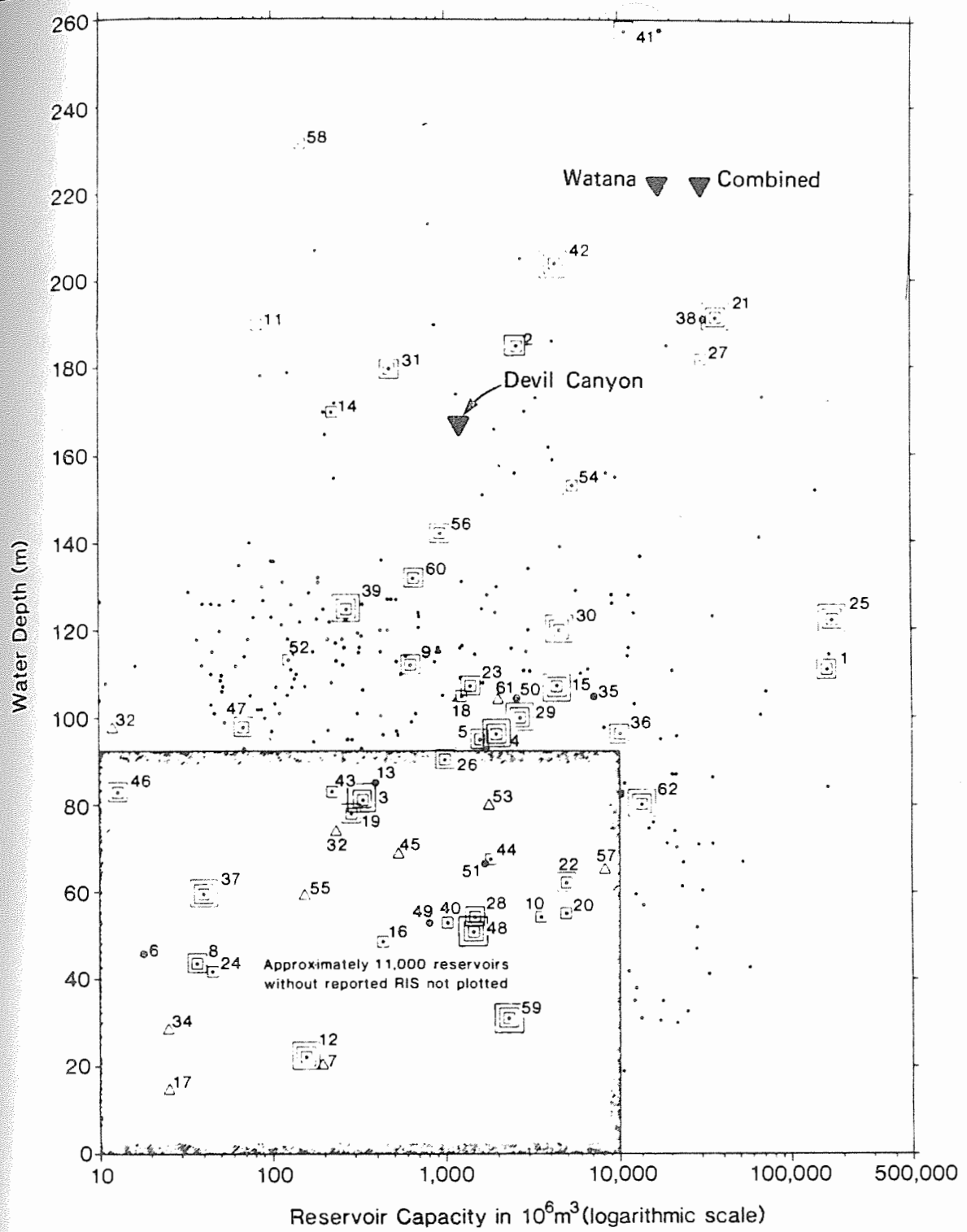

Note: The following reservoirs were not plotted because of insufficient data: Kinarsani, Sharavathi.

*41 - Nurek (USSR) depth is in excess of 285 m.

LEGEND

- Deep and/or very large reservoir
- Accepted case of RIS, maximum magnitude ≥ 5
- Accepted case of RIS, maximum magnitude 3-5
- Accepted case of RIS, maximum magnitude ≤ 3
- Questionable case of RIS
- Not RIS

PLOT OF WATER DEPTH AND VOLUME FOR WORLDWIDE RESERVOIRS AND REPORTED CASES OF RIS

7 - MAXIMUM CREDIBLE EARTHQUAKES (MCEs)

The approach to estimating the maximum credible earthquakes (MCEs) in a region, and thereby to establishing a basis for estimating the ground-motion parameters at a specific site, is based on the premise that significant earthquake activity is associated with faults with recent displacement. The evaluation of the MCE that may be associated with a given fault is closely related to the geologic and seismologic setting in the site region. Therefore, it is necessary to identify the characteristics of the faults with recent displacement in order to assess their seismic source potential. For this study, the only faults considered to have been subject to recent displacement within or adjacent to the site region are the Castle Mountain fault and the Denali fault. The Benioff zone passes at depth beneath the site and is also considered to be a potential seismic source. These three potential sources are the Talkeetna Terrain boundary faults discussed in Section 4.3.

In addition to assessing the MCE for seismic sources in or adjacent to the site region, the size of the maximum earthquake that could occur on a fault with recent displacement that might not have been detected by our geologic investigation was evaluated. This earthquake has been designated the detection level earthquake as discussed in Section 4.2.4.

The selection of ground-motion parameters for the project was based on both deterministic and probabilistic approaches (Section 8). For the deterministic approach, MCEs were estimated for each of the seismic sources and for the detection level earthquake. The closest distance of these sources from the Watana and Devil Canyon sites were estimated and used in the seismic design analysis. The MCEs and their distance from the sites are summarized in Table 7-1. The 13 significant features near

the sites were judged either not to be faults or to be faults without recent displacement; therefore, they were not included in this analysis.

The deterministic approach can be relatively conservative as it includes the assumptions that the MCE will occur during the lifetime of the facility and will occur at the closest approach of the respective sources to the sites. The approach does not take into account whether these assumptions are geologically or seismologically reasonable.

The probabilistic approach models the occurrence of earthquakes using the geological and seismological characteristics of the site region. Using this approach, estimates were made of the ground motions that might occur during the life of the Project. The MCEs estimated for the seismic sources are the same as those estimated for the deterministic approach. In addition, the recurrence interval, maximum rupture length, maximum displacement, fault geometry, and slip rate were estimated for each of the MCEs and their sources along with their b-slope. The MCE data used in the probabilistic ground-motion analysis are summarized in Table 7-1 and discussed in Section 8.

The probabilistic analysis specifies the contribution of each of the seismic sources to the overall ground motions. This approach is designed to provide a more realistic model of seismic ground motions to which the site may actually be subjected than does the deterministic approach. Using the probabilistic model, a systematic evaluation is made of the ground motions which could result from the MCE, not only at the closest distance to the site, but also at different locations along a particular seismic source. The approach also incorporates the recurrence interval of earthquakes on the sources and uses these data to assess the likelihood of occurrence during the lifetime of the project.

7.1 - Sources Outside the Talkeetna Terrain

The MCEs for sources outside the Talkeetna Terrain, such as the mega-thrust zone at the Aleutian Trench or the Fairweather fault, are not of significance to the Project because of the distance of these sources from the Project and because of the presence of seismic sources such as the Denali fault and the Benioff zone that are closer to the Project. Even if it is assumed that a magnitude (M_S) 8.5 event could occur on a known seismic source outside the Talkeetna Terrain, the resultant ground motions would be significantly less than those for the Denali fault or the Benioff zone. Consequently, MCEs associated with seismic sources outside the Talkeetna Terrain have not been considered further for this investigation.

7.2 - Talkeetna Terrain Boundary Sources

The MCEs were estimated for three of the boundaries of the Talkeetna Terrain. These boundary sources are the Castle Mountain fault to the south, the Denali fault system to the north and east, and the Benioff zone at depth.

7.2.1 - The Castle Mountain Fault

The MCE for the Castle Mountain fault is estimated to be a magnitude (M_S) 7-1/2 event. This estimate is based on the following assumptions:

1) The length of the Castle Mountain fault, 295 miles (475 km), is considered to be a discrete zone of crustal weakness that would be subject to an earthquake during a period of strain release;

2) The Castle Mountain fault is a strike-slip fault according to the definition of Bonilla and Buchanan (1970);

3) Using Slemmons' data (U.S. Nuclear Regulatory Commission, 1981) for strike-slip faults, the maximum rupture length that could occur during a single earthquake is estimated to be 55 miles (89 km); and

4) The rupture length cited in (3) would be expected to be associated with an MCE of magnitude (M_S) 7-1/2 using Slemmons' (1977b) relationship for magnitude vs. rupture length for strike-slip faults.

7.2.2 - The Denali Fault

The MCE for the Denali fault is estimated to be a magnitude (M_S) 8 event. This estimate is based on the following assumptions:

1) The part of the Denali fault closest to the Project sites includes the Togiak-Tikchik, Holitna, Farewell, and Shakwak Valley (west of the Totschunda fault) fault segments and the McKinley strand described by Grantz (1966) and discussed in Section 4.3. The total length of the fault considered for this analysis is 670 miles (1,080 km);

2) The fault length described in (1) above is the longest section of the Denali fault near the Project sites that appears to be a discrete zone of crustal weakness that could rupture in an earthquake;

3) The Denali fault is a strike-slip fault;

4) An estimated maximum rupture length of 178 miles (287 km) may be postulated to occur during a single earthquake using Slemmons' data (U.S. Nuclear Regulatory Commission, 1981) for strike-slip faults; and

5) The rupture length cited in (4) would be expected to be associated with an MCE of magnitude (M_S) 8, using Slemmons' (1977b) relationship for magnitude vs. fault rupture length for strike-slip faults.

7.2.3 - The Benioff Zone

Interplate Region

The MCE for the interplate region of the Benioff zone is estimated to be the equivalent of the 1964 Prince William Sound, Alaska, earthquake of M_W 9.2. (For consistency of presentation, elsewhere in the report we have used the M_S 8-1/2 magnitude designation for this same event. It is recognized that the M_S scale has substantial shortcomings as an adequate indicator of energy release and size when an earthquake reaches a magnitude of about (M_S) 8. However, the M_S 8-1/2 designation is used here to represent the 1964 Prince William Sound earthquake size and to correspond with the M_W 9.2 designation.) The closest approach of the interplate region to the Watana and Devil Canyon sites is 40 miles (64 km) and 57 miles (91 km), respectively. These distances are measured to the 22-mile (35-km) depth contour on the interface between the subducting Pacific plate and the North American plate (Figure 5-7). As discussed in Section 5, this depth is assumed to mark the down-dip limit of great shallow interplate earthquakes and the closest distance to the sites at which the MCE could occur.

The assumptions used to derive the interplate region MCE are summarized in the following paragraphs.

The MCE that could occur on the interface of any of the worldwide Benioff zone interplate regions is estimated to be magnitude (M_W, moment magnitude) 9.5. The fault rupture area and magnitude of this earthquake exceed the corresponding values for the 1964 Prince William Sound earthquake of magnitude (M_W) 9.2. In addition, the assumed magnitude (M_W) of 9.5 is equal to the magnitude of the largest earthquake that has occurred this century, namely the 1960 earthquake near Chile.

It is considered unlikely that an earthquake of magnitude (M_W) 9.5 would occur on the interplate region interface. Rather, it appears much more probable that future great earthquakes would rupture approximately the same plate boundary segment that ruptured in the 1964 earthquake in Alaska. As was the case in 1964, the magnitude (M_W, moment magnitude) would be expected to be 9.2 and the closest distances to the Watana and Devil Canyon sites would be 88 miles (142 km) and 108 miles (174 km), respectively. These distances to the sites are the closest approach of the area that ruptured in the 1964 earthquake and are considerably greater than those used for seismic design (i.e., 40 miles [64 km] and 57 miles [91 km], respectively).

One of the more conservative assumptions that could be made about the interplate region earthquake is that it could rupture from the surface down dip to the aseismic front (the latter is shown in Figure 5-7). The magnitude (M_W, moment magnitude) would be 9.5 and the closest distances to the Watana and Devil Canyon sites would be 40 miles (64 km) and 57 miles (91 km), respectively. However, such an assumption would be contrary to the expectation (based on the considerations outlined in Section 5)

that great interplate thrust events should not rupture farther down dip than 22 miles (35 km). If rupture of the deeper segment adjacent to the aseismic front were to occur, it would most likely occur independently of rupture on the shallow segment, and it would be unlikely to have a magnitude greater than (M_S) 7.5, as occurred during the 1978 Miyagi-oki, Japan, earthquake (Seno and others, 1980).

Intraplate Region

The MCE for the intraplate region of the Benioff zone is estimated to be magnitude (M_S) 7-1/2. This magnitude is based on an estimated maximum possible fault rupture area within the intraplate region and on historical seismicity (Section 5). The estimated maximum fault rupture dimensions of 9 miles (15 km) by 62 miles (100 km) yield a magnitude (M_W, Moment magnitude) of 7.2. A survey of the magnitudes of past intraplate earthquakes worldwide in the depth range 25 to 45 miles (40 to 70 km) reveals no events greater than magnitude (M_S) 7.6 (Section 5). The closest distance of the intraplate region of the Benioff zone to the Watana and Devil Canyon sites is 31 miles (50 km) and 38 miles (61 km), respectively.

7.3 - Talkeetna Terrain Sources

As discussed in Section 4.4 and at the beginning of Section 7, the 13 features in the Talkeetna Terrain near the Watana and Devil Canyon sites have been judged either not to be faults or to be faults without recent displacement. None of these features are considered to be seismic sources; thus, it is inappropriate to assign MCEs to them.

The absence of recognizable faults with recent displacement in the Talkeetna Terrain sets an upper limit on the magnitude of earthquakes that could occur on a fault (near one of the sites) that might not have been detected by our geological investigation. Consequently, an estimate was made of the size of earthquake that might have occurred without leaving detectable geologic evidence. This earthquake was designated the "detection level earthquake." The detection level earthquake for the Talkeetna Terrain is estimated to be magnitude (M_S) 6 (Section 4.2.4). The closest distance of this earthquake to either of the sites is estimated to be <6 miles (<10 km), as shown in Table 7-1.

7.4 - Effect of Reservoir-Induced Seismicity

The hydrologic effects of the proposed reservoirs are postulated to influence an elliptically shaped area that extends up to 19 miles (30 km) about the center (i.e., with a diameter of 37 miles [60 km]) of the proposed Devil Canyon-Watana reservoir, as discussed in Section 6. However, the reservoir and RIS will not affect consideration of MCEs along the faults outside the hydrologic regime of the reservoir, including the Castle Mountain and Denali faults and the Benioff zone.

Within the hydrologic regime of the reservoir, the influence of a reservoir is believed to be limited to that of a triggering mechanism (as discussed in Section 6). Thus, the reservoirs are not expected to cause an earthquake larger than that which could occur "naturally."

Moderate to large RIS events tend to have occurred where faults with recent displacement lie within the hydrologic regime of the reservoir. No faults with recent displacement have been observed within the

hydrologic regime of the proposed reservoir. Consequently, the effect of RIS is expected to be limited to the detection level earthquake, which is discussed in Section 4.2.4. This effect is expected to be relatively small, as discussed in Section 8.2.3.

TABLE 7-1

MAXIMUM CREDIBLE EARTHQUAKE (MCE) SUMMARY AND SEISMIC SOURCE DATA

Source	MCE	Closest Approach to		Fault[1,2,3]						MCE Rupture			Fault Recurrence[5]	Number of MCE Rupture Lengths[6]	b-Slope[3,7]	Fault Segment Recurrence[8]
	(M_S)[1]	Devil Canyon[2] miles (km)	Watana[2] miles (km)	Type	Strike	Dip	Length miles (km)	Width miles (km)	Slip rate in. (cm)/yr	Length[1] miles (km)	Width miles (km)	Displacement[4] feet (m)	years			years
Castle Mountain Fault	7-1/2	71 (115)	65 (105)	Strike-slip	N60° to 62°E	90°	295 (475)	12 (20)[9]	0.2 (0.5)	55 (89)	12 (20)[9]	7.5 (2.6)	235[10]	5.3	0.85[11]	1,245
Denali Fault	8	40 (64)	43 (70)	Strike-slip	N59° to 63°E	90°	670 (1080)	12 (20)[9]	0.4 (1.0)	178 (287)	12 (20)[9]	21.6 (6.6)	290[10]	3.8	0.85[11]	1,100
Benioff Zone (Interplate)	8-1/2	57 (91)	40 (64)	N/A	N45°E	7°NW	434 (700)	161 (260)[3]	N/A	434 (700)	124 (200)[3]	N/A	160[12]	N/A	0.85[13]	N/A
Benioff Zone (Intraplate)	7-1/2	38 (61)	31 (50)	N/A	N/A	N/A	N/A[14]	N/A[14]	N/A	62 (100)	12 (20)[3]	N/A	275[15]	N/A	0.68[13]	N/A
Detection Level Earthquake	6	<6 (<10)	<6 (<10)	N/A	N/A	N/A	N/A	N/A	N/A	5.2 (8.4)[2]	5.2 (8.4)[2]	N/A	2,700[16]	N/A	0.9[13]	N/A

Notes:

1. Analysis or data are discussed in Section 7.
2. Analysis or data are discussed in Section 4.
3. Analysis or data are discussed in Section 5.
4. Displacement is from relationships in Slemmons (1977b).
5. Estimated average return period of the MCE that may occur on the fault.
6. Calculated by dividing fault length by MCE rupture length.
7. Slope of earthquake recurrence curves that are shown in Figure 5-9.
8. Calculated by multiplying the fault recurrence by the number of MCE rupture lengths (e.g., for the Denali fault: 290 years x 3.8 = 1,100 years).
9. The fault, and fault rupture during an MCE, are assumed to extend to the base of the crust, i.e., 12 miles (20 km).
10. Estimate calculated using the procedures described in Appendix A.7.
11. These values are consistent with the b-slope that is used for the Talkeetna Terrain and are compatible with the b-slope for other major strike-slip faults.
12. Davies and others (1981).
13. These b-slopes are discussed in Section 5.4 and shown in Figure 5-9.
14. The intraplate earthquake was assumed to occur on a fault anywhere within a 10,425 square-mile (27,000-km^2) section of the intraplate region of the Benioff zone.
15. Woodward-Clyde Consultants, 1978.
16. Obtained in the b-slope shown in Figure 5-9.

8 - GROUND MOTIONS

8.1 - Introduction

The objective of this study is to develop estimates of the parameters of ground shaking at the Watana and Devil Canyon sites that may result from earthquakes in the site region. The ground motion parameters addressed in this report include peak acceleration, response spectra, and duration of strong shaking.

Deterministic estimates of ground motions are presented in this section for maximum credible earthquakes on significant faults with recent displacement in or adjacent to the site region. These faults are the Denali fault to the north of the sites and the interplate and intraplate regions of the Benioff zone beneath the sites. Deterministic estimates are also presented for an earthquake in the Talkeetna Terrain (designated the detection level earthquake, as discussed in Section 4.2.4), which, for purposes of these estimates, is assumed to occur close (within 6 miles [10 km]) to the sites.

A probabilistic analysis of ground motions has also been made for this study. The purpose of this analysis, referred to in this section as a seismic exposure analysis, is to assess the probabilities that values of peak ground acceleration may be exceeded at the sites and to identify the seismic sources that have a dominant contribution to the probability of exceedance. Also, the results of this analysis may be used to select design ground motion levels for appurtenant, less critical project facilities such as intake towers, powerhouse structures, and transmission towers.

This section is organized as follows. In Section 8.2, the seismicity environment of the sites is summarized, including the potential seismic

sources, maximum credible earthquakes on these sources, and recurrence of earthquakes on the sources. In Section 8.3, deterministic estimates of ground motions at the sites are presented. Section 8.4 describes the seismic exposure analysis and results. The use of the deterministic and probabilistic results in formulating criteria for ground-motion design for project facilities is discussed in Section 8.5.

8.2 - Seismicity Environment

8.2.1 - Potential Sources of Earthquakes

As described in Section 4, the Watana and Devil Canyon sites are located within a tectonic unit designated the Talkeetna Terrain. Known faults with recent displacement are present along the boundaries of the Talkeetna Terrain, as shown in Figures 1-1 and 4-1. These faults are considered to be potential seismic sources for the sites and include: the Castle Mountain fault, approximately 71 miles (115 km) south of the Watana site; the Denali fault, approximately 40 miles (64 km) north of the Watana site; and the interplate and intraplate regions of the Benioff zone, which underlie the Talkeetna Terrain. The interplate region is at a depth of 40 miles (64 km) south of and beneath the Watana site; the intraplate region dips downward to the northwest and is about 31 miles (50 km) below the Watana site at its closest approach. In addition to these seismic sources, a detection level earthquake is considered in this analysis; it is assumed that this earthquake would occur close to either site, that is, within approximately 6 miles (10 km) of either site.

For deterministic estimates of ground motions, the Denali fault, the interplate and intraplate regions of the Benioff zone, and the detection level earthquake are all considered to be potential

sources of earthquakes and ground motions. The Castle Mountain fault is not specifically addressed, because ground shaking at the sites due to a MCE on the Castle Mountain fault would be less intense than ground shaking from MCEs on the other boundary faults. For the probabilistic studies of ground motions, all of the potential earthquake sources mentioned above, including the Castle Mountain fault, were included. Table 8-1 summarizes the potential earthquake sources addressed in the deterministic and probabilistic studies and includes the closest distance of each source to the sites.

8.2.2 - Maximum Credible Earthquakes (MCEs)

As described in Section 7, estimates of MCEs have been made for the various potential seismic sources. The MCEs assigned to these potential sources are magnitude (M_S) 7-1/2 for the Castle Mountain fault, magnitude (M_S) 8 for the Denali fault, magnitude (M_S) 8-1/2 for the interplate region of the Benioff zone, and magnitude (M_S) 7-1/2 for the intraplate region of the Benioff zone. A maximum magnitude (M_S) of 6 has been assigned for the detection level earthquake. MCE magnitudes for each seismic source are summarized in Table 8-1.

8.2.3 - Earthquake Recurrence

The frequency of occurrence of different magnitude earthquakes is characterized by a Gutenberg-Richter relationship:

$$\log N(M) = a - bM$$

where N(M) = average annual number of earthquakes greater than or equal to magnitude M;

a, b = empirical constants.

The above relationship is considered valid for earthquakes up to the estimated maximum credible magnitude for a source. Table 8-2 summarizes the estimated values of a and b for each source, and the following paragraphs summarize the basis for these estimates.

Recurrence relationships were determined for the earthquake sources using historical seismicity data, geologic data, and information derived from the Susitna microearthquake network operated in 1980. These data and information are discussed in Section 4.3 (for the Denali and Castle Mountain faults) and in Section 5.4 (for the interplate and intraplate regions of the Benioff zone and the detection level earthquake).

The interplate region of the Benioff zone is the portion of the Benioff zone that ruptured in the 1964 Prince William Sound earthquake (magnitude [M_S] 8.4). Using the rate of convergence and the down-slip length of interaction between the Pacific and North American plates, Davies and others (1981) calculated a repeat time of about 160 years for a great earthquake at shallow depth along this portion of the Benioff zone. This recurrence interval and the size of the interplate region considered (approximately 69,498 square miles [180,000 km^2]) established the recurrence relationship for great earthquakes (Section 5.4). The b-value of 0.85 was selected on the basis of regional historical seismicity.

The recurrence relationship for the intraplate region of the Benioff zone was derived from the historical data compiled by the University of Alaska (Agnew, 1980) and from data collected during

operation of the 1981 microearthquake network (Woodward-Clyde Consultants, 1980b). The data collected by the network showed a b-slope of 0.68 (Section 5.4). During a 40-year period, Agnew (1980) observed one magnitude (M_S) 6 earthquake which he attributed to the deeper Benioff zone in a 6,564 square-mile (17,000 km^2) area beneath the sites. The relationship given in Table 8-2 appears to best fit the historical data and data obtained from the seismic network.

Geologic field studies conducted during the two-year investigation and reviews of pertinent literature were used to estimate earthquake recurrence for the Castle Mountain and Denali faults. A recurrence interval of 235 years was estimated for a magnitude (M_S) 7-1/2 earthquake on the Castle Mountain fault, which is about 295 miles (475 km) long; this estimate is based on observed slip rates (Section 4.3). A recurrence interval of 290 years was estimated for a magnitude (M_S) 8 earthquake on the 670-mile (1,080-km) length of the Denali fault west of the Totschunda fault (Figure 4-1). A b-value of 0.85 was chosen for both sources on the basis of historical seismicity in the region.

The recurrence relationship for the detection level earthquake source was determined using data from the 1980 microearthquake network and historical seismicity data. Few historical earthquakes have occurred in the area considered for the recurrence of the detection level earthquake, and the locations of the earthquakes are subject to uncertainty as a result of the sparse station coverage. Determining a recurrence relationship for the detection level earthquake is therefore subject to some uncertainty because of the limited quantity and quality of the historical seismicity data. Agnew (1980) observed five earthquakes of magnitude (M_S) ≥ 4 in 16 years in an area of 4,633 sqaure miles (12,000 km^2). The results of the 1980 microearthquake network indicate a recurrence

rate for magnitude (M_S) $\geq$4 earthquakes of approximately 0.40 events per year in the 6,564 square mile (17,000 km^2) micro-earthquake study area. Agnew (1980) did not observe any shallow earthquakes of magnitude (M_S) 6 or greater in this area. One event of magnitude (M_S) 6 in the area was located at great depth and is not considered to contribute to the shallow seismicity. A b-value of 0.9 was chosen for the detection level earthquake because it is the value considered to be most consistent with the historical seismicity data.

The influence of reservoir-induced seismicity (RIS) on the earthquake recurrence interval for the detection level earthquake was also evaluated and incorporated into the seismic exposure analysis. Section 6 describes the influence of RIS on earthquake recurrence. The added effect of reservoir-induced seismicity on the estimate of seismicity was characterized by a Gutenberg-Richter relationship as summarized in Table 8-2.

8.3 - Deterministic Estimates of Earthquake Ground Motions

Information on maximum credible earthquake magnitudes and closest distances of the faults from the sites (summarized in Table 8-1) was used to estimate levels of earthquake ground motions at the sites. The relationships employed for these estimates and the resulting ground-motion characteristics are described in the following paragraphs.

8.3.1 - Attenuation of Earthquake Ground Motion

Attenuation relationships were selected to describe the variation of peak ground acceleration and response spectral accelerations at the ground surface at the sites in relation to earthquake magnitude and distance of earthquakes from the site. These

attenuation relationships were selected on the basis of analyses of ground motions recorded during previous earthquakes, using recordings selected to be appropriate for conditions at the sites, i.e., rock at or very near the ground surface. The published work of Schnabel and Seed (1973), Seed, Muraka, and others (1976), Seed, Ugas, and Lysmar (1976), Woodward-Clyde Consultants (1978), Idriss (1978), Crouse and Turner (1980), Seed (1980) and the results of ground-motion studies at Woodward-Clyde Consultants were considered in the selection of the attenuation relationships.

Woodward-Clyde Consultants (1978), Idriss (1978), and Crouse and Turner (1980) indicate that ground motions from Benioff zone (subduction zone) earthquakes may attenuate differently than ground motions from shallow focus crustal earthquakes. To account for the possible differences, two sets of attenuation relationships were selected:

- A relationship for earthquakes occurring on the Benioff zone beneath the sites. This attenuation relationship was based primarily on analysis of recordings from South America and Japan for subduction zone earthquakes.

- A relationship for crustal earthquakes occurring on the Castle Mountain fault and Denali fault, and the detection level earthquake. The primary basis for this attenuation relationship was recordings from locations in California and other parts of the western United States.

The mean (average) attenuation relationships used in this study for peak ground acceleration are illustrated in Figure 8-1 for Benioff zone earthquakes and in Figure 8-2 for shallow focus crustal earthquakes.

The selected attenuation relationships were compared with limited data available from Alaska. This comparison is presented in Figure 8-3 and indicates reasonably good agreement between the Alaskan data and the attenuation curves used in this study.

8.3.2 - Estimates of Peak Ground Acceleration and Response Spectra at the Dam Sites

Using the attenuation relationships (Benioff zone or shallow focus) discussed above, mean peak ground accelerations at each site were estimated to be:

Earthquake Source	Mean Peak Ground Acceleration (g)	
	Watana Site	Devil Canyon Site
Denali fault	0.2	0.2
Benioff zone (Interplate region)	0.35	0.3
Detection Level Earthquake	0.5	0.5

It was found that the site ground motions from the Benioff zone are governed by the interplate region of the zone; therefore, the estimates for the intraplate region are not presented.

The response spectra of ground motions at the sites were also estimated for MCEs on each of these seismic sources. The resulting mean acceleration response spectra (damping ratios of 0.05 and 0.10) for the Denali fault and the interplate region of the Benioff zone earthquakes are illustrated in Figure 8-4 for the Watana site and in Figure 8-5 for the Devil Canyon site. The mean response spectra at either site for a detection level earthquake is shown in Figure 8-6.

8.3.3 - Estimates of the Duration of Strong Ground Shaking at the Dam Sites

The duration of strong ground shaking (significant duration) was estimated primarily on the basis of results presented by Dobry and others (1978). In that study, significant duration is defined as the time during which from 5 to 95 percent of the energy of an accelerogram is developed. The significant duration may be estimated from the following table:

Earthquake Magnitude	Significant Duration (seconds)
6	6
7	15
8	35
8-1/2	45

8.4 - Assessment of Seismic Exposure

8.4.1 - Methodology

Estimates of the probability of exceeding various levels of peak ground acceleration at the sites were made using the approach illustrated in Figure 8-7. As indicated in that figure, the probability analysis requires the characterization of certain input parameters. Specifically, these include:

- identification and geometry of seismicity sources;
- seismic activity (recurrence and maximum magnitude) of each source;
- relationship between rupture area and earthquake magnitude;

- ground motion attenuation relationships; and

- anticipated design time period of interest.

With these inputs, the exposure analysis was conducted to calculate the mean number of occurrences by which a given level of ground motion would be exceeded at each of the sites during the time period of interest, by combining the contributions of different magnitude earthquakes occurring on the various sources at different distances from the sites. The calculations were made using the computer program called PROGRAM SEISMIC EXPOSURE developed by Woodward-Clyde Consultants (in press).

The resulting mean number of occurrences that would exceed a given level of ground motion at a site within the time period of interest may then be used to estimate the probability of that level being exceeded at least once during that time period of interest. The analysis also provides an indication of the relative importance of an individual source based on its contribution to the total exposure of each site.

8.4.2 - Assessment of Inputs for Analysis

The earthquake sources considered in the analysis and the characterization of their seismic activity are summarized in Tables 8-1 and 8-2. The Castle Mountain and Denali faults were modeled as vertical planes extending in depth from 0 miles (0 km) (ground surface) to 12 miles (20 km). The Benioff zone was modeled as dipping planes at depth, representing the interplate and intraplate regions. The fault on which the detection level earthquake might occur was modeled as a series of vertical planes extending to a depth of 12 miles (20 km), simulating the possible location of a detection level earthquake at any location within the area of the Talkeetna Terrain.

In the analysis, it is assumed that an earthquake can occur with equal likelihood at any location on the planar surfaces defined for a given earthquake source. Because the attenuation relationships are defined in terms of closest distance from the fault rupture surface to the site, it is necessary to characterize the dimensions of fault rupture for given earthquake magnitudes. The relationships shown in Figure 8-8 between magnitude and rupture area, length, and width were used to characterize the dimensions of fault rutpure. A further constraint is necessary for the cases in which the fault width is limited by the fault geometry (e.g., to a width [depth] of 12 miles [20 km] for shallow crustal faults). For these cases, the rupture width was limited to the fault width, and the rupture length was selected to provide the total rupture area given in Figure 8-8.

The peak acceleration attenuation relationships (mean values) used in the analysis are shown in Figures 8-1 and 8-2. For a probabilistic evaluation, it is important to include the uncertainties in the predicted acceleration values for any given earthquake magnitude and distance. A random error term was used in the analysis to represent that uncertainty as a statistical distribution about the median values. A log normal distribution was assumed and the standard error term taken to be s = 0.40 for the shallow focus relationship and s = 0.60 for the Benioff zone relationship. The median (50th percentile), mean, and median-plus-standard-deviation (84th percentile) values of peak acceleration are related as follows:

$$a_{mean} = a_{median} \cdot e^{s^2/2}$$

$$a_{84th\ percentile} = a_{median} \cdot e^{s}$$

The methodology also provides for constraining the probability distribution of peak acceleration so that unrealistically high values of peak acceleration are not included in calculating probabilities of exceedance. An upper bound on peak acceleration was specified to be three standard deviations on the basis of the trends and bounds suggested by empirical data.

For this analysis, the design time period of interest was assumed to be 100 years.

8.4.3 - Results

Probabilities of exceedance were calculated for various levels of peak ground acceleration at the Watana site. The calculations were not repeated for the Devil Canyon site; however, the results would not be significantly different between the two sites because of their similar relative proximity to the seismic sources. (The probabilities of exceedance would be slightly lower at the Devil Canyon site because this site is somewhat further from the interplate region of the Benioff zone than is the Watana site). A plot of the probability of exceedance versus peak acceleration of the Watana site is shown in Figure 8-9. For probability of exceedance levels of 50%, 30%, 10%, 5%, and 1% in 100 years, the corresponding peak ground accelerations are the following:

Probability of Exceedance	Peak Ground Acceleration at Watana Site (g)
50%	0.28
30%	0.32
10%	0.41
5%	0.48
1%	0.64

The relative contributions of each seismic source to the probabilities of exceedance were also examined. The interplate region of the Benioff zone was found to contribute about 80 percent of the probabilities of exceedance. The reason for the dominance of this source on the results is primarily the projected high level of activity on the source, which is reflected in the recurrence relationships (Table 8-2) used in the analysis. The high maximum magnitude (M_S 8-1/2) for the interplate region of the Benioff zone and the higher acceleration attenuation curves used for the Benioff zone as compared to those used for shallow sources (Figures 8-1 and 8-2) are also reasons for the dominant influence of the interplate region of the Benioff zone on the results of the seismic exposure analysis.

Most of the rest of the contribution to the probabilities of exceedance comes from the intraplate region of the Benioff zone. The Castle Mountain fault, the Denali fault, and the detection level earthquake contribute only slightly to the probabilities of exceedance. The contributions of the Castle Mountain fault and the Denali fault are small primarily because of the relatively large distances of these faults from the site. The contributions of the detection level earthquake are small primarily because of the projected low level of activity for the Talkeetna Terrain.

8.5 - Use of Results of Ground Motion Studies in Selecting Design Ground-Motion Criteria

The results of the deterministic and probabilistic estimates of earthquake ground motions may be used in selecting ground-motion levels to be used for design of the dams and other project facilities.

The design of critical facilities, such as dams, has often been based on deterministic estimates of ground motion for MCEs. However, it is also desirable to take into account the probability of exceeding ground-motion levels in selecting design levels. The results of this study indicate that the most likely source of strong ground shaking at the site is the interplate region of the Benioff zone. The other sources are much less likely to cause the same levels of ground shaking at the site.

Possible design ground-motion criteria for the proposed dams have been formulated for a MCE occurring on the interplate region of the Benioff zone. For the Watana site, the estimated mean response spectrum for this earthquake is plotted in Figure 8-4. For a critical facility, the design is often made for ground motion at an 84th percentile level rather than at a mean level. In Figure 8-10, both the mean and the 84th percentile response spectrum are shown for the Watana site for a MCE on the interplate region of the Benioff zone.

Because the seismic analysis of Watana dam will be made using an acceleration time history rather than a response spectrum, a possible design acceleration time history was developed. A plot of this acceleration time history is shown in Figure 8-11, and the response spectrum of the time history is shown in Figure 8-10 superimposed on the smooth response spectra. As can be seen in Figure 8-10, the response spectrum of the time history lies between the mean to somewhat above the 84th percentile smooth spectra. It is anticipated that the fundamental period of Watana dam will be in the range of about 1 to 2 seconds. Figure 8-10 shows that the response spectrum of the time history is close to the 84th percentile smooth spectrum in this period range. Also, the significant duration of the time history is about 45 seconds, which is consistent with the duration expected for a magnitude 8-1/2 earthquake.

For the Devil Canyon site, mean and 84th percentile response spectra for a MCE on the interplate region of the Benioff zone are presented in Figure 8-12. Because the seismic analysis of the proposed Devil Canyon dam may be made using a rupture spectrum rather than an acceleration time history, a time history has not been developed for the Devil Canyon site. If a time history should be needed, it could readily be developed by modifying the time history shown in Figure 8-11. The modifications would involve scaling the time history shown in Figure 8-11 and modifying its frequency characteristics to provide response spectral values close to the 84th percentile level at the fundamental period of the dam.

Design ground-motion criteria for a maximum credible detection level earthquake could be formulated in a manner similar to that described above for a Benioff zone MCE. However, it is also appropriate to consider the relatively low likelihood of detection level earthquakes in comparison to Benioff zone earthquakes in developing design criteria for a detection level earthquake.

For non-critical facilities, such as a powerhouse or transmission tower, the results of the probabilistic studies can be used to aid in selecting design ground-motion criteria. Selection of the design criteria may include consideration of the acceptable levels of probabilities of exceedance, economics, and acceptable risks of damage to these facilities.

TABLE 8-1

SUMMARY OF EARTHQUAKE SOURCES CONSIDERED IN GROUND-MOTION STUDIES

Earthquake Source	MCE (M_S)	Closest Approach to Proposed Dam Sites (km)	
		Devil Canyon	Watana
		miles/(km)	miles/(km)
Castle Mountain fault	7-1/2	71 (115)	65 (105)
Denali fault	8	40 (64)	43 (70)
Benioff zone (Interplate)	8-1/2	57 (91)	40 (64)
Benioff zone (Intraplate)	7-1/2	38 (61)	31 (50)
Detection Level Earthquake	6	<6 (<10)	<6 (<10)

TABLE 8-2

SUMMARY OF EARTHQUAKE RECURRENCE ASSESSMENTS

Earthquake Source	Constants in Gutenberg-Richter Relationship[1] a	b	MCE (M_S)
Castle Mountain fault	5.30	0.85	7-1/2
Denali fault	5.33	0.85	8
Benioff zone (Interplate)	4.75	0.85	8-1/2
Benioff zone (Intraplate)	3.23	0.68	7-1/2
Detection Level Earthquake			
Natural seismicity only	3.97	0.9	6
Incremental seismicity resulting from RIS	2.65[2]	0.9	6

Notes:

1. Gutenberg-Richter Relationship: $\log N(M) = a - bM$. For the constants summarized herein, N(M) is the number of earthquakes per 100 years per 62 miles (100 km) of fault length (in the case of the Castle Mountain and Denali faults) and per 386 square miles (1,000 km^2) (in the case of the Benioff zone sources and the detection level earthquake source).
2. Reservoir induced seismicity (RIS) is considered for 10 years per 386 square miles (1,000 km^2).

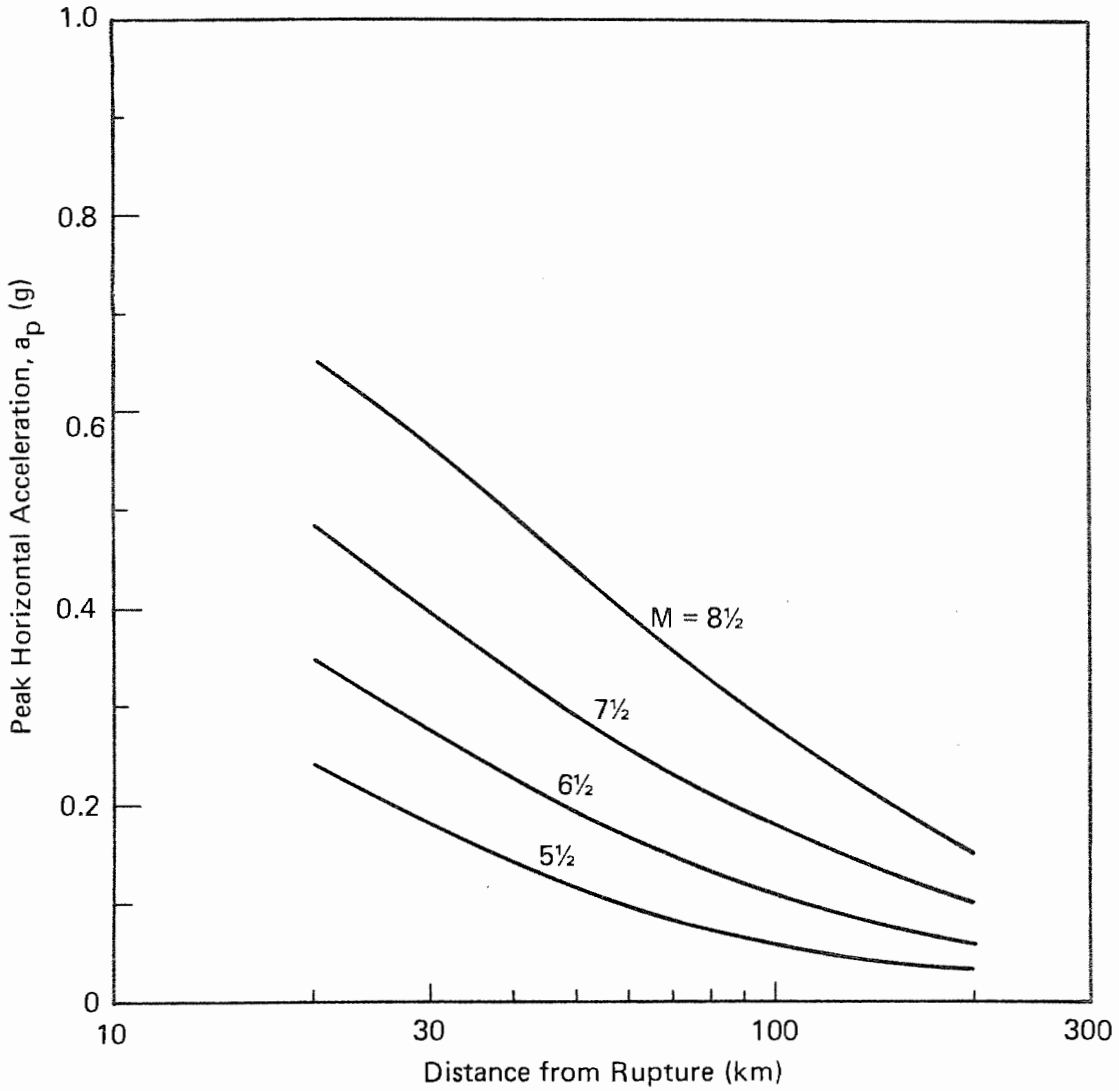

MEAN ATTENUATION RELATIONSHIPS FOR DEEP FOCUS (BENIOFF ZONE) EARTHQUAKES

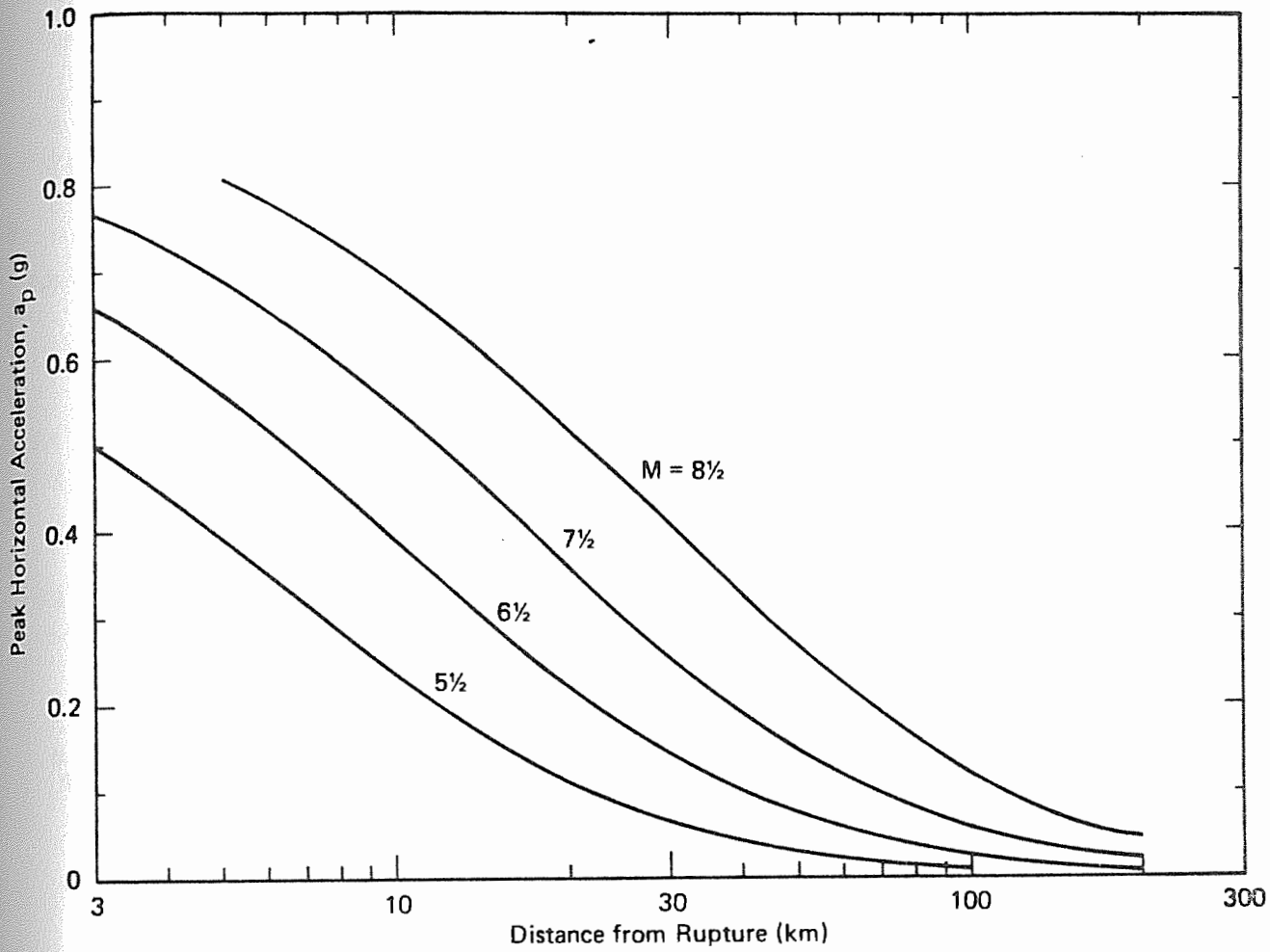

NOTE

1. Curves are applicable only within the distance range shown; at distances less than 3 km, peak accelerations are constant and equal to the values at 3 km.

MEAN ATTENUATION RELATIONSHIPS FOR SHALLOW FOCUS EARTHQUAKES

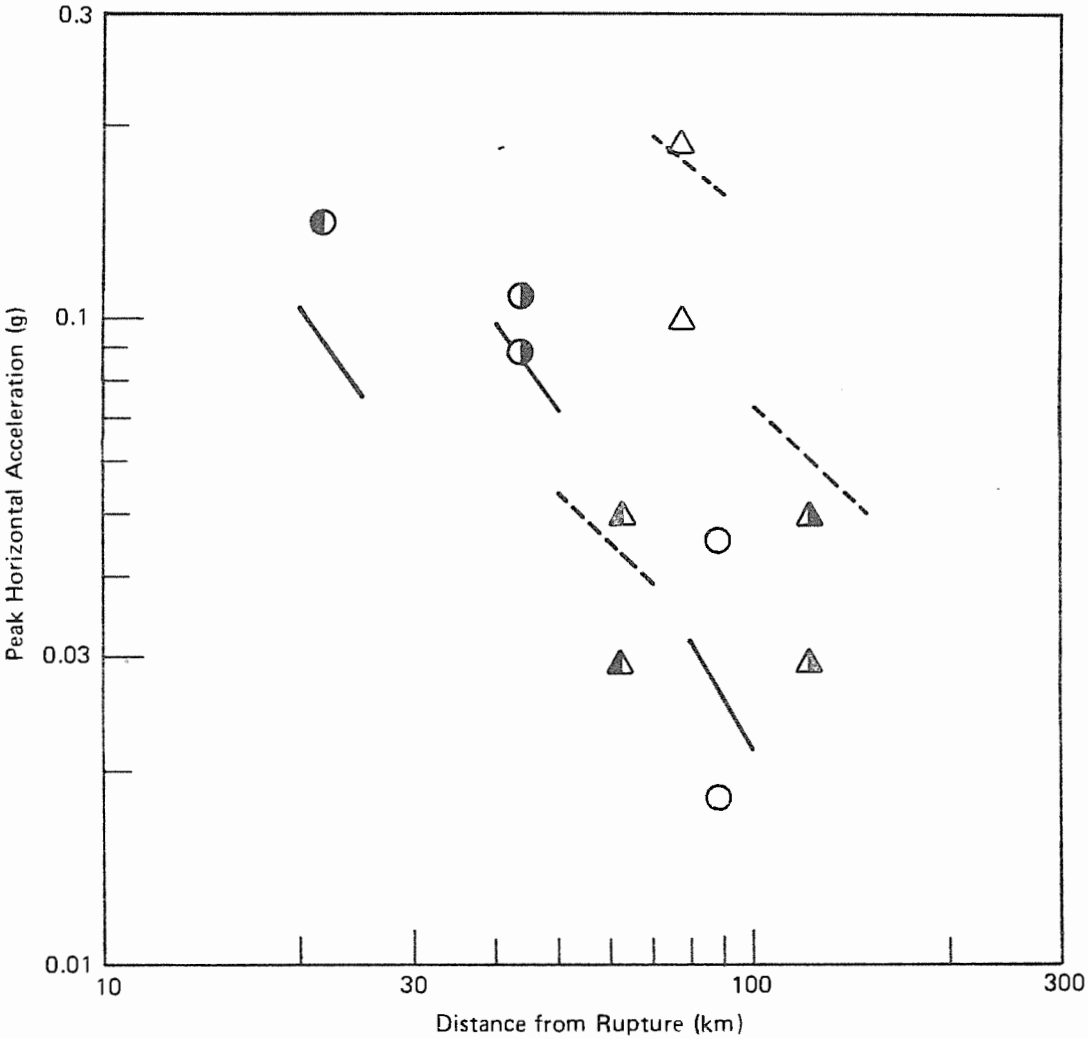

LEGEND

Attenuation Relationships for:

——— Benioff zone earthquakes (shown in Figure 8-1)

– – – – Crustal earthquakes (shown in Figure 8-2)

Alaskan Earthquakes

	Date	Magnitude	Focal Depth (km)
◐	21 June 1967	5.4	14
○	11 March 1970	6.4	29
△	1 May 1971	7.1	43
◑	30 July 1972	6.5	25
◭	10 Nov 1974	5.2	68
◭	21 Feb 1976	4.0	58

COMPARISON OF SELECTED ATTENUATION RELATIONSHIPS WITH DATA FROM ALASKA

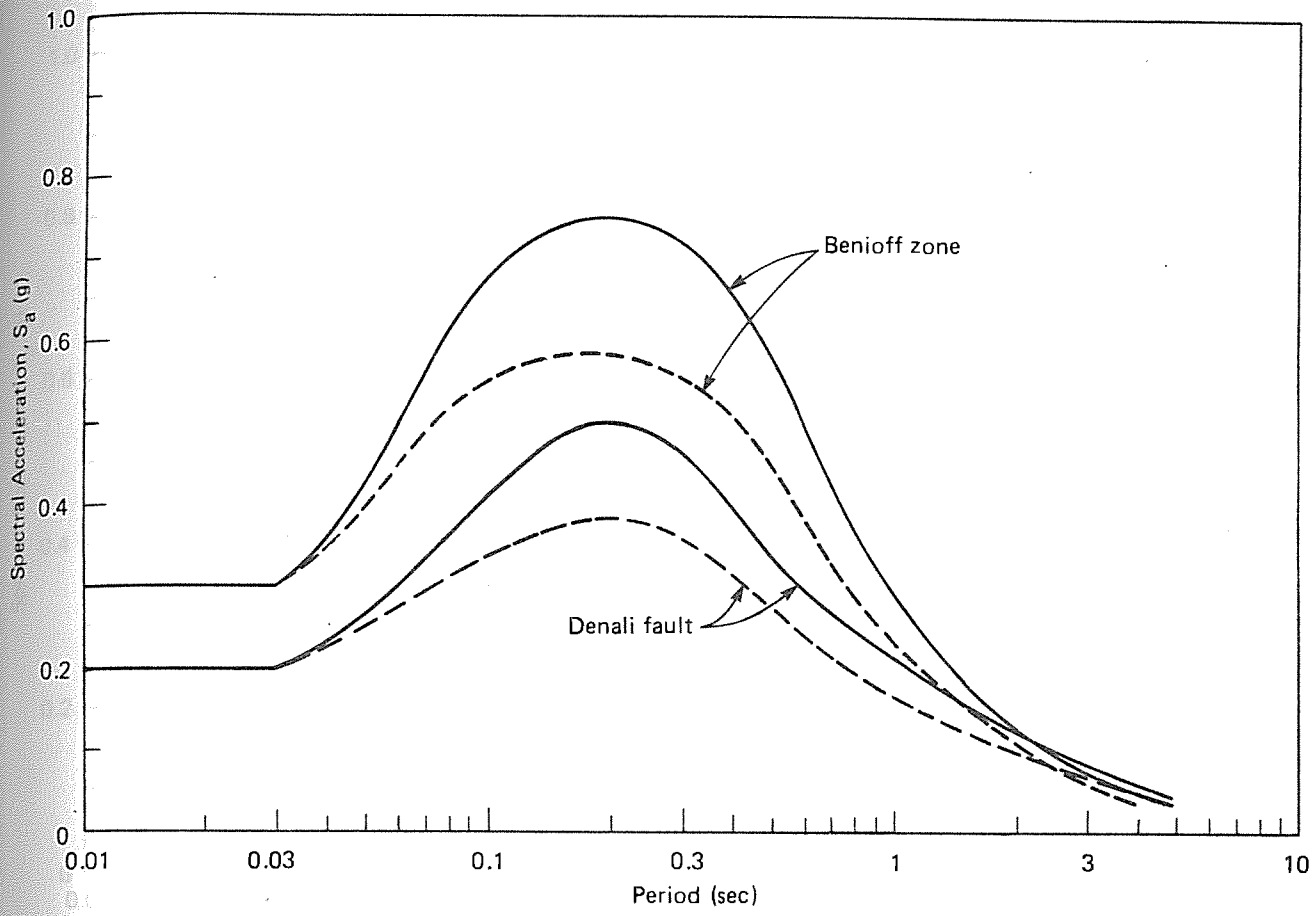

LEGEND

——— Damping ratio = 0.05

— — — — Damping ratio = 0.10

MEAN RESPONSE SPECTRA FOR MAXIMUM CREDIBLE EARTHQUAKES ON THE BENIOFF ZONE AND DENALI FAULT – WATANA SITE

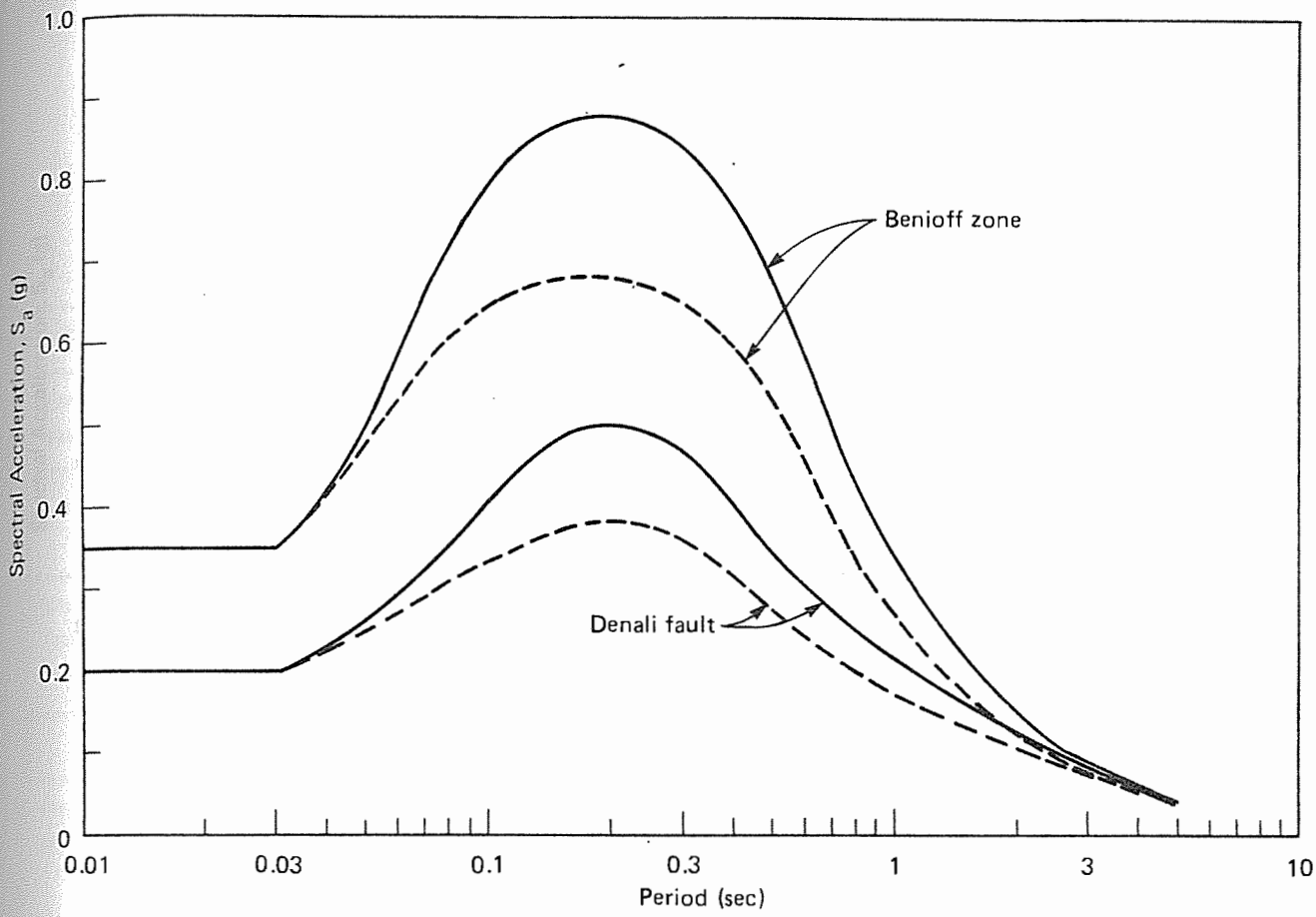

LEGEND

——— Damping ratio = 0.05

– – – – Damping ratio = 0.10

MEAN RESPONSE SPECTRA FOR MAXIMUM CREDIBLE EARTHQUAKES ON THE BENIOFF ZONE AND DENALI FAULT – DEVIL CANYON SITE

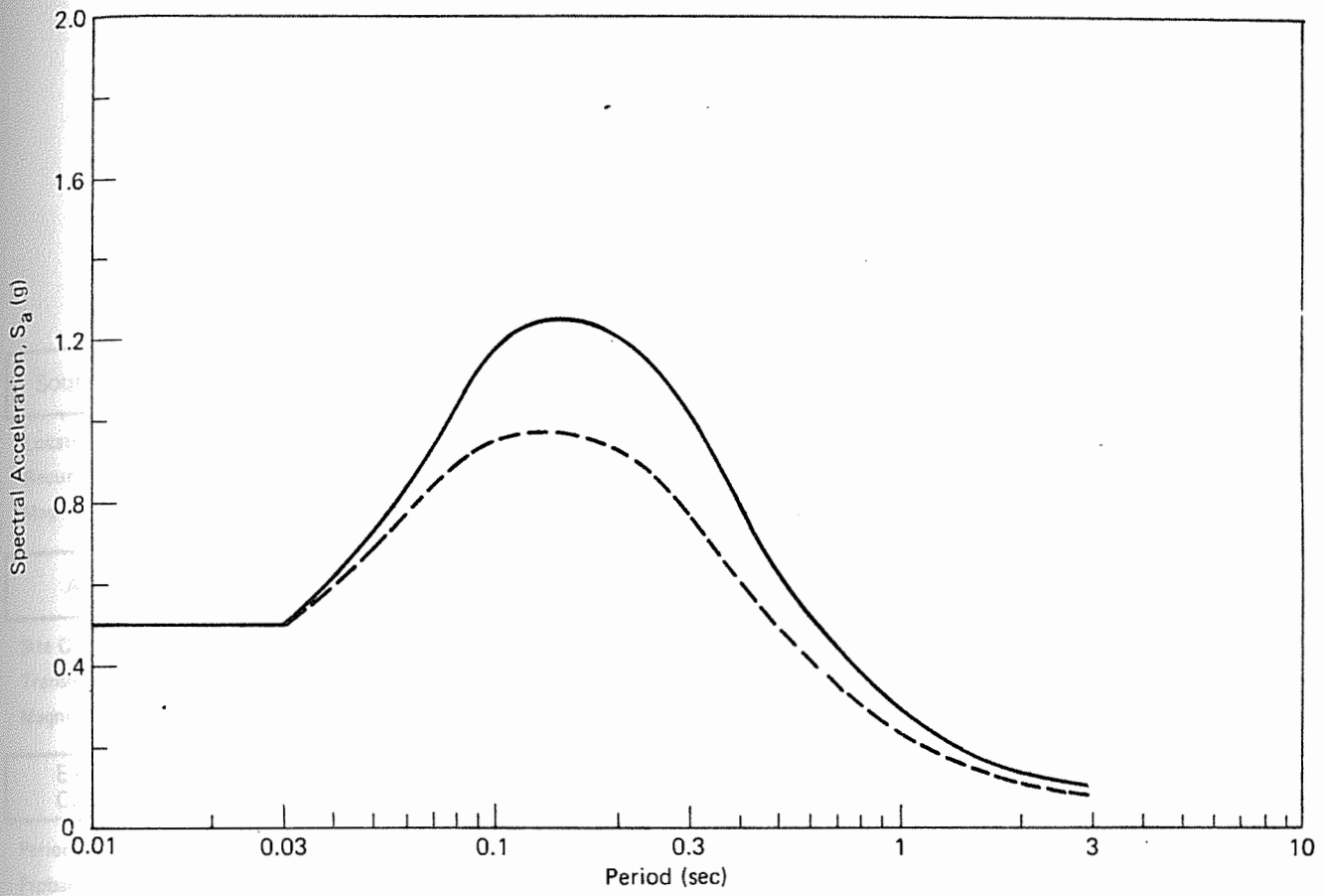

LEGEND

——— Damping ratio = 0.05

— — — Damping ratio = 0.10

NOTE

1. Spectrum applicable to both sites.

MEAN RESPONSE SPECTRA FOR MAXIMUM CREDIBLE DETECTION LEVEL EARTHQUAKE

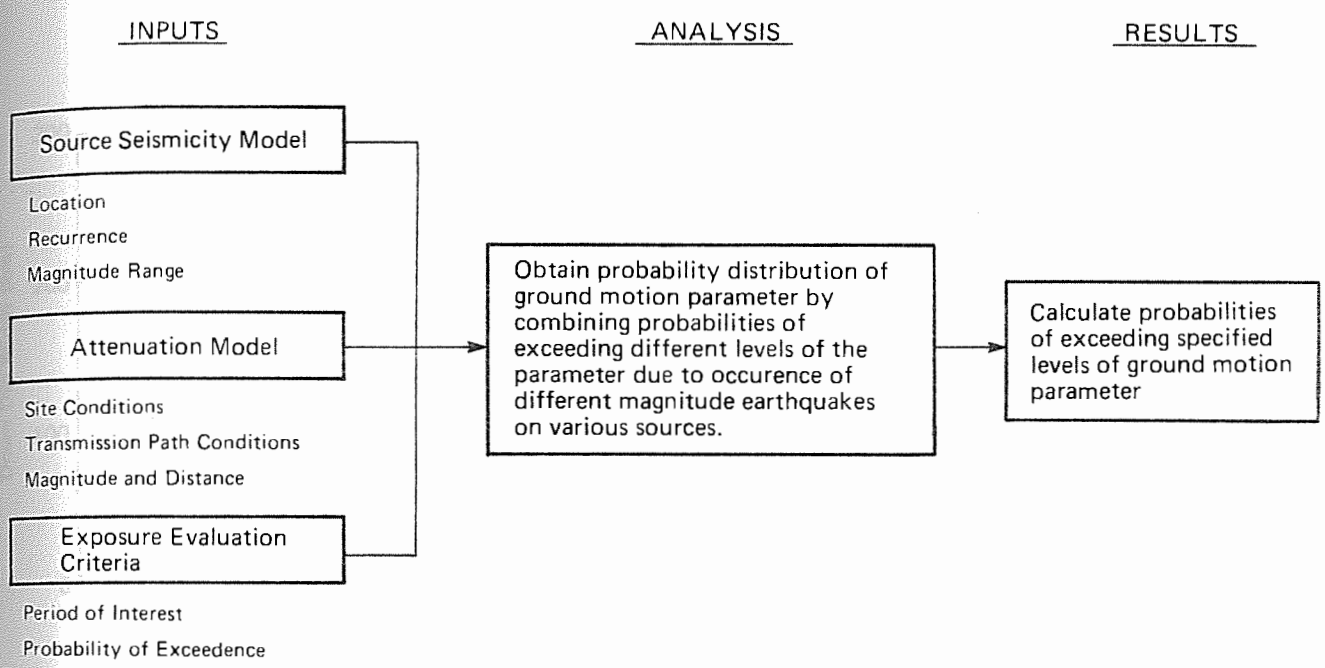

SCHEMATIC REPRESENTATION OF SEISMIC EXPOSURE ANALYSIS APPROACH

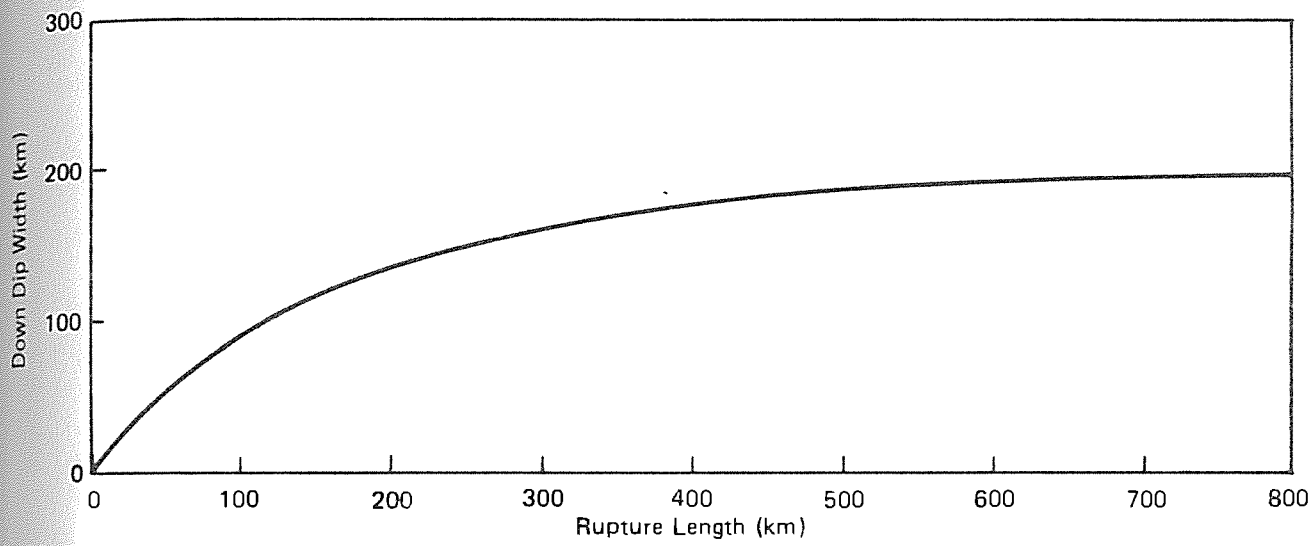

Magnitude (M_s)	Area[1] (sq. km)	Length[1] (km)	Down-dip[1] Width (km)
5.0	7	2.7	2.7
5.5	22	4.7	4.7
6.0	71	8.4	8.4
6.5	224	15	15
7.0	708	27	27
7.5	2240	47	47
8.0	7080	90	80
8.5	22,400	180	125

NOTE

1. Fault rupture dimensions are from Wyss (1979) and Woodward-Clyde Consultants (1978).

RELATIONSHIPS BETWEEN MAGNITUDE AND FAULT RUPTURE DIMENSIONS

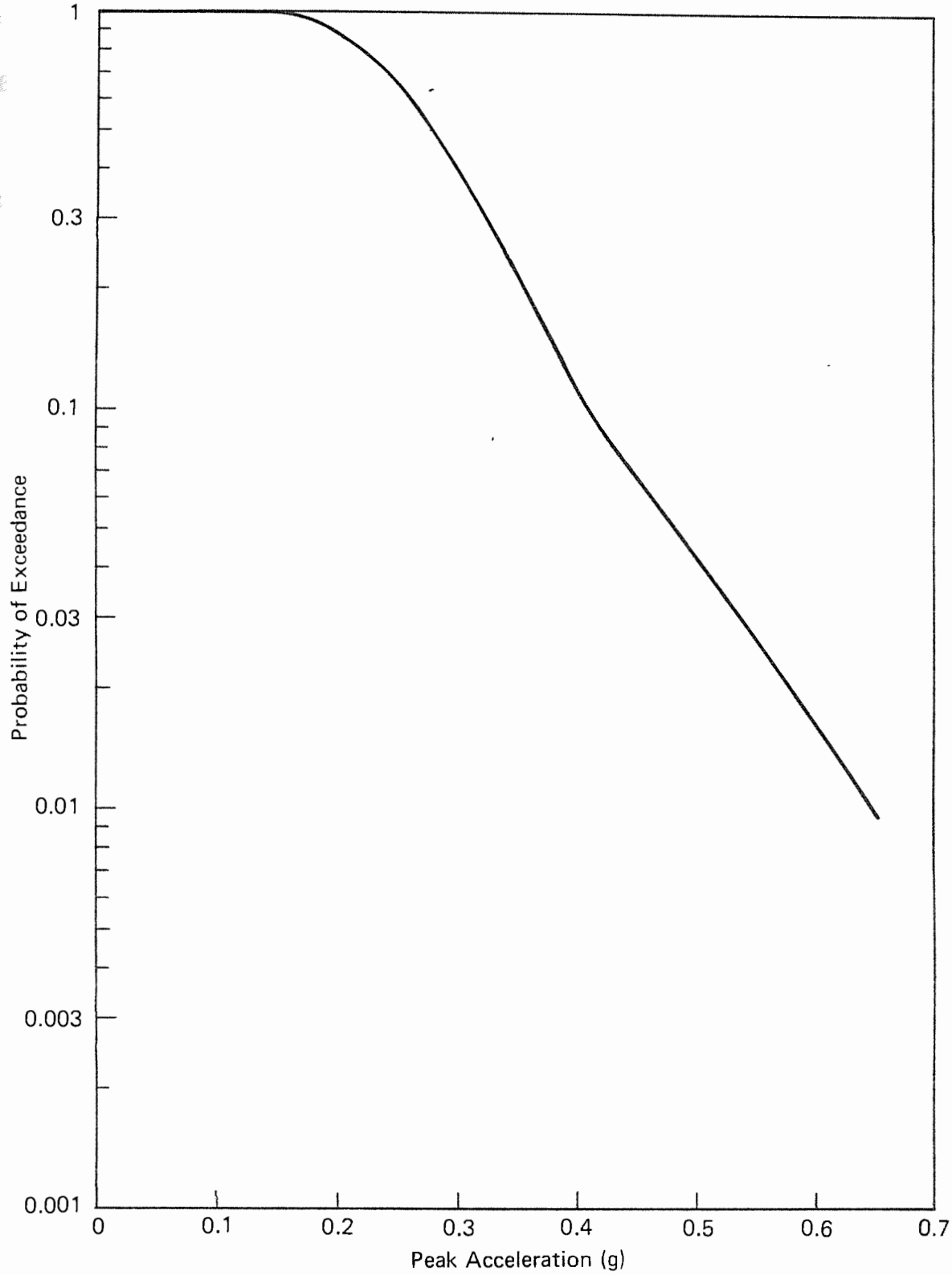

PROBABILITY OF EXCEEDANCE VERSUS PEAK GROUND ACCELERATION AT THE WATANA SITE

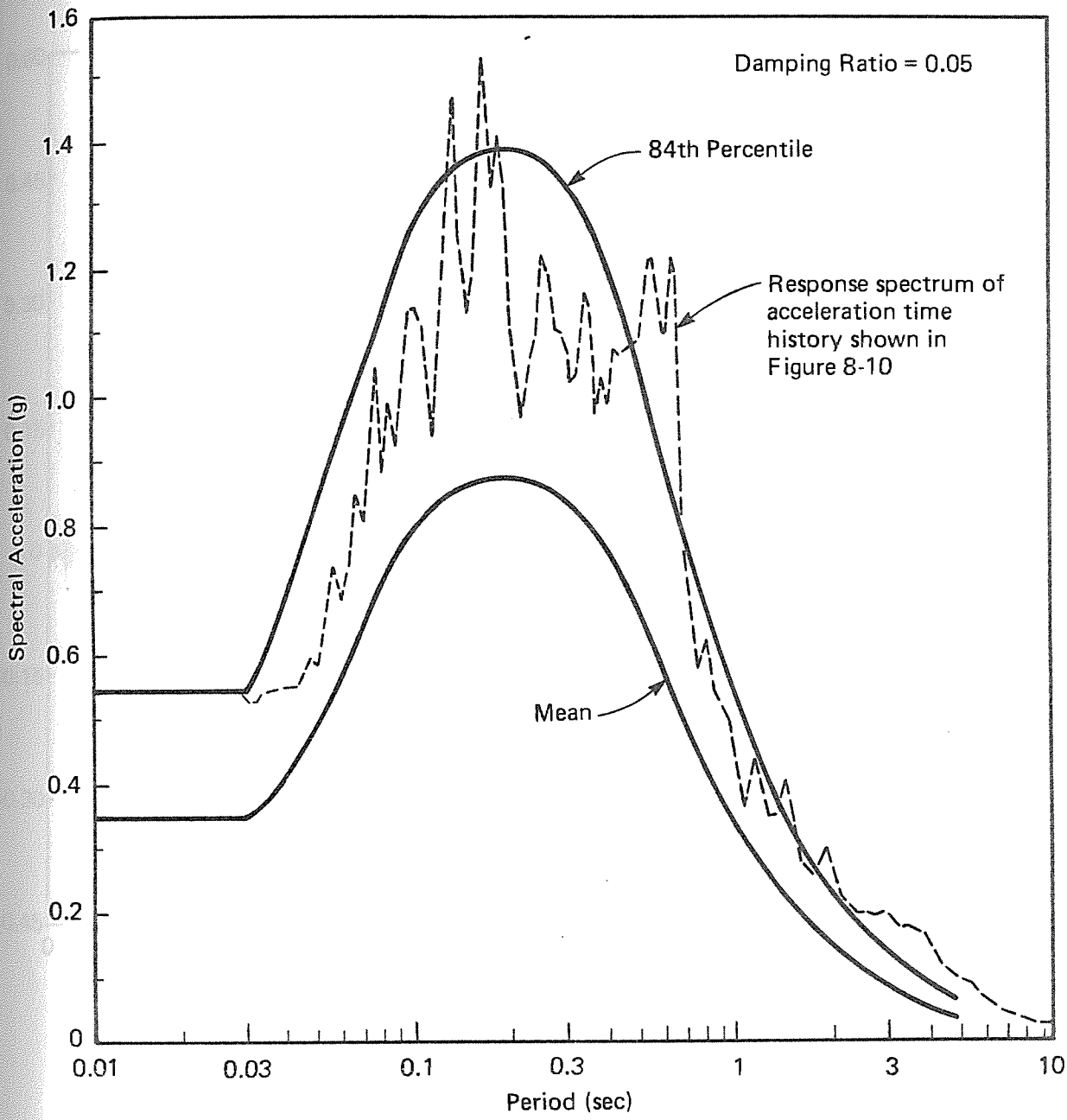

MEAN AND 84th PERCENTILE RESPONSE SPECTRA
FOR A MAXIMUM CREDIBLE EARTHQUAKE
ON THE BENIOFF ZONE–WATANA SITE

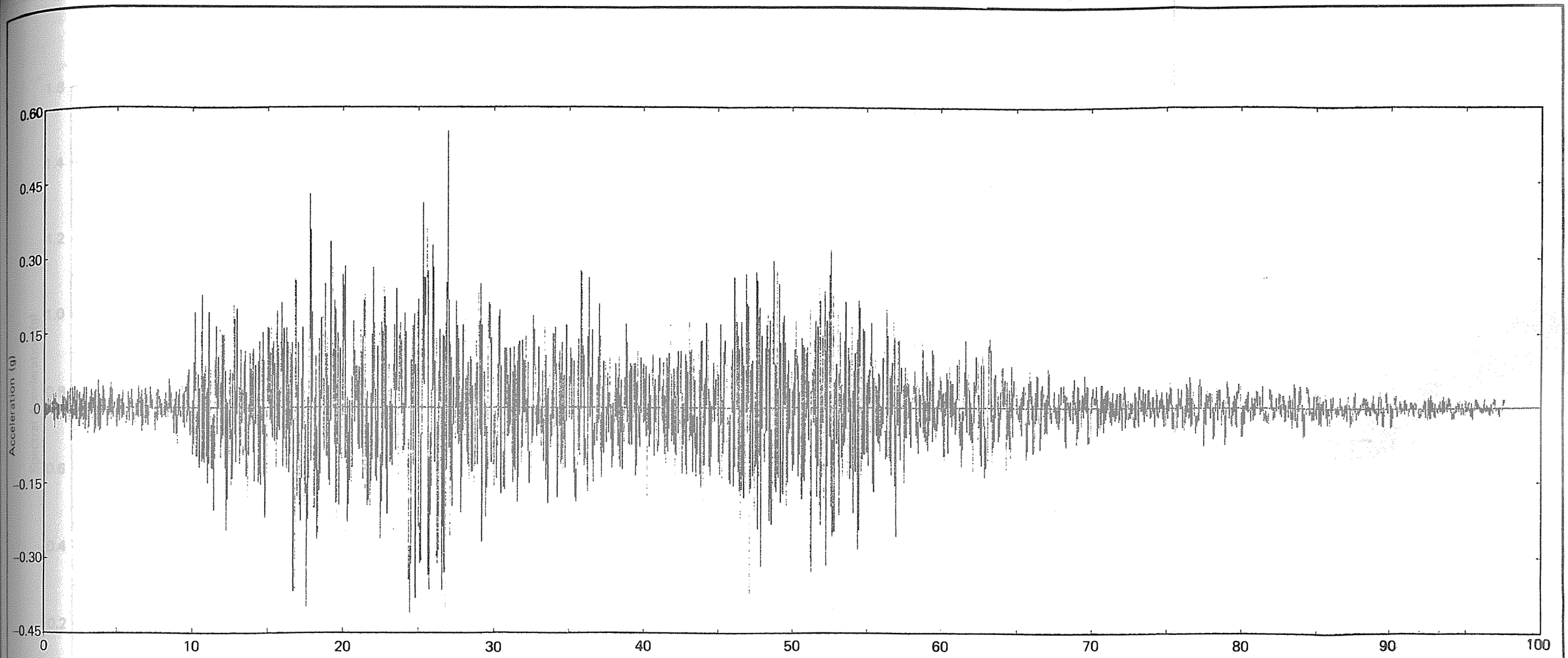

ACCELERATION TIME HISTORY FOR A MAXIMUM CREDIBLE EARTHQUAKE ON THE BENIOFF ZONE

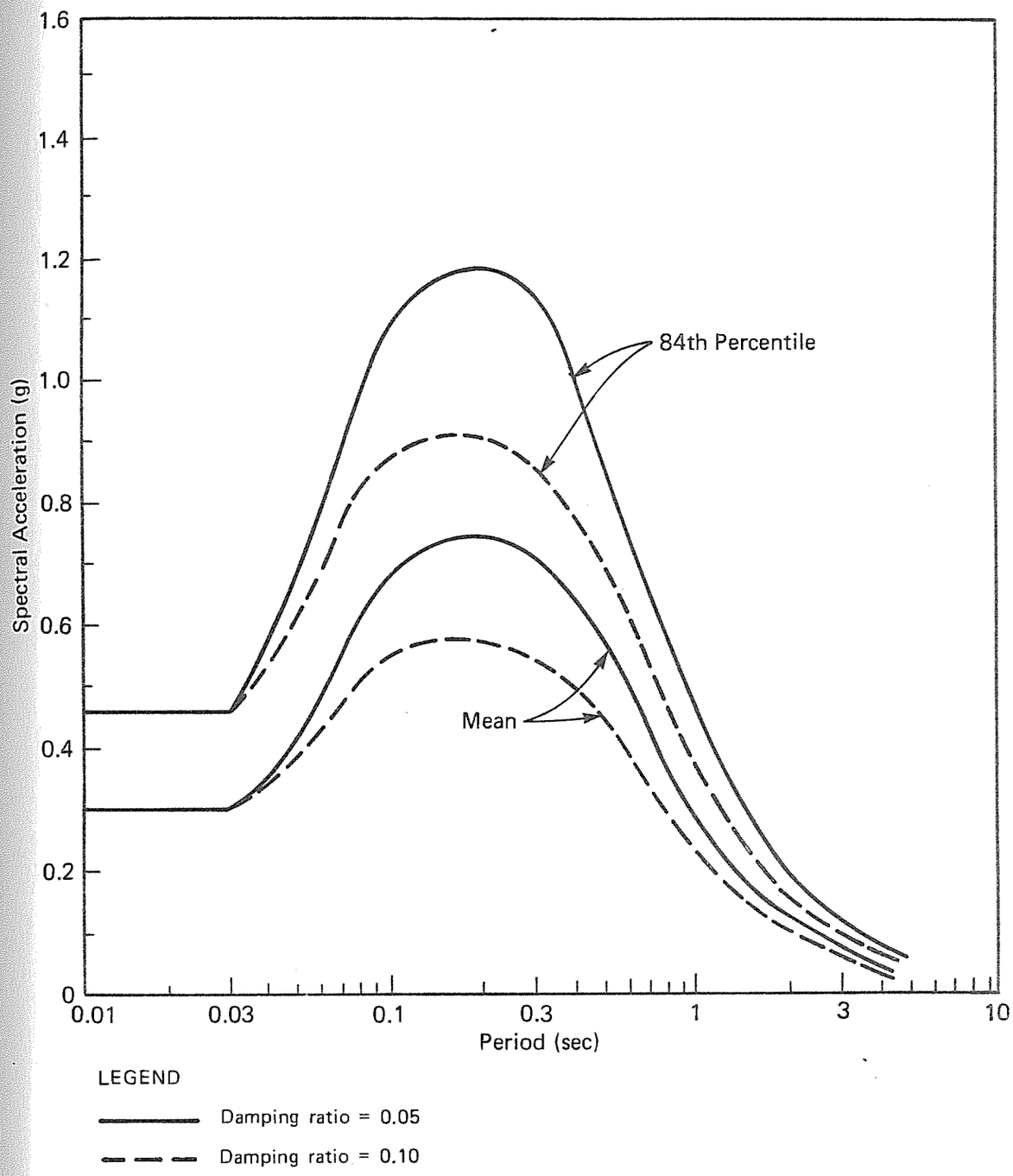

MEAN AND 84th PERCENTILE RESPONSE SPECTRA FOR A MAXIMUM CREDIBLE EARTHQUAKE ON THE BENIOFF ZONE–DEVIL CANYON SITE

9 - TRANSMISSION LINE AND ACCESS ROUTE SUSCEPTIBILITY TO SEISMICALLY INDUCED FAILURE

9.1 - Introduction

The objective of this part of the investigation was to provide input regarding the behavior of those areas along the transmission line and major access road routes that appeared to be underlain by soils that are potentially susceptible to seismically induced ground failure such as liquefaction or landsliding. The approach used to meet this objective was to interpret large scale and small scale aerial photographs along the rights-of-way and to review surficial geology mapping conducted by Woodward-Clyde Consultants during the 1981 field study (Section 3) and by R & M Associates, Inc. (1981).

The scope of this part of the investigation involved the interpretation of aerial photographs within 5 miles (8 km) of the three proposed routes shown in Figure 9-1. The photography used for the investigation was: U-2 false color near-infrared photography flown by the National Aeronautics and Space Administration (NASA) in 1977 at a scale of 1:125,000; color photography flown for Acres in 1980 at a scale of 1:24,000; low-sun-angle color near-infrared photography flown for Woodward-Clyde Consultants in 1981 at a scale of 1:24,000; and black and white photography flown by the U.S. Army in 1949, primarily at a scale of 1:40,000.

Criteria were established to guide the identification of two types of potentially hazardous areas. The two types of hazards are seismically triggered landslides and seismically induced liquefaction. The hazards were assumed to have the potential to occur in the site region during moderate to large earthquakes. No attempt was made to refine the analysis for different magnitude events occurring at various distances from the potential hazard areas.

Areas identified as having the potential for seismically induced landslides included:

a) areas with previous landslides and slumps;

b) river and stream valleys with steep slopes and overhanging promontories; and

c) areas with ground fracturing on slopes above river and stream valleys.

Criteria for areas of potential liquefaction were derived by reviewing reports of the areas that liquefied during the 1964 Prince William Sound earthquake (magnitude [M_S] 8.4). This review included reports by Foster and Karlstrom (1967), McCulloch and Bonilla, (1970), Plafker (1969), and Tysdal (1976). Liquefaction during the 1964 earthquake was concentrated in areas of unconsolidated deposits, particularly where the ground was saturated with water. Typically, these were areas underlain by glacial till, glaciolacustrine and glaciofluvial deposits, pro-glacial lake sediments, marine sediments, alluvium, loess, and clay.

Areas identified as having the potential for seismically induced liquefaction in and along the transmission and access routes included:

a) floodplain deposits along the margins of rivers and streams, and

b) areas underlain by glacial deposits, particularly kettles and deposits with standing or near-surface water.

Section 9.2 discusses each of the areas identified as potentially being susceptible to seismically induced landslides and/or liquefaction. It

should be emphasized that these locations have not been field checked. These locations and the selected right-of-way should be field checked prior to final design and construction.

9.2 - Areas of Potential Susceptibililty

This section presents the results of the study for each of the three transmission line and access route alternates. Each of the areas of potential susceptibility have been given a location number (T1-1, T1-2, etc.) and are shown in Figure 9-1.

9.2.1 - Alternate Route 1

Location T1-1 is located on a ridge 1-1/4 miles (2 km) northeast of Gold Creek (Figure 9-1). It consists of several depressions which may be kettles. The kettles appear to contain unconsolidated sediments and excessive water. This location may be an area of potential liquefaction under seismic loading conditions. The location of this area is indicated by the ground pattern and the brownish coloration of the vegetation within the depressions. At the point the Susitna bends eastward, upstream from Gold Creek, the floodplain (outwash material) contains kettles and pits (Figure 9-1; Location T1-2); this area may also contain areas of potential liquefaction.

Where Alternate Route 1 enters the stream valley southeast of Location T1-1, a site of possible landsliding is encountered (Location T1-3). At the top of the ridge east of the stream valley, Alternate Route 1 follows a colluvial deposit before reaching the Devil Canyon site (Location T1-4). The colluvium appears to contain numerous depressions where unconsolidated material is present and the water content is higher, as indicated

by the vegetation. These locations, T1-1, T2-2, and T1-4, have the potential for liquefaction. On the south side of the Susitna River, adjacent to the Devil Canyon site, an old river channel (associated with Feature KD5-43) on the hillside contains several similar depressions which may be susceptible to liquefaction (Location T1-5).

North of the Devil Canyon site, Alternate Route 1 trends northeast between several lakes in the High Lake area. The drainages from these lakes and the depressions in several low-lying areas may be areas of potential liquefaction and should be evaluated (Location T1-6). A bench of glacial till along Devil Creek at Location T1-7 is another area of potential liquefaction.

East of Devil Creek, numerous kettles and depressions at Locations T1-8 and T1-9 in till appear to contain saturated sediments that may present liquefaction problems. The route then crosses areas of extensive outwash that contain numerous depressions (Locations T1-10, 12, 13) that may be prone to liquefaction. North of the Watana site, the route crosses several stream valleys which have landslide scars at Locations T1-11 and T1-14. Near Tsusena Creek (Location T1-15) several landslides are present. South of Tsusena Creek, an area of extensive small lakes and drainage channels is present at Location T1-16. This area also has the potential for liquefaction. It is recommended that the route be carefully located to avoid the numerous depressions at Location T1-17 (a potential area of liquefaction) and the slide areas evident along Tsusena Creek.

9.2.2 - Alternate Route 2

Alternate Route 2 from Devil Canyon to the Watana site starts out at the intersection of Alternate Route 1, adjacent to a small lake

0.5 mile (0.8 km) south of the Devil Canyon site (Figure 9-1). It trends eastward on bedrock, but several stream valleys are crossed at Location T2-1. At each crossing, slide areas are present. Where the route crosses the bedrock exposures, several sites of glacial drift deposits are present (Location T2-2). Depressions containing what appear to be unconsolidated sediments that would be potentially susceptible to liquefaction are present at this location.

Southward of Location T2-2, the route is located on bedrock before turning eastward 6 miles (10 km) west of Stephan Lake. Near this bend, the route goes from bedrock to glacial deposits (Location T2-3). These deposits contain numerous depressions and hummocky areas and are underlain by relatively thick deposits of unconsolidated sediments. The vegetation indicates that the sediments are saturated in many of the sites. Near the west side of Stephan Lake, an outwash deposit is crossed and several boggy depressions are present (T2-4). Both of these locations (T2-3 and T2-4) are areas of potential liquefaction.

At the northeast end of Stephan Lake, the route passes several small lakes with intersecting drainages (Location T2-5). East of Location T2-5, the route enters an area of morainal sediments (Location T2-6). Several streams with evidence of slides are present near Location T2-6. During the 1981 field season, ground thawing and resultant slumping of surficial units occurred near Location T2-6. Locations T2-5 and T2-6 are areas that are potentially susceptible to liquefaction.

There are many slide areas where the route crosses Fog Creek; some are in ablation till (Location T2-7). This creek valley appears to be potentially unstable at numerous locations. Near Fog Lakes, there are numerous kettles in the glacial till, with possible

permafrost underlying the area (Location T2-8). Because of the potential susceptibility to liquefaction, the route location should be carefully planned through this area. Near the Susitna River and the Watana site, several slide areas are also present (Location T2-9).

9.2.3 - Alternate Route 3

Alternate Route 3 trends northward from the Watana site to the Denali Highway (Figure 9-1). North of the Watana site, a group of small lakes are present in the glacial deposits at Location T3-1. This area is potentially susceptible to liquefaction. These lakes and deposits continue northward to Deadman Creek. Several areas of outwash are present, and the vegetation pattern indicates sluggish drainage and potential sites of liquefaction at Location T3-2. On the high slopes above and west of Deadman Creek, bedrock is present. The only areas that are considered to be potentially susceptible to slide hazards are at stream crossings (Location T3-3). Northwest of Deadman Mountain, the route enters the Brushkana Creek area (Location T3-4). The entire area is pitted by kettles and depressions (particularly in Locations T3-5 through T3-8), is saturated, and has extensive areas of standing water. It is expected that the area is underlain by unconsolidated sediments and is potentially susceptible to liquefaction. The slide hazards in this region appear to be limited, except for small areas at stream crossings. Several scarps in a ground moraine are crossed four miles (seven km) south of the Denali Highway at the Seattle Creek Valley (Location T3-9). The route should be placed to avoid the areas containing these potential slide sites.

9.3 - Summary

In general, the areas which are expected to be potentially susceptible to landslides are those where steep slopes are encountered (particularly where they are underlain by weak or unstable rock and young, unconsolidated sediments), along river and stream drainages where previous landslides have occurred. An example of this type of area is the Susitna River banks upstream from the Watana site. It is recommended that these potential landslide areas, and areas with characteristics similar to those discussed previously in this section, either be avoided or examined carefully prior to final route selection for both the transmission line and the access route.

Areas generally expected to be susceptible to liquefaction are those underlain by saturated, cohesionless, unconsolidated sediments. These areas include river and stream floodplains, glacial depressions (such as kettles), and unconsolidated glacial sediments such as glaciolacustrine, glaciofluvial, outwash, and ice disintegration deposits. Prominent examples of these types of areas are the Susitna River floodplain, the Stephan Lake and Fog Lakes areas, the area between the Watana site and Deadman Lake, and the Brushkana Creek area. It is recommended that these potential liquefaction areas, and areas with characteristics similar to those discussed previously in this section, either be avoided or examined carefully prior to final route selection for both the transmission line and the access route.

LEGEND

AR-1	Alternate access and transmission line route and number
T1-4	Potential slide area and location number
T1-1	Potential area of liquefaction and location number

NOTES

1. Potential slide and liquefaction areas have been interpreted from aerial photography. Their location and extent should be field checked prior to design and construction along the selected right-of-way.
2. Route locations are from Acres American Inc. Drawing Sk-5700-C2-101 dated August, 1981.

N

TRANSMISSION LINE AND ACCESS ROUTES POTENTIAL HAZARDS MAP

0 5 10 Miles

0 5 10 Kilometers

FIGURE 9-1

10 - CONCLUSIONS

For the purpose of evaluating Project feasibility, two sets of conclusions were drawn from the results of the investigation: 1) the feasibility conclusions, i.e., those considered important in evaluating the feasibility of the Project; and 2) the technical conclusions related to the scientific data collected. The results upon which these conclusions were based should be reviewed when final design is considered.

10.1 - Feasibility Conclusions

1) The faults with known recent displacement closest to the Project sites are the Denali and Castle Mountain faults. These faults, and the Benioff zone associated with the subducting Pacific plate, are considered to be seismic sources. Maximum credible earthquakes (MCEs) for the Castle Mountain and Denali faults, and the interplate and intraplate regions of the Benioff zone, have been estimated as: a magnitude (M_S) 7-1/2 earthquake on the Castle Mountain fault, 71 miles (115 km) from the Devil Canyon site and 65 miles (105 km) from the Watana site; a magnitude (M_S) 8 earthquake on the Denali fault, 40 miles (64 km) from the Devil Canyon site and 43 miles (70 km) from the Watana site; a magnitude (M_S) 8-1/2 earthquake on the interplate region of the Benioff zone, 57 miles (91 km) from the Devil Canyon site and 40 miles (64 km) from the Watana site; a magnitude (M_S) 7-1/2 earthquake on the intraplate region of the Benioff zone, 38 miles (61 km) from the Devil Canyon site and 31 miles (50 km) from the Watana site.

2) Of the 13 significant features, nine were found to be lineaments and four were found to be faults. No evidence of faults with

recent displacement (displacement in the past 100,000 years) was found on features that pass through or adjacent to the Project sites; therefore, none of the 13 significant features near the sites are judged to be faults with recent displacement for purposes of seismic design.

3) The detection level earthquake (an earthquake that theoretically could occur on an undetected fault with recent displacement) was judged to be a magnitude (M_S) 6 earthquake that could occur within 6 miles (10 km) of either site.

4) Estimates of peak acceleration response spectra and duraction of strong shaking at the sites were made for the Denali fault, the interplate region of the Benioff zone, and the detection level earthquake. The results of the probabilistic ground-motion (seismic exposure) study indicate that the source most likely to cause ground shaking at the site is the interplate region of the Benioff zone. Possible design criteria have been formulated for the Benioff zone earthquake.

10.2 - Technical Conclusions

1) The site is located within the Talkeetna Terrain. This tectonic unit has the following boundaries: the Denali fault to the north and northeast; the Totschunda fault to the east; the Castle Mountain fault to the south; a broad zone of deformation and volcanoes to the west; and the Benioff zone at depth.

2) The northern, eastern, and southern boundaries of the Talkeetna Terrain are major fault systems along which displacement has occurred in Quaternary time. The Benioff zone beneath the Talkeetna Terrain represents the upper margin of the Pacific plate which

is being subducted beneath the North American plate. The western boundary does not appear to have brittle deformation occurring along a major fault.

3) The Talkeetna Terrain appears to be a relatively stable tectonic unit within the present stress regime. Major strain release occurs along the fault systems bounding the Terrain. Within the Terrain, strain release appears to be randomly occurring at depth within the crust. This strain release is possibly the result of crustal adjustments resulting from stress within the Terrain caused by the subduction of the Pacific plate and/or by stress imposed by fault displacement along the Terrain margin.

4) The only fault system within the site region (within 62 miles [100 km] of either Project site) which is known to have been subject to displacement in late Quaternary time (the past 100,000 years) is the Denali fault. This fault is approximately 40 miles (64 km) north of the sites at its closest approach. The only other fault near the site region that has been subject to recent displacement is the Castle Mountain fault which is immediately south of the site region. This fault has been subject to displacement in late Quaternary time.

5) Thirteen significant features were identified by the 1980 studies as needing additional investigation. These 13 features were selected on the basis of their seismic source potential and potential for surface rupture through either Project site. Four of these features are in the vicinity of the Watana site and include the Talkeetna thrust fault, the Susitna feature, the Fins feature, and the Watana lineament. Nine of the features are in the vicinity of the Devil Canyon site and include Faults KD5-2 and KC5-5, and lineaments KD5-3, KD5-9, KD5-12, KD5-42, KD5-43, KD5-44, and KD5-45.

6) No evidence that the Susitna feature is a through-going fault was recognized during this study. Aerial reconnaissance, ground checking, low-sun-angle aerial photograph interpretation, and trenching produced no evidence of a through-going fault in bedrock along the lineament, and no evidence of deformation in overlying surficial units.

7) The Talkeetna thrust fault is a northeast-southwest trending fault that extends from the town of Denali southwest to the Talkeetna River. The fault dips to the southeast except near Talkeetna Hill where the fault is near vertical. On the basis of aerial reconnaissance, ground checking, low-sun-angle aerial photograph interpretation, and trenching, the fault is classified as a fault without recent displacement.

8) The Broxson Gulch thrust fault is aligned with the Talkeetna thrust fault at Denali and dips in the opposite direction (to the northwest). Because of this dip reversal, the Broxson Gulch has been judged to be unrelated to the Talkeetna thrust fault within the present seismotectonic environment.

9) Seismicity within the Talkeetna Terrain can be clearly delineated as crustal events occurring at depths to approximately 5 to 12 miles (8 to 20 km) and as Benioff zone events occurring at greater depths. The depth to the Benioff zone increases from approximately 25 miles (40 km) in the southeastern part of the site region to more than 50 miles (80 km) in the northwestern part of the microearthquake study area, and to more than 78 miles (125 km) in the northwestern site region.

10) The Benioff zone can be divided into two regions, the interplate region and the intraplate region. The former includes the area where the Pacific plate is passing beneath, and in contact with,

the North American plate. The largest earthquakes associated with the Benioff zone occur on or adjacent to the interface between the plates in this region. The intraplate region dips to the northwest and is decoupled from the North American plate. This region has smaller maximum earthquakes than the interplate region.

11) The largest reported historical earthquake within the Talkeetna Terrain is the magnitude (M_S) 7.3 event of 1943 which occurred along the western margin of the Terrain approximately 90 and 107 miles (144 and 171 km) west of the Devil Canyon and Watana sites, respectively. Several lineaments in the epicentral area may represent faults that could have been the source on which this earthquake occurred.

12) The largest crustal event recorded within the microearthquake study area during three months of monitoring in 1980 was magnitude (M_L) 2.8. It occurred 7 miles (11 km) northeast of the Watana site at a depth of 9 miles (15 km) on 2 July 1980.

13) No association of microearthquake activity with any of the 13 significant features is apparent.

14) The two reservoirs are considered to be one hydrologic entity. This combined Devil Canyon-Watana reservoir would be among the deepest and largest in the world. After comparing this reservoir to similar reservoirs, our interpretation suggests that the mean likelihood of a reservoir-induced earthquake within the hydrologic regime of the proposed reservoir is 0.46 (on a scale of 0 to 1) with a standard deviation of 0.22.

15) Since no faults with recent displacement were found within the hydrologic regime of the proposed reservoir, the likelihood of a RIS event of magnitude (M_S) ≥ 4 is considered to be low. However,

the detection limits for faults with recent displacement in this region suggest that there is some likelihood that an RIS event up to magnitude (M_S) 6 could occur. This is the magnitude of the detection level earthquake.

APPENDIX A - METHODS OF STUDY

This appendix describes the methods used for conducting the 1981 field studies, including Quaternary geology, age dating, field mapping, trenching, geophysical surveys, and low-sun-angle photography acquisition. It also describes the methods used for estimating the recurrence intervals of maximum credible earthquakes for faults with recent displacement. Methods used for the 1980 studies are summarized in Appendix A of the Interim Report (Woodward-Clyde Consultants, 1980b).

A.1 - Quaternary Geology

A.1.1 - Scope of Studies

This section presents the methodology, procedures, and measuring techniques used to perform the Quaternary geology tasks during the 1981 study (described in Section 3). Section A.1.2.1 describes the pre-field subtasks used to identify the type, areal distribution, and relative age of the Quaternary surfaces. These pre-field studies included: literature acquisition and review; photogeologic interpretation; data transfer to topographic base maps; and preparation of a preliminary map of Quaternary surfaces. Field studies used to supplement, refine, and support the interpretations derived from the pre-field studies are described in Section A.1.2.2. The field studies included: aerial reconnaissance mapping and excavation of test pits; collection of samples for radiocarbon dating; and collection of relative (weathering) age data. Section A.1.3 and A.2.1 discuss the field techniques used for radiocarbon and relative (weathering) age dating of the surficial deposits. Subsequent to the field studies, radiocarbon age dates were

obtained for 11 samples. These dates along with a synthesis of the field data were used to refine the map of Quaternary surfaces (Figure 3-2).

Detailed evidence from which the maximum lateral and vertical limits of four chronologically distinct glaciations were derived are presented in Section A.1.4. This evidence is discussed for each of six subregions into which the Quaternary study region was divided. These six subregions are shown in Figure A-1 and discussed in Section A.1.4.

A.1.2 - Methods

A.1.2.1 - Pre-Field Studies

Published and unpublished literature was reviewed to provide a regional perspective of the Quaternary glacial history of south central Alaska. Applicable information was documented and briefly summarized from both regional and site specific studies that would help in the identification of glacial deposits in the Quaternary study region and in understanding their distribution and age. The results of this review are discussed in Section 3.2. A copy of the literature and recorded summaries are included in the project file.

Detailed photogeologic interpretation was used as the primary method for evaluating the glacial chronology of the Quaternary study region. Emphasis was placed on this method because the glaciogenic features that can be of diagnostic value in deciphering the geographic and elevational limits of glaciations lend themselves to identification on stereographic aerial photographs. Three stereographic aerial photo sets, each providing different levels of detail or resolution, were used to map the glaciogenic

features. The three sets of aerial photographs were: 1) 1:120,000-scale high altitude color near-infrared; 2) U.S. Army Corps of Engineers 1:40,000-scale black and white; and 3) Acres 1:24,000-scale color. Although they were not available during the pre-field photo analysis, low-sun-angle 1:24,000-scale color near-infrared photographs were used during aerial reconnaissance, field mapping, and field verification of glacial surfaces. For each set of photographs, photogeologic mapping was done on registered mylar overlays. The different mappable units were color coded or represented by symbolization.

In order to ensure as much objectivity as possible in identifying features and assessing their elevations, interpretation of aerial photographs was completed for all photographic sets before any data were transferred to the topographic base maps. In addition, each flight line was interpreted independently; data from adjacent flight lines were compared only during the transfer of data to the topographic base. Evaluation and analysis of the data began only after all of the data was transferred to the topographic base. The detailed maps are not presented here, but they are filed in the project file.

The photogeologic data were transferred from the photographs to the U.S. Geological Survey topographic quadrangle maps (1:63,360 scale) using a Bausch and Lomb zoom transfer scope. The transfer of these data to the maps introduced limitations in the accuracy of locations and elevations. The sources of accuracy limitations were: radial distortion at the photograph margins; lack of distinguishing features for precise registration of photograph and map; large variation in topographic elevation over small horizontal distances; and the small inherent distortions introduced by the transfer scope. The elevations of features, on which the conclusions and results of this study are based, are accurate to $\pm$200 feet (61 m).

Evaluation and analysis of the data on the topographic base maps allowed for construction of a preliminary morphostratigraphic map showing the maximum extent of each major glacial episode. The morphostratigraphic units show the elevational limits of geographical extents of ice-marginal glaciogenic features having similar morphologic, stratigraphic, or geographic expressions or relationships. These relationships were interpreted to provide a preliminary definition of the relative ages of each glacial episode. Characteristics used to assign a relative age to similar glaciogenic features or deposits are summarized in Tables 3-1 and 3-3.

A.1.2.2 - Field Studies

The field studies were designed to supplement and refine the interpretations and conclusions derived from the analysis of aerial photographs. The studies involved helicopter-supported low-level aerial reconnaissance of morphostratigraphic unit contacts and visual verification of glaciomorphologic evidence used to delineate the morphostratigraphic units. Lithologic characteristics of surficial deposits in natural exposures were identified during the aerial reconnaissance. This identification was supplemented, where needed and possible, by ground checking. Exposures with more than one lithologic unit and of significance in stratigraphic interpretation were measured and described to help define the glacial chronology and history. Descriptions of the lithologic units included lithology, grain size, color, structure, texture, other distinguishing characteristics, and unit thickness. Apparent unit thickness was measured by tape and the slope angle was measured by Brunton compass. The true thickness of the unit was calculated from these data.

During detailed ground study of the exposures, material suitable for radiocarbon age dating was collected where possible. Relative age (weathering) dating (referred to here as relative age dating) studies were also conducted.

A.1.3 - Age Dating

A.1.3.1 - Radiocarbon Age Dating

To increase the confidence in the ages assigned to various units in the Quaternary study region, selected samples collected from surficial deposits were radiocarbon age dated. During the aerial reconnaissance mapping and stratigraphic studies, exposures were identified that had a high likelihood of containing dateable material, i.e., lacustrine, deltaic, or glaciofluvial deposits. From these exposures, 28 samples of carbonaceous wood and plant material were collected. Of these 28 samples, 11 (at the 11 locations shown in Figure 3-2) were submitted to the Geochron Laboratory of Cambridge, Massachusetts, to obtain radiocarbon age dates. The results of the dating are summarized in Table 3-2.

The samples were collected in accordance with the guidelines and theory described in Woodward-Clyde Consultants (1975). To prevent contamination, samples were collected without hand contact and were wrapped in aluminum foil. Samples were marked with a locality designation and sample number (e.g., S34-1, as shown in Table 3-2 and Figure 3-2). Samples were dried and then wrapped in new foil and placed in marked, self-sealing plastic bags.

A.1.3.2 - Relative Age Dating

The discontinuous nature of radiocarbon age dated glaciogenic units and limited geologic exposures precluded continuous tracing

of these units to ice-marginal end moraines. Dating of these end moraines is important for understanding the age and extent of glaciation and Quaternary surfaces because of the spatial limits that end moraines place on glacial episodes. Quantitative and qualitative relative age dating techniques were applied to lateral moraine sequences in four key areas in the Quaternary study region (Figures 3-2, 3-5, and 3-6). The relative age dating results from these moraines were then compared to those from moraines that were relatively and absolutely age dated in the Alaska Range by Ten Brink and Waythomas (in press) and Werner (in press).

Relative age dating techniques measure variations in morphologic and soil weathering characteristics in similar glaciogenic deposits through time. The basic premise in all the relative age dating techniques is that, with age, surface weathering and erosion processes will alter and modify both the form of the moraine and the till deposits within the moraine. The degree of alteration or modification is a function of age. Therefore, if other weathering parameters such as slope, drainage, or climate are similar for the various moraines, then differences in the physical characteristics between moraines can be used as an indicator of relative age.

Relative dating techniques and measurement procedures used in this study were generally similar to those used by Ten Brink and Waythomas (in press) in glacial geology studies of the Alaska Range. Some modifications were made in these techniques and procedures to provide the information in a manner consistent with the scope of this investigation.

These modified techniques of Ten Brink and Waythomas (in press) were used because of: the close proximity of the Quaternary study region to the Alaska Range; the applicability of the technique to the scope of this study; and the successful application of these

techniques in the Alaska Range (including the south flank of the Alaska Range). The following discussion summarizes: the procedures that were used for field measurements at each field location; criteria that were followed for data collection; and the modified techniques that were used.

Rock weathering characteristics were measured on coarse-grained granitic rocks at the surface and near surface, and soil weathering characteristics were measured in the near surface. At each field location, these characteristics were measured at intervals along the crest of lateral moraines for a distance of up to approximately 1,000 feet (312 m).

The following method was established for data collection: 1) procedures were standardized for each relative-dating technique; 2) techniques were quantified as much as possible to minimize operator-induced bias; 3) the sample size was selected to cover the range of small-scale inhomogeneity of the rock and soil; 4) each technique was performed by the same operator at all localities; and 5) compilation and comparison of data from separate areas was not undertaken until all the data were collected.

Morphologic characteristics of lateral and end moraines that were measured included: inner and outer slope angles; crest width; local relief; and post-depositional modification. Comparison of the results obtained from field locations during this study showed that none of these characteristics were diagnostic in differentiating age. Therefore, the data obtained on morphologic characteristics are not presented here, but they are kept in the project file.

Surface weathering characteristics that were measured included: 1) boulder frequency per 1,000 feet (312 m); 2) percent of boulder

surface roughened by weathering; 3) ratio of the number of weathered boulders to fresh boulders; 4) ratio of boulders with pits to boulders without pits; 5) relief of individual grains above the surrounding rock surface of boulders; 6) ease of removal of individual grains from the surface of boulders; 7) size (depth and diameter) of weathering pits on boulder surfaces; and 8) total relief of boulder surfaces caused by direct weathering. The results for all of the surface weathering techniques have a large amount of scatter and overlap in three of the four key areas (Figure A-1) where they were applied. At the fourth area, the Butte Lake area, moraines were differentiated by two of the techniques: the size of the weathering pits and the total boulder surface relief. These techniques indicate a marked increase in degree of weathering between moraines BL6 and BL7. This break corresponds to a similar weathering-age contrast indicated by the subsurface weathering data (Table A-1). Although the data are not included here, they are kept in the project file.

Two techniques for measuring subsurface rock and soil weathering characteristics--the granite weathering ratio and depth of oxidation--were consistently found to be of diagnostic value in differentiating age in all four of the key areas shown in Figures 3-2, 3-5, and and 3-6. The granite weathering ratio is the percentage of 50 boulders taken from the B horizon that, when hit with a hammer, have the characteristic of being fresh, partly weathered, or completely weathered (rotten). It is a measure of the degree and ease with which the boulder fractures. There is an increase of approximately 50 to 100 percent between the values obtained for Early moraines and those obtained for Late Wisconsin moraines (Table A-1). To collect these data, five subsurface test pits were excavated by a backhoe at intervals along a 1,000 foot (312 m) length of crest on each moraine. Pit depth ranged from 2 to 4 feet (0.6 to 1.2 m). The depth of oxidation is the thickness of

the weathered zone above the unaltered parent material. The weathered zone contains iron minerals that are oxidized and stained orange. This depth generally corresponds to a gradational or sharp color break in the soil profile. Depths were measured by tape. Table A-1 shows the range of depth of oxidation in the soil profile exposed in five pits on each moraine for which measurements were obtained.

A.1.4 - Interpretation of Six Subregions of the Quaternary Study Region

The glacial chronology of the Quaternary study region is complex. Unlike the systematic sequence of alpine glacial events on the north side of the Alaska Range (Wahrhaftig, 1958; Ten Brink and Ritter, 1980; Ten Brink and Waythomas, in press), repeated convergant and multi-directional glacial flow occurred throughout much of the Talkeetna Mountains. Glaciers from the south side of the Alaska Range pushed southward through the areas of Butte Lake, Deadman Creek, Brushkana Creek, and Watana Creek (Figure A-1) to merge and coalesce in an intermountain basin with glaciers flowing from ice centers in the higher elevations of the Talkeetna Mountains. The intermountain basin includes the Watana site and extends approximately 25 miles (40 km) to the southwest, 10 miles (16 km) to the northeast, 3 miles (5 km) to the northwest; and 8 miles (13 km) to the southeast from the site (Figure A-1). It includes the Susitna River area (near the Watana site), the Fog Lakes area, the Stephan Lake area, the lower reaches of the Watana Creek area, and the Deadman Creek area. The Susitna River bisects the basin from east to west.

The Quaternary study region was divided into six subregions (Figure A-1) according to similarities in the physiography and character of the glacial morphology within each subregion. The six

subregions have been designated as: 1) Clear Valley-Fog Lakes; 2) Chunilna Plateau; 3) Portage Creek-Devils Canyon; 4) Tsusena Creek-Deadman Creek; 5) Butte Lake-Brushkana Creek; and 6) Kosina Creek-Black River. The four key areas discussed in Section 3.4 each lie within one of these subregions (Figure A-1).

The elevation, nature, and geographic extent of the glacial features in the six subregions (including the four key areas) form the basis for the delineation of Quaternary surfaces shown in Figure 3-2. Within each subregion, the major glacial features were identified. However, the scope of the study precluded identification and mapping of many small glaciogenic features that could alter or improve knowledge of the glacial geology.

Glacial episodes recognized in the subregions were assigned to the following ages: pre-Wisconsin, Early Wisconsin, Late Wisconsin, and Holocene. Assignment was made on the basis of relative and radiocarbon age determinations, similarities in geographic and elevational extent, comparison with similar chronologic sequences in adjacent areas of southcentral Alaska, and professional judgment. The following discussion describes the pre-Wisconsin, Early Wisconsin, and Late Wisconsin glacial activity and surfaces encountered in the Quaternary study region. Glacial activity and surfaces of Holocene age are discussed only in a cursory manner because the activity is generally restricted to higher intermountain valleys and cirque areas. The limited lacustrine and fluvial (deposits) occur in the intermountain basin. Because of their limited extent, these deposits, which are associated with Holocene glaciation, were not considered a significant part of the seismic geology evaluation.

A.1.4.1 - Clear Valley-Fog Lakes Subregion

This subregion includes the southern portion of the intermountain basin from the Susitna River on the north, southward to the Talkeetna River area (Figure A-1). The Clear Valley area, described in Section 3.4.2, lies in this subregion (Figures A-1, 3-6B).

Much of the subregion is mantled by fluted ground moraine deposits of inferred Late Wisconsin age. These deposits locally overlie highly oxidized glaciofluvial outwash deposits and angular colluvial deposits that were radiocarbon age dated at greater than 27,000 y.b.p. (Sample S34-1 shown in Table 3-2 and Figure 3-2). Oxidization of the outwash probably represents a major unconformity during an interglacial period prior to the Late Wisconsin glaciation.

Grooving on local bedrock nobs indicates that glaciers flowed to the southwest and west. These glaciers were probably piedmont glaciers that flowed through the intermountain basin in Early and Late Wisconsin time.

Data from the Clear Valley area (Section 3.4.2) were interpreted to show that the elevational limit of Early Wisconsin ice was at 3,100 to 3,300 feet (945 to 1,006 m) and the elevation limit of Late Wisconsin ice was at 2,500 to 2,700 feet (762 to 823 m). The upper elevational limit for Early Wisconsin ice appears to decrease from 3,100 to 3,300 feet (945 to 1,006 m) at Clear Valley to 2,900 to 3,100 feet (884 to 945 m) near the junction of the Talkeetna River and Prairie Creek southwest of the Clear Valley area. The evidence on which this conclusion is based includes trimlines, side glacial channels, and end moraines. The elevational decrease in the upper limit suggests that the ice surface for the Early Wisconsin piedmont glacier, which flowed through the intermountain

basin, sloped approximately 13 to 14 ft/mile (2.5 to 2.7 m/km) to the southwest. The maximum elevation of Early Wisconsin glacial features establishes that this glaciation was more extensive than the Late Wisconsin glaciation.

The elevational limit of Late Wisconsin ice in the subregion is indicated by prominent trimlines and morphologic contrasts between 2,500 and 2,700 feet (762 and 823 m) throughout the subregion. Ice marginal lacustrine deposits that have not been overriden by glacial ice are present at an elevation of 2,600 feet (793 m). The maximum elevation of Late Wisconsin ice at this locality is, therefore, limited to an altitude of 2,600 feet (793 m) or less.

Numerous ice-marginal features suggest that the piedmont glacier continued to decrease in size throughout successive stades of the Late Wisconsin glaciation in response to fluctuations in size of individual valley glaciers that coalesced with the piedmont glacier. Stephan Lake is presently dammed by a small moraine representing the last stages of the Late Wisconsin piedmont glacier as it retreated northward. The configuration and extents of individual moraines that are estimated to be of the last stade (Stade IV) of the Late Wisconsin stage, such as those in the Clear Valley area, indicate that the valley glaciers did not coalesce but were confined to individual valleys during the last stade of the Late Wisconsin glaciation. Extensive ice-disintegration deposits in the upper reaches of valley bottoms indicate rapid deglaciation at the end of the Late Wisconsin.

A.1.4.2 - Chunilna Plateau Subregion

This subregion is predominantly a glaciated bedrock plateau above 3,000 feet (915 m) elevation located south of the Susitna River and extending from the intermountain basin of the Clear Valley-Fog Lake

subregion westward to the Gold Creek area on the Susitna River (Figure A-1). Glacial grooving and other landform features produced by ice scour are common. These ice-scoured features suggest that ice flow was primarily to the west and southwest. Major drainages in plateau margins have sharp V-shaped valleys deeply incised into bedrock. This morphology suggests that a fluvial environment has existed without interruption since the glacial ice, which scoured the features, retreated from the subregion.

Prominant trimlines, grooving orientation contrasts, surface morphology differences, and side glacial channels on the margin of the plateau all suggest an upper elevational limit to the Early Wisconsin glaciation of 3,000 to 3,200 feet (915 to 976 m). The Late Wisconsin ice limit is not expressed on the plateau but is defined by ice-marginal features at lower elevations in adjacent subregions.

Scoured glacial features above 3,200 feet (976 m) indicate that the plateau was overridden in an earlier glaciation. The age of the earlier glaciation was not dated during this study but is estimated to be pre-Wisconsin. This old glacial surface was overridden by a younger glacial event in the Chunilna and Disappointment Creek areas. Valley profiles are U-shaped and floored by glaciofluvial sediments in the lower reaches. Grooving is oriented parallel to the valley, rather than obliquely, as it is higher on the older surfaces. The regional snowline as determined for the Wisconsinian shown by Pewé (1975) would suggest that the plateau elevations may have been just high enough for small valley glaciers to develop during the Early Wisconsin stage and possibly the first stade of the Late Wisconsin stage.

A.1.4.3 - Portage Creek-Devils Canyon Subregion

This subregion is a topographical continuation of the Chunilna Plateau subregion. The east-west trending Susitna River valley separates the two subregions. The plateau north of the river rises to merge with a major mountainous area in the northwestern Talkeetna Mountains (Figures A-1 and 3-2). This mountainous area was a major area of ice accumulation. Drainage from the mountains is controlled by the regional northeast-southwest trending structural grain. The plateau is dissected by these southwest-trending glaciated tributary valleys that drain to the Susitna River. These drainages contrast with those of the Chunilna Plateau that have all been cut by fluvial processes.

The elevational limit of pre-Wisconsin ice in this subregion appears to be approximately 4,000 feet (1,219 m). Grooved and beveled bedrock occurs up to at least 4,000 feet (1,219 m), suggesting that the plateau was almost completely overridden by ice during a pre-Wisconsin glacial episode. Later, less extensive, glaciations left substantially larger areas of bedrock (at lower elevations) above the glacier ice.

Markedly different surface weathering, trimlines, and the presence of end moraines between 3,000 and 3,300 feet (915 and 1,006 m) indicate that this elevation is the upper limit of Early Wisconsin ice. Relative age dating results suggest that Early Wisconsin ice formed prominent but very weathered-looking moraines at 3,000 to 3,200 feet (915 to 976 m) on the west side of the mountain ridge separating the Susitna River and Chulitna River valleys. The oxidation depth of 21 inches (53 cm) on the moraines is within the range of pre-Late Wisconsin data obtained in the Alaska Range and elsewhere in the Talkeetna Mountains (Table A-1).

The limits of Late Wisconsin ice are better defined than those of earlier glaciations. Along the southern portion of the Susitna River valley from Sherman Creek to Indian River (Figure 3-2), pronounced grooving orientation contrasts, deflected drainages, prominent trimlines, and kame terraces mark a sharp upper limit to the Late Wisconsin glaciation at an elevation of 2,100 feet (640 m). To the east through Devils Canyon, the upper limit rises slowly in elevation. It lies between 2,100 and 2,200 feet (640 and 671 m) at Portage Creek, as indicated by slope breaks, fluting truncations on older surfaces, surface weathering contrasts, trimlines, and end moraines. Topographic contrasts and side-glacial channels indicate an increase to 2,200 to 2,400 feet (671 to 732 m) in the High Lake area; in the Devil Creek area, trimelines, side-glacial channels, and surface weathering contrasts suggest an increase to 2,400 to 2,600 feet (732 to 793 m).

The maximum Late Wisconsin limit at Devil Creek of 2,600 feet (793 m) is similar to that found in the adjacent Clear Valley-Fog Lakes subregion (Section A.1.4.1). This suggests that the piedmont ice mass from the intermountain basin advanced through the topographic constriction at the western bend of the Susitna River (near Devil Creek) into Devils Canyon and merged with local valley glaciers from the northeast. Ice marginal features suggest that the ice was of sufficient extent for the piedmont and valley glaciers to coalesce and override the Devils Canyon area only during the first and possibly second stades of the Late Wisconsin stage.

The piedmont glacier and valley glaciers did not merge during later stades of the Late Wisconsin stage. In Portage Creek, the extent of subtle, heavily vegetated moraines and corresponding drainage profile changes indicate that the southwestern limits of glacial ice during Stade III and IV of the Late Wisconsin were

4 and 6 miles (6 and 10 km), respectively, upstream from the confluence of Portage Creek with the Susitna River. The valley profile of Devil Creek indicates that the extent of Late Wisconsin glacial stades in that creek was similar to the extent of stades in Portage Creek.

The age of the Susitna River canyon, which cuts across the Quaternary study region, is difficult to estimate. Extensive river terraces located in the Indian River area indicate that the Susitna River and associated tributaries served as major outlets for glacial meltwater and copious amounts of glacially derived sediments carried by the meltwater. The Susitna River at Devils Canyon and many adjacent tributary canyons are bedrock gorges that are 500 to 600 feet (152 to 183 m) deep in some places. They do not exhibit glacial modification in some areas that were clearly overridden by Early Wisconsin and early Late Wisconsin ice (e.g., the lower Portage Creek area). This suggests that the Devils Canyon is younger than Stade II of the Late Wisconsin stage (15,000 y.b.p). However, glaciofluvial outwash deposits located near river level approximately 1.2 miles (2 km) south of Fog Creek along the Susitna River were radiocarbon age dated by Terrestrial Environmental Specialists (1981) at 37,000 y.b.p. The location of these deposits suggests that the river canyon is at least 30,700 years old (i.e., the outwash sediments were deposited after the canyon was cut).

The apparent discrepancy in canyon age may be caused by deposition of older organic material from another (upstream) source into the outwash deposits. These outwash deposits are in the area that morphologically appears to have been glaciated until near the end of the Late Wisconsin stage (Figure 3-2). Thus, older organic material could have been reworked at this time.

Elsewhere along the Susitna River valley, hanging tributary drainages suggest rapid down-cutting by the Susitna River after retreat of the Late Wisconsin Stade II ice, 15,000 y.b.p. Alternatively, Devils Canyon and other bedrock canyons along tributary drainages could have been repeatedly filled and flushed during glacial advances and retreats and, therefore, not greatly modified by ice erosion. Following the second stade, individual valley glaciers were confined between valley walls, and the piedmont ice mass in the Stephan Lake area trough may have retreated north of the Susitna River. Retreat and deglaciation near the end of the Late Wisconsin stage would have produced large quantities of sediment-loaded meltwater. Isotatic readjustments during deglaciation and minor regional tectonic uplift may also have assisted down-cutting by effectively lowering the base level. River terraces adjacent to the Susitna River floodplain indicate that at least 50 to 100 feet (15 to 30 m) of down-cutting occurred during Holocene time.

A.1.4.4 - Tsusena Creek-Deadman Creek Subregion

This subregion forms the northern half of the intermountain basin which is divided by the westward-flowing Susitna River (Figure A-1). The Deadman Creek area, described in Section 3.4.4, lies in this subregion (Figures A-1, 3-6B).

The elevation of the basin floor rises gradually to the north and merges with major drainages and valleys that carried ice from the Alaska Range in the Butte Lake-Brushkana Creek subregion. Ice from the Alaska Range and the Talkeetna Mountains coalesced in the basin. The extent to which the glaciers coalesced during each glacial episode was different and was a function of the magnitude of each glacial episode and the restrictions to glacial flow caused by local topographic relief.

Surficial glaciogenic units in this subregion are predominantly hummocky ice-disintegration deposits and extensive lacustrine deposits which contrast sharply with the surface morphology of the south side of the Susitna River in the Stephan Lake-Fog Lakes subregion (Figure A-1). Fluted ground moraine or beveled bedrock outcrops are also present in the Tsusena Creek-Deadman Creek subregion.

The geomorphology of the subregion and relative and radiocarbon age dates from the deposits indicate that the sediments mantling the subregion are Late Wisconsin in age. The generalized cross-section (Figure 3-3) shows the stratigraphic relationships that were interpreted from numerous measured exposures. Highly oxidized outwash deposits overlie lacustrine deposits that are older than 37,000 y.b.p. (Sample S29-1, Table 3-2). The oxidized outwash deposits are overlain by till which in turn is overlain by ice-disintegration deposits. In the northern part of Watana Creek valley, the till (which stratigraphically correlates with the till described above) is overlain by younger lacustrine deposits and by glaciofluvial, deltaic, and ice disintegration deposits. These latter deposits are in turn overlain by lacustrine deposits that have a radiocarbon age date of 9,395 $\pm$200 y.b.p. (Sample S42-1, Table 3-2). These younger sediments (shown in measured Sections C, E, F, and G in Figure 3-3) date the last retreat of ice from the basin and are interpreted to represent a sequence of northward shrinking, retreating, and stagnating glacial ice that was debouching large amounts of meltwater and sediments toward the south.

Interpretation of relative age data for closely spaced lateral moraines west of Deadman Creek (Figure 3-6B) indicates that the elevational limit of Early Wisconsin ice was at least 4,200 feet (1,280 m) and that the limit of Late Wisconsin ice was 3,900 feet (1,189 m).

Local valley glaciers merged with glaciers from the Alaska Range that advanced southward down Deadman, Watana, Brushkana, and Butte Creeks during Early Wisconsin time and probably during early Late Wisconsin time. The glaciers merged to produce a piedmont glacier that filled the intermountain basin. During later stades of the Late Wisconsin stage, Alaska Range glaciers were of insufficient thickness to advance southward through the relatively high passes at Deadman Creek, Brushkana Creek, and Butte Lake, but still advanced southwestward through the northwest end of the Watana Creek valley as discussed in Section A.1.4.5. Northward-sloping slopes of morainal crests DC-1 and DC-2 at Deadman Creek and a concave southward arcuate terminal moraine (Figure 3-6B) at Big Lake suggest that local valley glaciers from Tsusena Creek flowed northward during later stades of the Late Wisconsin stage to fill areas that were left free of ice by the limited southward advance of Alaska Range glaciers.

The piedmont ice mass appears to have retreated north of the Susitna River by the last stades of the Late Wisconsin stage. Fluted ground moraine on the south side of the Susitna River contrasts with extensive younger lacustrine and ice-disintegration deposits on the north side. This contrast indicates ice was present north of the river and absent to the south during this time. The lower reaches of Watana Creek were dammed by ice during the later stades of the Late Wisconsin stage, and extensive lacustrine sediments were deposited in the Watana Creek area. Ice stagnation and ablation during the last stades of the Late Wisconsin stage caused large areas to be mantled with ice disintegration deposits, particularly in topographic low areas.

Near the end of the Late Wisconsin stage, the Tsusena Creek-Clark Creek valley glaciers extended southward into the Susitna River

valley south of the mouth of Tsusena Creek and modified the valley profile. Retreat and deglaciation produced hummocky ice-disintegration deposits north of Watana Camp near the Watana site. Ice-disintegration deposits in lower Deadman Creek formed a low dam that lasted well into the Holocene Epoch. The radiometric age of the lacustrine sediments is 3,450 ±170 y.b.p. (Sample S45-1, Table 3-2). This date suggests that the lake existed at least until this time, after which the stream profile was re-established by down-cutting through the ice disintegration deposits.

A.1.4.5 - Butte Lake - Brushkana Creek Subregion

This subregion includes the northern ends of the major valleys that drain southward and merge with the intermountain basin described in the Clear Valley-Fog Lakes and Tsusena Creek-Deadman Creek subregions (Section A.1.4.1 and A.1.4.4, respectively). The Butte Lake area, described in Section 3.4.3, lies in this subregion (Figures A-1, 3-6A).

Broad U-shaped valleys opening to the north and rounded topography are characteristic of this subregion. This topography was caused by extensive glacial scour and overridding by glaciers from the Alaska Range. Drainage patterns and directions have been altered by glacial erosion and deposition. Valley bottoms are predominantly mantled by till, and upper valley walls are extensively mantled by frost-shattered boulder fields and a type of patterned ground called nonsorted stripes. The boulder fields and nonsorted stripes formed in an ice-free periglacial environment. Their lower limit marks the upper limit of younger ice.

Numerous moraines in the Butte Lake area (Figures 3-2 and 3-6A) are interpreted to represent repeated southward glacial advances by Alaska Range glaciers. On the basis of morphologic contrasts and

relative age data (Table A-1), moraines at elevation 4,100 feet (1,250 m) and above are considered to be probably Early Wisconsin in age. The maximum elevation of Early Wisconsin ice may be marked by prominent trimlines at elevation 4,200 to 4,300 feet (1,280 to 1,311 m) that correspond to the lower limit of the extensive frost-shattered boulder fields. The surface morphology above elevation 4,300 feet (1,311 m) includes rounded topography, erosional features suggestive of glacial scour, and glacial erratics. This surface morphology indicates a pre-Wisconsin glaciation above elevation 4,300 feet (1,311 m).

The configuration and elevation of the moraines in the Butte Lake area suggest that only ice of the Early Wisconsin stage and Stade 1 of the Late Wisconsin stage was thick enough to advance southwestward through the passes of Brushkana Creek (at elevation 3,250 feet [991 m]) and Deadman Creek (at elevation 3,350 feet [1,021 m]) to merge in the intermountain basin with valley glaciers from the Talkeetna Mountains. Ice thickness during later stades was insufficient to allow ice to flow through the passes.

Elevations of the Late Wisconsin end moraines suggest that as many as nine individual end moraines of Late Wisconsin age are present in the Butte Lake area. The moraines have been tentatively grouped into four distinct Late Wisconsin stades according to clustering of end moraines, breaks in slope, kettle-frequency contrast, and surface-morphology contrasts (Figure 3-6A). These stades and their maximum elevation are: Stade 1, 3,900 feet (1,189 m); Stade 2, 3,600 to 3,800 feet (1,098 to 1,159 m); Stade 3, 3,200 to 3,300 feet (976 to 1,006 m); Stade 4, 3,000 to 3,100 feet (915 to 945 m).

Most evidence at the Butte Lake-Brushkana Creek subregion supports a maximum elevation of 3,800 to 3,900 feet (1,159 to 1,189 m) for Late Wisconsin ice. Prominent trimlines at 3,800 to 3,900 feet

(1,159 to 1,189 m) at Butte Lake are consistent in elevation with the upper limit of Late Wisconsin moraines in lower Deadman Creek (Section A.1.4.4). Some apparently contradictory evidence was found in Brushkana Creek where surficial lacustrine/deltaic deposits at elevation 3,000 feet (915 m) are older than 37,000 y.b.p. (Sample S12-2, Table 3-2). The age of the sediments suggest that they were deposited before Late Wisconsin time. Because the deposits have not been overridden, the maximum elevation of Early Wisconsin ice would have been at 3,000 feet (915 m) or less rather than 3,900 feet (1,189 m). Instead, the deposits are probably from the late stade of the Late Wisconsin substage deposited as Alaska Range glaciers retreated northward. The organic material may have been reworked from an older deposit into a Late Wisconsin ice marginal lake.

In contrast to Brushkana and Deadman Valleys, where the passes are higher than elevation 3,250 feet (991 m), the upper Watana Creek valley drainage divide is at elevation 2,850 feet (869 m). The lower elevation of this divide allowed Late Wisconsin ice of Stades II, III, and IV to advance through the Watana Creek valley into the intermountain basin where it coalesced with ice from local Talkeetna Mountain sources. This was the only route in the subregion along which glacial ice from the Alaska Range was able to advance into the intermountain basin following Stade I of the Late Wisconsin stage. Lacustrine deposits dated at 9,395 $\pm$200 y.b.p. (Sample S42-1, Table 3-2) just south of ice disintegration deposits in the northeast part of the Watana Creek valley (Figure 3-2) date the last retreat of Alaska Range ice from the Watana Creek valley area. During retreat northward, meltwater and sediment formed extensive deltaic, outwash, and lacustrine sediments in lower Watana Creek.

A.1.4.6 - Kosina Creek - Black River Subregion

This broad undulating bedrock platform south of the Susitna River in the eastern Talkeetna Mountains merges indistinguishably with the adjacent Copper River basin to the east. Three morphologically distinctive, glacially scoured topographic surfaces have been beveled into the platform by succeedingly less extensive glaciations (Figure 3-2). The Black River area, as described in Section 3.4.1, lies in this subregion (Figures A-1 and 3-5A).

An extensive glaciation of suggested Early Wisconsin age spread out over the platform. Side glacial channels, moraines, and discordant topography suggest an upper limit to this glaciation between 3,550 to 3,750 feet (1,082 to 1,143 m). A more extensive pre-Wisconsin glaciation above 3,750 feet (1,143 m) is indicated by rounded topography, glacial debris, and erosional features.

The distinction between Early and Late Wisconsin glaciations has been made on the basis of morphology and elevation of moraines, by relative age data from the Black River moraines (Tables A-1 and 3-3), and on the basis of valley morphology. The youngest or Late Wisconsin glaciation deeply incised and modified preexisting valleys and deposited four Late Wisconsin end moraines in the upper valleys of Tsisi Creek, Kosina Creek, and Black River. The maximum northward extent of the Late Wisconsin ice in the Black River area is identified by the arcuate termination of the uppermost lateral moraine (BR-3 on Table A-1), approximately 6 to 7 miles (10 to 11 km) south of the Susitna River. Downstream from the front of the maximum ice extent, the head of a sharp V-shaped fluvial-cut canyon also suggests the northernmost advance of ice in Black River. Similar morphology and configuration of end moraines in the Tsisi and Kosina Creek area suggest a similar order of magnitude for the extent of Late Wisconsin glacial events in this subregion.

Near the confluence of the Oshetna and Black Rivers (Figure A-1), conflicting radiocarbon age dates were collected during this study and by Terrestrial Environmental Specialists (1981). These differing dates have led to contrasting interpretations of the glacial history in this subregion. Within the exposure at this location, till interfingers with highly deformed lacustrine sediments. A wood sample (S47-4) obtained from the lacustrine deposits during this study provided a radiocarbon age date of >37,000 y.b.p. (Table 3-2). The relationship of the till to the lacustrine deposits and the radiocarbon age date suggest that the till is Early Wisconsin in age. In addition to these data, the extent of moraines and the relative age dating studies of these moraines in the Black River valley suggest that Late Wisconsin ice did not advance into the Susitna River west of the Copper River basin in the subregion (Figure 3-2).

Terrestrial Environmental Specialists (1981) obtained a radiocarbon age date for the same till unit, but somewhat higher in the stratigraphic section than the sample described above. This date was 24,900 $\pm$3,125 y.b.p. Terrestrial Environmental Specialists (1981) interpreted the sediments to be recessional ice-contact drift that was deposited by Late Wisconsin glacial ice.

This difference in the age of glacial surfaces in the eastern Talkeetna Mountains does not affect the interpreted age and extent of glacial surfaces in the vicinity of the Project sites. It does, however, point out the difficulty in interpreting the age and extent of glacial deposits where glaciers from different sources and different ages converge.

A.2 - Radiometric Age Dating

A.2.1 - Radiocarbon Age Dating

Radiocarbon age dates were obtained from 11 samples collected in the Quaternary study region (Figure 3-2). The dates measured by Geochron Laboratory are presented in Table 3-2. The procedures used to collect, store, and transport the samples are described in Section A.1.3.1. These procedures were in accordance with those described in Woodward-Clyde Consultants (1975).

A.2.2 - Potassium-Argon Age Dating

Whole rock potassium-argon age dates were obtained for three samples of andesite collected in the vicinity of the Talkeetna thrust fault. The purpose of obtaining the dates was to limit the area in which the fault is present upriver from the Watana site.

The locations from which the samples were collected are shown in Figure A-1. The procedures used to collect the samples were in accordance with those described in Woodward-Clyde Consultants (1975).

Analyses of the samples were conducted by Dr. Kenneth A. Foland at the Potassium-Argon Laboratory at Ohio State University. In addition to the whole rock age dates, thin sections were prepared of the samples, and petrographic descriptions of the thin sections were made. The results of the age dating are summarized in Table A-2. The procedures used to conduct the age dating and the thin section analysis are discussed in the following paragraphs.

A.2.2.1 - Sample Preparation

Samples for whole-rock dates were prepared from the hand-samples provided. Each sample was first trimmed of weathered rind using a rock saw with water as a cutting fluid. After drying, the trimmed sample was crushed with a jaw crusher and then was ground with a disc grinder. The ground rock was separated into size fractions by sieving with nested sieves on a Ro-Tap shaker. The size fraction falling between #40 and #60 U.S. standard sieve sizes was used for analyses. Prior to analysis, the #40 and #60 fraction was washed with water to remove adhering dust and with dilute hydrochloric acid (HCl) to remove undesirable carbonates. The procedure was: 10% HCl wash; reagent acetone wash; reagent ethanol wash; and, triplicate wash with doubly-distilled water. Each sample was then dried in an oven at 80°C.

A.2.2.2 - Argon Analysis

The concentrations of argon were determined by isotope dilution. The sample was fused by induction heating in a molybdenum crucible in a high vacuum system at pressures less than 5×10^{-7} torr. An ^{38}Ar tracer was added from a reservoir-gas pipette metering system. Argon was purified using hot CuO and Ti gettering. The purified argon was isotopically analyzed using a 6-inch gas mass spectrometer, Nuclide Corp. model SGA-6-60, operated in the static mode on line with a Hewlett Packard minicomputer.

A.2.2.3 - Potassium Analysis

Potassium concentrations were analyzed by flame photometry using an Instrument Laboratory Model 443 Flame Photometer with a lithium internal standard. Rock samples were fused as 850°C with lithium metaborate which serves as a flux and internal standard. The fused

samples were then dissolved in a 4% HNO_3 solution. The resulting solutions were then diluted and analyzed for potassium on the flame photometer which was calibrated with gravimetric standards.

A.2.2.4 - Age Calculation and Uncertainties

The averages of repetitive analyses were used to calculate K-Ar whole-rock dates using the following constants:

$$^{40}K = 1.167 \times 10^{-2} \text{ atom \% of K}$$
$$\lambda e = 0.581 \times 10^{-10} \text{ y}^{-1}$$
$$\lambda B = 4.962 \times 10^{-10} \text{ y}^{-1}$$
$$\lambda_{total} = 5.543 \times 10^{-10} \text{ y}^{-1}$$
$$(^{40}Ar/^{36}Ar) \text{ in air} = 295.5$$

The quoted age uncertainties reflect only analytical uncertainties and make no provision for those in the accepted and recommended above constants. Also, the quoted uncertainties do not reflect any "geological error," such as failure of the rock systems to behave as ideal systems. The K and Ar calibrations were checked by analyzing interlaboratory mineral standards.

A.2.2.5 - Petrographic Analyses

Thin sections were prepared for each sample along the marked orientation (if indicated). Two sections were prepared for each sample to ensure a representative petrographic description. The sections were studied with standard petrographic microscopes. Microphotographs were taken of the thin sections.

A.3 - Field Mapping

Geologic data were collected by aerial reconnaissance from helicopters and fixed-wing aircraft, interpretation of aerial photographs, and study of approximately 300 locations on the ground. Photographs were taken during these activities to document the aerial appearance of features.

The observed geomorphology, lithology, and geologic structure were described using methods described in geologic field texts such as Compton (1962). The orientation of features were measured with Brunton compasses. Samples were collected for later reference and comparison of rock types at different locations.

Ground locations were assigned outcrop location designations based on the first letter of the name of the geologist making the observation and on the consecutive number of the observations. For example, outcrop locations studied by Phillip Birkhahn have designations such as B-32, B-33, etc. Closely spaced observations were given the designation B-32A, B-32B, etc., as needed. Samples were labeled with the outcrop location designation and a number (for example, B-32-1, B-32-2, etc.).

Photography was done with 35 mm single-lens reflex, 35 mm rangefinder, and color and black-and-white Polaroid cameras. The rolls for the 1981 study were numbered consecutively beginning with S-200. The types of film used were: Kodachrome 64, Ektachrome 200, Plus-x pan, Polaroid Type 108, and Ektachrome near-infrared.

The geologic data collected were recorded in field books (J.L. Carling Corporation Field Book No. 350). The field locations of these data were plotted on U.S. Geological Survey maps at a scale of 1:63,380 and 1:24,000 on aerial photographs. Aerial photograph interpretations were marked on clear mylar overlays. Where appropriate, geologic maps were produced of selected areas using the data obtained.

The geologic data and photographs were also recorded on the following forms: Remote sensing lineament worksheet (SHP-4), Fault and lineament data summary sheet (SHP-3), Field observation documentation sheet (SHP-6), Photo log (SHP-7), Fault and lineament photo log (SHP-8), and Fault and lineament index sheet (SHP-5). The use of these forms is described in Appendix A of the Interim Report (Woodward-Clyde Consultants, 1980b), and copies of the forms are provided.

The data are on file in Woodward-Clyde Consultants office at Santa Ana, California, as follows: field locations and outcrops described in field notebooks; maps of the field locations plotted on a single set of 1:63,380-scale maps; photographs, slides, and negatives; field maps; and air-photo overlays.

A.4 - Trench Logging Methods

Trench logging and photography were conducted by Woodward-Clyde Consultants in three trenches excavated within 26 miles (41 km) of either site. Two of the trenches, Treches T-1 and T-2, were excavated across or near the Talkeetna thrust fault (Figures 4-11 and 4-7, respectively). One trench was excavated near the Susitna feature (Figure 4-17). The purpose of the logging and photograpy of these two trenches was to document the presence or absence of faults with recent displacement.

The trench logs which document the evidence of no fault displacement in the trenches are presented as Figures 4-12 and 4-18. Selected photographs of the trenches are presented as Figures 4-13, 4-14, and 4-19.

Interpretation of the stratigrahic relationships shown in the trench logs is presented in Section 4. The original trench logs and photographs of the trenches are in the Project file at Woodward-Clyde Consultants, Santa Ana, California.

The three trenches were excavated by R & M Consultants of Anchorage, Alaska. A track mounted John Deer 350 backhoe with a 0.07 cubic yard (0.05 m^3) bucket was then used to excavate the trench; subsequent to excavation, the trenches were shored using hydraulic aluminum shoring.

Also subsequent to excavation, one of the trench walls was selected for logging; the southwest wall was selected primarily because of lighting restrictions imposed by the spoils pile on the northeast wall. Horizontal and vertical control lines were then established. The horizontal control line (level line) was established using three strand nylon string and a K&E hand level or Stanley string level. After nailing the level line to the trench wall, horizontal distances were measured using 100-foot Keson plastic coated cloth tapes. The stationing system was established and recorded in feet southeast or northwest of the point where trench logging commenced. Vertical distances relative to the level line were measured using a standard six-foot wood carpenter's rule.

Following placement of the level line, the trench wall was cleared using a variety of techniques. A mason's hammer or a pick-axe was used to remove smear and slough material. A stiff-bristled brush or paint brush was used to clean and enhance stratigraphic relationships in sand and gravel deposits. In some instances the trench wall could not be prepared adequately for logging due to deep water and trench wall failures. These parts of the trenches were well away from the scarps and thus do not affect the conclusions regarding scarp origin.

After the trench wall was prepared for logging, stratigraphic relationships were documented by recording the relationships on trench logs and photographing the trench walls. Selected stratigrpahic units were logged to document the absence of fault displacement in the trench and to document stratigraphic relationships encountered in the trench.

Trench logging procedures and results were reviewed upon completion of the trench logging by Woodward-Clyde Consultants' project review team. Representatives of Acres and the Alaska Power Authority also examined the trenches.

In order to effectively log and display observed stratigraphic relationships, trench logs were drawn at a scale of 1 inch equal to five feet vertically and horizontally. Previous experience in logging trenches has demonstrated that this scale best portrays the observed stratigraphic relationships and adequately displays potentially significant features. For publication in this report, the trench logs were reduced to a scale of one inch equal to approximately ten feet vertically and horizontally (Figures 4-12 and 4-18).

The stratigraphic relationships were documented photographically with 35 millimeter SLR cameras equipped both with 35 millimeter 1.4 lenses and haze filters and with 50 millimeter 1.8 lenses and haze filters. Ektachrome film (ASA rating of 200) was used for color photography and Tri-X Panchromatic film (ASA rating of 400) was used for black-and-white photography.

An electronic flash was often used as a fill-in to illuminate the trench walls while photographing the exposed stratigrahic units. Photographs were taken at various spacings depending on trench width. After some experimentation, six-foot centers were selected to provide adequate photographic coverage without sacrificing necessary detail. This spacing also permitted relatively rapid photographic documentation of the trench wall. Locally, where the trench walls were narrow, or where the trench was deepened to expose significant features, photographs were taken on smaller centers. Generally, three-foot centers provided adequate coverage in these areas.

A.5 - Geophysical Studies

Geophysical studies in support of the geological portion of the investigation were undertaken during the summer field season of 1981. The objectives of these studies were to locate and delineate the subsurface trace of the Talkeetna thrust fault and possible sources of the Susitna feature and Feature KD5-3 (discussed in Section 4.4). Geophysical lines were conducted in areas believed to have faults or possible faults in order to confirm their extent, direction, and sense of movement. The techniques selected for use were seismic refraction and magnetic surveys. The scope of work consisted of the following tasks:

a) An evaluation of potential geophysical line sites to determine which method or methods would be most effective at each site.

b) A survey of the sites using the selected technique(s).

c) Interpretation and evaluation of the data to locate the desired faults and features.

A.5.1 - Field Operations

Thirteen geophysical profiles were obtained in the project region. The following sections cover the methods and equipment used.

A.5.1.1 - Seismic Refraction Measurements

Seismic refraction measurements were obtained on one line across the buried trace of the Talkeetna thrust fault near Fog Creek using a GeoMetrics model ES-1210F twelve-channel signal enhancement seismograph. The signal enhancement feature allows the signal-to-noise ratio of a low-energy source to be improved by adding

together 5 to 15 source inputs whose waveforms are consistent and therefore add, while noise being random tends to cancel out.

The source used for this survey consisted of 1 to 6 pound charges of ANFO. Triggering was obtained directly from the blaster. The seismic refraction lines were recorded using a 100 foot (30 m) geophone spacing except for the outside geophones which were moved inward 50 feet (15 m). The source locations were 50 feet (15 m) off each end of the line and midway in the line. Terrain constraints often caused some minor variations from the line of the survey and the geophone spacing.

Geophone and source locations were cleared of vegetation and soft surface material. Geophones were firmly planted away from disturbing influences such as tree roots, moving water, and wind disturbance.

A.5.1.2 - Magnetometer Measurements

The magnetometer readings were obtained along 12 profiles across the Talkeetna thrust fault, the Susitna feature, and Feature KD5-3 with a GeoMetrics Model G-816 portable proton magnetometer. This instrument measures the total magnetic field of the earth with an accuracy of 1 gamma under optimum conditions.

A base station was established at an accessible and magnetically stable point near each profile. Repeated readings were made at the base station in order to establish the diurnal variation in the earth's magnetic field during the survey period. Additional base stations were established on the longer profiles in order to minimize travel time. Stations were repeated when high diurnal drift rates occurred. Each station value was obtained by averaging the readings taken at four sites in a 10-foot (3-m) radius circle

around the station. Measurements were made every 200 feet (61 m) on all profiles except those at Talkeetna Hill where a 50 foot (15 m) spacing was used.

A.5.2 - Data Reduction and Interpretive Procedures

This section discusses the reduction procedures required to prepare the data for interpretation and describes the interpretative techniques utilized. Selected profiles are presented in Section 4. Originals of all profiles are in the Project file of Woodward-Clyde Consultants, Santa Ana, California.

A.5.2.1 - Seismic Refraction Measurements

The arrival times of the seismic waves were plotted for each shot to produce a continuous time-distance profile for the seismic line. The profile was interpreted using a two-layer model with lateral velocity variations. The velocities were obtained from the slopes of the plotted data. The depth to the second layer and lateral variations in the model were determined by using ray theory, as discussed in any basic geophysics text.

A.5.2.2 - Magnetometer Measurements

The plotted magnetic field values represent the average values at each station after correcting for diurnal variation. The unaveraged values at each station usually fall within a ten-gamma range. The diurnal variation was obtained from the plot of base station values as a function of time.

No attempt was made to correct for topographic effects. Where such effects do occur, they are noted in the discussions of the individual profiles.

Qualitative interpretations of the profiles are provided. Quantitative interpretation is not appropriate for the data obtained. Two features of the data are used for interpretation: the spatial frequency and the amplitude of the magnetic variations. A change in either characteristic implies a change in subsurface character which may be fault related.

A.6 - Low-Sun-Angle Aerial Photography

An aerial photographic survey of a 36 square-mile (100 km^2) area centered on each site and of a three-mile- (5-km-) wide strip along the Talkeetna thrust fault and Susitna feature was flown by Air Photo Tech of Anchorage, Alaska. The survey was made during May 1982. The survey was specially designed to emphasize the presence of faults with recent displacement.

The photographs were taken from a Piper Aztec aircraft at an elevation of 12,000 feet (3,630 m) above the terrain. The camera used was a Zeiss Jena MRB 15/2323 having a focal length of 6 inches (15.3 cm). The film was exposed using a Kodak Wratten number 12 filter. The film used was a 9.4 inch (24 cm) Eastman Kodak Aerochrome Infrared 2443 having an effective aerial film speed (AFS) of 40 daylight. Approximately 220 images were obtained at a scale of 1:24,000 and were printed on a 9 inch by 9 inch (23 cm by 23 cm) format as one set of positive transparencies and one set of Cibachrome prints. These are in the Project file at Woodward-Clyde Consultants, Santa Ana, California.

The photographs were taken when the angle of the sun above the horizon was 10° to 25°. The grazing angle of the sunlight enhanced the appearance of small topographic features such as fault scarps. Infrared film was used to enhance the appearance of any vegetation lineaments that might mark the location of a fault. Infrared film provides an exceptionally strong contrast between different types of vegetation.

A.7 - Earthquake Recurrence Calculations

The average recurrence interval of an earthquake is the average time between earthquakes of a given magnitude. Recurrence intervals are often obtained from field evidence of individual earthquakes that caused surface faulting and that left some permanent record to be interpreted by geologists. When direct geologic evidence cannot be obtained as evidence of recurrence interval, slip rates can be useful in estimating recurrence intervals based on theoretical seismology.

The recurrence calculations are primarily based on the magnitude-frequency relationship presented by Richter (1958):

$$\text{Log } N = a - b\,M \quad \text{Equation A-1}$$

where N = the number of earthquakes of magnitude M and larger occurring within a defined time interval for a group of faults or area of the earth's surface containing a group of faults;

a and b = empirical constants;

and M = magnitude.

Use of this relationship leads to numerical estimates for return period (recurrence) as a function of magnitude for that area of earth's surface.

Because faults are the sources of earthquakes, it is considered reasonable to apply the magnitude-frequency relationship to individual faults, although significant uncertainites exist in how the relationship is related to single faults. The uncertainty stems largely from a lack of historical data to verify the theoretical model. For example, from

the data available, it appears that the frequency of occurrence of earthquakes of a specific magnitude on a fault is highly variable and may be related to cyclic periods of activity and inactivity lasting many tens to hundreds of years. Thus, the geologic and historical data available in California for the past 50 to 180 years may provide evidence of consistency with a recurrence model, but they do not provide a basis for constructing the model.

An alternative to estimating recurrence intervals based on the magnitude-frequency relationship alone is to refine that estimate by incorporating geologic data into the calculation. If it is true that the total energy released by a fault in the form of earthquakes is related to the net offset occurring along the fault for the same time period, then the magnitude-frequency relationship can be adjusted to a single fault by using the slip rate of the fault. The measure of earthquake energy per event is often expressed in terms of moment, M_o:

$$M_o = \bar{d} \cdot A \cdot \mu \quad \text{. . . . . Equation A-2}$$

where $\bar{d}$ = the average slip per event occurring within a fault rupture area (A);

A = the fault rupture area;

and μ = the shear modulus.

Dividing this equation by a time period gives the rate of energy release (moment rate) for that period as a function of the average slip rate.

The assumptions made for the analysis of recurrence intervals are:

1) The total moment rate on a fault is given by the product of the area of the fault, the slip rate, and shear modulus.

2) All of the displacement is considered to occur seismically.

3) The magnitude-frequency relationship is considered to be linear with an assumed slope (b) of - 0.85 up to the maximum magnitude assigned to the fault. This slope is selected to be appropriate for the southern Alaska tectonic setting and seismicity.

Using these assumptions, we have calculated the recurrence intervals for possible earthquakes on the Castle Mountain and Denali faults with a slip rate of 0.5 and 1.0 cm/yr, respectively, for a possible maximum magnitude of 7.5 and 8.0, respectively. For each fault, the area of the fault is the product of MCE (maximum credible earthquake) rupture length and width from Table 7-1. The shear modulus was assumed to be $3x10^{11}$dyne/cm^2.

Anderson's method (1979) was used to calculate the "a" values for the maximum magnitude selected. Using the calculated "a" value and the assumed "b" value, we calculated the numbers of earthquakes expected annually within one-half magnitude ranges. The inverse of each of these numbers is the recurrence interval of earthquakes within the respective magnitude ranges. It is important to note that the recurrence intervals presented here represent a mathematical distribution within a half-earthquake magnitude range.

Using the above method, a magnitude (M_S) 7-1/4 to 7-3/4 event may be expected to recur on the Castle Mountain fault at an average rate of 235 years. A magnitude (M_S) 7-3/4 to 8-1/4 event may be expected to recur on the Denali fault at an average rate of 290 years.

TABLE A-1

RELATIVE AGE DATA IN THE TALKEETNA MOUNTAINS AND ALASKA RANGE

Study Area	Station Number[1]	Granite Weathering Ratio			Depth of Oxidation (inches)	Interpreted Age[2]
		%Fresh	%Partially Weathered	%Weathered		
A. TALKEETNA MOUNTAINS[3]						
Black River	BR-1	54	38	8	11 to 14	Late Wisconsin
	BR-2	52	40	8	11 to 13	
	BR-3	50	42	8	15 to 17	
	BR-4	42	32	26	21 to 22	Early Wisconsin
Clear Valley	CL-2	ND[4]	ND	ND	15 to 24	Late Wisconsin
	CL-4	ND	ND	ND	11 to 12	
	CL-6	ND	ND	ND	13 to 14	
	CL-8	ND	ND	ND	26 to 30	Early Wisconsin
	CL-10	ND	ND	ND	29	
	CL-12	64	30	6	35 to 40	
Butte Lake	BL-2[5]	50	32	18	11 to 16	Late Wisconsin
	BL-3	62	30	8	8 to 10	
	BL-4	58	32	10	10 to 12	
	BL-5	50	38	12	10 to 12	
	BL-6	53	35	12	10 to 12	
	BL-7	39	37	24	14 to 17	Early Wisconsin
	BL-8	20	56	24	29	
Deadman Creek	DC-1	46	40	14	10	Late Wisconsin
	DC-2	52	38	10	7 to 9	
	DC-3	50	40	10	8.5 to 12	
	DC-4	52	38	10	11 to 12	
	DC-5	40	40	20	17.5 to 18	Early Wisconsin
B. ALASKA RANGE[6]						
McKinley Park Glaciation	Stade MP-IV	38	60	2	6 to 13	10,500 to 9,500 y.b.p.
	Stade MP-III	58	42	0	15.5 to 17	12,800 to 11,800 y.b.p.
	Stade MP-II	50	46	4	10 to 17.5	15,000 to 13,500 y.b.p.
	Stade MP-I	28	66	6	11 to 19	25,000 to 17,000 y.b.p.
	Pre-Stade MP-I	16	66	18	17.5 to 35	>25,000 y.b.p.

Notes:

1. The locations of moraines are shown in Figures 3-5 and 3-6.
2. Interpreted age as estimated from photogeologic interpretation (Section A.1.2.1).
3. Data obtained during this investigation.
4. ND indicates that no data were obtained at this location because the rock types were primarily metamorphic and volcanic and because the few observed granitic rocks were transported to this location after deposition of the moraine.
5. The surface of the moraine was slightly disturbed by man-made activities.
6. Age determinations are from Ten Brink and Waythomas (in press); weathering data are from Werner (in press).

TABLE A-2

SUMMARY OF POTASSIUM-ARGON WHOLE ROCK AGE DATES

Sample No.[1]	K^2 (wt. %)	$^{40}Ar_{rad}$ ($\times 10^{11}$ mol/g)	$\frac{^{40}Ar_{rad}}{^{40}Ar_{tot}}$	Calculated age[3] (millions of years before present)
W-1	0.207			
	0.206	3.333	0.386	
	0.205	3.293	0.422	
	0.205			
Average:	0.206	3.313		90.2 ($\pm$2.3)
W-4	0.199			
	0.193	4.535	0.622	
	0.194	4.538	0.654	
	0.190			
Average:	0.194	4.536		130 ($\pm$3)

Notes:

1. Sample locations are shown in Figure A-1.
2. K is potassium, Ar is argon.
3. Uncertainties are given at the 68% confidence level and reflect analytical uncertainties of $\pm$2% in K and $\pm$1.5% in radiogenic ^{40}Ar.
4. Analyses were conducted by K. A. Foland, Ohio State University.

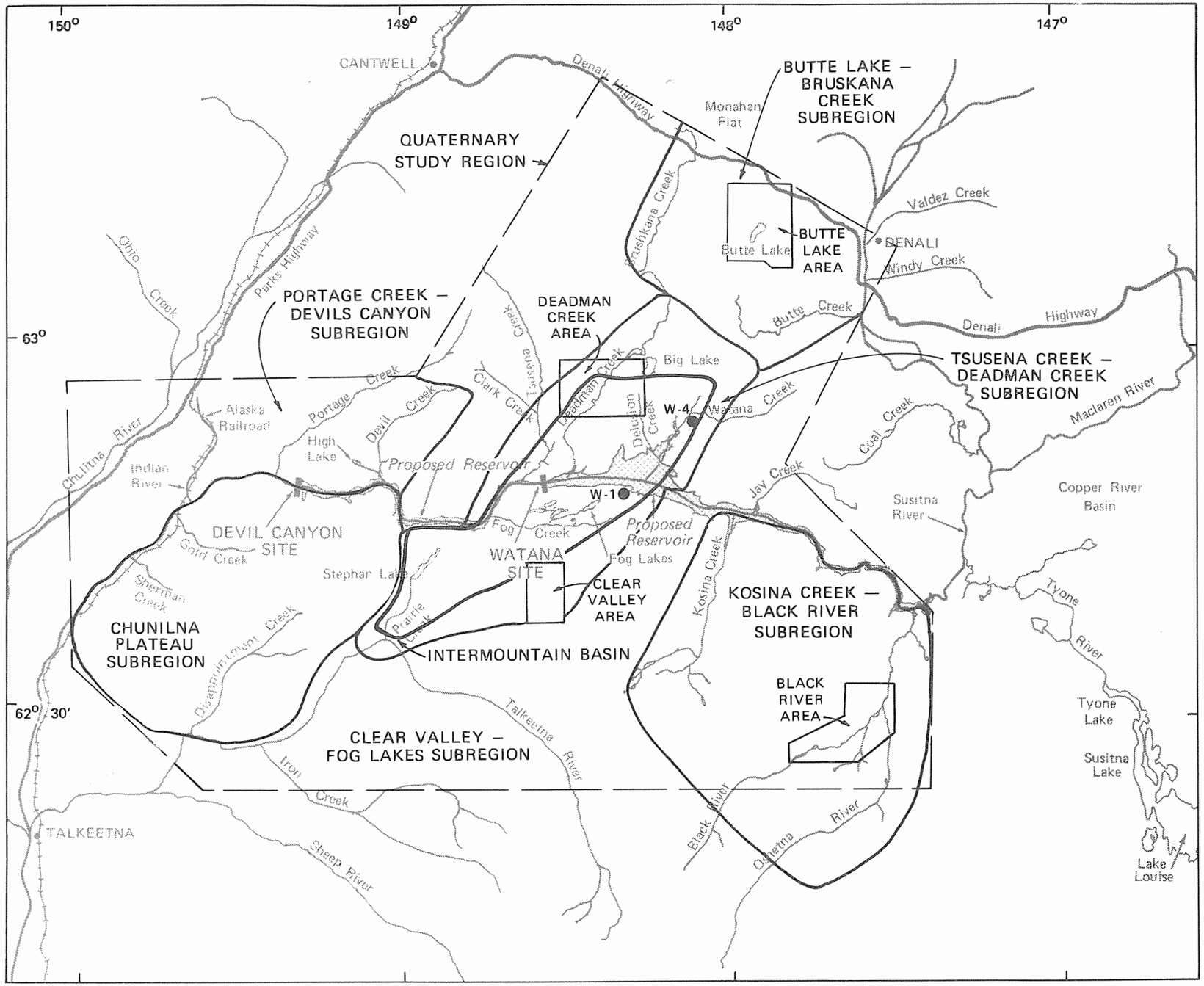

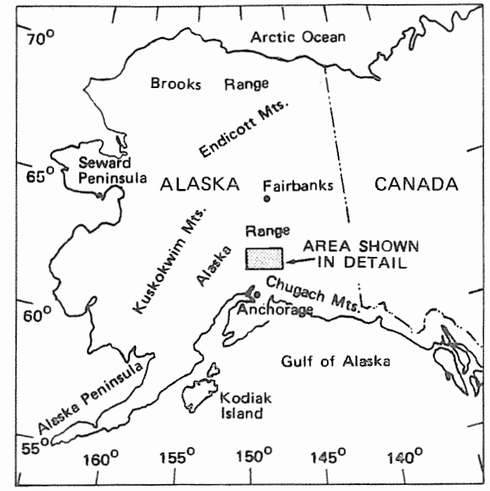

NOTE

1. Proposed reservoir configuration is after Acres American Inc. (In Press).
2. W-1 and W-4 are potassium-argon (K-Ar) sample localities.

N

QUATERNARY GEOLOGY
LOCATION MAP

0 5 10 15 20 Miles
0 10 20 30 Kilometers

FIGURE A-1

APPENDIX B - GLOSSARY

Ablation Till	Loosely consolidated rock debris, formerly contained by a glacier, that accumulated in place as the surface ice was removed by ablation.
Aleutian Megathrust	The major collision boundary between the Pacific and North American plates where the Pacific plate is descending into the earth's mantle.
Allochthonous	Formed or occurring elsewhere than in place; of foreign origin or introduced.
Alluvium	A general term for all sediment deposited in land environments by streams.
Amygdaloidal	Gas cavities in igneous rocks that have been filled with secondary minerals such as quartz, calcite, chalcedony, or zeolite.
Andesite	A type of volcanic rock that is believed to be associated with plate subduction.
Anelasticity	The effect of attenuation of a seismic wave; it is symbolized by Q.
Aseismic	An area of generally low seismicity that can have tectonic deformation which is not accompanied by earthquakes.

Autochthonous	Formed or occurring in the place where found; used for a rock or sediment derived in the place where it is now found.
Batholith	A large, generally discordant mass of igneous rock which was intruded originally at depth and now has more than 40 square miles (104 km^2) in surface exposure. It is composed predominantly of medium to coarse grained rocks, often of granodiorite composition.
Benioff zone	Seismicity associated with plates of the earth's crust which are sinking into the upper mantle. In Alaska, the Benioff zone is associated with underthrusting of the Pacific plate beneath the North American plate.
Candidate Feature	A term used in this study to identify faults and lineaments that may affect Project design considerations. Candidate features were selected by applying length-distance screening criteria prior to field reconnaissance studies.
Candidate Significant Feature	A term used in this study to identify faults and lineaments that may affect Project design considerations based on length-distance screening criteria and a preliminary assessment of seismic source potential and potential surface rupture through either site using the results of the field reconnaissance studies.

Cataclastic	The granular fragmental texture induced in rocks by mechanical crushing.
Cirque	A steep-walled, flat- or gently-floored, half-bowl-like recess or hollow, situated high on the side of a mountain and produced by erosive activity of mountain glaciers; it is commonly found at the head of a glacial valley.
Consanguineous	The relationship that exists between igneous rocks that are presumably derived from the same parent magma.
Crag and Tail	An elongate hill or ridge resulting from glaciation. The crag is a steep face or knob of ice-smoothed, resistant bedrock at the end of the ridge from which glacial ice came. The tail is a tapering, streamlined, gentle slope of intact weaker rock and/or till that was protected in part from the glacial ice by the crag.
Cryoturbation	A term to describe the stirring, churning, modification, and all other disturbances of soil resulting from frost action.
Dextral Fault	A strike-slip fault along which, in plan view, the side opposite the observer appears to have moved to the right.
Drift	All rock material transported by a glacier and deposited directly by the ice or by meltwater from the glacier.

Ductile	A rock that is able to sustain, under a given set of conditions, 5 to 10 percent deformation before fracturing or faulting.
Dynamometamorphism	The alteration of rock characteristics primarily by mechanical energy (pressure and movement).
End Moraine	A ridge of glacial sediments deposited at the margins of an actively flowing glacier.
Fault	A surface or zone of closely spaced fractures along which materials on one side have been displaced with respect to those on the other side.
Fault with Recent Displacement	As defined for this study, a fault that has been subject to displacement within approximately the last 100,000 years.
Flysch	A thick and extensive deposit largely of sandstone that is formed in a marine environment (geosyncline) adjacent to a rising mountain belt.
Geosyncline	A mobile downwarping of the crust of the earth, either elongate or basin-like, that is subsiding as sedimentary and volcanic rocks accumulate to thicknesses of thousands of meters. Geosynclines are usually measured in scores of kilometers.

Glacial Erratic	A rock fragment carried by glacier ice or floating ice, and deposited when the ice melted at some distance from the outcrop from which the fragment was derived.
Glacial Scour	The eroding action of a glacier.
Glaciogenic	Deposits or topographic forms derived from a glacial origin.
Gouge	Soft clayey material often present between a vein and a wall or along a fault.
Hypocenter	That point within the earth that is the center of an earthquake and the origin of its elastic waves.
Ice Pulses	Small advances of ice associated with a minor decrease in temperature during interglacial periods.
Intercalated	A material that exists as a layer or layers between layers or beds of other rock; interstratified.
Kame	A short ridge, hill, or mound of poorly stratified sediments deposited by glacial meltwater.
Kettle	A steep-sided, usually basin- or bowl-shaped hole or depression without surface drainage in glacial deposits.

Klippe	An outlying isolated remnant of an overthrust rock mass.
Lee	The side of a hill, knob, or prominent rock facing away from the direction from which an advancing glacier or ice sheet moved; facing the downstream side of a glacier.
Lineament	A linear trend with implied structural control (including but not limited to fractures and faults) typically identified on remotely sensed data.
Lit-par-lit	Having the characteristic of a layered rock, the layers of which have been penetrated by numerous thin, roughly parallel sheets of igneous material.
Lodgment Till	A basal till commonly characterized by compact fissile structure and containing stones oriented with their long axes generally parallel to the direction of ice movement.
Magnitude	Magnitude is used to measure the size of instrumentally recorded earthquakes. Several magnitude scales are in common usage (Richter, 1958). The differences in these magnitudes are caused by the way in which they are each calculated, specifically, by the periods (frequency) of the waves which are used in each measurement. M_L is the

	original Richter magnitude which was developed for Southern California earthquakes recorded on Wood-Anderson seismometers (free period 0.8 second) at distances of 372 miles (600 km) or less. M_S and m_b use signals recorded at teleseismic distances of 1,240 miles (2,000 km) or greater. M_S measures the amplitude of surface waves with periods of 20 seconds and the m_b is a measure of the 1 second body waves. M_W depends on the seismic moment according to the relation log W_O = 1.5 M_W + 11.8. The variations in the magnitude calculations result in part because different size earthquakes generate relatively different amounts of energy in these frequency bands.
Metabasalt	Volcanic rock (basalt) altered by temperature and pressure to a metamorphic rock.
Microearthquake	An earthquake having a magnitude (M_L) of three or less on the Richter scale; it is generally not felt.
Migmatite	A rock (gneiss) produced by the injection of igneous material between the laminae of a schistose formation.
Miogeosyncline	A geosyncline in which volcanism is not associated with sedimentation.
Modified Mercalli Scale	An earthquake intensity scale, having twelve divisions ranging from I (not felt by people) to XII (damage nearly total).

Morphostratigraphic	A distinct stratigraphic unit comprising a body of rock that is identified primarily from the surface form it displays.
Noncomformity	A substantial hiatus in the geologic record that typically implies uplift and erosion. The gap occurs between older igneous or metamorphic rocks and younger sedimentary rocks.
Nonsorted Stripes	Alternating bands comprising a form of patterned ground characterized by a striped pattern and nonsorted appearance due to parallel lines of frost-shattered rubble and intervening strips of relatively bare or vegetated ground.
Normal Fault	A fault along which the upper (hanging) wall has moved down relative to the lower wall (footwall).
Periglacial	Describing processes, conditions, areas, climate, and topographic features at the immediate margins of former or existing glaciers; influenced by the cold temperature of the ice.
Pluton	An igneous intrusion formed at great depth.

Potassium-Argon Age Dating	A type of age dating that is based on the decay rate of potassium-40 (an isotope of potassium) to argon-40. It is useful for dating rocks rich in potassium and is applicable for dating materials that are generally older than 100,000 year.
Pyroclastic	Formed by fragmentation as a result of a volcanic explosion or aerial expulsion from a volcanic vent.
Rejuvenation	Renewed downcutting by a stream caused by regional uplift or a drop in sea level.
Reservoir-Induced Seismicity	The phenomenon of earth movement and resultant seismicity that has a temporal and spatial relationship to a reservoir and is triggered by nontectonic stress.
Reverse Fault	A fault in which the upper (hanging) wall appears to have moved up relative to the lower wall (footwall).
Seismic Moment	Measurement of the "size" of an earthquake equal to the rupture area times the average displacement times the shear modulus.
Significant Feature	A term used in this study to identify the faults and lineaments that are considered to have a potential affect on Project design considerations pending additional studies. Selection of these features was made on the

	basis of length-distance screening criteria and final assessment of their seismic source potential and potential for surface rupture through either site using the results of the field reconnaissance studies.
Slickensides	A polished and smoothly striated surface that results from friction during movement along a fault plane.
Solifluction	The slow (0.2 to 2 inches/yr [0.5 to 5 cm/yr]) creeping of wet soil and other saturated fragmental material down a slope, especially the flow initiated by frost action and augmented by meltwater from alternate freezing and thawing of snow and ground ice.
Stade	A substage of a glacial stage; time represented by glacial deposits.
Stoss	The side or slope of a hill, knob, or prominent rock facing the direction from which an advancing glacier or ice sheet moved; facing the upstream side of a glacier.
Stoss and Lee Topography	An arrangement, in a strongly glaciated area, of small hills or prominent rocks having gentle slopes on the stoss side, and somewhat steeper, plucked slopes on the lee side.

Stratovolcano	A volcano composed of explosively erupted cinders and ash interbedded with occasional lava flows.
Time stratigraphic	A subdivision of rocks considered solely as the record of a specific interval of geologic time.
Whaleback	A small hill or hillock with a curved surface that is the result of abrasion by glacial ice. The resulting hillock has a smooth form resembling a whale's back.

APPENDIX C - REFERENCES

Abe, K., 1972, Mechanisms and tectonic implications of the 1966 and 1970 Peru earthquakes: Physics of the Earth and Planetary Interiors 5, 367-379.

---- 1974, Seismic displacement and ground motion near a fault; The Saitama earthquake of September 21, 1931: Journal of Geophysical Research, v. 79, p. 4393-4399.

---- 1975, Static and dynamic fault parameters of the Saitama earthquake of July 1, 1968: Tectonophysics, v. 27, p. 223-228.

---- 1977, Tectonic implications of the large Shioya-Oki earthquakes of 1938: Tectonophysics, v. 41, no. 4, p. 269-291.

Abe, K., and Kanamori, H., 1979, Temporal variation of the activity of intermediate and deep focus earthquakes: Journal of Geophysical Research, v. 84, p. 3589-3595.

---- 1980, Magnitudes of great shallow earthquakes from 1953 to 1977: Tectonophysics, v. 62, p. 191-203.

Acres American Inc., 1980, Design transmittal--Initial version--Preliminary licensing documentation: Alaska Power Authority, Anchorage, Alaska Task, 10.2, 60 p., 3 appendices.

---- 1982, Susitna Hydroelectric Project Feasibility Report: Prepared by Acres American Inc. for the Alaska Power Authority [in press].

Adams, C. E., Barnett, M. A. F., and Hayes, R. C., 1933, Seismological report of the Hawke's Bay earthquake of 3rd February, 1931: The New Zealand Journal of Science and Technology, v. XV, no. 1, p. 93-107.

Agnew, J. D., 1980, Seismicity of the Central Alaska Range, Alaska, 1904-1978: Master's Thesis, University of Alaska, Fairbanks, 95 p.

Ambraseys, N. N., 1965, An earthquake engineering study of the Buyin-Zahra earthquake of September 1st, 1962: Proceedings of the 3rd World Conference on Earthquake Engineering, New Zealand, v. III.

Ando, M., 1974, Faulting in the Mikawa earthquake of 1945: Tectonophysics, v. 22, p. 173-186.

Barnes, F. F., and Payne, T. G., 1956, The Wishbone Hill District, Matanuska Coal Field, Alaska: U.S. Geological Survey Bulletin 1016, 85 p.

Beikman, H. M., 1974a, Preliminary geologic map of the southwest quadrant of Alaska: U.S. Geological Survey Miscellaneous Field Studies Map MF-611, scale 1:2,000,000, 2 sheets.

---- compiler, 1974b, Preliminary geologic map of the southeast quadrant of Alaska: U.S. Geological Survey Miscellaneous Field Studies Map MF-612, scale 1:1,000,000, 1 sheet.

---- 1978, Preliminary geologic map of Alaska: U.S. Geological Survey, scale 1:2,500,000, 2 sheets.

---- 1980, Geologic Map of Alaska: U.S. Geological Survey, 2 sheets, scale 1:2,500,000.

Biswas, N. N., and Bhattacharya, B., 1974, Travel-time relations for the upper mantle P-wave phases from central Alaskan data: Bulletin of the Seismological Society of America, v. 64, p. 1953-1965.

Bolt, B. A., McEvilly, T. V., and Uhrammer, R. A., 1981, The Livermore Valley, California, sequence of January 1980: Bulletin of the Seismological Society of America, v. 71, p. 451-463.

Bonilla, M. G., 1979, Historic surface faulting--map patterns, relation to subsurface faulting, and relation to preexisting faults, in Evernden, J. F., convener, Proceedings of Conference VIII--Analysis of actual fault zones in bedrock: U.S. Geological Survey Open-File Report 79-1239, p. 36-65.

Bonilla, M. G., and Buchanan, J. M., 1970, Interim report on worldwide historic surface faulting: U.S. Geological Survey Open-File Report, 31 p.

Boore, D. M., and Stierman, D. J., 1976, Source parameters of the Pt. Mugu, California, earthquake of February 21, 1973: Bulletin of the Seismological Society of America, v. 66, p. 385-404.

Boucher, G. C., and Fitch, T. J., 1969, Microearthquake seismicity of the Denali fault: Journal of Geophysical Research, v. 74, p. 6638-6648.

Bowers, P. M., 1979, The Cantwell ash bed, a Holocene tephua in the central Alaska Range: Alaska Division of Geological and Geophysical Surveys, Geologic Report 61, p. 19-24.

Bruen, M., 1981, Personal communication, Project geologist for the Susitna Hydroelectric Project, Acres American Inc., Anchorage, Alaska.

Bruhn, R. L., 1979, Holocene displacement measured by trenching the Castle Mountain fault near Houston, Alaska: Alaska Division of Geological and Geophysical Surveys, Geology Department 61, p. 1-4.

Burford, R. O., and Harsh, P. W., 1981, 7.3 earthquake in Algeria reviewed: Geotimes, v. 26, no. 5, p. 18-20.

Cady, W. M., Wallace, R. E, Hoare, T. M., and Webber, E. J., 1955, The central Kuskakwim region, Alaska: U.S. Geological Survey Professional Paper 268, 132 p.

Cagnetti, V., and Pasquale, V., 1979, The earthquake sequence in Friuli, Italy, 1976: Bulletin of the Seismological Society of America, v. 69, p. 1797-1818.

Carder, D. S., 1945, Seismic investigations of the Boulder Dam area, 1940-1944, and the influence of reservoir loading on earthquake activity: Bulletin of the Seismological Society of America, v. 35, p. 175-192.

Cardwell, R. K., and Isacks, B. L., 1978, Geometry of the subducted lithosphere beneath the Banda Sea in eastern Indonesia from seismicity and fault plane solutions: Journal of Geophysical Research, v. 83, p. 2825-2838.

Cardwell, R. K., Isacks, B. L., and Karig, D. E., 1980, The spacial distribution of earthquakes, focal mechanism solutions, and subducted lithosphere in the Philippine and Northeastern Indonesia Islands, in The tectonic and geologic evolution of southeast asian seas and island: American Geophysical Union, Geophysical Monograph 23 (Hayes ed.), Washington, D.C., p. 1-35.

Castle, R., Church, J. P., Elliott, M. R., and Savage, J. C., 1977, Preseismic and coseismic elevation changes in the epicentral region of the Point Mugu earthquake of February 21, 1973: Bulletin of the Seismological Society of America, v. 67, p. 219-231.

Chapin, T., 1918, The Nelchina-Susitna region, Alaska: U.S. Geological Survey Bulletin 668, 67 p.

Chase, C. G., 1980, University of Minnesota, Minneapolis, personal communication.

Cipar, J., 1980, Teleseismic observations of the 1976 Friuli, Italy earthquake sequence: Bulletin of the Seismological Society of America, v. 70, p. 963-983.

---- 1981, Broadband time domain modeling of earthquakes from Friuli, Italy: Bulletin of the Seismological Society of America, v. 71, p. 1215-1231.

Coulter, H. W., Hopkins, D. M., Karlstrom, T. N. V., Pewé, T. L., Wahrhaftig, C., and Williams, J. R., 1965, Map showing extent of glaciations in Alaska: U.S. Geological Survey Miscellaneous Geologic Investigations Map I-415, scale 1:2,500,000.

Compton, R. R., 1962, Manual of field geology: New York, John Wiley and Sons, 378 p.

Crouse, C. B., and Turner, B. E., 1980, Processing and analysis of Japanese accelerograms and comparisons with U.S. strong motion data: Seventh World Conference on Earthquake Engineering, Istanbul, Turkey, v. 2, p. 419-426.

Csejtey, B., Jr., 1980, U.S. Geological Survey, Menlo Park, California, personal communication.

---- 1981, U.S. Geological Survey, Menlo Park, California, personal communication.

Csejtey, B., and Griscom, A., 1978, Preliminary aeromagnetic interpretative map of the Talkeetna Mountains quadrangle, Alaska: U.S. Geological Survey Open File Report 78-558-C, scale 1:250,000, 14 p., 2 plates.

Csejtey, B., Jr., Nelson, W. H., Jones, D. L., Silberling, N. J., Dean, R. M., Morris, M. S, Lanphere, M. A., Smith, J. G., and Silbermen, M. L., 1978, Reconnaissance geologic map and geochronology, Talkeetna Mountain Quadrangle, northern part of Anchorage Quadrangle, and southwest corner of Healy Quadrangle, Alaska: U.S. Geological Survey Open-File Report 78-558-A, 62 p.

Csejtey, B., and St. Aubin, D. R., 1981, Evidence for northwestward thrusting of the Talkeetna superterrane and its regional significance: U.S. Geological Survey Circular 823-B, p. B49-B51.

Csejtey, B., Stricker, G. D., Mullen, M. W., and Cox, D. P., 1980, The Denali fault of southern Alaska: The case for minor rather than major displacement (abs.): American Geophysical Institute (EOS) Transactions, v. 61, p. 1114.

Dames and Moore, 1975, Subsurface geophysical exploration--proposed Watana damsite on the Susitna River: U.S. Army Corps of Engineers, Alaska District, unpublished report, 12 p., 2 appendices.

Davies, J. N., 1975, Seismological investigations and plate tectonics in southcentral Alaska: Ph.D. dissertation, University of Alaska, Fairbanks, 192 p.

Davies, J. N., and House, L., 1979, Aleutian subduction zone seismicity, volcano-trench separation, and their relation to the great thrust-type earthquakes: Journal of Geophysical Research, v. 84, p. 4583-4591.

Davies, J., Sykes, L., House, L., and Jacob, K., 1981, Shumagin seismic gap, Alaska peninsula: history of great earthquakes, tectonic setting and evidence for high seismic potential: Journal of Geophysical Research, v. 86, p. 3821-3855.

Davis, T. N., 1960, A field report on the Alaska earthquakes of April 7, 1958: Bulletin of the Seismological Society of America, v. 50, p. 489-510.

---- 1964, Seismic history of Alaska and the Aleutian Islands: Bibliographical Bulletin of American Geophysics and Oceanography, v. 3, p. 1-16.

Davis, T. N., and Echols, C., 1962, A table of Alaskan earthquakes 1788-1961: University of Alaska, Geophysical Institute Research Report No. 8, 2 p.

Detterman, R. L., Plafker, G., Hudson, T., Tysdal, R. G., and Pavoni, N., 1974, Surface geology and Holocene breaks along the Susitna segment of the Castle Mountain fault, Alaska: U.S. Geological Survey Miscellaneous Field Studies Map MF-618, scale 1:24,000, 1 sheet.

Detterman, R. L., Plafker, G., Tysdal, R. G., and Hudson, T., 1976, Geology of surface features along part of the Talkeetna segment of the Castle Mountain-Caribou fault system, Alaska: U.S. Geological Survey Miscellaneous Field Studies Map MF-738, scale 1:63,360, 1 sheet.

Dibblee, Jr., T. W., 1955, Geology of the southeastern margin of the San Joaquin Valley, California, in Earthquake in Kern County during 1952: California Division of Mines and Geology Bulletin 171, p. 23-34.

Dobry, R., Idriss, I. M., and Ng, E., 1978, Duration characteristics of horizontal components of strong motion earthquake records: Bulletin of the Seismological Society of America, v. 68, p. 1487-1520.

Dunbar, W. S., Boore, D. M., and Thatcher, W., 1980, Pre, co and post-seismic strain changes associated with the 1952 M_L=7.2 Kern County, California earthquake: Bulletin of the Seismological Society of America, v. 70, p. 1893-1905.

Everingham, I. B., Gregson, P. J., and Doyle, H. A., 1969, Thrust fault scarp in the western Australian shield: Nature, v. 223, p. 701-703.

Ferrians, O. J., and Schmoll, H. R., 1957, Extensive proglacial lake of Wisconsin age in the Copper River basin, Alaska: Geological Society of America Bulletin, v. 68, p. 1726.

Finetti, I., Pursi, M., and Slejko, 1979, The Friuli earthquake (1976-1977): Tectonophysics, v. 53, p. 261-272.

Flint, R. F., 1971, Glacial and Quaternary geology: New York, John Wiley and Sons, 892 p.

Forbes, R. B., Turner, D. L., Stout, J., and Smith, T. E., 1973, Cenozoic offset along the Denali fault, Alaska (abs.): American Geophysical Union (EOS) Transactions, v. 54, p. 495.

Foster, H. M., and Karlstrom, T. N. V., 1967, Ground breakage and associated effects in the Cook Inlet area, Alaska, resulting from the March 27, 1964 earthquakes: U.S. Geological Survey Professional Paper 543-F, 28 p.

Fujita, K., and Kanamori, H., 1981, Double seismic zones and stresses of intermediate depth earthquakes: Geophysical Journal of the Royal Astronomical Society, v. 66, p. 131-156.

Gedney, L., Berg, E., Pulpan, H., Davies, J., and Feetham, W., 1969, A field report on the Rampart, Alaska earthquake of October 29, 1968: Bulletin of the Seismological Society of America, v. 59, p. 1421-1423.

Gedney, L., and Shapiro, L., 1975, Structural lineaments, seismicity and geology of the Talkeetna Mountains area, Alaska: Unpublished report prepared for the U.S. Army Corps of Engineers, Alaska Division, 18 p.

Geller, R. J., and Kanamori, H., 1977, Magnitudes of great shallow earthquakes from 1904 to 1952: Bulletin of the Seismological Society of America, v. 67, p. 587-598.

Geller, R. J., Kanamori, H., and Abe, K., 1978, Addenda and corrections to "Magnitude of great shallow earthquakes from 1904 to 1952": Bulletin of Seismological Society of America, v. 68, p. 1763-1764.

Gettrust, J. F., Hsu, V., Helsley, C. E., Herrero, E., and Jordan, T., 1981, Patterns of local seismicity preceding the Petatlan earthquake of 14 March 1979: Bulletin of the Seismological Society of America, v. 71, p. 761-769.

Grantz, A., 1966, Strike-slip faults in Alaska: U.S. Geological Survey Open-File Report, 82 p.

Griscom, A., 1978, Aeromagnetic map and interpretation, Talkeetna Quadrangle, Alaska: U.S. Geological Survey Miscellaneous Field Studies Map MF-870B, Scale 1:250,000, 2 sheets.

---- 1979, Aeromagnetic interpretation of the Big Delta Quadrangle, Alaska: U.S. Geological Survey Open-File Report 78-529-B, 10 p.

Guptill, P. D., Brogan, G. E., and Turcotte, T., 1981, Tectonic setting of the Gulf of Alaska: Marine Geotechnology, v. 4., no. 3, p. 223-241.

Gutenberg, B., 1955, The first motion in longitudinal and transverse waves of the main shock and the direction of slip, in Earthquakes in Kern County during 1952: California Division of Mines and Geology Bulletin 171, p. 165-170.

Gutenberg, B., and Richter, C. F., 1954, Seismicity of the earth and associated phenomena: Princeton, New Jersey, Princeton University Press, 310 p.

Hanks, T. C., and Kanamori, H., 1979, A moment magnitude scale: Journal of Geophysical Research, v. 84, p. 2348-2350.

Hasegawa, A., Umino, N., Takagi, A., and Suzuki, Z., 1979, Double planed deep seismic zone and anomalous structure in the upper mantle beneath northeastern Honshu (Japan): Tectonophysics, v. 57, p. 1-6.

Helmberger, D. V., 1968, The crust-mantle transition in the Bering Sea: Bulletin of the Seismological Society of America, v. 58, p. 179-214.

Hickman, R. G., and Craddock, C., 1973, Lateral offsets along the Denali fault, central Alaska Range, Alaska (abs.): Geological Society of America Abstracts with Programs, v. 5, p. 322.

Hickman, R. G., Craddock, C., and Sherwood, K. W., 1976, The Denali fault system and the tectonic development of southern Alaska (abs.): International Geological Congress Abstracts, v. 3, p. 683.

---- 1977, Structural geology of the Denali Fault system, central Alaska Range: Geological Society of America Bulletin, v. 88, p. 1217-1230.

---- 1978, The Denali fault system and the tectonic development of southern Alaska: Tectonophysics, v. 47, p. 247-273.

Hopkins, D. M., 1967, The Bering Land Bridge: Palo Alto, California, Stanford University Press, 495 p.

Huang, P., 1981, Focal parameters of October 29, 1968 Rampart, Alaska earthquake and its tectonic implications: Massachusetts Institute of Technology [in press].

Idriss, I. M., 1978, Characteristics of earthquake ground motions, state-of-the-art paper: Specialty Conference on Earthquake Engineering and Soil Dynamics, Geotechnical Engineering Division of the American Society of Civil Engineers, Pasadena, California, Proceedings, v. 3, p. 1151-1263.

Iida, K., 1965, Earthquake magnitude, earthquake fault and source dimensions: Journal of Earth Science, Nagoya University, v. 13, p. 115-132.

Isacks, B. L., and Barazangi, M., 1977, Geometry of Benioff zones: Lateral segmentation and downwards bending of the subducted lithosphere, in Island areas, deep sea trenches and back-arc basins, Ewing series, American Geophysical Union, Washington, D.C., v. 1, p. 99-114.

Isacks, B., Oliver, J., Sykes, L. R., 1968, Seismology and the new global tectonics: Journal of Geophysical Research, v. 73, p. 5855-5896.

Jones, D. L., and Silberling, N. J., 1979, Mesozoic stratigraphy, the key to tectonic analysis of southern and central Alaska: U.S. Geological Survey Open File Report 79-1200, 37 p.

Kachadoorian, R., and Moore, G. W., 1979, Reconnaissance of the recent geology of the proposed Devils Canyon and Watana dam sites, Susitna River, Alaska, in U.S. Army Corps of Engineers, Southcentral railbelt area, Alaska-upper Susitna river basin: U.S. Army Corps of Engineers, Alaska District, Appendix Part 1, Exhibit, D-2, 42 p.

Kanamori, H., 1977, The energy release in great earthquakes: Journal of Geophysical Research, v. 82, p. 2981-2987.

Kanamori, H., and Anderson, D. L., 1975, Theoretical basis of some empirical relations in seismology: Bulletin of the Seismological Society of America, v. 65, p. 1073-1095.

Karlstrom, T. N. V., 1964, Quaternary geology of the Kenai lowland and glacial Cook Inlet region, Alaska: U.S. Geological Survey, Professional Paper 443, 69 p.

Karlstrom, T. N. V., Coulter, H. W., Jernald, A. T., Williams, J. R., Hopkins, D. M., Pewé, T. L., Drewes, H., Huller, E. H., and Candon, W. H., 1964, Surficial Geology of Alaska: U.S. Geological Survey Miscellaneous Geologic Investigations Map I-557, scale 1:1,584,00, 2 sheets.

Kawasaki, I., 1975, The focal process of the Kita-Mino earthquake of August 19, 1961, and its relationship to a Quaternary fault, the Hatogaya-koike fault: Journal of Physics of the Earth, v. 24, p. 227-250.

Keith, C. M., Simpson, D. W., and Soboleva, O. V., 1979, Induced seismicity and deformation at Nurek reservoir, Tadjik, USSR: Unpublished manuscript, 28 p.

Kelleher, J. A., 1972, Rupture zones of large South American earthquakes and some predictions: Journal of Geophysical Research, v. 77, p. 2087-2103.

Kelleher, J. A., and Savino, J., 1975, Distribution of seismicity before large strike-slip and thrust-type earthquakes: Journal of Geophysical Research, v. 80, p. 260-271.

Kelleher, J. A., Savino, J., Rowlett, H., and McCann, W., 1974, Why and where great thrust earthquakes occur along island arcs: Journal of Geophysical Research, v. 79, p. 4889-4899.

Kelley, T. E., 1963, Geology and hydrocarbons in Cook Inlet Basin, Alaska, in Childs, D. E., and Beebe, B. W., eds., Backbone of the Americas Symposium: American Association of Petroleum Geologists Memoir 2, p. 278-296.

Kuno, H., 1936, On the displacement of the Tanna fault since Pleistocene: Bulletin of the Earthquake Research Institute, University of Tokyo, v. 14, p. 619-631.

Lahr, J., 1975, Detailed seismic investigation of Pacific-North America plate interaction in southern Alaska: Ph.D. thesis, Columbia University, New York, 88 p.

Lahr, J. C., and Plafker, G., 1980, Holocene Pacific-North American plate interaction in southern Alaska: Implications for the Yakataga seismic gap: Geology, v. 8, p. 483-486.

Lander, J., ed. 1969, Seismological notes: Bulletin of the Seismological Society of America, v. 59, p. 1023-1030.

----, ed., 1970, Seismological notes: Bulletin of the Seismological Society of America, v. 60, p. 685-693.

Langston, C. A., 1978, The February 9, 1971, San Fernando earthquake: a study of source finiteness in teleseismic body waves: Bulletin of the Seismological Society of America, v. 68, p. 1-30.

Langston, C. A., and Helmberger, D. V., 1975, A procedure for modeling shallow dislocation sources: Geophysical Journal of the Royal Astrological Society, v. 42, p. 117-130.

Lee, W., Herd, D. G., Cagnetti, V., Bakun, W., and Rapport, A., 1979, A preliminary study of the Coyote Lake earthquake of August 6, 1979 and its major aftershocks: U.S. Geological Survey Open File Report 79-1621, 43 p.

Matsuda, T., 1977, Estimation of future destructive earthquakes from active faults on land in Japan: Journal of Physics of the Earth, v. 25, Supplement, p. S251-S260.

McCann, W., 1981, Research Associate, Lamont-Doherty Geological Observatory, Palisades, New York, personal communication.

McCulloch, D. S., and Bonilla, M. G., 1970, Effects of the earthquake of March 27, 1967, on the Alaska Railroad: U.S. Geological Survey Professional Paper 545-D, 161 p.

Meyers, H., 1976, A historical summary of earthquake epicenters in and near Alaska: National Geophysical and Solar-Terrestrial Data Center, Boulder, Colorado, NOAA Technical Memorandum EDS NGSDC-1, 57 p., 7 appendices.

Miller, R. D., and Dobrovolny, E., 1959, Surficial geology of Anchorage and vicinity, Alaska. U.S. Geological Survey Bulletin 1093, 128 p.

Mogi, K., 1969, Some features of recent seismic activity in and near Japan, activity before and after great earthquakes: Bulletin Earthquake Research Institute, Tokyo University, v. 47, p. 395-417.

National Oceanic and Atmospheric Administration, 1981, Hypocenter data file (computer tape and cards): Boulder, Colorado, Environmental Data Services.

Nokleberg, W., 1981, U.S. Geological Survey, Menlo Park, California, personal communication.

Okada, A., and Ando, M., 1979, Active faults and earthquakes in Japan: Science (Japanese publication), v. 49, p. 158-169 (in Japanese).

Packer, D. R., Brogan, G. E., and Stone, D. B., 1975, New data on plate tectonics of Alaska: Tectonophysics, v. 29, p. 87-102.

Packer D. R., Cluff, L. S., Knuepfer, P. L., and Withers, R. J., 1979, Study of reservoir induced seismicity: Final Technical Report to the U.S. Geological Survey, Contract 14-08-0001-16809, 222 p.

Packer, D. R., Lovegreen, J. R., and Born, J. L., 1977, Earthquake evaluation studies of the Auburn Dam area--Volume 6--Reservoir induced seismicity: U.S. Bureau of Reclamation, Denver, Colorado, Contract 6/07/DS/72090, 124 p., 7 appendices.

Page, R. A., 1968, Aftershocks and microaftershocks of the great Alaska earthquake of 1964: Bulletin of the Seismological Society of America, v. 58, p. 1131-1168.

---- 1972, Crustal deformation on the Denali fault, Alaska, 1942-1970: Journal of Geophysical Research, v. 77, p. 1528-1533.

Page, R. A., and Lahr, J., 1971, Measurements for fault slip on the Denali, Fairweather, and Castle Mountain faults, Alaska: Journal of Geophysical Research, v. 76, p. 8534-8543.

Pascal, G., 1979, Seismotectonics of the Papua New Guinea-Solomon Islands region: Tectonophysics, v. 57, p. 7-34.

Perman, R. C., Packer, D. R., Coppersmith, K. J., and Knuepfer, P. L., 1981, Collection of data for data bank on reservoir induced seismicity: Report to the U.S. Geological Survey, Contract No. 14-08-0001-19132, Final Technical Report, 45 p.

Pettijohn, F. J., 1949, Sedimentary rocks: New York, Harper and Brothers, 513 p.

Pewé, T. L., 1975, Quaternary geology of Alaska: U.S. Geological Survey Professional Paper 835, 145 p.

Pewé, T. L., Hopkins, D. M., and Giddings, J. L., 1965, Quaternary geology and archeology of Alaska, in Wright, H. E., Jr., and Frey, D. G., eds., The Quaternary of the United States: Princeton, New Jersey, Princeton University Press, p. 355-374.

Plafker, G., 1969, Tectonics of the March 27, 1964, Alaska earthquake: U.S. Geological Survey Professional Paper 543-I, 74 p.

Plafker, G., Hudson, T., Bruns, T. R., Rubin, M., 1978, Late Quaternary offsets along the Fairweather fault and crustal plate interactions in south Alaska: Canadian Journal of Earth Science, v. 15, p. 805-816.

Plafker, G., Hudson, T., and Richter, D. H., 1977, Preliminary observations on late Cenozoic displacements along the Totschunda and Denali fault systems, in Blean, K. M., ed., The United States Geological Survey in Alaska: Organization and status of programs in 1977: U.S. Geological Survey Circular C 751-A, p. B67-B69.

R & M Associates Inc., 1981, Photointerpretation report and terrain unit maps: Susitna Hydroelectric Project Report for Subtask 5.02 submitted to Acres American Inc., 5 sheets, 18 maps at a scale of 1:24,000.

Real, C. R., Toppozado, T. R., and Parke, D. L., 1978, Earthquake epicenter map of California 1900-1974: California Division of Mines and Geology Map, Sheet 39, scale 1:1,000,000.

Reyners, M., and Coles, K. S., 1982, Fine structure of the dipping seismic zone and subduction mechanics in the Shumagin Islands: Journal of Geophysical Research, v. 87, p. 356-366.

Rial, J. A., 1978, The Caracas-Venezuela earthquake of July 1967: A multiple source event: Journal of Geophysical Research, v. 83, p. 5405-5414.

Richter, C. F., 1958, Elementary Seismology: San Francisco, California, W. H. Freeman and Company, 768 p.

Richter, D. H., 1967, Geology of the Portage Creek - Susitna River area: Alaska Division of Mines and Minerals Geological Report No. 3, scale 1:24,000, 2 sheets.

Richter, D. H., and Matson, N. A., Jr., 1971, Quaternary faulting in the eastern Alaska Range: Geological Society of America Bulletin, v. 82, p. 1529-1539.

Rogers, G. C., and Hasegawa, H. S., 1978, A second look at the British Columbia earthquake of June 23, 1946: Bulletin of the Seismological Society of America, v. 58, p. 653-675.

Rojan, C., Brogan, G. E., and Slemmons, D. B., 1977, Preliminary report on the San Juan, Argentina Earthquake of November 23, 1977: Conference on Earthquake Engineering, San Salvador, 1978, reprint.

Ryall, A., Van Wormer, J. D., and Jones, A. E., 1968, Triggering of microearthquakes by earth tides, and other features of the Truckee, California, earthquake sequence of September 1966: Bulletin of the Seismological Society of America, v. 58, p. 215-248.

St. Amand, P., 1957, Geological and geophysical synthesis of the tectonics of portions of British Columbia, the Yukon Territory and Alaska: Geological Society of America Bulletin, v. 68, p. 1343-1370.

Schmoll, H. R., Szabo, B. J., Rubin, M., and Dobrovolny, E., 1972, Radiometric dating of marine shells from the Bootlegger Cove Clay, Anchorage area, Alaska: Geological Society of America, v. 83, p. 1107-1114.

Schnabel, P. B., and Seed, H. B., 1973, Accelerations in rock for earthquakes in the western United States: Bulletin of the Seismological Society of America, v. 63, p. 501-516.

Seed, H. B., 1980, University of California at Berkeley, Revisions to Schnabel and Seed (1973), personal communication.

Seed, H. B., Murarka, R., Lysmer, J., and Idriss, I. M., 1976, Relationships of maximum accelerations, maximum velocity, distance from source and local site conditions for moderately strong earthquakes: Bulletin of the Seismological Society of America, v. 66, p. 1323-1342.

Seed, H. B., Ugas, C., and Lysmer, J., 1976, Site-dependent spectra for earthquake resistant design: Bulletin of the Seismological Society of America, v. 66, p. 221-243.

Seno, T., 1981, International Institute of Seismologic and Earthquake Engineering, Ministry of Construction, Tsukuba, Japan, personal communication.

Seno, T., and Pongsawat, B., 1981, A triple-planed structure of seismicity and earthquake mechanisms at the subduction zone off Miyagi Prefecture, Northern Honshu, Japan: Earth and Planetary Science Letters, v. 55, p. 25-36.

Seno, T., Shimazaki, K., Somerville, P., Sudo, K., and Equchi, T., 1980, Rupture process of the Miyagi-Oki, Japan earthquake of June 12, 1978: Physics of the Earth and Planetary Interiors, v. 23, p. 39-61.

Shannon and Wilson, 1978, Seismic refraction survey, Susitna hydroelectric project--Watana and Devils Canyon dam sites: Report to U.S. Army Corps of Engineers, Alaska District, 27 p.

Sherard, J. L., Cluff, L. S., and Allen, C. R., 1974, Potentially active faults in dam foundations: Geotechnique, v. 24, p. 367-428.

Shimazaki, K., 1975, Nemuro-oki earthquake of June 17, 1973: A lithospheric rebound at the upper half of the interface: Physics of the Earth and Planetary Interiors, v. 9, 314-327.

Shimazaki, K., and Somerville, P., 1979, Static and dynamic parameters of the Izu-Oshima, Japan earthquake of January 14, 1978: Bulletin of the Seismological Society of America, v. 69, p. 1343-1378.

Silberling, N. J., Richter, D. H., and Jones, D. L., 1981, Recognition of the Wrangellia and vicinity, south-central Alaska: U.S. Geological Survey Circular 823B, p. B51-B55.

Simpson, D. W., 1976, Seismicity changes associated with reservoir loading: Engineering Geology, v. 10, p. 123-150.

Simpson, D. W., and Negnatullaiv, S. K. H., 1978, Induced seismicity studies in south central Asia: Earthquake Information Bulletin, v. 10, p. 209-213.

Singh, S. K., Bazan, E., and Esteva, L., 1980, Expected earthquake magnitude from a fault: Bulletin of the Seismological Society of America, v. 70, p. 903-914.

Slauson, W. F., and Savage, J. C., 1979, Geodetic deformation associated with the 1946 Vancouver Island, Canada earthquake: Bulletin of the Seismological Society of America, v. 69, p. 1487-1496.

Slemmons, D. B., 1977a, Faults and earthquake magnitude: U.S. Army Corps of Engineers, Waterways Experiment Station, Vicksburg, Mississippi, Miscellaneous Paper S-73-1, Report 6, 129 p.

---- 1977b, State-of-the-art for assessing earthquake hazards in the United States; Part 6: Faults and earthquake magnitude with appendix on geomorphic features of active fault zones: U.S. Army Engineer Waterways Experiment Station, Vicksburg, Contract No. DACW 39-76-C-0009, 12 p., plus 37 p. appendix.

Smith, T. E., 1973, Alaska Department of Geology and Geophysical Surveys, Fairbanks, Alaska, unpublished geologic maps, scale 1:24,000.

---- 1980, University of Alaska, Fairbanks, Alaska, personal communication.

---- 1981, Alaska Department of Geology and Geophysical Surveys, Fairbanks, Alaska, personal communication.

Snow, D. T., 1972, Geodynamics of seismic reservoirs: International Association of Engineering Geologists, Symposium on Percolation through Fissured Rocks, Stuttgart, Germany, Proceedings, p. TJ1-TJ19.

Stauder, W., 1968, Mechanism of the Rat Island earthquake sequence of February 4, 1965, with relation to island arcs and sea-floor spreading: Journal of Geophysical Research, v. 73, p. 3847-3858.

---- 1975, Subduction of the Nazca plate under Peru as evidenced by focal mechanisms and by seismicity: Journal of Geophysical Research, v. 80, p. 1053-1064.

Stout, J. H., Brady, J. B., Weber, F., and Page, R. A., 1973, Evidence for Quaternary movement on the McKinley strand of the Denali fault in the Delta River area, Alaska: Geological Society of America Bulletin, v. 84, p. 939-947.

Stout, J. H., and Chase, C. G., 1980, Plate kinematics of the Denali fault system: Canadian Journal of Earth Sciences, v. 17, p. 1527-1537.

Sudo, K., 1972, The focal process of the Taiwan-Oki earthquake of March 12, 1966: Journal of Physics of the Earth, v. 20, p. 147-164.

Sykes, L. R., 1971, Aftershock zones of great earthquakes, seismicity gaps, and earthquake prediction for Alaska and the Aleutians: Journal of Geophysical Research, v. 76, p. 8021-8041.

---- 1981, Lamont-Doherty Geological Observatory, Palisades, New York, written communication to Acres included as part of the Review of Woodward-Clyde Consultants Interim Report on Seismic Studies--Final Draft dated 23 February 1981.

Sykes, L. R., and Quittmeyer, R. C., 1981, Repeat times of great earthquakes along simple plate boundaries: in Simpson, D. W., and Richards, P. G., eds., 1981, Maurice Ewing Series No. 4, Earthquake prediction and international review: Washington, D. C., American Geophysical Union, p. 217-246.

Ten Brink, N. W., and Ritter, D. F., 1980, Glacial chronology of the north-central Alaska Range and implications for discovery of early-man sites (abs.): Geological Society of America, Abstracts with Programs, v. 12, p. 534.

Ten Brink, N. W., and Waythomas, C. F., 1982, Late Wisconsin glacial chronology of the north-central Alaska Range--A regional synthesis and its implications for early human settlements: Accepted for publication in the Geological Society of America Bulletin, 27 p. [in press].

Terrestrial Environmental Specialists, Inc., 1981, Environmental studies annual report 1980 Subtask 7.06, Cultural resources investigation: Report prepared for Acres American Inc., Buffalo, New York and the Alaska Power Authority, Anchorage, Alaska, by Terrestrial Environmental Specialists, Inc., Phoenix, New York, 257 p.

Thatcher, W., and Rundle, J. B., 1979, A model for the earthquake cycle in underthrust zones: Journal of Geophysical Research, v. 84, p. 5540-5556.

Thorson, R. M., and Hamilton, T. D., 1977, Geology of the Dry Creek site: A stratified early man site in interior Alaska: Quaternary Research, v. 7, p. 149-176.

Tobin, D. G., and Sykes, L. R., 1966, Relationship of hypocenters of earthquakes to the geology of Alaska: Journal of Geophysical Research, v. 71, p. 1659-1667.

Toppozada, T. R., Real, C. R., and Pierzinski, D. C., 1979, Seismicity of California January 1975 through March 1979: California Geology, v. 7, p. 139-142.

Trainer, F. W., and Waller, R. M., 1965, Subsurface stratigraphy of glacial drift at Anchorage, Alaska: U.S. Geological Survey Professional Paper 525-D, p. D167-D174.

Tsai, Y., and Aki, K., 1970, Source mechanism of the Truckee, California, earthquake of September 12, 1966: Bulletin of the Seismological Society of America: v. 60, p. 1199-1208.

Turner, D. L., and Smith, T. E., 1974, Geochronology and generalized geology of the central Alaska Range, Clearwater Mountains, and northern Talkeetna Mountains: Alaska Division of Geological and Geophysical Surveys Open-File Report 72, 11 p.

Turner, D. L., Smith, T. E., and Forbes, R. B., 1974, Geochronology of offset along the Denali fault system in Alaska (abs.): Geological Society of America Abstracts with Programs, v. 6, p. 268-269.

Tysdel, R. G., 1976, A preliminary evaluation of selected earthquake-related geologic hazards in the Kenai Lowland, Alaska: U.S. Geological Survey Open File Report 76-270, 30 p.

U. S. Army Corps of Engineers, undated, Upper Susitna River basin-Watana reservoir, surficial geology: U.S. Army Corps of Engineers, Alaska District, scale 1:63,360, Plate 5.

---- 1979, Southcentral railbelt area, Alaska, Upper Susitna River basin, Hydroelectric power supplemental feasibility report: U.S. Army Corps of Engineers, Alaska District, main report and appendices 1 and 2.

U. S. Bureau of Reclamation, 1960, Devil Canyon project, Alaska, feasibility report: Bureau of Reclamation, Alaska District, 99 p.

U. S. Nuclear Regulatory Commission, 1981, Safety evaluation report related to the operation of San Onofre Nuclear Generating Station, Units 2 and 3: U.S. Nuclear Regulatory Commission, Washington, D.C., NUREG-0712, Supplement No. 1, p. E-16 and E-17.

Urhammer, R. A., 1980, Observations of the Coyote Lake, California earthquake sequence of August 6, 1979: Bulletin of the Seismological Society of America, v. 70, p. 559-570.

Van Eysinga, F. W. D., 1978, Geological timetable: New York, Elsevier Scientific Publishing Company, 1 sheet.

Vieth, K. F., 1974, The relationship of island arc seismicity to plate tectonics: Ph.D. thesis, Southern Methodist University, Dallas, Texas.

Wahrhaftig, C. A., 1958, Quaternary geology of the Nenana River valley and adjacent parts of the Alaska Range: U.S. Geological Survey Professional Paper 293, p. 1-70.

Wahrhaftig, C. A., Turner, D. L., Weber, F. R., and Smith, T. E., 1975, Nature and timing of movement on Hines Creek strand of Denali fault system, Alaska: Geology, v. 3, p. 463-466.

Weber, F. R., Hamilton, T. D., Hopkin, D. M., Repenning, C. A., and Haas, H., 1980, Canyon Creek: A Late Pleistocene vertebrate locality in interior Alaska: Quaternary Research, v. 16, no. 2, p. 167-180.

Werner, A., 1982, Glacial Geology of the McKinley River area, Alaska: with an evaluation of various relative age dating techniques: Master's thesis, Southern Illinois University at Carbondale, Illinois, 147 p. [in press].

Withers, R. J., 1977, Seismicity and stress determination at man-made lakes: Ph.D. Dissertation, University of Alberta, Canada, 241 p.

Withers, R. J., and Nyland, E., 1978, Time evolution of stress under an artificial lake and its implication for induced seismicity: Canadian Journal of Earth Sciences, v. 15, p. 1526-1534.

Wood, H. O., and Neumann, F., 1931, Modified Mercalli Intensity Scale of 1931: Bulletin of the Seismological Society of America, v. 21, p. 277-283.

Woodward-Clyde Consultants, 1975, Age dating of geologic materials--A survey of techniques: San Francisco, Professional Development Committee, Woodward-Clyde Consultants, 183 p.

---- 1978, Offshore Alaska Seismic Exposure Study, Volumes I-VI: Unpublished report prepared for the Alaska Subarctic Offshore Committee, Exxon Corporation, Houston, Texas, Project Administrator, by Woodward-Clyde Consultants, Orange, California.

---- 1980a, Final Report--Susitna Hydroelectric Project--Seismic Refraction Survey--Summer, 1980: Unpublished report prepared for R & M Associates, Anchorage, Alaska, 17 p., 1 appendix.

---- 1980b, Interim Report on Seismic Studies for Susitna Hydroelectric Project: Report prepared for Acres American Inc., Buffalo, New York, by Woodward-Clyde Consultants, Orange, California, 225 p, 8 Appendices.

---- 1980c, Preliminary Seismic Hazards Study for the Ituango Project; Colombia--Phase I: Report submitted to Integral, LTDA, Medellin, Colombia, 7 Sections, 2 Appendices, 15 plates.

---- 1982, Susitna Hydroelectric Project Seismic Refraction Surveys 1981: Unpublished report prepared for R & M Consultants, Anchorage, Alaska, by Woodward-Clyde Consultants, Santa Ana, California, 59 p., 3 Appendices.

Wyss, M., 1979, Estimating maximum expectable magnitude of earthquake from fault dimensions: Geology, v. 7, p. 336-340.

Yerkes, R. F., 1973, Effects of the San Fernando earthquake as related to geology in San Fernando, California earthquake of February 9, 1971: National Oceanographic and Atmospheric Administration, Washington, D.C.

Yoshii, T., 1975, Proposal of the "aseismic front": Zisin 2, v. 28, p. 365-367 (in Japanese).

---- 1979, A detailed cross-section of the deep seismic zone beneath northeastern Honshu, Japan: Tectonophysics, v. 55, p. 349-360.